Protein Kinase C Iota in Mammalian Cell Polarity and Cancer

Mark Linch

University College London

and

Cancer Research UK London Research Institute

PhD Supervisor: Prof Peter Parker

A thesis submitted for the degree of

Doctor of Philosophy

University College London

September 2011

Declaration

I Mark Linch confirm that the work presented in this thesis is my own. Where information has been derived from other sources, I confirm that this has been indicated in the thesis.

Abstract

Protein Kinase C iota (PKCι) is a serine/threonine kinase that is involved in epithelial polarity and malignancy where polarity is typically abrogated. The aim of this thesis was to characterise the role of PKCι in oncogenic signaling in the context of polarity loss. This work set out to identify activators, binding partners and downstream effectors of PKCι with a view to informing rational therapeutic design.

Madin Darby Canine Kidney (MDCK) cells, grown as polarised cysts containing a central lumen in Matrigel, developed a multiple-lumen phenotype on perturbation of PKCι, suggesting a threshold requirement for normal lumenogenesis. When transfected with oncogenic Ras, MDCK cells formed large spheres lacking a lumen and polarity. Upon PKCι inhibition with siRNA or small molecules, polarity was partially rescued indicating that PKCι lies downstream of Ras in this polarity loss pathway.

Structural studies have enabled two distinct approaches to identify effectors of PKCι. A novel protein-protein interaction motif (RIPR) within PKCι was identified and shown here to be responsible for interaction with a subset of target proteins, including LLGL2. MDCK cysts expressing a PKCι mutated in this motif developed a multiple-lumen phenotype. In a second approach, use was made of an inhibitor bound complex of PKCι to design a drug insensitive mutant. Expression of the resistant mutant in HEK293 cells led to resistance to inhibitor induced dephosphorylation of LLGL2 and protected MDCK cells from developing inhibitor induced multiple lumens and loss of polarity. This tool has been used to screen for PKCι substrates.

In summary, PKCι lies downstream of H-Ras in MDCK polarity signalling. The site at which PKCι binds LLGL2 is defined and shown to contribute to normal lumenogenesis. A drug insensitive PKCι mutant is described that can be utilised for substrate and biomarker identification.

Acknowledgements

Firstly I would like to thank Peter Parker for giving me the chance to work in his laboratory and for all his help. In particular, his encouragement of my ideas and his willingness to share his passion for science. A huge thanks goes to all the members of the Parker Lab, both past and present who have created an atmosphere conducive of work and great fun. A special mention goes to Carine and Katrina who introduced me to atypical PKC and provided my initial laboratory training.

A key influence on this work was the atypical PKC interest group: Peter Parker, Neil McDonald, Angus Cameron, Sven Kjaer, Erika Soriano and Philippe Riou. These meetings were intriguing, stimulating, exciting and sometimes bewildering and I thank you all. I would also like to thank Jon Roffey and Christian Dillon for helpful discussions and embracing me within the PKCι drug development program at Cancer Research Technology.

There are countless people around the London Research Institute who have gone out of their way to help me with this PhD: Julie Bee and the animal facility, Chris Madsen for help with the lung colonisation assay, Emma Nye for histopathology, Mark Skehel for mass spectrometry, Richard Mitter for bioinformatics support and David Bacon for software training and help with this document. Thanks to everyone in IS for their brilliant support. I would also like to thank my friend Mark Barraclough for his invaluable help with Adobe Illustrator.

Finally, I would like to thank my wife Anna for her love, support and for the sacrifices she has made while I have been engrossed in this work.

Table of Contents

Table of figures

List of tables

Abbreviations

Å	angstoms
Ala	alanine
aPKC	atypical PKC
Arg	arginine
Asp	aspartate
ATP	adenosine triphosphate
BIM1	bisindolylmaleimide 1
BSA	bovine serum albumin
^{o}C	degrees centigrade
cPKC	classical PKC
Da	daltons
DAG	diacylglycerol
DMSO	dimethyl sulphoxide
DNA	deoxyribonucleic acid
EDTA	ethylene diamine tetra-acetic acid
EGF	epidermal growth factor
FCS	oetal calf serum
GFP	green fluorescent protein

g	grams
Glu	glutamate
GST	glutathione S-transferase
IB	immunoblot
IF	immunofluorescence
IP	immunoprecipitation
Lys	lysine
M	molar
M	milli
μ	micro
MEF	mouse embryonic fibroblast
n	nano
nPKC	novel PKC
p	pico
PCR	polymerase chain reaction
PKC	protein kinase C
PKN	protein kinase novel (also referred to as PRK)
Pro	proline
Ser	serine

Thr	threonine
w/v	weight/volume
v/v	volume/volume

Chapter 1. Introduction

1.1 Overview of Introduction

In biological systems, cells are continuously exposed to a diverse array of stimuli. Cells must sense their environment and then relay this information into the cells where it is interpreted and responded to appropriately. This biological information flow is known as cell signalling. Failure of cells to correctly sense their environment or interpret the information flow can lead to diseases including cancer. This thesis focuses on the role of protein kinase C iota (PKCι), a signalling molecule that has been implicated in cancer when it is inappropriately activated. The first section of the introduction will aim to provide an overview of normal signalling, highlighting areas pertinent to this thesis. In particular, I will describe how post-translational modifications of proteins, protein-protein interactions and protein dimerisation or oligomerisation can impact on signal transduction. I will discuss how feedback mechanisms help to regulate and increase the complexity of signalling and provide a few classical examples of where erroneous signalling results in disease. The second section will formally introduce PKCι, describe the current understanding of where it sits in the signalling cascade and the functional roles of PKCι in cells. In addition, evidence for abrogated PKCι signalling in human cancer and the current potential therapeutic strategies will be addressed.

1.2 Cell Signalling

1.2.1 Introduction to signalling

Cells from multicellular organisms must constantly communicate with each other to facilitate their multitude of functions. The life history of cells encompasses birth from cell proliferation and differentiation into specific cell types with specific functions such as migration and senescence through to cell death. In particular cells, processes such as

sensory perception, secretion and mounting of an immune response are also performed. Cell signalling is the transfer of biological information required to orchestrate these processes (Berridge, 2006, see Downward, 2001 for review).

There has been an explosion in the characterisation of signalling components and pathways. It is evident that different pathways are combined and adapted to control a diverse array of cellular processes in varying spatial and temporal contexts. Despite this diversity, there are common mechanisms that have evolved. Receptors sense the environmental cues and transfer information across the membrane using a range of transducers and amplifiers. These then connect the vast repertoire of intracellular signalling molecules comprised of messengers, sensors and effectors and this relay of information ultimately results in cellular responses (Berridge, 2006).

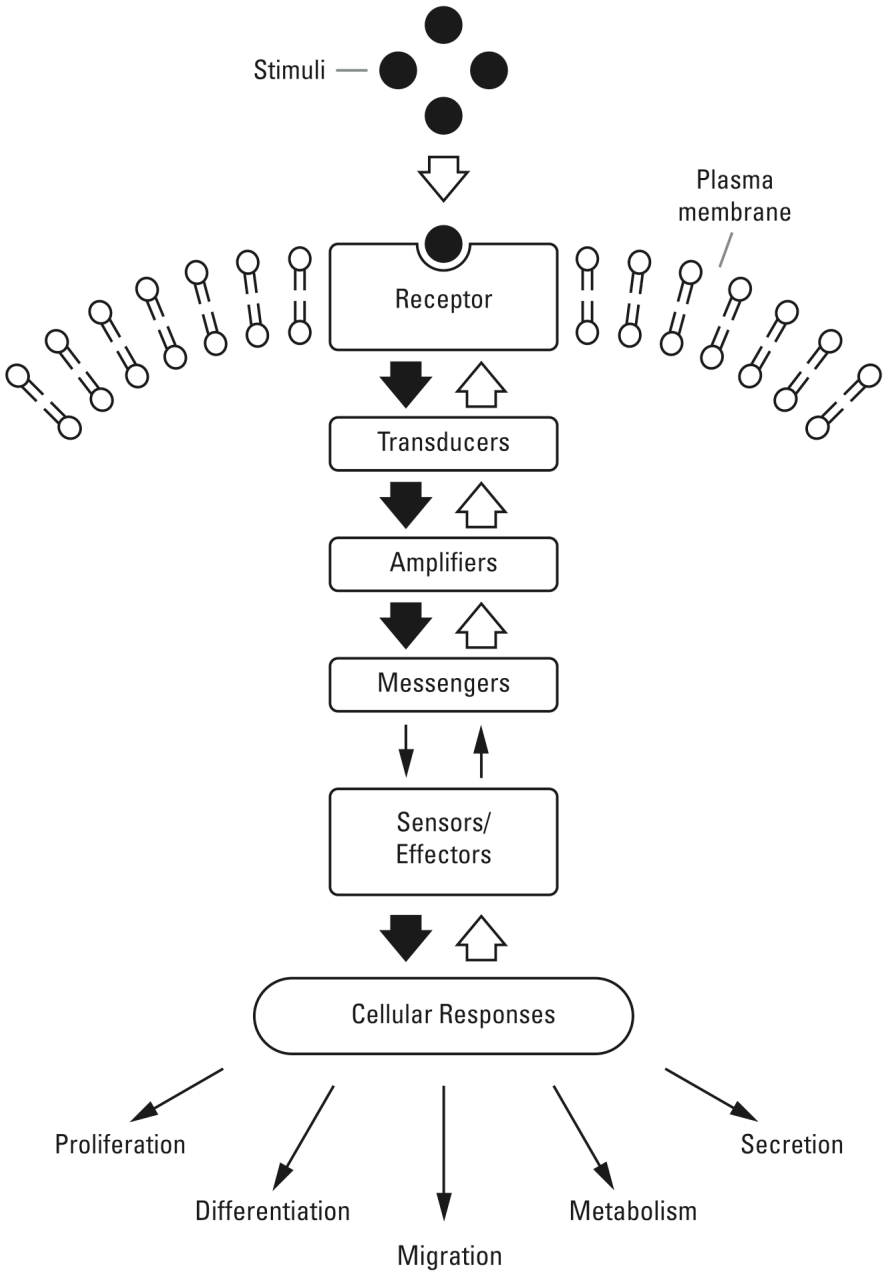

Figure 1.1 Signalling overview
The scheme is adapted from (Berridge, 2006).

1.2.2 Stimuli and Receptors

The two-way cellular discourse that is necessary in multicellular organisms occurs through electrical, physical and chemical signals. Electrical signals are usually fast and require cells to be coupled together through low resistance pathways such as gap junctions. These junctions allow passing electrical charge and are large enough for small metabolites and second messengers to diffuse from one cell to another. Some chemical signals, such as steroid hormones, are able to diffuse through the lipophilic plasma membrane to gain access to cytoplasmic or nuclear receptors. However, most water-soluble stimuli including growth factors, hormones, nutrients and neurotransmitters, require a means to relay the extracellular information into the cell without physically traversing the plasma membrane. Soluble signals can be derived locally from the same cell (autocrine) or neighbouring cells (paracrine) or distally and carried around the blood stream (endocrine). Additionally, stimuli can remain tethered to the cell membrane (juxtacrine) or be insoluble extracellular matrix components (Singh and Harris, 2005, Berridge, 2006).

Receptors at the plasma membrane function as embedded molecular antennae. Upon complementary binding of a signal (ligand) to the receptor, the receptor undergoes a conformational change that alters the intracellular receptor activity. The largest family of receptors is the G-protein coupled receptors that respond to a diverse array of signals. The ligand bound conformational change in these 7-transmembrane/heptahelical receptors enables their guanine nucleotide exchange factor (GEF) activity, exchanging GDP for GTP in their associated G proteins (see (Wettschureck and Offermanns, 2005)for review). One of the most common receptor families is the tyrosine kinase receptors, that includes the epidermal growth factor and insulin receptors. The epidermal growth factor receptor dimerises in response to its ligand, EGF, and undergoes autophosphorylation of several tyrosine residues in the intracellular C-terminal domain. This phosphorylated EGFR is capable of binding to signal transducers such as the Src homology 2 containing effector and adaptor proteins which recognise phosphotyrosine in a sequence specific context (Pawson et al., 2001). Other receptors trigger the opening of gated ion channels in response to ligand binding, for example, the nicotinic acetylcholine receptor (McGehee, 1999).

In order to detect and respond to this multitude of signal inputs a wide range of receptors have evolved. One means of increasing specificity of the receptors is by the formation of heterodimers and/or co-operative receptor response. An example of receptors that require heterodimerisation for function is the integrin family that is comprised of α and β subunits. In mammals there are 24 α,β heterodimers made up of 18 α and 8 β integrin subunits. While multiple receptors can recognise the same signals, the integrin-ligand combination elicit specific signals although the precise mechanism for this is currently unknown (for review see Byron et al., 2010). As well as responding to environmental stimuli the integrins are also able to propagate inside-out signalling where they reveal the status of the cell to the outside (Qin et al., 2004).

1.2.3 Transducers and Amplifiers

The signal in the form of receptor conformational changes is transduced and amplified by second messengers. This is well exemplified by cyclic AMP signalling where the signal from G-protein coupled receptors (GPCR) is transduced by heterotrimeric G proteins that can either activate or inhibit the amplifier adenylate cyclase (AC). In the case of activation, the GEF activity of GPCR causes dissociation of the heterotrimeric G protein into Gβγ and $G\alpha_s$-GTP and this later subunit is capable to activating adenylate cyclase by allosteric maturation of its active site. Adenylate cyclase is a transmembrane enzyme that converts ATP into the second messenger cyclic-AMP. Adenylate cyclase can generate multiple molecules of the second messenger for each ligand bound to GPCR and in doing so amplifies the signal (Lynch et al., 2006). Other prevalent second messengers include diacyclglycerol (DAG) (Carrasco and Merida, 2007), calcium and inositol 1,4,5-triphosphate (IP_3) (Berridge, 2009).

1.2.4 Post translational modifications

Post translational modifications (PTMs) are various processing events that change the maturity, activity, and/or turnover of proteins. More that 200 different forms of PTM

have been identified and more are expected to be found (Zhu et al., 2003). This section will concentrate on phosphorylation, an important modification upon which much of thesis is based and glycosylation which is the most abundant protein modification (Larkin and Imperiali, 2011). Examples of other common and functionally important PTMs are show in Table 1.1.

Phosphorylation involves the transfer of a phosphate group from the terminal phosphate of nucleoside triphosphates, usually ATP, on to the hydroxyl group of specific protein residues, typically a serine, threonine or tyrosine. This reaction is carried out by protein kinases. A single phosphate group can dramatically alter the protein conformation and/or activity. A single molecule of protein kinase that is catalytically activated can process many thousands of substrate molecules. If the substrate is itself an enzyme, the amplification effects can be magnified further. Dephosphorylation is achieved by protein phosphatases and thus the balance between kinases and phosphatases determines the steady state of protein phosphorylation. Through the control of phosphorylation therefore, protein kinases act as rapid, sensitive and reversible molecular switches (Mann et al., 2002, Li et al., 2009).

The human genome project identified 518 putative protein kinases that is about 2% of the genome (Manning et al., 2002). In addition there were 100 phosphatases (Venter et al., 2001). The kinases form 3 classes based on their substrate specificity; the serine/threonine kinases, the tyrosine kinases and dual specificity kinases. At any one time in the cell it is estimated that the phospho-amino acid content ratio is 1800:200:1 (pSer:pThr:pTyr) (Mann et al., 2002). These kinases may be further classified based on their distinct catalytic domains, regulatory domains or biological function (Manning et al., 2002).

The covalent attachment of a phosphate group to a target protein can have a variety of effects on the function of the protein. Phosphorylated proteins have acquired a bulky negative charge that is capable of protein interactions. Typically the phosphoryl group mediates hydrogen bonding to main-chain amide groups or salt bridging to arginine residues (Johnson and O'Reilly, 1996). Phosphorylation can affect the target protein in several ways. Firstly it can change the activity of the protein. For example

phosphorylation of glycogen phosphorylase at Ser14 results in a marked allosteric shift of the serine side chain by 50Å leading to rearrangement of subunit-subunit contacts and active site activation (Barford and Johnson, 1989). However, phosphorylation of Src kinase at Tyr-527 by other tyrosine kinases is inhibitory (Kmiecik and Shalloway, 1987, Thomas et al., 1991). Secondly, phosphorylation can provide new recognition sites for binding proteins (see section 1.1.5).

Proteins that are destined to be placed on the cell surface or secreted into the extracellular environment commonly undergo covalent modification by the attachment of carbohydrate molecules at specific residues. This modification is termed glycosylation and specific enzymes are required to catalyse these reactions. There are three major types of glycosylation in nature; N-linked, O-linked and GPI-anchored. N-linked involves the transfer of an oligosaccharide onto the side chain amide nitrogen of asparagine residues. In O-linked glycosylation monosaccharides are sequentially added to the hydroxyl oxygen of predominantly serine or threonine residues. In the third major type, a complex glycosylphosphatidylinositol (GPIanchor) moiety is transferred to the C-terminus of a target protein, tethering it to the cell membrane. Glycosylation is thought be involved in intracellular targeting, cell signalling, cellular trafficking and the immune response (Larkin and Imperiali, 2011).

Table 1.1 Post translational modifications.
Selected common and functionally important post-translational modifications. Adapted from (Mann and Jensen, 2003).

Post Translational Modification	Functional
Glycosylation	Cell-cell recognition Signalling Membrane tethering
Phosphorylation	Activation/inactivation Modulation of protein interaction Signalling
Acetylation	Protein stability Protein-DNA interactions
Acylation eg. Myristoyl, Farnesyl, Palmitoyl	Membrane targeting Stability Protein-protein interactions
Methylation	Regulation of gene expression
Ubiquitination	Degradation Protein (in)activation Traffic
Sulphation	Modulator of protein-protein and receptor ligand interactions

1.2.5 Protein interaction domains

Signalling proteins commonly contain modular interaction domains (also known as recognition modules) that facilitate multi-protein complex formation (Kuriyan and Cowburn, 1997). During signal transduction these interaction domains determine the specificity of signal complex assembly and target them for a defined subcellular localization that in turn specifies which regulators and targets they are exposed to (Pawson et al., 2001).

Interaction domains are independently folded modules, typically 35-150 residues in length that can still bind their target ligands if expressed independently of the full-length protein. This domain organisation has evolved such that different domains may be strung together in a combinatorial manner without disrupting function (Pawson et al., 2002, Pawson and Nash, 2003).

Interaction domains are often arranged into distinct groups whose members have related, but not identical, sequence binding. Common protein interaction domain families include Src-homology 3 (SH3), WW domains and EVH1 that all bind to proline rich sequences. PDZ domains bind predominantly to the extreme c-termini of their target proteins. In addition there are the common phospholipid interacting domains critical for membrane compartment targeting including pleckstrin homology (PH) domains, that bind to phosphoinositides such as $PI(4,5)P_2$ and $PI(3,4,5)P_3$, and FYVE, phox homology (PX), C1 domains and some WD40 domains (Pawson et al., 2002, Pawson and Nash, 2003).

Other interaction domains bind specifically to sequences containing post-translational modifications. These include 14.3.3, Forkhead-associate (FHA), p21-binding domain (PBD) and some WD40 repeats which all bind to phospho-theonine/serine motifs. A further group requiring PTMs are Src-homology 2 (SH2) and some Phosphotyrosine-binding domains (PTB) which require phosphotyrosine sites (Hunter, 2000, Yaffe, 2002, Yaffe and Elia, 2001). WD40 and 14.3.3 binding domains are described here in further detail as they pertain to this thesis. WD40 repeats contain conserved tryptophan and aspartic acid residues ('WD') and are approximately 40 amino acids in length. Their functions include adaptor modules in signal transduction, pre-mRNA processing, cytoskeletal assembly, gene transcription activation and cell cycle control. It has emerged that multiple WD40 repeats associate and form β-propeller structures, typically comprising 7 blades, that act as a platform for binding partners, particularly those with post-translational modifications (Xu and Min, 2011)

14.3.3 is a family of small 30kDa acidic proteins that form cup-shaped homo and heterodimers. Each subunit of the dimer contains a highly conserved phospho-peptide binding pocket separated by ~34Å. 14.3.3 isoforms have been reported to have a number of effects on the target protein; conformational change, steric hindrance or scaffolding. Two modes of binding have been defined that have distinguishing primary sequence recognition motifs: Mode I, R-S-X-pS/T-X-P and Mode II R-X-X-X-pS/T-X-P. Several target proteins were found to contain multiple 14.3.3 binding sites, which enhances binding affinity. Furthermore, many target proteins contained one high affinity site and one suboptimal site that had low affinity binding by itself but acted

synergistically with a high affinity site. It was hypothesised that the suboptimal site (gatekeeper) may facilitate dissociation and therefore reversibility of the interaction (Yaffe, 2002, see Bridges and Moorhead, 2005 for review). Functional studies and the crystal structure of PKCε-14.3.3ζ have subsequently supported the gatekeeper model (Saurin et al., 2008, Kostelecky et al., 2009).

1.2.6 Dimerisation/oligomerisation

Proteins can bind identical proteins through complementary binding surfaces and form complexes that range from dimers to filaments. The formation of protein polymers has broad implications for protein function including their role as scaffolds (as described for 14.3.3 above) and allosteric protein activation. The latter is well illustrated by the epidermal growth factor receptor (EGFR).

Different inhibitor bound structures of EGFR have demonstrated both a symmetrical and asymmetrical dimer and thus provided an insight into the possible mechanism of activation. Unlike the original model, whereby ligand binding induced receptor dimerisation, it appears that EGF causes a shift from a symmetrical dimer to an asymmetrical dimer (Schlessinger, 2002, Garrett et al., 2002, Zhang et al., 2006b). In activated structures the kinase domains form a head to tail configuration in which the αH helix in the C-lobe of one kinase (activator kinase) docks with the αC helix in the N-lobe of its partner kinase (receiver). This interaction causes a conformational change in the αC helix and activation loop to facilitate catalytic activity. However, this interaction is weak and also requires a second intermolecular binding event; the juxta-membrane segment of the receiver kinase loops around to interact with the C-lobe of the activator kinase (Zhang et al., 2006b, Jura et al., 2009). These models developed from structural biology studies indicate how intricate and elegant protein interactions can be.

1.2.7 Feedback Control

Feedback loops are processes that connect output signals back to their inputs. Such feedback loops are abundant in and critical for signal transduction pathways. Negative feedback is necessary for maintaining homeostasis within a system (see Brandman and Meyer, 2008 for review). For example, the p53 pathway is critical for the stress response in cells and is tightly regulated by multiple homeostatic feedback mechanisms. p53 requires serine phosphorylation by p38 MAP kinase for activation. Upon p53 activation one of its transcriptional targets, Wip-1 is up regulated. Wip-1 is a phosphatase that reverses the serine phosphorylation and thus decreases the activity of p53 (Harris and Levine, 2005).

Positive feedback mechanisms are necessary to amplify a signal. A good example is the inositol 1,4,5-triphosphate (IP_3)-receptor at the endoplasmic reticulum (ER). This IP_3 receptor is partially activated by binding of IP_3 molecules that result in slight Ca^{2+} release from the ER. The Ca^{2+} release fully activates the receptor causing further calcium release into the cytosol (Finch et al., 1991, Bezprozvanny et al., 1991). These positive feed back mechanisms help to establish molecular "on/off" switches (see (Berridge, 2009)for review). The threshold upon which the switch is activated depends, among other things, on the sensitivity of the regulatory step for a specific pathway, the stability of the signalling outputs and temporo-spatial parameters.

Signalling networks involving both positive and negative feedbacks are likely to contribute to the complicated array of signalling outputs from a single stimulus that we observe in nature. The possible complexity of multiple feedback loops is further enhanced by interaction with other signalling pathways. Experimental reports on such integrated signalling networks with multiple feedbacks is limited and this probably reflects our ingrained approach to studying individual pathway components. There are several situations where multi-threshold responses are apparent and it has been proposed that this may be regulated by the combination of feedback loops. These combinations of feedback loops includes diverse behaviours such as the response to morphogens in *Xenopus* and the induction of tolerance in T-cells under the control of

Lymphocyte-specific protein tyrosine kinase (Lck) (Green et al., 1994, Stefanova et al., 2003)

1.2.8 Signalling and disease

There is a vast array of interconnecting signalling pathways. Despite a high degree of plasticity to cope with changing demands, pathway defects still occur. Given the fundamental role of signalling in all physiological processes, such aberrations have a great significance for the onset of human disease. Pathological organisms and viruses can interfere with signalling pathways as can inherited or somatic mutations to the genes encoding signalling molecules.

An excellent example of an infective disruption of signalling is the affect of cholera toxin on cAMP generation by adenylate cyclase (see section 1.2.3). Active efflux of chloride ions across the intestinal epithelium into the lumen is regulated in part by cAMP. Cholera is a disease characterized by severe watery diarrhoea. It is caused by the gram negative bacterium Vibrio cholerae that secretes cholera toxin. The cholera toxin catalytic subunit couples the adenosine disphosphate (ADP)-ribose moiety of intracellular nicotinamide adenine dinucleotide to a critical residue in $G\alpha_S$, the subunit of the heterotrimeric G protein. This ribosylation inhibits the ability of $G\alpha_S$ to hydrolyse GTP, which means that the G protein is locked in its active configuration. This maintains activation of adenylate cyclase and thus cAMP production and intestinal secretion (Farfel et al., 1999).

Retinoblastoma (Rb) is the prototype of an inherited cancer linked to sequential loss or inactivation of both alleles of a tumour suppressor gene, the Rb1 gene. In order to explain the pathogenic mechanism Knudson in 1971, based on epidemiological studies, proposed the “two-hit theory”. The theory states retinoblastoma is inherited by two sequential mutational events, the first via the germline and the second occurring spontaneously in somatic cells. Inactivation of Rb was shown to have profound effects on the control of the cell cycle. E2F transcription factors associate with a second subunit, DP1 or DP2, to form a heteromeric transcription factor capable of binding to

DNA promoters of cell cycle (G1/S) target genes. Phosphorylation of Rb enables an inhibitory interaction with E2F. In cancer cells, loss of the pRb brake leads to E2F-dependent G1/S gene expression even in the absence of mitogens (Weinberg, 1995, Sherr and McCormick, 2002). Further intensive study of the role of Rb in cancer has added huge complexity to this picture and it is now recognised that in addition to serving as a G1 checkpoint Rb has many other cellular roles. Rb is also identified as a somatic mutation in a wide range of human cancers. Contemporary epidemiologists have suggested that the Knudson two hit theory was indeed flawed but perhaps this can be explained by the multiple non-inherited roles, the influence of other factors and incomplete penetrance (Burkhart and Sage, 2008, Mastrangelo et al., 2009).

While a proportion of malignancies may be attributed to germline mutations the vast majority have been shown to be due to an accumulation of 3-7 somatic mutations and has been described as the multistep nature of cancer (Vogelstein and Kinzler, 1993). Somatic mutations of the Ras gene are the most frequently detected in human cancer. It is now 30 years since it was recognised that fragments of DNA from human cancer derived cells could induce malignant transformation in fibroblasts. It was later demonstrated that for the first of these, the active component was the cellular homolog of H-Ras, an oncogene found in the Harvey rat sarcoma retrovirus (see Downward, 2006 for review). There are four major isoforms of Ras: H-ras, N-Ras, K-RasA and K-RasB. The principal isoform differences are their post-translational modifications that determine their compartmental localization. The first defined function of Ras was as a transducer of tyrosine kinase receptors. Upon ligand occupation the tyrosine kinase receptors dimerise and autophosphorylate enabling Grb2, an adaptor protein containing SH2/SH3 binding domains, to interact with the intracellular receptor domain. Grb2 contributes to the localization of Son-of-sevenless (SoS), a Ras guanine nucleotide exchange factor (RasGEF). SoS binds to the SH3 domain of Grb2 where it can facilitate the exchange of GDP for GTP generating activated Ras-GTP. Switching off activated Ras requires the hydrolysis of GTP to GDP by Ras. Ras GTPase-activating proteins (RasGAPs) are required to accelerate this “off” reaction. Activated Ras is now known to relay signals to multiple pathways including Raf, PI3-K, phospholipase Cε and RalGEFs (Buday and Downward, 2008, Ferro et al., 2008).

Somatic K-Ras mutations are common in cancer and are particularly high in malignancies of the pancreas (59%), colon (32%), lung (18%) and ovary (15%) (Wang et al., 2010). Common activating mutations of Ras include the G12V mutation that renders activated Ras insensitive to GAPs and Q61K that reduces the rate of Ras-GTP hydrolysis. In colon cancer the G12V mutation was predictive for shorter time to treatment failure and reduced overall survival (Andreyev et al., 2001). Knowledge of patients K-Ras mutation status also helps to guide treatments. For example, in patients with chemotherapy refractory metastatic colorectal cancer only those patients with wild type K-Ras gain a benefit from treatment with Cetuximab, a monoclonal antibody against EGFR (Karapetis et al., 2008).

1.3 Atypical Protein Kinase C

1.3.1 aPKC primary structure and organisation

The Atypical Protein Kinase Cs (aPKC) consist of iota (ι) and zeta (ζ) gene products and are members of the Protein Kinase C (PKC) branch of the AGC kinases (protein kinases A,G and C). PKC lambda (λ) is the murine homolog of human PKCι. The PKCs are serine/theonine protein kinases that share similar catalytic domains and are divided into four separate classes based on their more divergent regulatory domains - conventional, novel, atypical and PKN (Figure 1.2). The Conventional PKC (cPKC) isotypes, that include PKCα, the alternatively spliced βI and βII and γ, are activated through a combination of DAG and phosphatidylserine binding to two tandem C1 domains (Hurley et al., 1997) and Ca^{2+} - dependent phospholipid binding to the C2 domain. These phospholipids include phosphatidylinositol-4,5-bis phosphate (PIP_2). The C1 domain also binds to tumour promoting phorbol esters such as PMA (Ono et al., 1989). Novel PKC (nPKC) isotypes that include PKC δ, ε, η and θ also contain the tandem C1 domains and are therefore DAG sensitive but have a 'novel' C2 domain that does not bind to Ca^{2+} or participate in membrane association. The atypical PKCs do not have a C2 domain and have an 'atypical' C1 domain with a highly basic cleft that prevents ligand binding, rendering aPKCs insensitive to both DAG and Ca^{2+} (Pu et al., 2006). The C1 domain is a cysteine rich sequence that co-ordinates zinc ions and the atypical C1 domain has been reported to mediate interactions with proteins such as PAR-4 (see section 1.3.3.5)(Hommel et al., 1994).

All PKC isoenzymes have a regulatory domain pseudosubstrate sequence that occupies the substrate binding pocket in the absence of lipid binding (or allosteric activators) and maintains the kinase in an autoinhibited state. Upon binding to second messengers or allosteric activators, typically at the plasma membrane, the docking of the regulatory domain, including the pseudosubstrate region, is released allowing the activation of PKC (Pears et al., 1990).

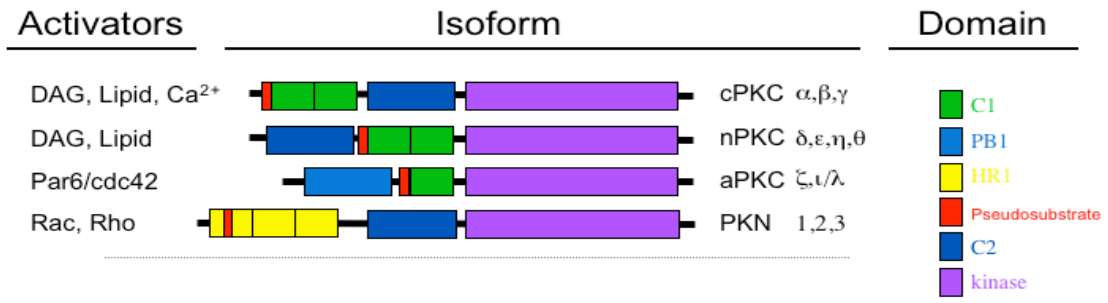

Figure 1.2 The domains of PKC

Both PKC and PKN have protein-protein binding domains, the Phox and Bem1p (PB1) and homology region 1 (HR1) domains respectively. PB1 domain interactions associated with aPKC are formed when the conserved acidic segment (termed the OPCA motif) of one PB1 domain forms a salt bridge with the conserved basic residues (typically lysines) on another (Wilson et al., 2003, Hirano et al., 2005). For examples of PB1 proteins see section 1.3.3.5. The bivalent engagement of HR1 motifs by the Rho-family GTPases Rho or Rac disengages the PKN pseudosubstrate and results in kinase activation (Shibata et al., 1996, Flynn et al., 1998).

All AGC kinases require phosphorylation on conserved Ser or Thr residues that for PKC are termed priming phosphorylations. These priming phosphorylations stabilise the kinase and achieve a catalytically competent state that can be rapidly activated upon second messenger generation. cPKCs and nPKC have 3 priming phosphorylation sites, one at the activation loop and two at the C-terminus referred to as the turn motif and the hydrophobic motif. However, PKCι/ζ only have the activation loop (Thr403/410) and turn motif (Thr555/556) phosphorylation sites with the hydrophobic site S/T substituted with an acidic residue (E), that can potentially act as a phosphomimetic; a similar situation pertains in PKN where an aspartate sits at the equivalent hydrophobic site (see

Parker and Murray-Rust, 2004 for review). The activation loop phosphorylation is catalysed by the upstream kinase phosphoinositide-dependent kinase-1 (PDK-1), which docks onto the hydrophobic motif or phosphomimetic site and has its enzymatic activity near the entrance to the aPKC active site (Le Good et al., 1998, Balendran et al., 2000). This correctly aligns residues within the aPKC active site for catalysis (Toker and Newton, 2000, see Mora et al., 2004 for review).

For atypical PKC the mechanism of priming phosphorylation of the turn motif has not been well described, but it may be reasonable to extrapolate from our more extensive knowledge of other PKC family members. Phosphorylation at the C-terminus depends on the activity of the mammalian target of rapamycin 2 complex (mTORC2), a complex of mTOR, mLST8, rictor, proctor and sin1 (Facchinetti et al., 2008, Ikenoue et al., 2008, Cameron et al., 2011). For aPKC priming a recent study has speculated that all the mTORC2 subunits except rictor are dispensable for priming phosphorylation. Presumably the adaptor protein rictor would mediate an interaction between aPKC and an as yet unknown kinase (Zhang et al., 2010). In vitro the carboxyl terminal sites are efficiently autophosphorylated (Behn-Krappa and Newton, 1999). The recent finding in cells that priming phosphorylations at the C-terminal sites are dependent on nucleotide occupation of the kinase rather than catalytic activity would suggest that autophosphorylation of PKC is not what determines priming phosphorylations in vivo (Cameron et al., 2009). The steady state levels of the priming phosphorylation is also determined by agonist dependent dephosphorylation. Prolonged activation of PKC, that induces an open conformation of the kinase, increases the sensitivity to phosphatases such as PP2A and results in down-regulation of PKC (Hansra et al., 1996, Parker et al., 1995).

1.3.2 AGC/PKC tertiary structure

Eukaryotic protein kinases are dynamic molecules with a diverse array of structures, modes of regulation and substrate specificity but with strict organisation of the internal architecture. The AGC kinases, of which PKCι is a member, have a conserved catalytic structure. They share a bilobal catalytic domain of about 250 residues. The smaller N-

lobe is dominated by a five-stranded β-sheet, which is coupled to a helical sub-domain that typically consists of the C-helix. The large C-lobe contains mostly α-helices plus a β sheet. The helices provide a stable core and substrate tethering sites whereas the β sheet contains most of the catalytic machinery. There are a number of important structural elements to a kinase identified from the sequence and main chain geometry (see Table 1.2).

Utilising an analysis technique called Local spatial pattern (LSP) alignment new structure modules have been identified that coordinate kinase function. LSP considers residues within the crystal structure as an individual vector arrayed in space. As such, conserved residues may be identified independently of their sequence or main chain geometry. In this way, strands of conserved spatial position residues that span both N- and C-lobes of the kinase were seen to align and were termed the regulatory (R) spine and the catalytic (C) spine. The R-spine includes a C-helix Leu, an activation loop Phe (from DFG) and Tyr (from the H/YRD motif) in the catalytic loop. In addition to the role of DFG in coordinating the Mg^{2+} ion, the aligned Phe and Tyr stabilise the active conformation. The C-spine contains an Ala (from AxK), the adenosine ring from ATP and a β7 Leu. The Leu is flanked by two further Leucines that provide a hydrophobic contact with a short D helix that in turn contacts the F-helix, a highly hydrophobic region that is integral to the organisation of the kinase core. The D-helix therefore has an important function in contributing to the positioning of ATP with respect to the rigid hydrophobic core. This LSP form of analysis has uncovered a previously unrealised and critical role of the D-Helix, has highlighted the importance of the activation loop Phe and focused attention on the newly defined regulatory and catalytic spines (Taylor and Kornev, 2011).

Table 1.2 Common conserved features of AGC kinases
Summarised from reviews by (Taylor and Kornev, 2011) and (Pearce et al., 2010).

Motif	Function	Lobe of Kinase
Activation loop	Contains catalytic elements such as DFG. Upon phosphorylation there is a conformational change which then allows coordination of hydrogen bonds between Glu and the C-Helix, Lys on the N-lobe and phosphates on ATP.	C-lobe
C-terminal tail	Wraps around both lobes and contains elements essential for catalysis. 1) completes the ATP binding pocket, 2) glycine rich loop positioned for catalysis and 3) docking of hydrophobic motif into the N-lobe stabilizes the C-helix. 4) C-terminal phosphorylation sites are embedded in the tail.	C-lobe
F-Helix	Highly hydrophobic and is a rigid core around which the kinase domain is organised.	C-lobe
GHI domain	Segment that includes the G, H and I helices. Substrate, regulator and allosteric binding, stabilises kinase	C-lobe
DFG	Aspartic acid residue in the activation segment that binds the Mg2+ ions that coordinate the β and γ phosphates of ATP in the binding cleft	C-lobe
H/YRD	Aspartic acid functions as a base acceptor to achieve proton transfer. The Tyr aligns with the Phe from the DFG and Leu in the C-Helix to coordinate the N & C lobes poised for catalysis.	C-lobe
P+1 loop	This provides a docking site for the P+1 residue of the peptide substrate.	C-lobe
APE	Site of anchorage for the GHI domain to the activation loop. Demarcates the end of the activation loop.	C-lobe
AxK	Lysine residue interacts with α and β phosphates of ATP to anchor to the C-Helix and orientates ATP.	N-lobe
Glycine rich loop	GxGxxG/A. The loop folds over the nucleotide and positions the γ-phosphate of ATP for catalysis. Makes a hydrophobic contact to the base (purine moiety) of ATP.	N-lobe
P-Loop	GxxxxGKT/S. Anchors nucleotide bound phosphates and binds to the γ-phosphate.	N-lobe
C-Helix	Dynamic regulatory element. Important position between the 2 lobes. N-terminus interfaces with the activation loop and its positioning is critical for catalysis.	N-lobe

Two groups have published the coordinates of PKCι in the Apo form, ATP bound and BIM1 bound determined to 2.1 Å, 2.0Å and 3.0Å respectively (Takimura et al., 2010, Messerschmidt et al., 2005). Overall the ATP bound form was almost identical to the BIM1 complex in these structures. PKCι displays most of the characteristics of the AGC kinases but there are a number of notable features elicited in these PKCι structures. The glycine rich loop (GXGXXA) is unusual in that it has an alanine in the last position rather than the typical glycine of other AGC family members. It forms a fixed and intermediate open conformation that could be because of the 'fixed' alanine or due to the presence of a tyrosine in the loop. The catalytically important residues are all conserved as is the geometry of the priming phosphorylations at Thr403 and Thr555. The substitution of the glutamate residue at the hydrophobic motif does not impact on its spatial positioning compared to other AGC kinases. Interestingly, the side chain of Phe543 protrudes into the ATP binding pocket and interacts with the adenine moiety of ATP. Finally the B-helix in the N-lobe, unlike the well-formed B-helices in other AGC kinase structures, is partially unfolded and not helical in the PKCι structures (Messerschmidt et al., 2005, Takimura et al., 2010).

1.3.3 Regulators and Effectors of aPKC

1.3.3.1 Introduction

aPKC is influenced by and regulates a vast array of intracellular signalling pathways and these differ depending on cellular context. Regulation has been reported following aPKC manipulation at multiple levels of the signalling cascade that can be broadly grouped as stimuli and receptors, transducers, amplifiers and metabolites (see section 1.2.1). A schematic overview of oncogenic aPKC signalling is depicted in Figure 1.3.

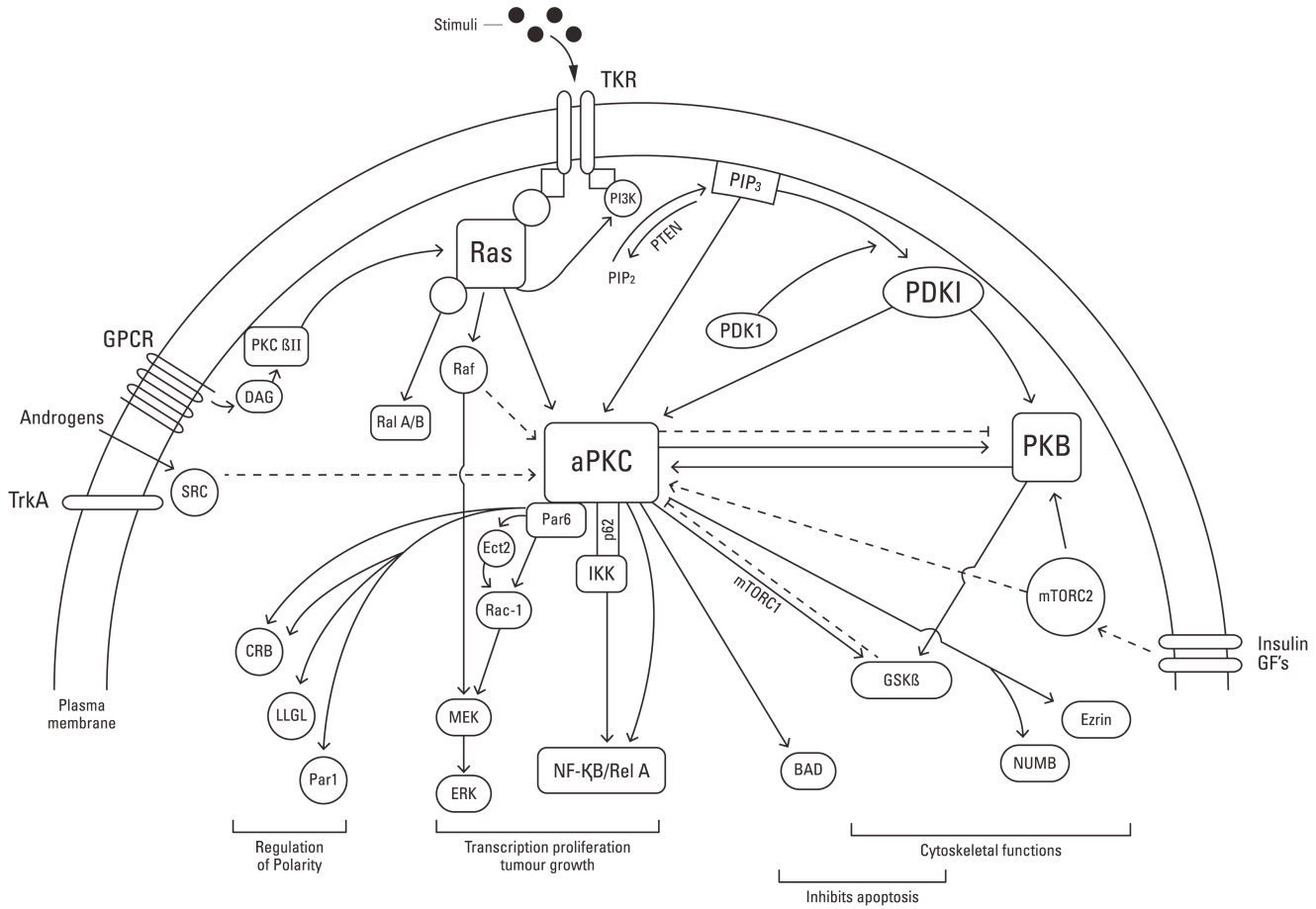

Figure 1.3 Schematic overview of oncogenic aPKC signalling
Atypical PKCs are involved in several major signalling pathways implicated in cancer. The dotted lines represent weaker level of evidence (see section 1.3.3 for details)

1.3.3.2 Stimuli and Receptors

The first growth factors recognised to modulate aPKC in cells were EGF and PDGF. Phosphorylation and re-localisation of aPKC in Cos cells occurred in response to this growth factor stimulation in a phosphoinositol-3-kinase (PI3K) dependent manner (Akimoto et al., 1996). Subsequently, aPKC was demonstrated to be involved in the signalling downstream of at least two members of the Epidermal growth factor receptor family – EGFR (ErbB1) and Her2 (ErbB2). The four members of this family, that also includes ErbB3 and ErbB4, are a group of transmembrane tyrosine kinase receptors that homo- or heterodimerise in response to ligand binding. Epidermal growth factor (EGF), the ligand for EGFR, promotes chemotaxis in A549 and MDA-MB-231 cells and this can be reduced by PKCζ siRNA knockdown or chemical inhibition (Sun et al., 2005, Liu et al., 2008). ErbB2 forced dimerisation has been shown to disrupt polarity in an aPKC dependent manner. This was demonstrated in 3D cultures of MCF10a cells by reversing ErbB2 driven hyperproliferation, loss of apoptosis and disruption of apical-basal polarity with a Par6 mutant that was unable to bind to aPKC (Aranda et al., 2006). Several other studies have implicated PDGF as an activator of aPKC. The immunocomplex activity of PKCζ from COS-1 cells is enhanced following PDGF treatment and the PDGF induced proliferation of fibroblasts was inhibited by expression of a dominant negative kinase dead mutant of PKCζ (Doornbos et al., 1999, Diaz-Meco et al., 1994).

The regulation of aPKCs may also be influenced by external triggers. Nerve growth factor (NGF), that induces differentiation of PC12 cells via the TrkA neurotrophin receptor family, has been shown to induce tyrosine phosphorylation of PKCι in a Src dependent manner (Wooten et al., 2001). In an androgen starved prostate cell line, LNCaP, addition of a synthetic androgen leads to increased phosphorylation of aPKC (T403/410) in a mechanism that seems to be downstream of c-Src activation (Kobayashi et al., 2010). Agonists such as nicotine and glucose also regulate aPKC but the mechanisms for this remain unclear (Xu and Deng, 2006, Bandyopadhyay et al., 2001, Chuang et al., 2003).

1.3.3.3 Signal transducers and amplifiers in aPKC signalling

Ras

Ras was shown to co-immunoprecipitate with aPKC and bind directly to the regulatory domain of PKCζ by the Moscat Laboratory in 1994 (Diaz-Meco et al., 1994). Bjorkoy et al showed that constitutive activation of ERK1/2 and Elk1 in response to oncogenic Ras could be reversed by transfecting a dominant negative PKCλ construct (Bjorkoy et al., 1997). The morphological changes of H-Ras expressing NIH3T3 cells, that include dissolution of actin stress fibres, were blocked by dominant negative mutants, RNAi and a chemical inhibitor against aPKC (Uberall et al., 1999). Similarly the inhibition of differentiation of mouse skeletal muscle cells induced by expression of oncogenic H-Ras were overcome with a dominant negative PKCι/λ construct or Gö6983, the pan-PKC inhibitor (Fedorov et al., 2002). Furthermore, exogenous expression of Ras and PKCι in an ovarian cancer cell line has been shown to be synergistic for the size and number of colonies in a soft agar assay (Zhang et al., 2006a). Seemingly, PKCι can interact with Ras in multiple cellular contexts and the Ras associated phenotypes are PKCι dependent.

The significance of PKCι, downstream of oncogenic Ras, has also been born out of murine models. Expression of a dominant negative PKCι in A549 cells, known to harbour a K-ras mutation, resulted in reduced xenograft tumour formation in nude mice (Regala et al., 2005a). In an orthotopic model of pancreatic cancer, using a K-Ras mutant cell line, RNAi induced knockdown of PKCι led to decreased tumour burden, decreased markers of angiogenesis and fewer distant metastases (Scotti et al., 2010). Transgenic mice that contain a latent oncogenic K-ras allele that is activated by spontaneous recombination developed aberrant crypt foci (ACF) of the intestine. ACFs are likely precursors to colon cancer in mice and humans (Takayama et al., 1998) and their frequency is predictive of colon tumour formation in rodents (Magnuson et al., 1993). Bi-transgenic mice that express the latent oncogenic K-Ras and kinase dead PKCι developed fewer ACFs than K-Ras mice (Murray et al., 2004).

Transgenic mice that expressed oncogenic K-Ras after Cre-mediated recombination developed lung tumours following intra-tracheal Cre-administration. Bitransgenic mice that simultaneously expressed oncogenic K-Ras but lost PKCι expression upon Cre-delivery had significantly reduced tumour burden (Regala et al., 2009). Similarly, mice expressing oncogenic K-Ras but knock out for p62, an adapter protein that binds to aPKC, also has a reduced lung tumour formation (Duran et al., 2008). On the other hand, PKCζ would appear to negatively regulate Ras induced tumourigenesis of the lung in a bi-transgenic mouse model (Galvez et al., 2009).

SRC

Src is the prototype of the Src family of non-receptor tyrosine kinases that have dual adaptor and kinase functions. It forms an immunocomplex with PKCι and the TrkA neurotrophic receptor and this interaction is enhanced by NGF stimulation of PC12 cells. The SH3 binding domain of Src binds to the proline rich motif in PKCι (aa98-114). Sites of Src dependent PKCι tyrosine phosphorylation were identified from kinase assays performed on a PKCι peptide array (Y256, Y271 & Y325) and the functional significance was confirmed using the non-phosphorylatable mutants (Tyr>Phe) (Wooten et al., 2001). Tyrosine phosphorylation of aPKC by Src has been shown to be required for an association with Rab2, a small GTPase necessary for endocytic transport, and could be inhibited by the Src kinase inhibitor-PP2 (Tisdale and Artalejo, 2006). Several reports have suggested that aPKC is required for Src mediated transformation. Knockdown or inhibition of c-Src led to decreased aPKC activation loop phosphorylation in a Rac1 dependant manner and reduced proliferation in androgen dependent prostate cancer cells (Kobayashi et al., 2010). Additionally, perturbation of aPKC by dominant negative constructs or RNAi, decreased invasion, 2D cell polarity and matrix degradation in v-Src transformed NIH3T3 cells (Rodriguez et al., 2009).

Raf

PKCζ was reported to phosphorylate and activate Raf-1 (van Dijk et al., 1997). In COS cells, PKCζ was reported to immunoprecipitate with Raf-1 and this interaction was enhanced by co-transfection of 14.3.3 isoforms, and was weaker for wild type PKCζ constructs than kinase dead constructs. These data would suggest that PKCζ, Raf-1 and 14.3.3 form a ternary complex that is phosphorylation dependent (Van Der Hoeven et al., 2000). In the 10 years since this work, however, no group has published on the signalling or functional relevance of this interaction.

PKCβII

Over-expression of PKCβII induced an invasive phenotype in rat intestinal epithelial cells (RIE) in a PKCι dependent manner. Using small G-protein GTP assays transfection of PKCβII was shown to increase both Ras and Rac1 activities but not RhoA. Inhibition of PKCβ by LY379196 reduced invasion that could be overcome by expression of constitutively active Rac1 suggesting that the Ras effector Rac1 is downstream of PKCβII (Zhang et al., 2004). Taken together with the results discussed in the Ras section above, these data would be consistent with a model whereby PKCβII induces invasion in RIE cells through activation of a PKCβII>Ras>PKCι/Rac1 signalling axis.

PKB

PKCζ was reported to co-immunoprecipitate with PKB in COS cells and this interaction was mediated by the pleckstrin homology domain of PKB (Doornbos et al., 1999, Mao et al., 2000). PDGF induced activation of PKB was negatively influenced by PKCζ as defined by immunocomplex kinase assays, phosphorylation at its Ser473

site and lack of substrate phosphorylation (GSK3). Further evidence that PKCζ acts at the same level (or downstream) of the signalling pathways comes from the observation that it is still able to inhibit a constitutively active form of PKB whose activity is independent of its upstream kinase PI3K (Doornbos et al., 1999). Contrary to these results, more recent studies have suggested that PKCζ is able to activate PKB. Recombinant PKCζ has been shown to directly phosphorylate PKB at 3 separate sites; Ser124, Ser473 and Thr308 with a 3:1:1 stoichiometry. Knockdown of PKCζ in embryonic fibroblasts significantly reduces phosphorylation of Ser473 and Thr308, the principal priming sites of PKB (Joshi et al., 2008, Cantley, 2002). Knockdown of Rictor, a component of TORC2 that regulates PKB Ser473 phosphorylation, prevents Ser473 phosphorylation. One interpretation of these data is that PKCζ principally phosphorylates PKB at Ser124 which in turn modulates TORC2 regulation of PKB Ser473 and PDK1 regulation of Thr308 (Joshi et al., 2008). Alternatively Rictor may be a necessary adaptor protein for aPKC dependent phosphorylation in vivo.

PI3K

Over-expression of one of the catalytic subunits of PI3K, p110α, increased PKCι/λ phosphorylation and increased PKCι/λ dependent transcriptional activity in a luciferase reporter assay in response to PDGF and EGF. A dominant negative PI3K construct had the opposite effect (Akimoto et al., 1996). The PI3K lipid metabolite, PIP_3, was shown to promote in vitro activation of aPKC, potentially by direct binding to the cysteine rich sequence and resulting release of pseudosubstrate autoinhibition or indirectly via PDK1 (Standaert et al., 2001). However, the role of PI3K in the activation of aPKC is likely to be via PDK1 as in vitro studies have shown PIP_2 to be equally as effective as PIP_3 at activating aPKC (Palmer et al., 1995). Chemical inhibition of PI3K by LY294002 decreased PKCι phosphorylation in glioma cells (Baldwin et al., 2008) and lung cancer cells (Liu et al., 2008). Over-expression of wild type PTEN, a lipid phosphatase that promotes the conversion of PIP_3 to PIP_2, in the glioma cells also resulted in decreased PKCι phosphorylation (Baldwin et al., 2008). PDK1 binds to PIP_3 causing co-location with target kinases also on membranes; for aPKC this enables efficient phosphorylation

of the Threonine in the activation loop (Le Good et al., 1998, Balendran et al., 2000). Knockdown of PDK1 by siRNA inhibited priming phosphorylation of PKCι (Thr555) and reduced expression levels in glioma cells (Desai et al., 2011). Increased PDK1 mRNA expression was commonly indentified in epithelial malignancies such as breast cancer, and while not oncogenic it dramatically enhanced the ability of upstream oncogenic lesions, such as ErbB2, to form tumours (Maurer et al., 2009).

1.3.3.4 Other lipid metabolites

The sphingolipid ceramide has been implicated in the regulation of aPKC. Ceramide activates both recombinant and HEK293 cell endogenous aPKC. In response to insulin ceramide promotes phosphorylation of the JNK pathway. (Bourbon et al., 2000). Using lipid vesicle-mediated affinity chromatography ceramide was demonstrated to bind to PKCζ. Low concentrations of ceramide were observed to stimulate PKCζ activity but high concentrations were inhibitory both in vivo and in vitro (Wang et al., 1999). In primitive ectoderm cells that form a central cavitation, pharmacological inhibition of ceramide resulted in aPKC mislocalisation, impaired ectoderm morphology and increased central apoptosis (Krishnamurthy et al., 2007). A further lipid that was found to associate with PKCζ is Phosphatidic acid (PA), a diacylglycerol (DAG) metabolite. PA caused autophosphorylation of PKCζ immunocomplexes and a mobility band shift consistent with a PKCζ-PA complex (Limatola et al., 1994)). Despite an appreciable time lapse since some of these reports, publication of corroborative studies are still outstanding.

1.3.3.5 Protein-Protein Interactions

aPKC is comprised of modular protein-protein interaction domains that allow multiple interactions that both regulate aPKC function and couple it to various signalling pathways. aPKCs are the only PKC isoforms to have PB1 domains which allow

interaction with other PB1 domain containing proteins including Par6 (see section 1.3.5), ZIP/p62 and Mek5.

In a yeast-two-Hybrid screen PKCζ was found to bind to an adaptor protein termed zeta interacting protein (ZIP/p62) (Puls et al., 1997, Sanchez et al., 1998). ZIP/p62 binds to PKCζ via the PB1 domain and links upstream transduction to NF-κB (transcription factor) signalling via aPKC. Disruption of the p62-PKCζ interaction by ursolic acid suppressed NF-κB activity and resulted in down-regulation of MMP-9 protein and decreased TNF-α induced glioma cell invasion (Huang et al., 2008). P62 is up-regulated in a transcription dependent manner by Ras and is required for lung tumourigenesis in a Ras dependent lung cancer mouse model (Duran et al., 2008). P62 has also been shown to be required for IKK activation (Duran et al., 2004, Martin et al., 2006). MEK5 and aPKCs formed a complex upon EGF stimulation and have been implicated in proliferation and anti-apoptotic signalling through the NF-κB pathway (Diaz-Meco and Moscat, 2001).

The cysteine rich region of aPKC (C1-related domain) binds to prostate androgen response-4 (PAR-4) and Lambda interacting protein (LIP). PAR-4 was originally identified as an apoptotic gene in prostate cancer and is distinct from the partitioning defective 4 gene (Par4) identified in *C.Elegans* as a polarity regulator (Diaz-Meco et al., 1996). PAR-4 interacts with and inhibits PKCζ in vitro and in vivo. Tissue of PAR-4 null mice demonstrated increased levels of activated aPKC, PKB and NF-κB. Increased catalytic activity of aPKC was present in immunocomplex kinase assays from lung extracts (Joshi et al., 2008). The interaction of PAR-4 with PKCζ in immunocomplexes was reported to be mediated by ceramide. In the absence of PAR-4 ceramide activated PKCζ but in the presence of PAR-4 ceramide led to decreased PKCζ activity and reduced NF-κB transcription (Wang et al., 2008a).

Mouse models have demonstrated that PAR-4 knockout results in susceptibility to malignancy. Female mice demonstrated a preponderance for endometrial adenomas and male mice showed prostate hyperplasia (Moreno-Bueno et al., 2007, Garcia-Cao et al., 2005). Bi-transgenic mice expressing a conditional Ras oncogene and knockout for PAR-4 have a higher lung tumour grade and burden than single transgenic Ras mice

(Joshi et al., 2008). There are also examples of human malignancy where PAR-4 expression is reduced including lung adenocarcinoma and prostate carcinoma (Joshi et al., 2008, Galvez et al., 2009).

Over-expression studies in cell lines show that PAR-4 inhibition of serum induced PKB Ser473 phosphorylation could be overcome by forced over-expression of PKCζ. Taken together the results could suggest that PAR-4 negatively regulates PKCζ and that is then unable to potentiate activation of PKB (Joshi et al., 2008). These results do not exclude the possibility that PAR-4 can also directly inhibit PKB and that the affect of PKCζ is the sequestration of PAR-4 thus releasing its inhibition of PKB .

LIP binds to the cysteine rich region of PKCλ/ι but not that of PKCζ. It was shown to activate PKCλ/ι both in vivo and in vitro but has subsequently been identified as the C-terminus of Serine/threonine-protein kinase 1 (SMG1). The function of the full length SMG1 has not been assessed in relation to aPKC and is otherwise thought to be involved in nonsense-mediated mRNA decay (Diaz-Meco et al., 1996, Yamashita et al., 2001).

1.3.4 Downstream Effectors of aPKC

Rho Family Members

Rac 1 and Cdc42 are functionally similar Rho-GTPases but have distinct functions (Qiu et al., 1995). Both proteins play important roles downsteam of PKCι in cytoskeletal remodelling. Levels of activated Rac1-GTP were suppressed in A549 cells expressing the dominant negative PKCι (PKCι-K274W) construct or when treated with the aPKC pseudosubstrate inhibitor (Regala et al., 2005a). Over-expression of PKCι-K274W in A549 cells resulted in decreased non-adherent cell growth and tumourigenesis in nude mice but both of these phenotypes were recovered by co-expression of a constitutively active Rac-1 allele indicating that Rac1 may be required for PKCι dependent transformation. Rac1 is thought to regulate a p21 activating kinase (PAK) that in turn phosphorylates MEK1/2. Expression PKCι-K274W in A549 cells also led to reduced

phosphorylation of the downstream effectors of the ERK pathway – MEK1/2 at both the Raf and PAK phosphorylation sites and the canonical sites on ERK1/2. This was rescued by activated Rac1 expression (Regala et al., 2005b). Together this data supports a role for an aPKC>Rac1>PAK1>MEK1/2>ERK1/2 signalling axis that plays a role in non-adherent growth and tumourigenesis.

Ect2 is a Rho-GTPase nucleotide exchange factor. It is located on chromosome 3q26, the same region as PKCι that is commonly overexpressed in squamous cell carcinoma (Yang et al., 2008). Both Ect2 and PKCι genes were identified to be the drivers of amplicons on chromosome 3q (Haverty et al., 2009). Ect2 is thought to play a role in cytokinesis and has recently been identified, via co-immunoprecipitation with PKCι-Par6 followed by mass spectrometry, as a PKCι substrate. PKCι phosphorylated Ect2 at Thr328 in vitro and siRNA knockdown of PKCι (or Par6) led to decreased phosphorylation of Ect2 and decreased activity of Rac1 (Justilien et al., 2010). Ect2 RNAi decreased non-adherent lung cancer cell growth (H1703 cell line) and this could be rescued by WT Ect2 but not a phosphorylation deficient mutant. Ect2 has been reported to be over-expressed at a protein level in lung cancer (Justilien and Fields, 2009). In summary Ect2 is a recently identified human oncogene that requires phosphorylation by PKCι for its transformed behaviour. It should be noted however that the sequence flanking Thr328 is a very unusual aPKC substrate site.

Transcription Regulation

A number of transcriptional targets have been cited as being downstream of aPKC. One of the most extensively studied pathways is that involving NF-κB, a transcription factor that is activated by numerous stimuli and is involved in the regulation of processes such as immune response, cell survival and angiogenesis (Kisseleva et al., 2006). There are three main families of proteins that comprise the NF-κB signalling pathway; NF-κB, inhibitor of NF-κB (IκB) and inhibitor of NF-κB kinase (IKK). NF-κB is comprised of 5 family members that form homo or heterodimers and include RelA (p65), RelB, c-Rel, NF-κB1 (p50) and NF-κB2 (p52). NF-κB dimers are retained in the cytoplasm by

IκB but upon pathway activation IKK phosphorylates IκB and targets it for ubiquination and proteasomal degradation. This releases NF-κB to translocate to the nucleus and affect transcription (Karin, 1999).

Perturbation of PKCι or PKCζ via pseudosubstrate inhibitors, antisense oligonucleotides or transfection with kinase dead mutants all impair NF-κB activation (Dominguez et al., 1993, Diaz-Meco et al., 1996). PKCζ has been reported to regulate at least two different parts of the NF-κB pathway. In mouse embryonic fibroblasts PKCζ phosphorylated NF-κB (RelA) at Ser311 and established a complex with CBP, a coactivator necessary for transcription (Duran et al., 2003). Additionally PKCζ interacted with and phosphorylated IKK in TNF-α stimulated HEK293 cells. Recombinant protein studies suggest that this interaction could be direct and identified the PKCζ substrate sites on IKKβ as Ser177 and Ser181 (Lallena et al., 1999). PKCι phosphorylated and activated IKK in TNF-α treated prostate carcinoma cells but not in a TNFα treated non-transformed prostate cell line possibly suggesting specificity towards transformed cells (Win and Acevedo-Duncan, 2008).

NF-κB has also been implicated as mediating PKCι dependent chemoresistance. Antisense expression of PKCι decreased NF-κB (RelA) transcriptional activity and sensitised a chronic myelogenous leukaemia cell line to paclitaxel induced apoptosis (Murray and Fields, 1997).

One of the targets of NF-κB signalling is IL-6, a cytokine involved in immune and haematological function. The IL-6 promoter contains recognition sites for both NF-κB and a second transcription factor AP-1. In hormone refractory prostate cancer high levels of AP-1, NF-κB and consequently IL-6 levels were seen and could be reduced following PKCι RNAi (Ishiguro et al., 2009). PKCζ has been shown to repress histone acetylation of the IL-6 promoter resulting in lower levels of the cytokine (Galvez et al., 2009). Seemingly therefore, aPKC can both enhance and repress IL-6 production via different pathways.

Transcription of MMP10, a matrix metalloproteinase, in lung tumours from K-Ras over-expressing transgenic mice was elevated upon Cre induction. The increase in

MMP10 mRNA upon Cre induction was negated in a bi-transgenic mouse with concomitant PKCι knockout (Frederick et al., 2008, Regala et al., 2009). Studies in human lung tumours with Ras mutations have not corroborated the finding of elevated MMP10 mRNA or protein (Zhang et al., 2007). Using a bioinformatics approach employing 3 separate publicly available gene expression data sets, the Fields laboratory indentified 4 functionally distinct genes that were co-ordinately expressed with PKCι in lung adenocarcinoma. Knockdown of PKCι reduced transcription of all four genes (COPB2, ELF3, RFC4, PLS1). Knock down of each of the four genes phenocopied the PKCι knockdown exhibiting a reduction in non-adherent cell growth (Erdogan et al., 2009).

mTOR/P70S6Kinase

P70S6 kinase is a ribosomal S6 protein kinase that upon phosphorylation and activation in turn phosphorylates the S6 component of the 40S ribosome subunit and leads to increased protein synthesis. mTORC1 is the best described activator of p70S6K but there are multiple others that are less well defined, for example aPKC. PKCλ was found to directly associate with p70S6K and dominant negative kinase deficient PKCλ mutants suppress serum activation of p70S6K (Akimoto et al., 1998). Inhibition of aPKC using a myristolated pseudosubstrate (PS) peptide suppressed androgen induced phosphorylation of p70S6K. Phosphorylation of both aPKC and p70S6K proteins were correlated in human prostate tissue microarrays (Inoue et al., 2006). In a follicular lymphoma cell line an anti-CD20 antibody, a B-cell surface antigen of uncertain role, decreased aPKC and p70S6K phosphorylation and reduced aPKC activity in an immunocomplex kinase assay. The same results were attained with the aPKC PS inhibitor and an aPKC kinase dead construct and the anti-CD20 antibody treatment affects could be overcome by a constitutively active aPKC construct (Leseux et al., 2008). These results suggest that p70S6K may be a down stream effector of aPKC in multiple cellular contexts.

Apoptosis pathways

It has recently been demonstrated that aPKC can inactivate the apoptotic machinery through its kinase activity. In glioma cells PKCι formed immunocomplexes with BAD (BCL2-associated agonist of cell death) and phosphorylated it at 3 distinct sites (Ser112, Ser136 and Ser155). Usually BAD promotes apoptosis by binding to Bcl-X_L. Phosphorylation of BAD immunocomplexes by purified PKCι led to BAD/Bcl-X_L dissociation and promoted the inactive BAD/14.3.3 association. The phosphorylation of BAD by PKCι was shown to be direct in recombinant protein kinase assays. In cells, aPKC was seen to co-localise with BAD and knockdown of PKCι led to increased apoptosis (Desai et al., 2011).

Morphological pathways

aPKC/Par6 inactivated GSK3β by phosphorylation at Ser9 and prevented GSK3β driven apoptosis (Kim et al., 2007). Expression of a non-aPKC binding mutant of Par6 in MDCK cells led to decreased GSK3β phosphorylation, increased JNK activation and increased apoptosis. In Rat astrocytes exogenous PKCζ phosphorylated and dissociated from GSK3β. This process was shown to be vital for directed migration (see section 1.3.6). Intriguingly GSK3β has recently been shown, in a *D.melanogaster* epidermis model, to directly phosphorylate aPKC leading to its ubiquitin mediated proteosomal degradation (Colosimo et al., 2010).

Ezrin is a cytosolic protein that upon phosphorylation of Thr567 becomes localised under the cell membrane where it connects actin filaments to membrane proteins (Wald et al., 2008). Ezrin is phosphorylated at the Thr567 by several kinases including members of the PKC family (Ng et al., 2001, Ren et al., 2009, Wald et al., 2008). Treatment of an osteosarcoma cell line, K7M2, with Gö6976 (a classical PKC inhibitor) decreased migration and invasion which could be rescued by expression of a constitutively activate Ezrin construct, demonstrating that Ezrin is downstream of PKC

in the signalling cascade (Ren et al., 2009). In differentiating mouse intestinal crypts, a temporospatial model, activated PKCι and Ezrin were co-localised apically. In Caco2 cells PKCι knockdown led to mislocalisation and decreased phosphorylation of Ezrin (Wald et al., 2008). Recently LGN (named after ten Leucine-Glycine-Asparagine tripeptides in its N-terminal region), a protein involved in spindle orientation during mitosis, was shown to be phosphorylated by aPKC (for more details see section 1.3.7).

Numb is an evolutionary conserved signalling adapter that was originally identified in Drosophila as a protein involved in asymmetrical cell division and was therefore a cell fate determinant (Uemura et al., 1989). It is therefore considered in this cytoskeletal section although it has a complex pattern of functions, probably due to its diverse isoforms and heterogeneity of interacting proteins (see (Gulino et al., 2010) for review). It contains a phosphotyrosine binding region and a proline rich region. Numb was found to bind to aPKC and Par3 in HeLa cell immune complexes. It was phosphorylated by aPKC at Ser7, Ser265 and Ser284. Truncation mutants have revealed that Numb binds within the C-terminal coiled-coil region of Par3 (aa937-1038) (Nishimura and Kaibuchi, 2007). Src activation or HGF treatment led to increased interaction of Numb with aPKC and Par6 but decreased interaction with Par3 and E-cadherin. This led to disrupted cell-cell adhesion and is proposed to contribute to Src dependent epithelial to mesenchymal transition (EMT) (Wang et al., 2009, Nishimura and Kaibuchi, 2007). In addition to its roles in cell fate determination and cell adhesion Numb is involved in integrin endocytosis (Hutterer et al., 2004) and directed cell migration (see section 1.3.6).

Others

Finally, other proposed downstream substrates of aPKC for which the mechanisms are less well described include S-phase kinase associated protein (SKP2) (Liu et al., 2011), hASIP (Jin et al., 2008), cdk7 (Win and Acevedo-Duncan, 2009, Acevedo-Duncan et al., 2002) and the heat shock protein, HSP70B (Boellmann and Thomas, 2010).

1.3.5 Apical-Basal Polarity

One of the major functions of aPKC is the regulation of polarity. Deregulation of polarity proteins often causes a more invasive phenotype in malignant tumours (Igaki et al., 2006, Bilder, 2004). Loss of the apical-basal polarity in epithelial cells is one of the hallmarks of aggressive and invasive cancers (Thiery, 2002). Cellular polarity refers to the restricted pattern of cellular components to regions of the cell. Polarity is essential for a range of normal cellular functions including asymmetric cell division, maintenance of epithelial integrity and cell migration. The core polarity machinery seems to be well conserved between cell types and is comprised of a number of protein complexes. In epithelial cells there are three major complexes – Par, Crumbs and Scribble. aPKC interacts with and/or phosphorylates each of these complexes and in doing so specifies their cellular localisation. This section will introduce the architecture of a polarised epithelial cell, discuss the polarity machinery, the antagonistic interactions between complexes and potential polarity cues.

1.3.5.1 Polarised structure of mammalian epithelial cells

Mammalian epithelia, such as Mardin Darby canine kidney (MDCK) cells are characterised by three different polarised domains; apical, lateral and basal (St Johnston and Ahringer, 2010). The apical domain is made up of the brush border of microvilli beneath which lie actin and spectrin filaments. These filaments are linked to the plasma membrane by ezrin, moesin and radixin (ERM family proteins). The apical and lateral membranes are separated by tight junctions (Tepass et al., 1990). Tight junctions contain a number of homotypic adhesion molecules such as junctional adhesion molecules (JAMs), Claudin, Occludin and Tricellium. These adhesion molecules associate with the MAGUK (membrane associated guanylate kinase like homology) proteins, ZO-1 and ZO-2, which are able to interact with the cytoplasmic tails of Claudin and Occludin via their N-terminal PDZ domains (Tsukita et al., 2001). It was thought that tight junctions formed a physical barrier to the diffusion of cellular proteins. This model has been challenged by the finding that knockdown of MAGUKs does not effect the polarised membrane protein distribution despite a loss of tight

junctions and altered transepithelial resistance. Based on the evidence from the MAGUK knockout mouse, which are embryonic lethal, tight junctions would be predicted to play a fundamental cellular role. Whether this includes the initiation or maintenance of polarity remains to be seen (see Tsukita et al., 2008 for review).

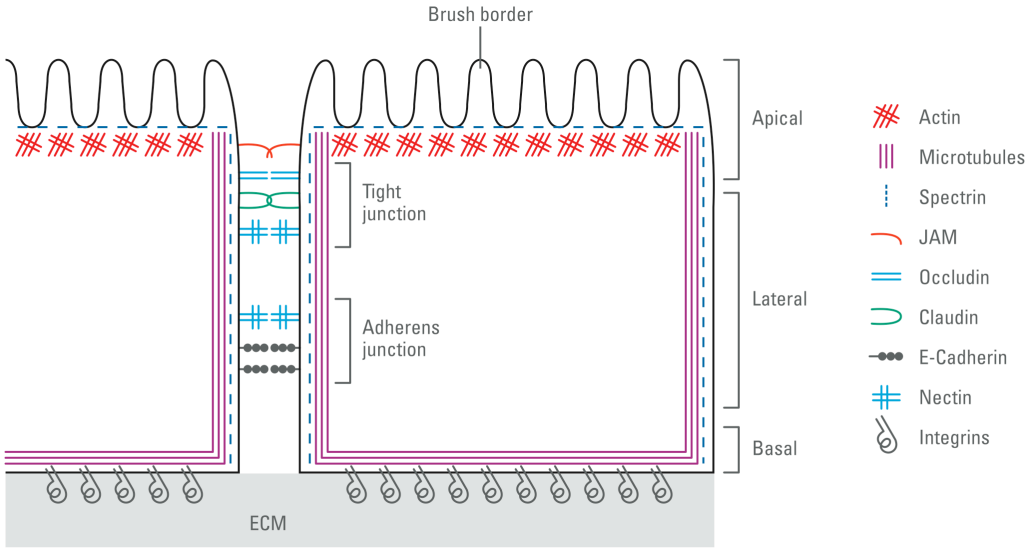

Figure 1.4 Architecture of a mammalian epithelial cell
Adapted from (St Johnston 2010). Mammalian epithelial cells contain an apical, lateral and basal region. Tight junctions act as the partition between the apical and lateral regions and are comprised of JAM, claudin, occludin and nectin. The lateral adherens junctions contain nectin and E-cadherin. Cytoskeletal proteins surround the cell cortex (see text). Basally located integrins interact with the extracellular matrix (ECM).

Below the tight junctions and located in the lateral domain of the cell, lies the adherens junctions which provide the main mechanical link between adjacent cells. These junctions are characterised by the presence of calcium dependent adhesion molecules, the cadherins, and their adapter proteins beta- and alpha catenin. The cadherin-catenin complex indirectly mediates actin cytoskeleton reorganisation and this process is regulated by both phosphorylation and endocytosis (see Nelson, 2008 for review). Similarly another class of homophilic transmembrane adhesion molecules, the nectins, are found predominantly at the adherens junctions but also play a role in establishing

tight junctions (Fukuhara et al., 2002). At adherens junctions nectins are coupled to the cytoskeleton with the help of the adapter protein Afadin/AF-6 (Takai et al., 2008).

The basal domain of the cell is the interface between the cell and the extracellular matrix. This region is highly enriched in matrix receptors such as the integrins and dystroglycan and is depleted of intercellular adhesion molecules (St Johnston and Ahringer, 2010).

1.3.5.2 Par Complex

The 'Par complex' is made up of Par3, aPKC, and Par6 proteins (Hung and Kemphues, 1999, Joberty et al., 2000). The respective genes were first identified in an RNAi screen of defective cell partitioning in *C.elegans* embryos (Tabuse et al., 1998, Watts et al., 1996). These 3 genes are highly conserved through metazoan evolution (Izumi et al., 1998). The functional importance is also conserved, for example when Drosophila Par6 was silenced, cells failed to undergo the normal process of asymmetrical division (Petronczki and Knoblich, 2001) and in mammalian cells a dominant negative aPKC construct prevented normal tight junction formation (Suzuki et al., 2001).

aPKC and Par6 form a stable dimer that is capable of interacting with Par3 to form the trimeric complex (Joberty et al., 2000). The interaction between aPKC and Par6 is mediated by their respective PB1 domains (see section 1.2.5) (Hirano et al., 2005). It is proposed that Par6 stabilises aPKC, by preventing proteolytic degradation (Durgan et al., 2011). Additionally some studies, but not all, have suggested that Par6 suppresses the catalytic activity of aPKC (Lin et al., 2000, Qiu et al., 2000). Cdc42, a small Rho GTPase interacted with Par6 via the partial CRIB/PDZ domain of Par6 and caused increased aPKC activity in an immunocomplex kinase assay. These data could be interpreted as Par6 restrains the aPKC kinase domain which is allosterically released upon Cdc42 binding (Lin et al., 2000, Yamanaka et al., 2001).

Par3 interacts directly with the aPKC kinase domain via a 26 amino acid minimal binding region of Par3 (aa816-841) and induces phosphorylation in vivo at Ser827.

Additionally, Par3 interacts with Par6 via their respective PDZ domains completing the trimeric Par complex (Gao et al., 2002)). The Par complex is apically situated and there are a number of features of Par3 that suggest that it is this protein that drives the localisation. Firstly, the N-terminal PDZ of Par3 binds to the c-terminal PDZ binding domains of JAM and nectin, the apical-lateral junction proteins (Ebnet et al., 2001). Secondly, the next PDZ binds to phosphoinositides located in the membrane lipid bilayer (Wu et al., 2007). Thirdly the N-terminal CR1 domain of Par3 homo-oligomerises which assists apical localization in Drosophila and mammals and potentially provides a large scaffold for binding (Benton and St Johnston, 2003, Feng et al., 2007, Mizuno et al., 2003). Fourthly, upon tight junction association Par3 recruits protein phosphatase 1α that protects Par3 from inactivating phosphorylations (Traweger et al., 2008).

When recruited to the apical membrane there is evidence to suggest that Par6-aPKC does not remain associated with Par3 and that aPKC-Par6 is dispensable for tight junction formation. Firstly, in contrast to earlier studies that reported aPKC-Par6 and Par3 co-localisation, (Hirose et al., 2002) recent work has suggested that they are not truly co-localised, in fly and mammals, with the aPKC-Par6 located apical-laterally and Par3 slightly basal to this (Morais-de-Sa et al., 2010). Secondly, aPKC-Par6 dissociates from Par3 following aPKC dependent phosphorylation of mammalian Par3 at Serine 827 and a non-phosphorylation mutation at this site disrupts tight junction formation (Nagai-Tamai et al., 2002). The evidence that tight junction formation may be dispensable for Par6-aPKC came from MDCK lacking endogenous Par3. This caused disrupted (delayed) tight junction formation but was rescued by an exogenous Par3-mutant that was unable to bind to aPKC or Par6. Furthermore, an alternative complex including Par3 and the Rac exchange factor, TIAM1, has been implicated as being required for tight junction formation (Chen and Macara, 2005).

Several recent studies have carefully distinguished between tight junction formation and apical domain formation (Horikoshi et al., 2009, Ishiuchi and Takeichi, 2011). In this respect it has been reported that apical membrane formation requires Par6-aPKC binding to Par3 in a process that also involves trafficking of Par6-aPKC containing vesicle-like structures. Consistent with the work of Chen et al tight junction formation

was independent of Par6-aPKC. How Par3 recruits the Par6-aPKC containing vesicles to an apical region where Par3 is not detected is currently unexplained (Horikoshi et al., 2009). A further study has shown that Willin, a FERM domain protein, can recruit aPKC-Par6 to apical domain sites independently of Par3 (Ishiuchi and Takeichi, 2011). Therefore Par6-aPKC is necessary for apical domain formation and Par3 can direct this localisation but redundant pathways may exist.

Par1, another partition defective protein identified in *C. elegans*, is a posteriorly localised protein kinase that associates with membranes. It is not part of the Par complex but is discussed here as it illustrates well how aPKC is able to spatially restrict polarity proteins (Figure 1.5A). In mammalian cells Par1 is capable of phosphorylating Par3 at S144 and S285 creating binding sites for a stable interaction with 14.3.3 protein (Hurd et al., 2003, Hurov et al., 2004). If left unattended Par1 would result in sequestration of Par3 from the anterior compartment. Par1 that strays into the apical compartment is phosphorylated at Thr585 and translocates from the membrane to the cytosol away from the apical complexes (Hurov et al., 2004). The human pathogen H.pylori CagA abrogates cell polarity by impairing the aPKC induced inactivation of Par1, most likely by steric hindrance (Saadat et al., 2007).

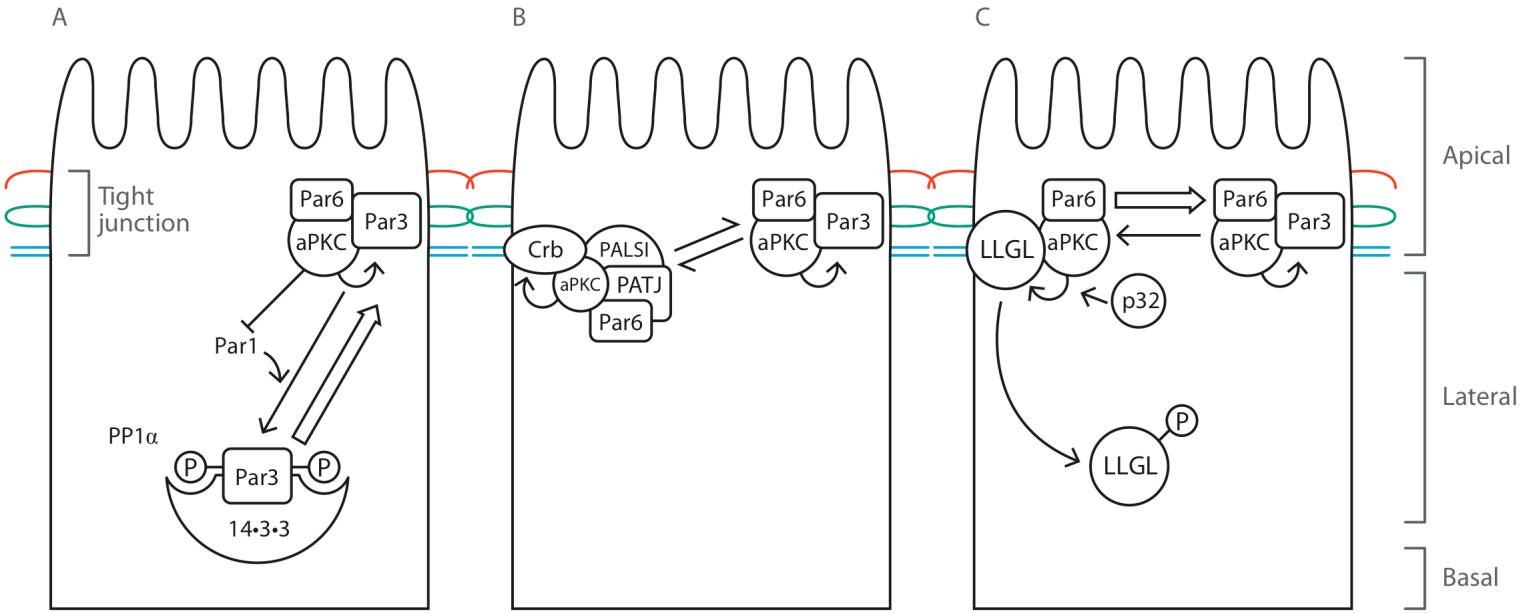

Figure 1.5 Control of polarity complex localisation by aPKC

A, the apical Par3 complex can be disrupted by Par1 phosphorylation of Par3 (see text). This is averted by inhibition of Par1 and stabilisation of membrane associated Par3 by aPKC phosphorylation. Protein phosphatase 1α (PP1α) inhibits Par3 association with 14.3.3. B, The Crb and Par complexes are both apically located and in equilibrium. Changes in the levels of Par3 or Crb would lead to disruption of this balance. C, LLGL forms a basolateral complex. It is capable of interacting with Par6-aPKC but becomes inactivated and dissociates form the membrane upon phosphorylation by aPKC. p32 facilitates aPKC-induced phosphorylation of LLGL. Thick arrows represent the direction of the reaction. Arrows indicate phosphorylation and blunt arrows represent phosphorylation inhibition.

1.3.5.3 Crumbs Complex (Crb)

Closely associated with the Par complex is a second group of apically located proteins called the Crumbs complex (Tepass et al., 1990). The mammalian Crumbs complex contains a transmembrane protein (Crb) and two cytoplasmic scaffolding proteins (PALS1 and PATJ) (Michel et al., 2005). Within a centrally conserved region in the middle of the Crb protein are two functional subdomains; the FERM binding domain (F for 4.1 protein, E for ezrin, R for radixin and M for moesin) that is known to bind proteins or phosphoinositides (Chishti et al., 1998) and the PDZ binding motif. Crb binds to PATJ via the PDZ motif and PATJ interacts with the aPKC-Par6 dimer facilitating, at least in Drosophila, aPKC mediated phosphorylation of the cytoplasmic tail of Crb that is necessary for epithelial cell polarity (Sotillos et al., 2004). These data would suggest that the two apical complexes, Crb and Par, compete for binding of aPKC-Par6 and therefore can negatively regulate the other (Figure 1.5B).

1.3.5.4 Scribble Complex

Scribble, discs large and lethal giant larvae form a group of tumour suppressor proteins known as the scribble complex. They act co-dependently for polarity based on genetic and biochemical studies in Drosohila (Bilder et al., 2000b). Lethal giant larvae has been reported to bind to the LRR region of Scribble but aside from this the physical interactions of the Scribble complex proteins are not well defined (Kallay et al., 2006). In view of the work performed during this thesis the remainder of this section will concentrate on Lethal giant larvae.

<u>Discovery and conservation of LLGL</u>

Drosophila lethal (2) giant larvae (D-Lgl) was the first tumour suppressor gene described in modern scientific literature. In 1933 Bridges identified its chromosome locus (Hadorn, 1938), mutant alleles were generated and studied in the 1970's (Gateff,

1978) and the gene was cloned in 1985 (Mechler et al., 1985). Its descriptive name reflects the phenotype seen in mutant Drosophila larvae. The imaginal disks and brain overgrow and the resultant larvae die before entering metamorphosis. The gene is highly conserved between Drosophila and vertebrates (Figure 1.6). There are 2 homologs of D-Lgl in vertebrates, LLGL1 and LLGL2. There are further proteins with sequence homology to LLGL1/2 – Sro7 and Sro77 in *S. cerevisiae* and Tomosyn in metazoans. There are no reports of enzymatic activity of LLGL.

Structure of LLGL

The structure of LLGL1/2 has not yet been solved but predictions can be made based on the published structures of Sro7 and Tomosyn. The structure of Sro7 reveals two 7 bladed WD40 β-propellers that would be predicted to be present in LLGL1/2 (Hattendorf et al., 2007). Between the two β-propellers the sequence (in Tomosyn and LLGL) is a highly positively charged low complexity region (LCR) that contains the aPKC phosphorylation sites and may act as a hinge region (Betschinger et al., 2005). Sro7 also contains a 60 residue long tail that is bound to the surface of the amino-terminal propeller but LLGL1/2 lacks sequence homology (Hattendorf et al., 2007).

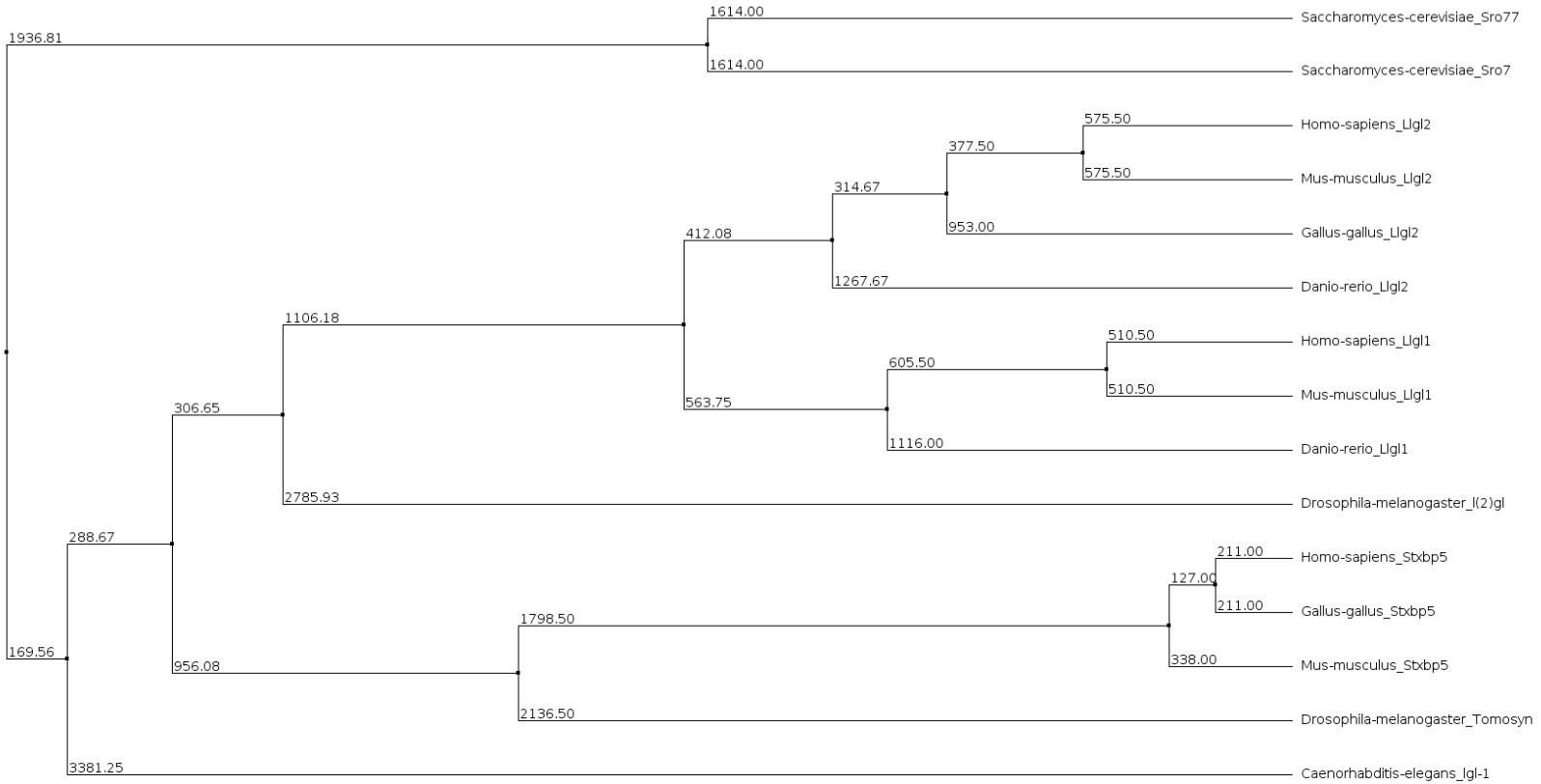

Figure 1.6 Conservation of Lgl family proteins
The phylogenetic tree of Lgl, Sro7//77 and Tomosyn/Stxbp5 (refer to text). The tree was constructed by aligning the protein sequences with ClustalW and then using an Average Distance algorithm based on a BLOSUM 62 distance metric. Large numbers represent greater phylogenetic distances.

Interactions of LLGL

D-Lgl from Drosophila embryos is found within large protein complexes after gel filtration and demonstrates homotypic binding in a phosphorylated LLGL overlay assay suggesting homo-oligomerisation (Strand et al., 1994). Interspecies co-immunoprecipitation experiments using species-specific antibodies for Dlgl and human LLGL show protein interactions suggesting the possibility of heterocomplex formation (Grifoni et al., 2004).

The requirement for LLGL in normal polarity is extensively described in model systems from the initial description of imaginal disc polarity (Gateff and Schneiderman, 1969, Manfruelli et al., 1996, Bilder et al., 2000a) asymmetric cell division of Drosophila neuroblasts, epithelial polarity in the frog (Dollar et al., 2005) and junctional formation in the zebrafish (Sonawane et al., 2009). There are several overlapping theories by which LLGL affects polarity; mutual antagonism (Yamanaka et al., 2003), regulation of the actomyosin cytoskeleton (Strand et al., 1994) and regulation of polarised transport (Musch et al., 2002).

Mutual antagonism between LLGL and the Par complex is very similar to the mechanism already described for the Par complex and Par1 (Figures 1.5A & C). LLGL1/2 co-immunoprecipitates with Par6 in MDCK cells (Yamanaka et al., 2003) and recombinant protein studies show that the direct interaction is between the N-terminus of LLGL and the CRIB/PDZ region of Par6 (Plant et al., 2003). Exogenous LLGL2 in MDCK cells competes with Par3 for Par6-aPKC binding (Yamanaka et al., 2003, Horikoshi et al., 2009) and similarly, D-Lgl binds to Par6 exclusive of Par3 in Drosophila (Betschinger et al., 2003). LLGL is therefore capable of disrupting the apically localised Par3 complex and Crb complex.

Atypical PKC has been shown in a number of studies to phosphorylate and mislocalise LLGL. It does this by phosphorylating the LLGL hinge region at multiple sites, possibly resulting in an inhibitory intramolecular interaction between the C- and N-termini, leading to a change of cellular location from the cortex to the cytoplasm (Betschinger et al., 2005, Hutterer et al., 2004). By doing so aPKC is able to exclude active LLGL from the apical region. The aPKC-induced phosphorylation of LLGL is

potentiated by interaction between aPKC and the LLGL-associated p32, a novel regulatory protein that causes actin-enrichment of the apical membrane and is required for MDCK cyst polarity (Bialucha et al., 2007).

A potential role in cytoskeletal regulation was proposed when myosin II, a motor protein and actin crosslinker, was found to be the most abundant D-Lgl binding protein in co-immunoprecipitation studies in Drosophila (Strand et al., 1994). In normal metaphase Drosophila neuroblasts myosin II is located in an apical crescent. The D-Lgl hypomorphic mutant neuroblast shows membrane associated myosin that is not apically restricted. The constitutively phosphorylated D-Lgl mutant shows cytosolic myosin distribution (Barros et al., 2003). The C-terminus of D-Lgl interacts with myosin II and is located cortically but, as previously mentioned, phosphorylation of D-Lgl results in detachment from the membrane and actin cytoskeleton. It may be speculated therefore that D-Lgl negatively regulates the localisation of myosin II which, through it motor protein function, effects the polarisation of other proteins. Similar interplay between LLGL and myosin have not so far been reported in mammalian epithelium.

The close homologs of LLGL, Sro7/77 and Tomosyn, have both been implicated in regulating polarized exocytosis (Lehman et al., 1999, Sakisaka et al., 2004). Mammalian LLGL may also contribute to epithelial polarity by interacting with Syntaxin-4 (and SNAP-23) which has been demonstrated in MDCK cell lysates. Syntaxin-4 is a basolaterally located t-SNARE that has been implicated in promoting exocytosis and thus the polarised delivery of molecules to the cell (Musch et al., 2002). In MDCK cells, vesicles containing apical proteins form upon depolarization with calcium depletion. In LLGL knockdown MDCK clones, however these intracellular vesicles fail to form and the apical proteins remain apical (Yamanaka et al., 2006). Upon repolarisation by calcium switch the trafficking back to the membrane is Par3 dependent but is unaffected by LLGL knockdown (Yamanaka et al., 2006, Horikoshi et al., 2009). LLGL is known to compete with Par3 for complex formation so it is possible that LLGL negatively regulates Par3 dependent polarized exocytosis.

Tumour Suppressor role.

It is well established through the genetic manipulation of Drosophila that Dlgl is a tumour suppressor gene (Bilder, 2004). Loss of function Dlgl mutants in Drosophila lead to loss of polarity, proliferation and growth of neoplastic lesions. This phenotype is rescued by expression of human LLGL1 indicating conservation of function across the species (Grifoni et al., 2004). LLGL2 knockout Zebrafish are unable to form hemidesmosomes (that connect the epidermis to the basement membrane), and display hyperproliferation and disorganization of the basal epidermis (Sonawane et al., 2009).

Whether the effects of LLGL manipulation are conserved in mammals is less well documented. The mammalian LLGL studies have been conducted principally in MDCK cells. Stable knockdown of LLGL in MDCK led to an early selective relocation of apical proteins to the basal membrane while those basal proteins stained for were unaffected. Subsequent cystogenesis and lumen formation were perturbed resulting in a cell aggregate predominant phenotype (Yamanaka et al., 2006). Overexpression of wild type LLGL results in abnormal tight junction formation in MDCK cells (Yamanaka et al., 2003) and abnormal lumen formation in MDCK cysts (Horikoshi et al., 2009). Expression of non-phosphorylatable, membrane localized (active) LLGL mutant (LLGL-3A) also disrupts tight junction formation in MDCK cells and decreases the ability of mouse embryonic fibroblast cells to polarise in a scratch wound assay (Plant et al., 2003). Both over-expression and under-expression of LLGL in MDCK cells seems to result in similar defects in polarised protein localisation suggesting a threshold behaviour.

Studies in mammals have also explored the role of LLGL knockout. LLGL1 knockout mice develop severe brain dysplasia and die shortly after birth from hydrocephalus (Klezovitch et al., 2004). Surprisingly, in view of the Zebrafish data, LLGL2 knockout mice are viable and only have a mild phenotype. The pups are initially small due to placental defects caused by impaired polarised invasion of trophoblasts during placental development (Sripathy et al., 2011).

A few studies have looked at whether LLGL is altered in human cancer. LLGL1 mRNA and protein was decreased in melanoma cell lines and most tumour samples. Over-expression of LLGL1 in these cell lines reduced invasion and migration but proliferation and non-adherent growth were unaffected (Kuphal et al., 2006). Loss of LLGL1 is associated with advanced stage, particularly lymph node metastases, in colorectal cancer (Schimanski et al., 2005). Mutant LLGL1 transcripts were identified in 32.5% of 80 sequenced hepatocellular carcinoma samples most of which were predicted to disrupt WD40 interaction domain folding. Mutant transcripts correlated with larger tumour size and worse histological grade. Over-expression of mutant LLGL1 proteins in an HCC cell line promoted invasion, migration and tumorigenicity in nude mice but wild type LLG1 had the opposite effect (Lu et al., 2009). Serous and mucinous ovarian carcinomas were shown to have cytoplasmic distribution of LLGL1 whereas the normal ovarian tissue showed polarised basolateral membranous localisation (Grifoni et al., 2007). LLGL2 protein expression is lower in gastric dysplasia and adenocarcinoma compared to normal matched tissue (Lisovsky et al., 2009). Low grade pre-malignant pancreatic lesions express basolateral LLGL whereas highly dysplastic and malignant pancreatic lesions have lost or aberrantly located LLGL2 (Lisovsky et al., 2010). The published evidence to date, while limited to a select few tumour types, suggests that both human LLGL1 and LLGL2 act as tumour suppressors.

1.3.6 Migration

Atypical PKC has been shown to be involved in migration in multiple contexts. In vivo, aPKC as part of the activated Par complex is required for migration of neuroblasts in *C Elegans* (Welchman et al., 2007), control of *X. laevis* gastrulation (Hyodo-Miura et al., 2006) and border cell migration in *D. melanogaster* (see (Boeckeler et al., 2010) for review). In mice the migration of granule cell precursors (GCP) in the developing cerebellum in response to growth factors such as BDNF was dependent on the activation of aPKC and its interaction with the adaptor protein Numb and the TrkB nerve growth factor receptor (Zhou et al., 2011).

In cancer specific cell models PKCζ was required for EGF induced migration of human breast cancer and lung cancer cells and CSF-1 chemotaxis of macrophages and acute monocytic leukaemia cells (Sun et al., 2005, Liu et al., 2008, Guo et al., 2009). Following EGF stimulation aPKCζ recruited Smurf1, a HECT domain E3 ubiquitin ligase, to cellular protrusions where it negatively regulated the local levels of RhoA, a small GTPase protein that regulates the actin cytoskeleton. PKCι has been shown to promote nicotine-induced migration and invasion of lung cancer cells via phosphorylation of m- and μ-calpains and this was blocked by PKCι inhibition (Xu and Deng, 2006). aPKC phosphorylation of Numb during cervical cancer cell migration resulted in dissociation from integrins and clathrin-coated structures, integrin endocytosis and thus enabled migration. (Nishimura and Kaibuchi, 2007).

In an astrocyte scratch wound assay, cdc42 and Rac were recruited to the wound edge. The recruitment of cdc42 was triggered by integrin induced Src signalling and activation by the βPIX exchange factor (Osmani et al., 2006). βPIX also recruited Rac1 but did not activate it. βPIX recruitment was dependent on Arf 6, a small GTPase that regulates membrane endocytosis and recycling (Osmani et al., 2010). Cdc42 recruited and activated Par6/PKCζ to the leading edge where it phosphorylated and inactivated GSKβ. Adenomatous polyposis coli tumour suppressor protein (APC), a substrate of GSKβ, consequently associated with microtubule plus ends at the leading edge and enabled centrosome and golgi reorientation (Etienne-Manneville and Hall, 2003)). For polarisation of the microtubule cytoskeleton it was necessary for APC to interact with puncta in the plasma membrane containing discs large protein, Dlg1. This interaction was also promoted by cdc42 at the leading edge (Etienne-Manneville et al., 2005).

Distinct aPKC dependent migratory pathways that do not involve cdc42/Par6 have been identified using scratch wound assays in Normal Rat Kidney cells (NRK). Using siRNA and chemical inhibitor approaches, aPKC was shown to be required for migration (Rosse et al., 2009). Localisation at the membrane of aPKC was mutually dependent on the Exocyst complex, a complex of 8 proteins mainly associated with membranes (Rosse et al., 2006). During cell migration Kibra, a scaffold protein, formed a complex with aPKC-Exocyst and translocation of this complex coincided with activation of ERK, JNK and the focal adhesion protein Paxillin. Inhibition of aPKC

decreased ERK and paxillin phosphorylation (Rosse et al., 2009). The compartment specific requirement of aPKC in ERK pathway dependent paxillin phosphorylation was demonstrated by means of a Rapalogue dimerisation approach. Using this approach exogenous paxillin, which becomes located at the leading edge of migrating cells, was inducibly coupled to an upstream effector of the ERK pathway, MEK1, resulting in paxillin phosphorylation and increased focal adhesion turnover despite global aPKC blockade (Boeckeler et al., 2010). This provides direct evidence that aPKC is required for activation of ERK at the plasma membrane of migrating cells.

In summary aPKC is critical to polarized migration both in vivo and in a number of cell based models. It promotes signalling at the migration front by its direct interaction with migration effectors and through its regulation of endo and exocytosis.

1.3.7 Mitotic spindle orientation

Formation of epithelial sheets requires that cell division occurs in the plane of the sheet. Several polarity proteins have been implicated in spindle pole orientation during epithelial cell division including LGN , LLGL2, aPKC, cdc42 and the cdc42 specific exchange factors Tuba and Intersectin-2. Activated cdc42 can bind to the par6-aPKC complex and activate aPKC (Jaffe et al., 2008, Qin et al., 2010, Rodriguez-Fraticelli et al., 2010, Yasumi et al., 2005, Liu et al., 2006). Knockdown of Par3 or Par6 disrupts spindle orientation and aPKC localization but does not disrupt apical basal polarity per se (Durgan et al., 2011, Hao et al., 2010). LGN, the human homologue of *D.melanogaster* Pins, is able to bind to NuMA, a microtubule binding protein, and thus attach astral microtubules to the cortex ensuring correct orientation of the mitotic spindle (Du and Macara, 2004, Zheng et al., 2010). LGN's localization at the membrane is determined by its interaction with cortical GαI. aPKC has recently been shown to phosphorylate LGN at Ser401 resulting in binding of the adaptor protein 14.3.3 (Hao et al., 2010). This inhibits LGN's interaction with GαI consequently restricting LGN to the cytoplasm. In this way, apically located aPKC excludes LGN

and astral microtubules from the apical surface ensuring that mitosis only occurs in the plane of the epithelial sheet (Hao et al., 2010)

1.3.8 Polarity Cues

While the identification of polarity molecules and their complexes has been widely cited the cues that initiate the process for tissues are less well defined. Extracellular cues are obtained from cadherin-dependent cell-cell interactions and adhesion to the extracellular matrix (Yeaman et al., 1999). The intercellular interactions involve the homophilic binding of the extracellular domains of nectin. This therefore defines the site of cell-cell interaction and Par3 is known to bind to the intracellular domain of nectin via N-terminal PDZ thus localising the polarity machinery to this site.

Integrins bind to the extracellular matrix and provide a spatial polarity cue. Sites of Integrin-ECM interaction provide another likely spatial polarity cue. Laminin, an extracellular matrix protein, binds and activates integrin signalling. In MDCK cysts embedded in collagen dominant negative Rac1 led to a reversal of apical-basal polarity with apical protein being detected at the basal (outside in contact with the ECM) membrane. Deficient laminin assembly was identified on the cyst surface and correct apical-basal polarity could be rescued by exogenous laminin (O'Brien et al., 2001). MDCK cysts deficient of β-Integrin or grown in suspension cultures, and therefore lacking the influence of the ECM, also had reversed polarity. Taken together this would suggest that integrin-ECM interaction signals to Rac1 that is required for normal extracellular laminin assembly and basal membrane determination.

Clearly the identification and mechanistic basis behind polarity cues are vital to our understanding of the process. There is a great deal still to uncover in this field of research.

1.3.9 Asymmetric cell division

The role of aPKC in the asymmetric cell division in *C.elegans* and *D.melanogaster* neuroblasts is well characterised. While the molecules implicated in this process are well conserved in vertebrates it is less clear if this function is preserved. Recently a study explored stem cell fate determination in mammalian adult stem-cells. Using haematopoietic specific deletions of PKCζ and/or PKCλ the function including polarisation, self renewal, engraftment and differentiation were assessed and shown to be entirely unaffected (Sengupta et al., 2011). Further studies will be required in different cellular contexts to address whether this function holds true in mammals.

1.3.10 PKCι and PKCζ functional redundancy

PKCι and PKCζ, the two mammalian isoforms of aPKC, demonstrate marked overall amino acid sequence homology (72%) and strong sequence homology of the kinase domain (86%). What is more, the features identified from the respective crystal structures of the PKCι and PKCζ are highly conserved (communication with the Structural Biology Laboratory). Northern blot studies performed by the Ohno Laboratory showed that PKCλ RNA was ubiquitously expressed in mouse tissue whereas PKCζ was largely confined to brain, intestine, kidney and testes (Akimoto et al., 1994). Numerous cell-based and xenograft studies have suggested that the two isoforms play divergent functional roles. There are a number of reasons to interpret these data with caution as firstly these are inter-experimental comparisons. Secondly, the reagents used to assign isoform specific function were often of poor quality. Assessment of commonly used PKCι and PKCζ antibodies have been shown to be non-isoform specific (Appendix 1) and the same applies to the ζ pseudosubstrate inhibitor.

More robust genetic techniques have been utilized and provide further insight. The PKCι knockout mouse is embryonic lethal at day 9.5 whereas PKCζ knockout mice display mildly impaired NF-κβ and IL-4 signalling only. Cell lines derived from viable chimeric PKCι deficient mice showed alterations in stress fibres and focal adhesions but

responded normally to activators of NF-κβ such as TNF, serum and lipopolysacchride (Soloff et al., 2004). The critical experiment to elicit whether the apparent differences are due to expression patterns or intrinsic structural properties would be to place the PKCζ allele downstream of the PKCι promoter in a PKCι and PKCζ null background and see if embryonic lethality can be rescued.

The most convincing cell based study to date to assign a tumour suppressor phenotype to PKCζ was from the Moscat Laboratory. They crossed mice with lung specific inducible oncogenic Ras and PKCζ knockout or wild type mice. After 2 months there was a 4 fold increase in total lung tumour area in the PKCζ knockout strains and at 3 months all the knockout mice demonstrated worse histological grade of lung tumour. They went on to show that the Oncogenic Ras/PKCζ knockout mice had high levels of IL-6 staining. Use of IL-6 RNAi decreased the rate of subcutaneous tumour formation in nude mice inoculated with embryonic fibroblasts lacking PKCζ (Galvez et al., 2009).

1.3.11 The role of PKCι in human cancer

The literature overwhelming supports the oncogenic role of PKCι. An oncogene is a gene that, when mutated or over-expressed transforms a normal cell into a malignant cell (see (Croce, 2008)for review).

PKCι is located on chromosome 3q26, one of the most frequent amplicons in human cancer (Han et al., 2002). While there are several potentially important cancer associated genes within this region, including PIKC3A, Ect2 and MDS1 a direct link between 3q26 amplification, PKCι and transformed cell growth has been established in several studies. In ovarian cancer tissue high PKCι gene copy number was associated with increased mRNA and protein expression. siRNA inhibition of PKCι in an ovarian cancer cell line decreased non-adherent cell growth confirming the transforming function of PKCι (Zhang et al., 2006a). Using a high resolution SNP array dataset in 52 ovarian tumours an analysis showed that the genes for PKCι and Ect2 were putative drivers of two distinct amplicons on chromosome 3q (Haverty et al., 2009). The high

PKCι copy number and protein expression was correlated to a short progression free survival (Eder et al., 2005). High PKCι protein expression correlates with gene amplification in lung squamous cell carcinoma (SCC) but not lung adenocarcinoma (Regala et al., 2005b). In oesophageal squamous cell carcinoma a FISH analysis identified that the PKCι gene was frequently amplified and the protein expression, from a 180 patient tissue microarray, was correlated to stage and lymph node metastasis (Yang et al., 2008). PKCι gene amplification and protein over-expression are correlated with hepatocellular carcinoma grade, stage and junctional markers (Wang et al., 2008b). Chromosome 3q amplification has also been reported in SCC of the head and neck (Snaddon et al., 2001) and cervix (Sugita et al., 2000). No oncogenic mutations of PKCι have been reported to date.

There are multiple reports where PKCι protein is elevated in the absence of any genetic aberrations. High PKCι protein expression was found in lung adenocarcinoma and correlates with patient survival. It is worth mentioning here that the K-Ras mutation, that has been shown to drive PKCι dependent oncogenesis in cell and murine models, is commonly found in lung adenocarcinoma and not lung SCC (Regala et al., 2005b). Other immunohistochemistry based studies have shown a link between protein expression and patient prognosis or grade in tumours of the breast (Kojima et al., 2008), pancreas (Scotti et al., 2010), stomach (Takagawa et al., 2009), bile duct (Li et al., 2008) and brain (Patel et al., 2008) (Table 1.3).

What accounts for the apparent discrepancy between elevated PKCι protein and lack of genetic abnormalities? Mutational analyses of cancer patient samples to date tend not to have been exhaustive so important mutations in PKCι may have been missed particularly if they are of low frequency. Alternatively the increased PKCι protein expression in these tumours may be due to post-translational modifications or signal cross-talk at a transcription level that have not yet been identified. One example of the latter is that the Bcr-abl fusion protein was able to up-regulate PKCι transcription in Chronic myelogenous leukaemia cells by induction of the PKCι promoter (Gustafson et al., 2004). In view of the compelling link between the increased expression of PKCι

and worse cancer prognosis, studies designed to identify somatic PKCι mutations and signal cross talk in human cancer are warranted.

Malignancy	Patient No.	Genetic Aberration (1)	Protein Expression (2)	Outcome/Phenotype	Reference
Ovarian cancer	67	ND	⇑ PKCι	⇓ Median Survival ⇑ tumour grade ⇑ tumour stage	Weichert et al 2003
Ovarian cancer	54	⇑ PKCι mRNA	⇑ PKCι	⇑ tumour grade[2] ⇑ tumour stage[2]	Zhang et al 2006
Ovarian cancer Epithelial	441	⇑ Copy N	⇑ PKCι ⇑ Cyclin-E	⇓ Progression Free Survival[2] ⇓ Overall Survival	Eder et al 2005
Lung cancer Adenocarcinoma SCC	 37 37	 ⇑ Copy N (70%) ⇑ Copy N (3%)	 ⇑ PKCι ⇑ PKCι	 High protein (all): 2.6x RR death High protein (stage I-II): 11x RR death	Regala et al 2005
Primary Breast Cancer	110	ND	⇑ PKCι	⇑ tumour grade	Kojima et al 2008
Cholangiocarcinoma	41	ND	⇑ PKCι ⇓ E-cadherin	⇑ tumour grade ⇑ tumour stage ⇓ Disease Free Survival	Li et al 2008
Oesophageal SCC	180	⇑ Copy N	⇑ PKCι	⇑Lymph node metastasis (independent of tumour size)[2] ⇑stage[2]	Yang et al 2008
Hepatocellular carcinoma	43	⇑ Copy N	⇑ PKCι ⇑ Cyclin-E	⇑ tumour grade[2] ⇑ tumour stage[2]	Wang et al 2008
Pancreatic cancer	28	⇑ PKCι mRNA	⇑ PKCι	High vs low protein levels Median Survival: 16.4 vs 22.7 months	Scotti et al 2010
Gastric Carcinoma	177	ND	Higher in intestinal type than diffuse type	High protein: ⇓ Disease Free Survival	Takagawa et al 2010
Prostate Cancer	29	⇑ PKCι mRNA	⇑ PKCι	High protein: associated with shorter time to serum PSA elevation[2]	Ishiguro 2009

Table 1.3 PKCι expression in human cancer

Immunohistochemical studies comparing PKCι protein expression with clinicopathological outcomes. Unless stated these studies are normal vs cancer. mRNA or copy number information is indicated if performed. ND, not done; RR, relative risk; MS, median survival; PSA, prostate specific antigen.

1.3.12 PKCι and therapeutics

The identification of PKCι as an oncogenic kinase that correlates with prognosis in a range of human malignancies has directed research towards its affect on conventional cancer therapy and development of new therapeutics.

PKCι was found to be activated upon paclitaxel treatment in a Chronic Myelogenous Leukaemia (CML) cell line containing Bcr-Abl, a chimeric oncogenic tyrosine kinase that mediates chemotherapy resistance (Murray and Fields, 1997). Over-expression of PKCι in a CML cell line lacking Bcr-Abl also resulted in insensitivity to paclitaxel induced apoptosis. An aPKC inhibitor was found to have a synergistic affect on 5-fluorouracil induced apoptosis in human breast cancer cell lines that overexpress hASIP, a PKCι substrate (Jin et al., 2008). Zhang et al were unable to induce chemoresistance to cisplatin by overexpressing PKCι in ovarian carcinoma cell lines and there was no correlation between PKCι mRNA expression and platinum sensitivity in a panel of ovarian cancer cell lines (Zhang et al., 2010). Taken together this would suggest that PKCι expression in cancer cells can lead to chemoresistance and that PKCι inhibition may act synergistically with conventional chemotherapies but the effects are likely to be cell type and chemotherapy specific.

Aurothiomalate (ATM) was identified in a fluorescence resonance energy transfer (FRET) assay as an inhibitor of PKCι-Par6 interactions. ATM inhibition of this PB1-PB1 domain interaction reduces colony formation in soft agar and tumourgenicity in vivo (Stallings-Mann et al., 2006). ATM has been widely used in the treatment of rheumatoid arthritis and it is thought that it works by the formation of gold-cysteine adducts with cellular targets (see Messori and Marcon, 2004 for review). The crystal structure of PKCι-Par6 has been solved and molecular modelling of this structure combined with ATM predicts adduct formation between ATM and Cys69, a cysteine unique to the PKCι PB1 domain. Mutation of Cys69 to either an isoleucine or valine retains Par6 binding but renders it ATM insensitive (Erdogan et al., 2006). In a lung cancer cell line panel, sensitivity to ATM correlated with PKCι mRNA and protein expression (Regala et al., 2008). Based on the proposed selective inhibition of PKCι-Par6 and the in vitro and in vivo suppression of cell transformation phase I clinical trials

of the ATM compound in cancer are currently in accrual. Oncrastin-1 is a small molecule inhibitor identified in a synthetic lethal screen in immortalised mutant K-ras ovarian epithelial cells. While the precise mechanism of action of Oncrastin-1 is unknown, PKCι and mutant Ras expression were required for its cytotoxic activity. Additionally upon Oncrastin-1 treatment there was nuclear accumulation of PKCι (Guo et al., 2008).

A number of other groups, including our collaborators at Cancer Research Technology have active drug development programs for ATP competitive PKCι inhibitors. To date the only compound to be published in this drug class is ICA-1 that has a biochemical IC_{50} of 100nM and is at least 50 fold more potent against PKCι than PKCζ. In neuroblastoma cells ICA-1 was shown inhibit phosphorylation of cdk7, a cell cycle regulator shown to be a PKCι substrate (Pillai et al., 2011) (Acevedo-Duncan et al., 2002). In this neuroblastoma cell line ICA-1 inhibited proliferation and induced apoptosis but this did not occur in a non-transformed neuronal cell line suggesting possible specificity for transformed cells (Pillai et al., 2011).

It is anticipated that over the next few years, several PKCι inhibitors will be tested in clinical trials, either in combination with chemotherapy or as a single agent, and hopefully identify a clinical benefit for cancer patients.

1.4 Overarching aims of this thesis

The work carried out in this thesis was stimulated by the role of PKCι in epithelial malignancy and the ambition to drive rational therapeutic design through a greater understand of PKCι biology. This work sought to identify a robust cancer dependent PKCι cell phenotype in which to analyse potential PKCι activators and to establish a platform for identification of clinically relevant PKCι downstream effectors.

Chapter 2. Materials and Methods

2.1 Materials

2.1.1 Reagents

Agarose

Ampicillin

dNTP

Enhanced Chemiluminesce (ECL) solution – Amersham

Filter Paper (3MM) – Whatman

Full Range Rainbow marker (RPN800E, Amersham)

GFP-TrapM (Chromotek)

Immobilon-FL PDVF membranes IPFL00010 Millipore

Immobilon-P PDVF membranes IPVH00010 Millipore

Kanamycin

Matrigel Growth factor reduced BD 354230

Mini Trans Blot Electrophoretic transfer cell – Bio Rad

NuPAGE 4-12% Bis-Tris Gels Invitrogen NP0335BOX

NuSEP 8-16% NuSEP NH21-816

Photographic Film – Fuji

Pfu Turbo

Pfu Ultra

QIAquick PCR purification kit (28104), QIAquick Gel Extraction Kit (28704)

QIAFilter Plasmid Maxi Kit (12263)

Restriction Enzymes – NEB

SDS Page Electrophoresis mini tank – Invitrogen

TopTEN chemically competent E. coli - Invitrogen

2.1.2 Plasticware

All plasticware was purchased from Corning international unless otherwise stated. Polypropylene round bottom tubes, 8-well chamber slides and polystyrene round bottom tubes with cell strainers and gel loading pipettes were obtained from BD Fisher. Microscope cover glass 24x60 #1 were obtained from Erie Scientific Company.

2.1.3 Buffers

Colloidal Comassie Buffer: GelCode Blue Stain Reagent (ThermoScientific 24590)

DNA loading Buffer (x2): 13% (w/v) sucrose, 2mM Tris-HCl (pH 7.5), 2mM EDTA, 0.06% (w/v) Bromophenol Blue. This was a 1:5 dilution of BlueJuice (Invitrogen) in D_20.

LDS loading Buffer(x2): 50% (v/v) 4xLDS Nupage buffer (Invitrogen) in D20 supplemented with 100mM DTT (Melford)

TAE: 0.04M Tris, 0.1% glacial acetic acid, 1mM EDTA (pH 8.0)

TBS: 0.9% (w/v) NaCl, 20mM Tris

TBS-T: TBS and 0.1% (v/v) Tween-20

Running Buffer1 TRIS-HEPES-SDS (NuSEP, BG-163)

Running Buffer2 MOPS-SDS (NuPAGE, Invitrogen NP0001), 500µl of Antioxidant (Cat no. NP0005, Lot no. 283034; Store at +4oC)

5xTrypsin/EDTA: 2.5g/l Trypsin, 8g/l NaCl, 1.15g/l Na2HPO4, 200mg/l KH2PO4, 1g/l EDTA and 1% v/v Phenol Red, pH 7.2. (Cell Services, CRUK)

Transfer Buffer: 25mM Tris, 192mM glycine, 10% methanol

Kinase Dilution Buffer: 5% glycerol v/v, 50mM Tris, 1mM EDTA, 1mM DTT

Substrate Dilution Buffer: 100mM HEPES (pH 7.5) and 2mM EGTA

L-Broth (LB): 10g/l Bacto-Typtone, 5g/l Yeast extract, 10g/l NaCl

L-Agar: 15g agar/l. Autoclaved for 15 mins

Distilled Water (D_2O): Ultra-pure Millipore water, autoclaved for 20 mins

Stripping Buffer: 5% (v/v) acetic acid in D_2O

S.O.C Medium: 2% Tryptone, 0.5% Yeast Extract, 10mM NaCl, 2.5mM KCl, 10mM $MgCl_2$, 10mM $MgSO_4$, 20mM glucose (Invitrogen)

Phosphate Buffered Saline – Ca^{2+}/Mg^{2+} free (PBS): 8g/l NaCl, 250mg/l KCl, 1.43g/l $NaHPO_4$, 250mg/ml KH_2PO_4, pH 7.2 (Cell Services, CRUK)

Dulbecco's PBS (DPBS): PBS, 534mg/l $CaCl_2$, 400mg/l $MgCl_2$, pH7.2 (Cell Services, CRUK)

Mounting Medium: Prolong Gold antifade reagent, Invitrogen P369343

Co-Immunoprecipitation Lysis Buffer: 1%Triton X 100, 20mM Tris (pH 8), 130mM NaCl, 1mM DTT, 10mM NaF, Protease Inhibitor (CoMplete, Roche) and Phosphatase Inhibitors (Calbiochem, II & IV)

Co-Immunoprecipitation Wash Buffer: 1%Triton X 100, 20mM Tris (pH 8), 130mM NaCl, 1mM DTT, 10mM NaF, Protease Inhibitor (CoMplete, Roche)

Immunofluorescence (IF) Buffer: 0.2% Triton X-100, 0.04% Tween-20, 130mM NaCl, 13mM Na_2HPO_4, 3.5mM NaH_2PO_4 , pH 7.4 and filter sterilized

Matrigel washing buffer: 5mM EDTA, 1mM Na3VO4, 1.5mM NaF, Phosphatase inhibitor cocktail sets II & IV (Calbiochem)

Permeabilization buffer: 0.5% Triton X-100 in PBS

IF-Blocking buffer: IF buffer, 10% goat serum (v/v)

Primary Antibody Blocking Buffer: 3% (v/v) BSA in TBS-T

Secondary Antibody Blocking Buffer: 5% (w/v) dried skimmed milk powder (Marvel) in TBS-T

PolyLysine-PBS: 10% (v/v) Poly-L-lysine (Sigma P4707) in PBS

PBS-EDTA: 5mM EDTA, 1mM Na_3VO_4, 1.5mM NaF in PBS

Transfer Buffer: 25mM Tris, 150mM Glycine, 20% (v/v) methanol in D_20.

Pfu Buffer: Stratagene

2.1.4 Antibodies

Table 2.1 Primary Antibodies

Name	Description	Source & code	Use	Dilution
α-Tubulin	Mouse monoclonal [B-5-1-2]	Sigma T5168	WB	1:10000
PKCλ	Mouse monoclonal	BD 610608	WB IF	1:500 1:300
aPKC	Rabbit polyclonal [C-20]	Santa Cruz 216	WB IF	1:500 1:100
PKCζ	Goat polyclonal	Santa Cruz 7262	1/1000	1/500
PKCζ	Mouse monoclonal [H1]	Santa Cruz 17781	WB IF	1:1000 1/50
PKCζ	Rabbit monoclonal	Cell Signaling C24E6	WB	1:1000
aPKC	Mouse monoclonal	CRUK 524/1	WB	1:1000
ZO-1	Rabbit polyclonal	Zymed 40-2200	IF	1/100
Cleaved Caspase-3	Rabbit polyclonal (Asp175)	Cell Signaling 9661S	IF	1:100
Ki-67	Rabbit polyclonal	Zymed 18-0191Z	IF	1:100
pPKCι[p555]	Rabbit polyclonal	Invitrogen 44-968G	WB	1:500
pPKCζ/λ [T410/403]	Rabbit polyclonal	Cell Signaling Technology 9378	WB	1:1000
α-6-Integrin	Rat monoclonal [Go H3]	Abcam ab 19765	IF	1:200
β-catenin	Mouse monoclonal	BD 610154	IF	1:100
GM130	Mouse monoclonal	BD 610823	IF	1:100
LLGL2	Mouse monoclonal	Abcam ab55423	WB	1/500
pLLGL1/2 [S650/654]	Rabbit polyclonal	Abnova PAB4657	WB	1:500
pSrc [Y416]	Rabbit Polyclonal	Cell Signaling Technology 2101	WB	1:1000
PI3 Kinase p110α	Rabbit monoclonal [C73F8]	Cell Signaling Technology 4249	WB	1:1000
Pan-Ras	Mouse monoclonal [RAS 11]	Calbiochem OP41	WB	1:500

Her2	Rabbit monoclonal [29D8]	Cell Signaling Technology 2165	WB	1:1000
Par3	Rabbit polyclonal	Millipore 07:330	WB	1:1000
Par6	Rabbit Polyclonal [H64]	Santa Cruz 67392	WB	1:500
C-Raf	Mouse monoclonal	Cell Signaling 610151	WB	1:1000
B-Raf	Rabbit polyclonal	Upstate 07-453	WB	1:1000
pErk[T202/204]	Rabbit monoclonal	Cell signaling	WB	1:500
GST	Rabbit Polyclonal	Sigma	Protein overlay	1:1000

Table 2.2 Secondary Antibodies

Name	Description	Source & code	Use	Dilution
Alexa Fluor 555	Goat anti-rabbit	Invitrogen A21429	IF	1:300
Alexa Fluor 555	Goat anti-mouse	Invitrogen A21422	IF	1:300
Alexa Fluor 488	Goat anti-mouse	Invitrogen A11001	IF	1:300
Alexa Fluor 488	Goat anti-rabbit	Invitrogen A11008	IF	1:300
ECL Mouse HRP	Sheep anti-mouse IgG linked to HRP	Amersham NA931V	WB	1:5000
ECL Rabbit HRP	Donkey anti-rabbit IgG linked to HRP	Amersham NA934V	WB	1:5000
Goat HRP	Donkey anti-goat IgG linked to HRP	Santa Cruz 2020	WB	1:5000
LI-COR 800	Goat anti-Mouse IRdye	LI-COR 926-3221G	WB	1:4000
Alexa Fluor 680	Goat anti-Rabbit IgG	Invitrogen A21109	WB	1:4000
IgG F(ab')2	Goat anti-mouse	Jackson ImmunoResearch Labs 115-007-003	Blocking	1:100
FITC anti-rat	Donkey anti rat linked to FITC	Jackson Laboratories 712-095-150	IF	1:200

2.1.5 Immunofluorescent Probes

Table 2.3 Immunofluorescent Probes

Name	Structure stained	Source & code	Use	Dilution
Phalloidin Alexa Fluor 546	F-actin	Invitrogen A22283	IF	1:200
Hoechst	DNA	Invitrogen	IF	1:5000
DAPI	DNA	Invitrogen	FACS	1:5000
TOPRO-3 (642/661)	DNA	Invitrogen	IF	1:5000

2.1.6 Pharmacological Agents

Table 2.4 Pharmacological Agents

Name	Source	Action
Go6983	Calbiochem	Pan-PKC inhbitor
BimI	Calbiochem	Inhibits cPKC & nPKC (not aPKC)
CRT66854	CRT	aPKC specific inhibitor
CRT31	CRT	aPKC specific inhibitor
CRT92	CRT	aPKC specific inhibitor
MG132	Calbiochem	Proteosome inhibitor
PP1	TOCRIS	Selective inhibitor of Src
NaPP1	TOCRIS	Selective inhibitor of Src
PP2	TOCRIS	Selective inhibitor of Src

2.1.7 Media and Growth Supplements

DMEM, DMEM/F12 and McCoys's 5A media were obtained from GIBCO. PenStrep was also obtained from GIBCO and used at a final concentration of 100U/ml penicillin and 100mg/ml streptomycin. Foetal bovine serum (FBS) was obtained from PPA and Horse serum (324831), Hydrocortisone (H-0888), Cholera toxin (C-8052) and Insulin (1882) were purchased from Sigma. EGF was obtained from Calbiochem. Media Filtration products were obtained from Nalgene.

2.2 Methods

2.2.1 Cell Culture

2.2.1.1 Parental Cell Lines

Mardin Darby Canine Kidney (MDCK), HeLa, HEK293 and A549 cells were obtained from CRUK cell production services and cultured in DMEM supplemented with 10% FBS and PenStrep. HCT116 cells were also obtained from CRUK cell production services but cultured in McCoy's 5A Media supplemented with 25mM HEPES, 10% FBS and PenStrep.

MCF10a cells were a gift from Joan Brugge, Harvard Medical School. Maintenance of these cells, such that they are suitable for 3D cultures, has been described in detail elsewhere (Debnath and Brugge, 2005). In brief, cells were cultured in DMEM/F12 supplemented with 5% Horse serum, 20ng/ml EGF, Hydrocortisone, 100ng/ml Cholera toxin, 10μg/ml Insulin and PenStrep. Importantly, early passage cells were maintained in log phase growth and discarded if they reached confluence.

MDCK cells were obtained from Cell Production, cancer research UK. Isoenzyme and SNIP analysis was performed by cell services to authenticate the origin of these cells. Cells were maintained in DMEM supplemented with 10% FBS and PenStrep.

2.2.1.2 Stable Cell lines

Stable MDCK cell lines expressing V12-Ras, p110 CD2, v-Src or Raf-CAAX were a gift from Julian Downward, London Research Institute (Khwaja et al., 1997). Further MDCK cell lines were generated by reverse transfection of MDCK cells in a poly-L-Lysine coated dish. For a 35mm dish 3μg of cDNA, 10μl of Lipofectamine 2000 (Invitrogen) and $5x10^5$ MDCK cells were used. After 24h the cells were trypsinised (Cell services CRUK) and re-plated in a 10cm dish containing appropriate antibiotic-resistance markers, typically 750μg/ml G418 (GIBCO) or 5mg/ml Puromycin (Sigma P9620). Subpopulations of these polyclonal cell lines, expressing similar levels of GFP,

were established by 2 successive rounds of Fluorescent Activated Cell Sorting (FACS, CRUK FACS facility).

Table 2.5 Stable cell lines obtained during this thesis

Stable Cell Line	Expression vector	Source
MDCK-p110*	pcDNA3- myc-p110α-CAAX	Julian Downward
MDCK-V12-Ras	pcDNA3- V12-Ras	Julian Downward
MDCK-Raf-CAXX	pEFH6 PLINK - Raf-CAXX	Julian Downward/ Richard Morais
MDCK-vSrc	pSG5- vSrc	Julian Downward

Table 2.6 Stable cell lines made during this thesis

Stable Cell Line	Expression vector	Mammalian resistance marker
MDCK-EV	pEGFP-C1	G418
MDCK-PKCι	pEGFP-FL.PKCι	G418
MDCK-PKCι(DN)	pEGFP-FL.PKCι (D368N)	G418
MDCK-PKCι(CA)	pEGFP-FL-PKCι(A120E)	G418
MDCK-PKCι(AIPA)	pEGFP-FL.PKCι(D471A/D474A)	G418
MDCK-PKCι(DIM)	pEGFP-FL.PKCι(D330A/D373A)	G418
GFP-MDCK-V12-Ras	pBABE-GFP-CAAX-puro	Puromycin
Cherry-MDCK-V12-Ras	pBABE-Cherry-puro	Puromycin
GFP-MDCK-vSrc	pBABE-GFP-CAAX-puro	Puromycin
Cherry-MDCK-vSrc	pBABE-Cherry-puro	Puromycin
GFP-MDCK	pBABE-GFP-CAAX-puro	Puromycin
Cherry-MDCK	pBABE-Cherry-puro	Puromycin
MDCK-ErbB2-YVMA	pEGFP	G418

2.2.2 Protein Overlay

The peptide array was obtained from the Peptide Synthesis Laboratory at Cancer Research UK. The array was designed to have sequential overlapping PKCι peptides of 20 amino acids each differing from the previous peptide by a single amino acid.

The membranes were blocked in 3% BSA/DTT/Tween for 1 hour. This was followed by a 20 minute incubation with both recombinant GST tagged PKCι kinase domain (50ug/ml, 1ml total volume) and CRT66855 (1.2μM, obtained from Cancer Research Technology) in 3%/BSA/DTT/Tween. The membranes were then rapidly washed in

3% BSA/DTT/Tween, cross linked with 0.5% Formaldehyde in D_2O for 5 minutes and quenched with 2% glycine – PBS for 5 minutes.

The arrays were washed a further 2 times, firstly in 3%-BSA/DTT/Tween and then in PBS/Tween. The membranes were incubated with anti-GST antibody (Sigma) overnight at 4 degrees and detected using a rabbit-HRP secondary antibody and chemiluminescence (see section 2.2.20.3).

2.2.3 Polymerase Chain Reactions

Polymerase Chain Reaction (PCR) mix consisted of 1U Pfu Turbo, 1xPfu buffer, 0.2mM dNTP mix, 0.3μM of forward primer, 0.3μM of reverse primer and 20ng DNA template made up to 50μl with distilled water. The mix, in a polypropylene tube tube, was placed in a thermocycler (DNA Engine DYAD, MJ Research) and the following program used:

Step 1: 95°C, 5 mins
Step 2: 95°C, 30 secs
Step 3: Lowest primer Tm -4°C, 30 secs
Step 4: 70°C, 1 min per kBase
Step 5: Repeat steps 2-4 x25
Step 6: 70°C, 10 mins
Step 7: 6°C, Forever

2.2.4 Agarose gel electrophoresis

PCR products were identified by agarose gel electrophoresis. The gel consisted of 1% agarose (w/v) and 6% (v/v) ethidium bromide in TAE buffer. Samples were mixed 3:1 with DNA loading buffer (x2), run along side a 1kb DNA ladder and separated at 100V. Bands were identified using the uv transilluminator, excised and purified using QIAquick gel extraction kit (Qiagen).

2.2.5 Restriction Digests

In separate reaction mixes 2μg purified insert and the vector DNA were mixed with restriction enzymes, appropriate buffer and BSA according to the manufacturers guidelines. Typically the mix was incubated at 37°C for 1-2h. The vector mix alone was then mixed with calf intestine alkaline phosphatase at 37°C for 30mins. The solutions were again purified using QIAquick spin (Qiagen).

2.2.6 Ligation Reactions

The ligation mix was comprised of 400U T4 DNA ligase, 1 x ligase buffer, 100ng digested vector and insert DNA. Typically a 3:1 molar ratio of vector to insert was used. As a control a vector only reaction was concomitantly performed. The reaction mixes were incubated overnight at 16°C and terminated by heating at 65°C for 10 mins.

2.2.7 Transformation

50 μl of chemically competent E.coli (Top10, Invitrogen) were mixed with 150ng of plasmid DNA or 3μl of ligation reaction and incubated on ice for 25mins. DNA uptake into the cells was promoted by heat shock in a 42°C water bath for 30 secs. The cells were incubated on ice for 2 mins and then 250μl of SOC was added and the mix placed on a shaker at 37°C for 1h. Cells were then plated onto LB containing plates with an appropriate selection antibiotic (100μg/ml Ampicllin or 50μg/ml Kanamycin) and incubated overnight at 37°C.

2.2.8 Plasmid DNA preparation

A transformed *E.coli* colony was picked from the LB selection plate and grown overnight in 5 ml of LB containing appropriate selection antibiotics. 1 ml of this

bacterial preparation was retained in the fridge while 4ml was used to generate a small quantity of DNA using the mini-prep kit (Qiagen). The correct plasmid DNA was confirmed either by a unique restriction digest pattern on an agarose gel or, in the case of mutagenesis, by sequencing (see below). DNA preparations were then scaled up by using the retained 1ml bacterial prep to inoculate 200ml LB and further incubation overnight on the shaker at 37^{o}C. The DNA was prepared using a plasmid maxi-prep kit (Qiagen). DNA concentration was confirmed using Nanodrop ND-1000 UV-Vis Spectrophotometer at 280nm, and the quality was deemed acceptable if the OD_{260}/OD_{280} ratio was between1.6-1.8.

2.2.9 DNA Sequencing

DNA sequencing was performed using the ABI BigDye Terminiator v3.1 system as per the manufacturers guidelines. Typically the reaction mix comprised of 150ng plasmid DNA, 3.2pmol primer, 1x BigDye Terminator Mix made up to a volume of 20µl with distilled water. The following programme was used on the thermocycler:

Step 1: Ramp to 96^{o}C at 2.5^{o}C/sec
Step 2: 95^{o}C, 1 mins
Step 3: 95^{o}C, 10 secs
Step 4: Ramp to (primer Tm -3) ^{o}C at 1^{o}C/sec
Step 5: (primer Tm -3) ^{o}C, 5 secs
Step 6: Ramp to 60 ^{o}C at 1^{o}C/sec
Step 7: 60^{o}C, 4 mins
Step 8: Repeat steps 3-7 x 24
Step 9: 2^{o}C, forever

Sequencing products were purified using the DyeEx 2.0 Spin Kits (Qiagen) and sequenced by CR-UK services on an Applied Biosystems 3730 DNA Analyser. Sequencing results were viewed and analysed using EditView and ClustralX software respectively.

2.2.10 Cloning

PKC iota constructs were cloned by PCR using human PKCi cDNA in pcDNA3.1 as a template (from Dr Scott Parkinson). The Entrez Nucleotide accession number is NM_002740.5. The cDNA contains two start codons at bp1-3 and bp28-30. For consistency with published literature the second methionine is denoted as the first amino acid of the protein. PCR primers (see Table 2.7) were used to introduce 5'-SalI and 3'-BamHI sites to the PKCι sequence to allow ligation into the corresponding restriction sites in pEGFP-C1. In addition the PCR primers were used to introduce a 5' Myc tag sequence.

PKC zeta constructs were cloned by PCR using human PKCζ cDNA in pMT2 vector (from Dr Sven Kjaer). The Entrez Nucleotide accession number is NM_002744.4. Our stock contains a silent mutation at G1164A and a gly>asp mutation resulting from G18A substitution (note the asp is present in rat PKCζ). PCR primers were used to introduce 5'SalI and 5'XmaI restriction sites to the PKCζ sequence to enable ligation into pEGFP-C1. The PCR primers were also designed to add 5' Myc tag sequence.

Table 2.7 Cloning primers

Name	Primers (5'→3')	Key
FL.PKCι Forward	taatGTCGACgccaccATGGAGCAGAAGCTGATCTCA GAGGAGGACCTGccgacccagagggacagcag	SalI, Kozak, MYC TAG, PKCι
FL.PKCi Reverse	attaGGATCCtcagacacattcttctgcag	BamHI, PKCι
KDom.PKCι Forward	tgcGTCGACctcgccaccatgagtctaggtctcagg	SalI, Kozak, PKCι
FL.PKCi Reverse	cgGGATCCtcagacacattcttctgc	BamHI, PKCι
PKCζ Forward	acgcGTCGACgccaccATGGAGCAGAAGCTGATCTC AGAGGAGGACCTGcccagcaggaccggccc	SalI, Kozak, MYC TAG, PKCζ
PKCζ Reverse	tcccCCCGGGtcacaccgactcctcggtgg	XmaI, PKCζ

2.2.11 Constructs

Table 2.8 Cloning and expression vectors

Vector	Selection (bacterial/mammalian)	Source
pEGFP-C1	Kanamycin/G418	Clontech
pcDNA3.1	Ampicillin/Neomycin	Invitrogen
pBABE-GFP(CAAX)	Ampicillin/puromycin	Erik Sahai
pBABE-Cherry	Ampicillin/puromycin	Erik Sahai

Table 2.9 Constructs obtained during the course of this thesis

Name	Expression vector	Restriction sites	Source
LLGL2	pEGFP-C1	EcoR1-SalI	Tony Pawson
PKCι	pCDNA3.1	XhoI-XbaI	Scott Parkinson (PP Lab)
ErbB2-YVMA	pEGFP-N1 (A206K)	XhoI - HindIII	Tony Ng
PKCι	pEGFP-C1	BspEI - Sal I	Gavin Greenland, CRT.
PKCι (D330A)	pEGFP-C1	BspEI - Sal I	Gavin Greenland, CRT.
PKCι (I323A)	pEGFP-C1	BspEI - Sal I	Gavin Greenland, CRT.

2.2.12 Mutagenesis

Mutants were generated using QuikChange site directed mutagenesis according to the manufacturers guidelines. In brief the mutant DNA was sythesised by PCR (see 2.2.3) using high fidelity DNA polymerase and purified plasmid DNA as a template. A typical reaction mix contained 1xPfu buffer, 250μM dNTP, 400ng/ml template DNA, 2% v/v Pfu Ultra and 500nM of a forward primer, and the reverse complements, containing the desired point mutations. The reaction mix was made up to 50μl with distilled water and the following program was used on the Thermocycler.

Step 1: 95^{o}C, 30 secs
Step 2: 95^{o}C, 30 secs
Step 3: 55^{o}C, 1 min
Step 4: 68^{o}C, 8min
Step 5: Repeat steps 2-4 x 18

The methylated DNA template was then digested with 1µl of Dpn1 at 37°C for 1 hour. The newly synthesised non-methylated DNA was then transformed, purified and sequenced (see 2.2.7, 2.2.8 & 2.2.9) to confirm the presence of the intended mutation.

Table 2.10 Constructs generated by mutagenesis during this thesis

Template	Derived Mutant	Primers
pEGFP-myc-FL.PKCι	GFP-myc-FL.PKCι (A120E)	F: atctaccgtagaggtgAacgccgctggagaaag
	GFP-myc-FL.PKCι (R471A/R474A)	F:gttattttggaaaaacaaattgccataccagcttctctgtctgtaaaagc
	GFP-myc-FL.PKCι (D368N)	F:gagcgagggataatttatagaaatttgaaactggacaatgtattactgg
	GFP-myc-FL.PKCι (K274M)	F: cgtatttatgcaatgaTGgttgtgaaaaaagagc
	GFP-myc-FL.PKCi (S477A)	F: caaattcgcataccacgttGCctgtctgtaaaagc
	GFP-myc-FL.PKCi (S477E)	F: caaattcgcataccacgttTCctgtctgtaaaagc
	GFP-myc-FL.PKCi (R471C)	F: ggaaaaacaaattTgcataccacgttctctg
	GFP-myc-FL.PKCi (Y421C)	F: gaggagaagattGtggtttcagtgttgactgg
	GFP-myc-FL.PKC (D373A)	F: agagatttgaaactggCcaatgtattactggac
pEGFP-myc-KDom.PKCι	GFP-myc-KDom.PKCι (A120E)	F: atctaccgtagaggtgAacgccgctggagaaag
	GFP-myc-KDom.PKCι (R471A/R474A)	F:gttattttggaaaaacaaattgccataccagcttctctgtctgtaaaagc
	GFP-myc-KDom.PKCι (D368N)	F:gagcgagggataatttatagaaatttgaaactggacaatgtattactgg
pcDNA3-PKCι	PKCι (D368N)	F:gagcgagggataatttatagaaatttgaaactggacaatgtattactgg
	PKCι(R471A/R474)	F:gttattttggaaaaacaaattgccataccagcttctctgtctgtaaaagc
	Myrist-GFP-myc-PKCi	
pEGFP-PKCι(D330A)	PKCι (D330A/D373A)	F: agagatttgaaactggCcaatgtattactggac

2.2.13 *In Vitro* Kinase Assay

In this thesis 2 different *in vitro* kinase assay protocols were adopted that I have called the Classical and the Modified Kinase Assays. The classical kinase assay utilised ATP[γ-^{32}P] and has been extensively used to assess AGC kinases (Hastie et al., 2006).

The second modified protocol was developed in order to test the activity of high concentrations of PKCι. In essence this necessitated a lower temperature, shorter incubation time and smaller reaction volumes. Recombinant human PKCι kinase domain was expressed in and purified from insect cells (Protein Production Laboratory, CRUK). As a substrate for the reaction either PKCε pseudosubstrate peptide (PKCεPS , produced by Peptide Synthesis Laboratory, CRUK) or purified LLGL2 (made by Phil Knowles form the Structural Biology Laboratory, CRUK) was used.

2.2.13.1 Classical Kinase Assay

The final reaction mix contained 200μM ATP, 10mM $MgCl_2$, 2.5-5μg/ml PKCι in kinase dilution buffer and 250-1000μg/ml of substrate in substrate buffer. Typically the reaction was carried out in 40μl. The kinase was made up to 10μl in kinase buffer and placed in a screw cap tube on ice. A Master Mix containing the ATP, magnesium and substrate was spiked with 0.25μl of ATP[γ-^{32}P](~0.125μCi). 30μl of this mix was added to the enzyme to start the reaction and incubated at 30^{o}C with shaking (Thermoshaker) for 10 minutes. This procedure was applied to the different samples sequentially and carefully timed. The reaction mix was then spotted onto pre-cut p81 filter paper tabs and the reaction terminated by washing in 30% acetic acid. Alternatively the reaction was stopped by adding LDS loading Buffer(x2) directly to the reaction mix, boiling for 10 minutes, resolving by SDS PAGE and drying overnight (Gel-Dry solution, Invitrogen). The p81 tabs or cut gel bands were placed in a scintillation vial and incorporated γ-p32 was measured over 1 minute in a Beckman Scintillation LS6000IC machine. A known volume of the spiked Master Mix was placed directly onto the p81 tab and scintillations counted so that the specific activity (SA) of ATP in the mix could be calculated.

SA (ATP) = CPM/pmol dNTP

From the scintillation counts for the experimental reaction mixes, the concentration of ATP incorporated into substrate could be calculated and thus the specific activity of the kinase.

SA (kinase) = μMol substrate/mg kinase/min of reaction

2.2.13.2 Modified Kinase Assay

The final reaction mix contained 500μM ATP, 12mM $MgCl_2$, 5-3000μg/ml PKCι kinase domain in kinase dilution buffer and 1200μg/ml of PKCεPS in substrate buffer. The reaction was carried out in a 96-well PCR plate on ice. To facilitate high kinase concentration assays it was necessary to scale down the reaction volumes to 10μl and limit the incubation time to 15secs. As with the Classic Kinase Assay, the reaction was commenced by adding the Master Mix to the kinase. However, unlike the Classic Assay the reaction was terminated by directly adding concentrated acetic acid to give a final concentration of 30% acetic acid. To minimise differences in these short incubation times the different samples were processed concomitantly, in groups of eight, using a multi-channel pipette. Scintillation counting and subsequent specific activity calculations were carried out as described for the Classical Kinase Assay.

2.2.14 Immunocomplex Activity and Inhibition Assays

HEK293 cells were reversed transfected with GFP tagged cDNA (see transfection of DNA) and after 36 hours was co-immunoprecipitated using the GFP-TrapM system (see co-IP section). After the final wash of the co-immunoprecipitation the immunocomplexes were resuspended in 40µl of kinase dilution buffer and placed on ice. This provided enough protein for 3 Classical Kinase Assays (10µl each) and 10µl that was mixed with LDS Sample Buffer (x2), separated by SDS PAGE and immunoblotted. In immunocomplex drug inhibition experiments, 30µl of spiked Master Mix containing 100µM ATP, 10mM $MgCl_2$ and 250µg/ml of PKCεPS in substrate buffer was added to 5µl immunocomplex in kinase dilution buffer and 5µl of inhibitor at various concentrations. Scintillation counting was performed and a relative activity was calculated and adjusted for protein loading as determined by densitometry of the resulting Coomasie gel or PKCι immunoblot.

2.2.15 Co-Immunoprecipitation

Immunoprecipitation of GFP tagged proteins was performed using GFP-TrapM. GFP-TrapM is a 13kD single domain antibody from Lama Alpaca that is stable, has a dissociation constant with GFP of 0.59nM and is coupled to magnetic beads. HCT116 or HEK293 cells were seeded (eg. $3x10^6$ HCT116 cells /10cm dish) and transfected (see transfection section) with cDNA in a pEGFP-C1 vector. 36 hours after transfection cells were washed twice in DPBS and then extracted from the dish with Co-Immunoprecipitation Lysis Buffer and a cell scraper. The lysate was incubated on ice for 10mins and then spun at 1300g for 10minutes at 4^oC. The supernatant was transferred to a pre-cooled eppendorf of which 50µl was retained for analysis by Western Blot. The pellet was discarded. The GFP-TrapM beads were washed twice in Wash Buffer and 20µl (original GFP-TrapM volume) was added to the supernatant followed by gentle rotation for 90 minutes at 4^oC. After 3 quick washes with the Wash Buffer the beads were resuspended in 40µl LDS loading Buffer(x2). For protein

identification a high concentration (30µl) was loaded onto a NuPAGE gel and for Western Blotting 5µl of immunocomplexes was loaded onto a NuSEP gel.

2.2.16 Mass Spectrometry

Mass spectrometric was performed by the Protein Analysis and Proteomics Laboratory at CRUK London Research Institute. Co-immunoprecipitation samples were separated by mass on a polyacrylamide gel and protein was stained with GelCode Blue to look for any differences between the experimental conditions. Single differential bands or whole lanes were cut from the gel and sent for analysis.

Polyacrylamide gel slices (1-2 mm) containing the purified proteins were prepared for mass spectrometric analysis using the Janus liquid handling system (PerkinElmer, UK). Briefly, the excised protein gel pieces were placed in a well of a 96-well microtitre plate and destained with 50% v/v acetonitrile and 50 mM ammonium bicarbonate, reduced with 10 mM DTT, and alkylated with 55 mM iodoacetamide. After alkylation, proteins were digested with 6 ng/µL Trypsin (Promega, UK) overnight at 37 °C. The resulting peptides were extracted in 2% v/v formic acid, 2% v/v acetonitrile. The digest was analysed by nano-scale capillary LC-MS/MS using a nanoAcquity UPLC (Waters, UK) to deliver a flow of approximately 300 nL/min. A C18 Symmetry 5 µm, 180 µm x 20 mm µ-Precolumn (Waters, UK), trapped the peptides prior to separation on a C18 BEH130 1.7 µm, 75 µm x 100 mm analytical UPLC column (Waters, UK). Peptides were eluted with a gradient of acetonitrile. The analytical column outlet was directly interfaced via a modified nano-flow electrospray ionisation source, with a hybrid linear quadrupole fourier transform mass spectrometer (LTQ Orbitrap XL/ETD, ThermoScientific, San Jose, USA). Data dependent analysis was carried out using a resolution of 30,000 for the full MS spectrum, followed by eight MS/MS spectra in the linear ion trap. MS spectra were collected with an automatic target gain control of $5x10^5$ and a maximum injection fill time of 100 ms over a m/z range of 300–2000. MS/MS scans were collected using an automatic gain control value of $4x10^4$ and a threshold energy of 35 for collision induced dissociation. LC-MS/MS data were then

searched against a protein database (UniProt KB) using the Mascot search engine programme (Matrix Science, UK) (Perkins et al., 1999). Database search parameters were set with a precursor tolerance of 5 ppm and a fragment ion mass tolerance of 0.8 Da. One missed enzyme cleavage was allowed and variable modifications for oxidized methionine, carbamidomethyl cysteine, pyroglutamic acid, phosphorylated serine, threonine and tyrosine were included. MS/MS data were validated using the Scaffold programme (Proteome Software Inc., USA) (Keller et al., 2002). All data were additionally interrogated manually.

Following identification of peptides in individual samples, a subtractive approach was employed to identify proteins that were specifically purified in the PKCι or PKCι(RIPR>AIPA) pulldowns and not in the control pulldowns. Data were then consolidated by identifying proteins that were both common in independent experiments and abundant (>3 separate unique peptides identified). Candidate immunoprecipitations were carried out to validate the findings (see 2.2.15).

2.2.17 Transfections

The optimal transfection reagents and conditions were determined for individual cell lines as described below.

2.2.17.1 Transfection of Plasmid DNA

Transient reverse transfections of HEK293 and MDCK cells were performed using Lipofectamine 2000 and Poly-L-lysine precoated plates. DNA and lipofectamine 2000 were mixed together in a 1:1 (μg:μl)ratio in Optimen, incubated for 20 mins and added directly to cells recently plated in antibiotic free media. HCT116 and HeLa cells were transfected 24hours after plating using FuGENE HD. DNA and FuGENE at a 1:3 ratio were added to Optimen, incubated for 15 mins and then added to the adherent cells. For

both transfection conditions media was refreshed after 20h and typically further manipulation took place after 36h post transfection.

2.2.17.2 Transfection of siRNA

Reverse transfections of MDCK were performed using Lullaby and Poly-L-Lysine precoated plates. For a six well plate, 25nM siRNA and 10µl Lullaby were mixed together in Optimen, incubated for 20 mins and added to 2-3 $x10^5$ cells/well. HeLa cells underwent reverse transfection using HiPERFECT and 10-20nM siRNA. Media was refreshed at 20h and typically further manipulation took place 72h post transfection.

Table 2.11 Short Interfering RNAs

Name	Source	Target DNA sequence (5'→3')*
HsPKCi.Q5	Qiagen	AACAGGTGGTACCTCCCTTTA
HsPKCi.Q8	Qiagen	ACGCCGCTGGAGAAAGCTTTA
HsPKCi.Q10	Qiagen	CAGATTGTTCTTTGTTATAGA
HsPKCi.Q11	Qiagen	GTGCCGGTACATTTACTTAAA
HsPKCz.Q1	Qiagen	CACCGACAACCCGGACATGAA
HsPKCz.Q3	Qiagen	CACGCGTTCTTCCGCAGCATA
HsPKCz.Q5	Qiagen	CGGAAGCATGACAGCATTAAA
HsPKCz.Q6	Qiagen	GACCAAATTTACGCCATGAAA
cfPKCi.1	Qiagen	AGTTCTGTTGGTGCGATTA
cfPKCi.2	Qiagen	AAGCTCTGATAACCCGGATCA
cfSCRAM.1	Qiagen	AATGAGTGAGTAGTCTTTGCT
cfSCRAM.2	Qiagen	AAGGCCCAACGAAACCATACA
HsPKCi.D4	Dharmacon	CAAAUTCGCATACCACGTT

* The antisense and sense RNA strands were designed based on the Target DNA sequence.

2.2.18 Soft Agar Assay

HeLa cells in log phase growth were trypsinised and resuspended at a concentration of $3x10^3$ cells/ml in 2 x RPMI supplemented with 20% FCS. The cell suspension was mixed in a 1:1 ratio with 0.7% molten agarose cooled to 37°C in a waterbath. 3ml of

the agarose-cell mix was added to each 35mm well that had been pre-coated with 1.5ml of 0.5% agarose. Plates were incubated at 4°C for 20 mins to allow the agarose to set before placing in the 37°C incubator for 10-14 days. Colonies were stained with 0.005% crystal violet for 1h after which images were taken using light microscope (Zeiss Axiovert 40 CFL) and colony number was quantified using ImageJ (version 1.40g) analysis.

2.2.19 Three Dimensional Cultures in Matrigel

The 3D culture of MCF10a and MDCK cells were performed as previously described by the Laboratories of Joan Brugge, Mina Bissel and Keith Mostov (Debnath et al., 2003, Lee et al., 2007, O'Brien et al., 2001) As this technique formed an integral part of the work in this thesis a detailed overview is presented. Further information may be obtained from my methods file stored in the Protein Phosphorylation laboratory.

Cells in log phase growth were trysinised and resuspended in standard media. The cell suspension was mixed well at a 1:1 ratio with standard media supplemented with 4%-low growth factor Matrigel in order to form a single cell suspension with a final Matrigel concentration of 2%. Each well of an 8-well chamber slide was pre-coated with 30µl of 100% Matrigel to which 400µl of the cell suspension-Matrigel mix was added (see table for cell numbers). After 4h a further 300µl of media-2% Matrigel was added. The cultures were maintained for up to 12 days and the media-2% Matrigel was replenished on alternate days.

2.2.19.1 Immunofluorescence

At the end of the assay the media was removed by inverting the chamber slide and the cultures were fixed using 400µl of 2% formaldehyde-PBS for 20 minutes. They were then washed 3 times, for 3 minutes each, with 400µl PBS and gentle agitation. 400µl of permeabilisation buffer was then added followed by 2 further quick washes with PBS.

At this stage the cultures were either directly stained with fluorescent dyes or immunostained.

2.2.19.1.1 Fluorescent Dye staining

Hoechst, TOPRO-3 or Phalloidin dyes were diluted (see table 2.3 for concentrations) in IF-Blocking buffer and incubated with the cultures for 30-60mins at room temperature. After a quick rinse with PBS the cultures were mounted (see below).

2.2.19.1.2 Immunostaining

IF-Blocking buffer supplemented with 20μg/ml F(ab')2 goat anti mouse Fab fragments was added for 1h following which the cultures were incubated with primary antibody diluted in the IF-Blocking buffer/anti-Fab.

Incubation conditions varied for individual antibodies but typically it was overnight at 4^{o}C with gentle agitation. The cultures were then washed 3 times for 10 mins each with IF buffer and incubated with the secondary antibody in IF-Blocking buffer for 1h at room temperature. Subsequent manipulations proceeded under low light conditions to prevent photobleaching. The cultures were washed a further 3 times, for 10 mins each with IF buffer. The cultures could then be counterstained with Fluorescent dyes or proceed straight to mounting.

2.2.19.2 Mounting of chamber slides

Chamber slides were inverted on filter paper to rid of excess buffer. The chamber compartment was cleaved off the slide using the accompanying plastic guillotine and residual liquid at the edge of the slide was removed with a tissue. The specimen was mounted with a hard set mounting medium. To avoid crushing of the specimen a drop

of nail polish was applied to the four corners of the slide and a coverslide was added. The specimens were allowed to cure at room temperature in the dark for 48h prior to confocal imaging.

2.2.19.3 Scoring of Apical Lumen

MDCK cysts that had their F-Actin stained with Phalloidin were visualised with a confocal microscope (Zeiss 510) and an apical lumen assessment made. The middle of a cyst in the z plane was identified and the following criteria applied to determine whether the cyst has a 'predominantly single lumen': 1) there must have been a clear continuous F-actin defined lumen 2) The luminal actin staining must have been more intense than the basal (outside) staining 3) The uni-dimentional measurement of this lumen must have been at least 1/3rd of the cyst diameter and 4) the uni-dimentional measurement of the lumen must have been at least twice the size of any other luminal structure.

2.2.19.4 Image Acquisition of 3D Cultures

High resolution confocal microscope (Zeiss 510) images were acquired using x25, x40 or x63 oil objectives. Typically the images were taken of the middle of a spheroid where the lumen is its largest. To enhance image quality the following parameters were used: 1 airy unit pinhole, low speed imaging, averaging image x8 and a pixel resolution of at least 512x512.

2.2.19.5 Protein Analysis of 3D Cultures

Cells in log phase growth were diluted in 1.5ml of 2% Matrigel-media and pipetted into a 6 well plate pre-coated with 600µl of 100% Matrigel. An additional 1 ml of 2% Matrigel-media was added after 4h and then replenished on alternate days. At the end

of the experiment the media was aspirated and rinsed with ice cold DPBS twice. 2ml of ice cold Matrigel washing buffer was added and using a p1000 pipette with a cut off tip the cell/Matrigel mixture was dislodged and transferred to a pre-cooled 15ml conical tube. This was repeated 2-3 times until all the cell-gel mixture was transferred. The tubes where shaken in the cold room for 1h to dissolve the Matrigel and then centrifuged for 5 minutes at 1000rpm at 4^{o}C. The supernatant was aspirated, 2xLDS loading buffer was added and then the sample was frozen at -20^{o}C

2.2.20 Western Blot Analysis

2.2.20.1 Protein Extraction and SDS Electorphoresis

Adherent cells were washed once with cold PBS and then solubilised using LDS loading buffer (x2). Samples were boiled for 10 mins followed by sonication for 6 seconds to shear genomic DNA. Samples were centrifuged at 13,000rpm for 60 seconds and loaded, along with Rainbow marker, onto a SDS page gel in running buffer. Electophoresis was set to run at 90V (150-80mA).

2.2.20.2 The Transfer of Proteins form the Gel to the Solid Support

Gel sized 3MM filter paper and fibre pads were soaked in distilled water and PDVF membranes were hydrated in methanol. On the black cathode of the mini-transblot cassette was placed: 1)fibre pad 2)Filter paper 3) the gel 4) PDVF membrane 5)the another filter paper and 6)another fibre pad, that was in contact with the red anode. To ensure good contact between the gel and the nitrocellulose any air bubbles were extruded using a plastic tube. The cassette was placed in the Mini Trans Blot Electrophoretic transfer cell containing transfer buffer and a cooling pack and transfer took place in the cold room at 250mA for 2.5h or 100mA overnight.

2.2.20.3 Western Blotting Probing and Development

After electrode disassembly the PDVF membranes were labelled, rehydrated with methanol and placed in 3% BSA-TBST for 1h at RT. The membranes were incubated with primary antibody in 3% BSA-TBST overnight at 4^{o}C (Table 2.1 Primary Antibodies), washed 3 times with TBST and then incubated with species-specific secondary antibody in blocking buffer for 1h. Standard blots were then washed thrice, incubated with ECL solution and immunoreactive bands were visualised by autoradiography on film. On blots where quantification was sought, the Infrared emitting secondary antibodies were used and florescence detected on the LiCOR Oddessy. The quantification of the bands was performed using the Gel function on ImageJ version 1.40g.

2.2.20.4 Stripping and Reprobing Membranes

To allow blots to be re-probed the antibodies (predominately secondary antibodies) were removed from the PDVF membrane by submerging in stripping buffer for 20 mins followed by D_20 washes for 30 mins. At this stage membranes could be re-blocked and the Western Blotting protocol followed once again.

2.2.21 Immunofluorescence

Cells grown on a coverslip or Matex dish were fixed using 4% paraformaldehyde. Cells were permeabilised with 0.5% triton for 10 mins, washed 3 times with PBS and then blocked using 10%FCS-PBS for 1 h. Cells were incubated overnight with primary antibodies in blocking solution, washed 3 times with PBS and incubated with species-specific fluorescent secondary antibody in blocking solution for 1h. The cells were then washed 3 times in PBS and mounted with Prolong Gold.

2.2.22 Short-term Lung Colonisation Assay (STLCA)

Animal experimentation was carried out under the UK Home Office Project Licence PPL80/2329. Animals were maintained in specific pathogen free conditions in the CRUK Biological Resources Unit.

The methods for the STLCA were adapted form those developed by Eric Sahai (Medjkane et al., 2009)(Cancer Research UK). For the assay fluorescently labelled Ras-MDCK cells were used that had been transfected with siRNA 48h before use. PKCι-depleted and control cells ($0.5x10^6$ each and labelled with different fluorophores), were injected into the tail vein of NOD-SCID mice and $5x10^4$ cells from the mix were seeded on a poly-lysine coated Matex dish and fixed in paraformaldehyde as an input control. After 48 h the mice were culled, the lungs dissected, washed in cold PBS and confocal images were taken of the fluorescent cells present in the lungs. The total sum of cell area from at least 10 separate images was derived using Volocity software. A ratio between the control and siRNA treated cells was obtained and this was normalised to the ratio obtained in the input control.

2.2.23 Proliferation assay

10μl of 5mg/ml MTT (3-(4,5-Dimethylthiazol-2-yl)-2,5-diphenyltetrazolium bromide) was added to each well of a 96 well plate and incubated for 30minutes at 37°C. The media/MTT mix was removed by inversion of the plate and tapped 3 times. 50μl of DMSO was added to each well to solubilise the mitochondrial dependent formazan product and incubated for 10mins at 37°C followed by 10mins of agitation at 37°C. The absorbance was measured using a spectrophotometer at 570nm. Linearity of the MTT assay was tested for each cell line by performing a serial dilution of cells and then adding the reagent once cells had become adherent.

Chapter 3. Establishment of a PKCι dependent cancer-related cellular model

3.1 Introduction

Genetic manipulations in Drosophila have identified a clear role for aPKC in cell proliferation and polarity. In mammalian cells, multiple groups have also implicated PKCι in control of proliferation and apoptosis, although these older studies tend to use dominant negative PKCι constructs and non-specific PKC inhibitors. The role of aPKC has often been extrapolated from observing the phenotypic affects of inhibitors such as Gö6983 (inhibits all PKC classes) and BIM1 (inhibits classical and novel PKCs) and any difference between them attributed to aPKC function. Through collaboration with Cancer Research Technology (CRT) access was provided to a number of more specific atypical PKC inhibitors based on a favourable inhibition profile against a commercial kinase panel.

The work conducted in this chapter utilized siRNA/RNAi technology and the novel specific inhibitors in order to confirm or refute the principles of previous published work. The main aim was to identify a robust PKCι dependent cancer associated phenotype.

3.2 Results

3.2.1 HeLa cell proliferation is unaffected by PKCι inhibition

Adherent cell growth has previously been described as being aPKC dependent. Initial experiments set out to confirm these results in a cell model. The HeLa cell line, derived from cervical epithelial cancer, was chosen to study due to its known high PKCι protein expression and its tractability as a cell culture model. HeLa cells were treated for 24, 48 or 72 hours with three structurally distinct PKCι inhibitors. An MTT assay, which was shown to be linear between $2x10^3$ and $7.5x10^4$ cells/well, was used to estimate relative cell number at each time point (figure 3.1A). There was a similar trend for decreased cell number associated with inhibitor treatment at all three time points. The 24-hour time point is represented (see figure 3.1B) but in an analysis of variance no statistical difference was demonstrated. To ensure that a true inhibitor effect on adherent proliferation was not being missed, the cell cycle profile was assessed using fluorescence activated cell sorting analysis (see figure 3.1C). For this analysis adherent HeLa cells were treated with the competitive PKCι inhibitor, CRT66854, at two contrasting doses. At 48h there was no difference in G1/G2 ratio between inhibitor treated and DMSO control cells at either dose. Nor was there a substantial pre-G1 (apoptotic) population of cells. To corroborate these findings, siRNA against aPKC were employed. Maximal knockdown of PKCι in HeLa had previously been demonstrated to occur at 72h (communication from Dr Carine Rosse , Protein Phosphorylation Laboratory). Reverse transfection was performed and the level of knockdown and cell number in a MTT assay were assessed. Up to 75% knockdown of PKCι was attained (see figure 3.1D) but no evidence of any effect on cell number was seen (figure 3.1E).

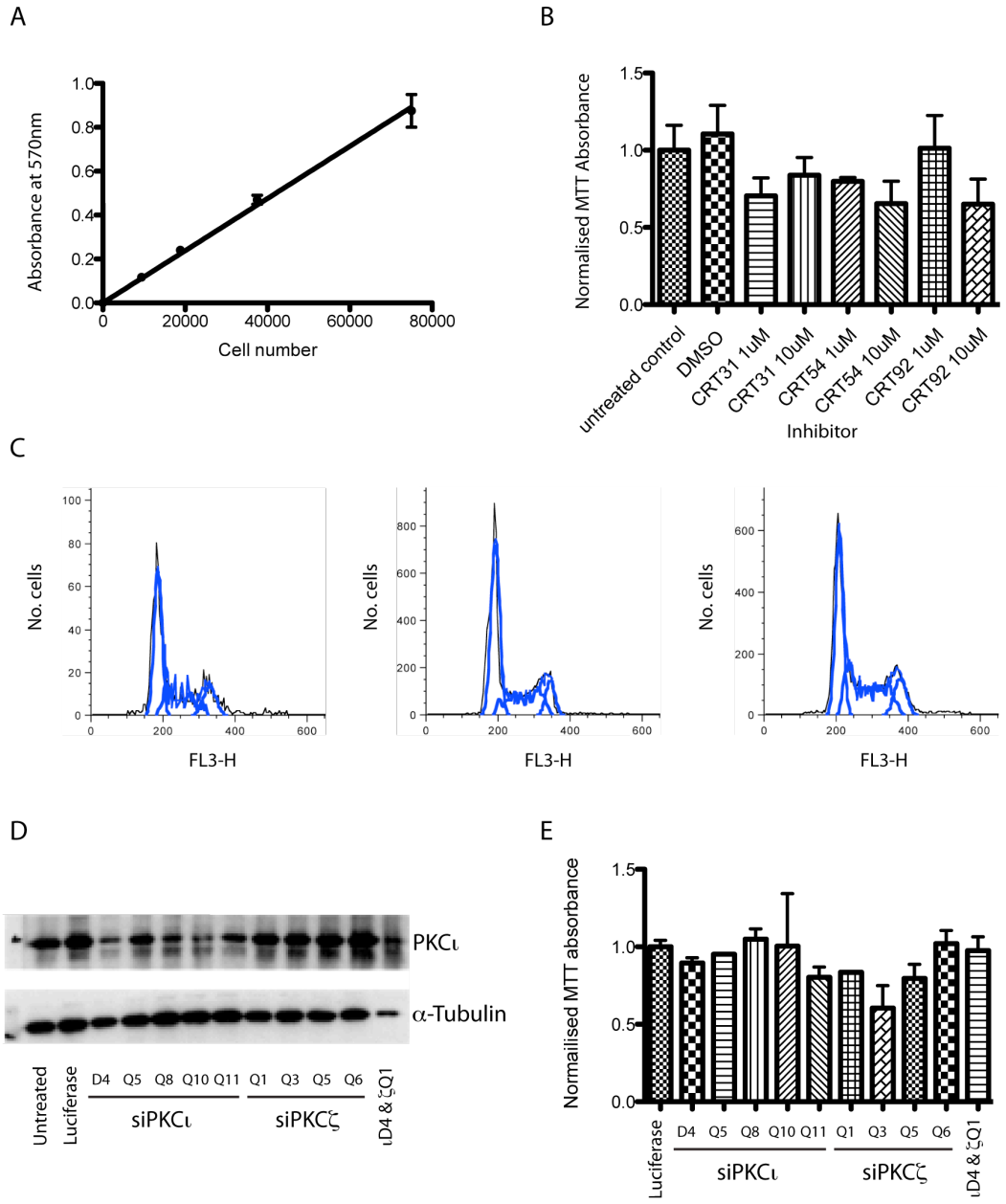

Figure 3.1 PKCι is dispensable for adherent HeLa cell growth.
A, HeLa cells were seeded over a range of concentrations in a 96 well plate and after 2h an MTT assay was performed and absorbance measured at 570nm. B, HeLa cells were seeded at $1x10^4$ cells/well and treated with PKCι inhibitors. Relative cell number after 24 hours of inhibitor treatment was estimated with the MTT assay and the mean ± SEM is presented of 3 separate experiments. C, Cells fixed in ethanol were treated with propidium iodide and DNA content at a wavelength of 670nm (FL3-H) was measured using FACS. Shown are cell cycle profiles for the HeLa cells treated with DMSO (Left panel), 3μM CRT66854 (Middle panel) or 12μM CRT66854. The profiles are representative of 2 separate experiments. D, Western blot of PKCι knockdown by different aPKC siRNAs after 72h of transfection. E, The effect of 72h of siRNA-aPKC on the cell number as determined in an MTT assay. Mean ± SEM is presented of 3 separate experiments. No statistically significant differences were detected.

3.2.2 HeLa cell colony formation is reduced by PKCι inhibition

The most prominent reported role of aPKC is in the regulation of 3D growth and polarity (see section 1.3.5). To test whether PKCι plays a role in non-adherent growth, a soft agar assay was carried out in six well plates. HeLa cells were seeded as a single cell suspension in agarose and treated with 3 structurally distinct atypical PKC inhibitors of varying potency. After 12 days colonies were stained with crystal violet solution, a CCD image was taken (Figure 3.2A) and colony number was estimated using image J software. Initial experiments showed that the automated counting technique was consistent with manual counting of the digital image and was robust for colony numbers of 0 to 400. The higher potency compounds, CRT31 and CRT54, caused a reduction in colony formation even at the lowest treatment concentration of 0.1 μmol whereas the less active enantiomeric pairs, CRT15 and 90, only resulted in a statistically significant reduction in colony formation at 10μM (figure 3.2B). CRT92, a non-ATP competitive compound, was the least potent compound and this was reflected by the low extent of colony growth inhibition. There was a strong relationship between the biochemical inhibition of PKCι kinase activity and the reduction in colony formation in this assay (R^2=0.89, $p<0.05$) (see figure 3.2C). Gö6983 and BIM1 were used at 1μM, which is 15 times and one fifth of their reported IC50s respectively (Gschwendt et al., 1996). At these concentrations it was predicted that Gö6983 would inhibit PKCι whereas BIM1 would not. However, no differential affect on colony inhibition was seen between the two agents. Again, in an attempt to corroborate the findings of a possible aPKC dependence on non-adherent growth, siRNAs against aPKC were used. The siRNA treated cells used in the soft agar assay were also seeded on plastic in a 6-well plate for assessment of the 72h transfection knockdown efficiency. At 12 days there was no difference in non-adherent colony formation. The lack of effect seen with the PKCι siRNA was not unexpected as the half-life of the siRNA is likely to be significantly shorter than the duration of this 12 day soft agar assay and the extent of the knock-down was not complete. This result therefore, while not collaborating the inhibitor induced 3D growth suppression results, is not contradictory.

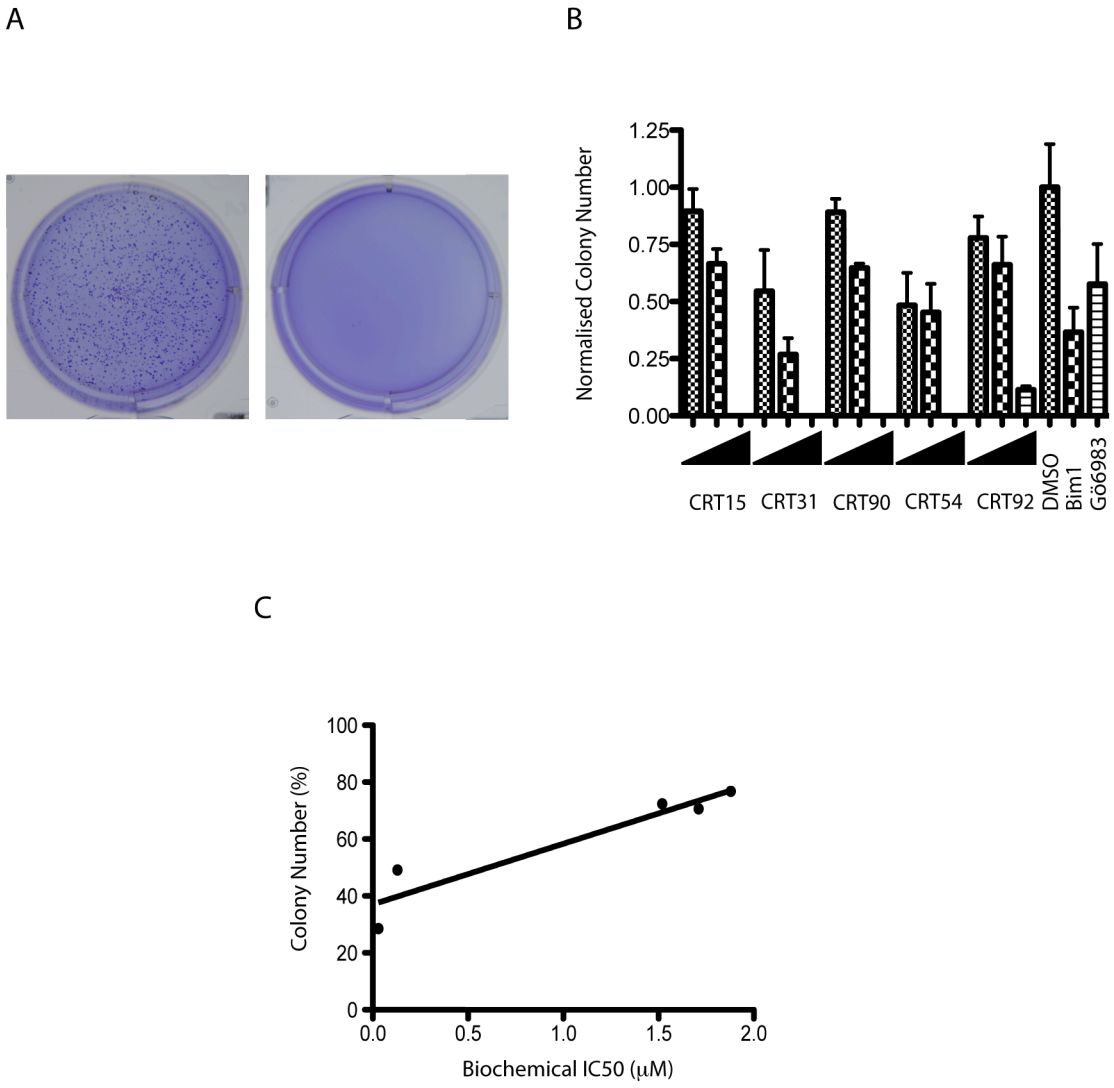

Figure 3.2 Structure-activity relationship of PKCι inhibitors

A, $4.5x10^3$ HeLa cells were cultured in soft agar for 14 days, stained with crystal violet and images of the 35mm well taken using a digital camera with a 18-55mm lens. B, The affect of aPKC inhibitors, replenished on alternate days, on HeLa colony growth was quantified and the mean ± SEM is calculated from 3 separate experiments. Each CRT inhibitor was doses at 0.1, 1 or 10μM as indicated by the increment bar. C, The mean colony number present with 1μM of the CRT inhibitors is plotted as a function of the biochemical IC50. Bim1 and Go6983 are not plotted as their Biochemical IC50s were not evaluated in this experiment. The R^2 calculated from Pearson coefficient is 0.89.

The use of the soft agar assay had provided inhibitor-derived evidence that non-adherent HeLa cell growth is PKCι dependent. Attempts were therefore made to develop a model that could provide morphological information in a physiologically relevant context. The model chosen for development was the growth of MCF10a acini in Matrigel. MCF10a are human non-transformed immortalised mammary cells that recapitulate characteristics of mammary ducts when cultured in Matrigel. Collaboration with the Bentires-Alj Laboratory provided instruction on the assay, some reagents and advice. Using early passage MCF10a cells from the Brugge Laboratory, and in collaboration with the Bentires-Alj Laboratory, 7 batches of low growth factor Matrigel were tested for the characteristic morphological development. While the cells did form spheroids with a clear basal aspect, as demonstrated by α-6-intergrin or β-catenin (basolateral) staining, the spheroids did not demonstrate significant caspase 3 staining or cell clearance in the central region (central apoptosis) which made assessment of the apical domain difficult (see figure 3.3A&B). In addition, the spheroids did not exhibit terminal growth arrest as demonstrated by the persistence of Ki67 staining at days 12 and 18 (Figure 3.3C). In an attempt to identify a cause for this aberrant growth pattern, aside from Matrigel constituents, a separate batch of MCF10a cells (from cell services at the London Research Institute), a different serum batch, a new Epidermal Growth Factor (EGF) batch and a range of EGF concentrations were tried in sequential studies. The optimal EGF concentration for central lumen formation was 5ng/ml, the same as the original protocol (see Figure 3.3D). The serum batch made no difference and the new MCF10a cells demonstrated no lumen formation at all.

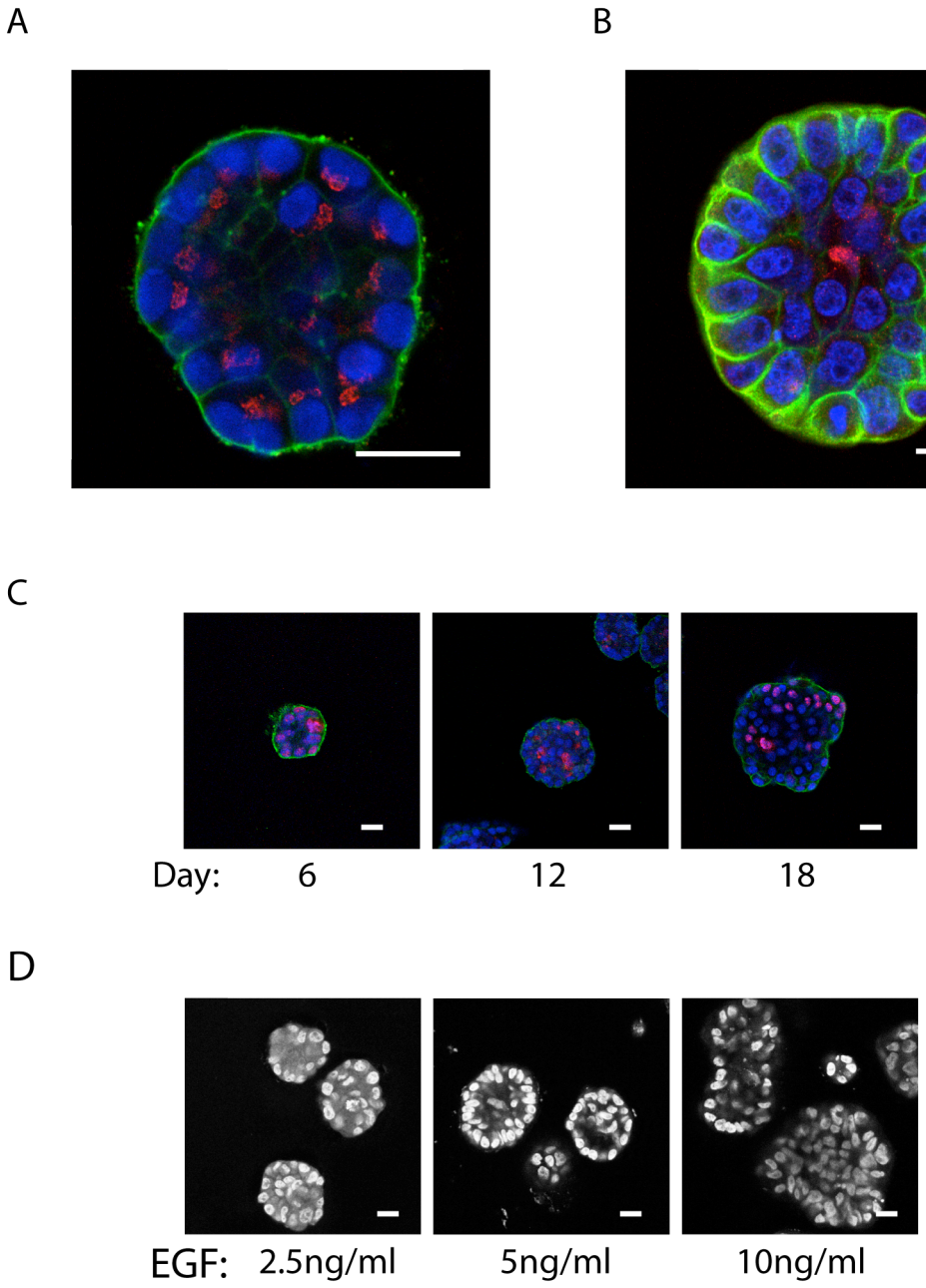

Figure 3.3 Three-dimensional cultures of MCF10a cells on Matrigel
MCF10a cells were cultured on Matrigel in an 8 well chamber slide. Representative confocal images of cross-sections through the middle of acini are shown. Day 8 acini are stained with A, the basal marker α-6-Intergrin (green), the apical marker GM130 (red) and Dapi counter stain (Blue); B, the basolateral marker β-catenin (green), cleaved caspase 3 (red) and Dapi counter stain (Blue). C, Acini cultured for 6, 12 or 18 days were stained with α-6-Intergrin (green), the proliferation marker Ki67 (red) and Dapi counter stain (Blue). D, Acini were incubated with the indicated concentrations of EGF for 12 days and the acini morphology is represented by nuclear staining (white). Scale bars, 20μm.

3.2.3 Attempted long-term knockdown of PKCι

In parallel to the MCF10a studies, RNAi systems for long-term knockdown were explored. The RNAi system investigated was human TRIPZ shRNA from Open Biosytems; constructs that are both doxycycline inducible and have turbo-RFP marker. In order to optimise transfection and induction conditions, prior to embarking on viral infections, 2 constructs were chosen (1 PKCι and 1 PKCζ oligo) and transiently transfected into HEK293 cells. 24h post transfection 2 separate doses of Doxycycline induction was commenced and 48h post transfection tRFP fluorescence could be visualised. There was no difference in the total fluorescence between 1mg/ml and 2mg/ml Doxycycline. In the absence of doxycycline induction no tRFP was detected and the optimal ratio of DNA to transfection reagent (Fugene) was 1:3 (Figure 3.4A). Despite the bright signal only about 10% of cells were positive for RFP. When knockdown of PKCι protein was analysed 72h post induction there was no evidence of protein silencing (Figure 3.4B). In case this lack of efficacy was as a result of the poor transfection efficiency, cells were FACS sorted for RFP after 72h of induction, centrifuged and total cell extracts were made. The FACS sorting confirmed the low transfection efficiency of 10% but there was still no knock down of PKCι protein on an immunoblot using the pure RFP cell population. A further 4 constructs were tested by transient transfection without any evidence of PKCι knockdown.

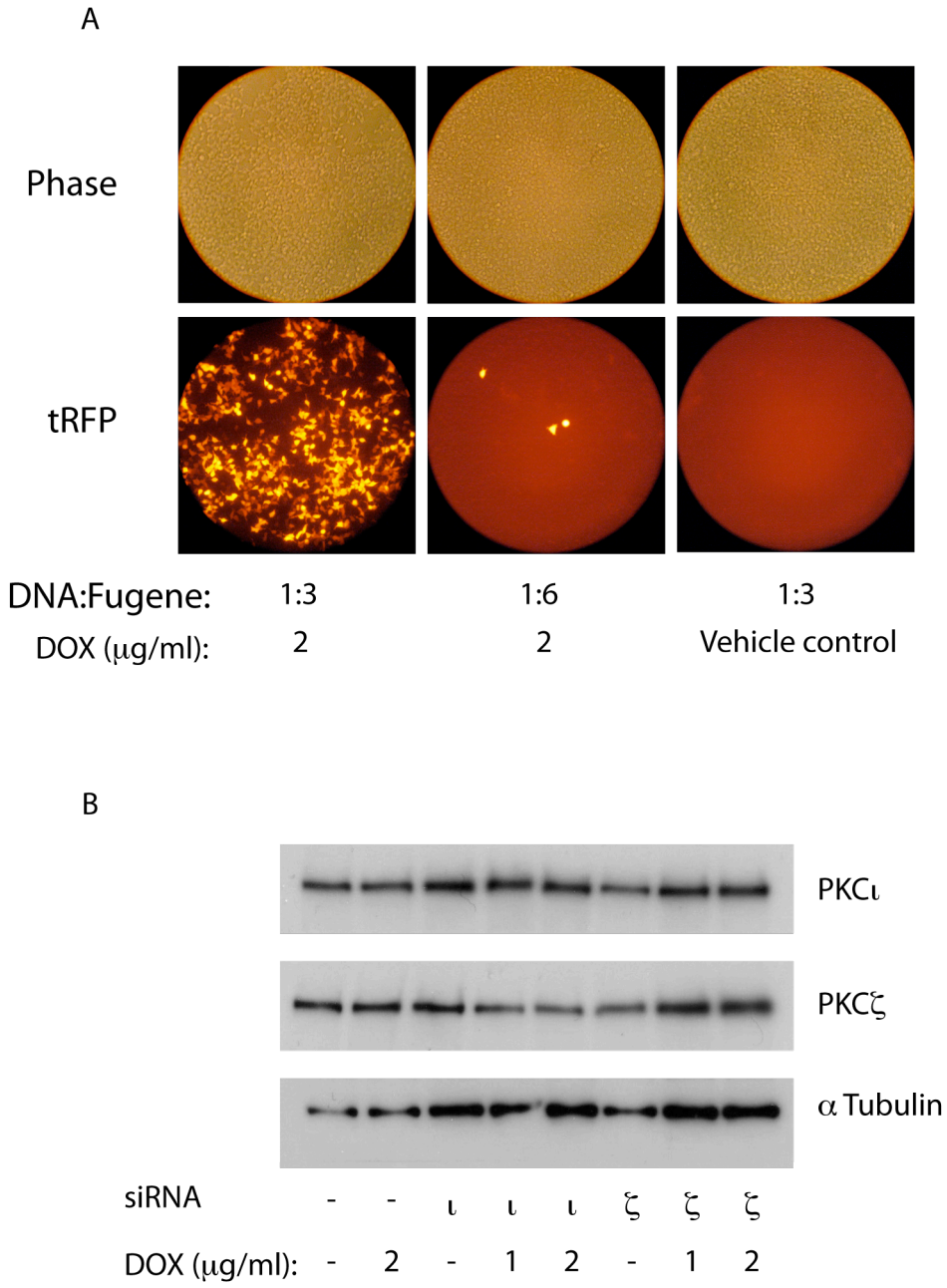

Figure 3.4 Transfection of PKCι shRNA in HEK293 cells.
HEK293 cells were transiently transfected with selected shRNA for PKCι and PKCζ in TRIPZ constructs. A, 24h post transfection the cells were induced with 2mg/ml of doxycycline or vehicle control. The level of transfection was estimated by counting the number of tRFP positive cells in a x10 objective field using an epi-fluorescent microscope. The images presented are representative of 2 separate experiments. B, Knockdown of PKCι and PKCζ were assessed 72h post doxycycline induction by Western Blot. The blots are representative of 2 separate experiments.

3.2.4 MDCK cells grown in Matrigel provide a robust model for apical lumen formation

In view of the significant difficulties in attaining a MCF10a acini model with a well-defined apical lumen, the cell type was switched to Mardin Darby canine kidney cells (MDCK). MDCK have long been shown to be a robust model for cell polarity. Typically, when grown in collagen, these cells develop hollow spheres (known as cysts) that recapitulate the morphological features of the renal collecting ducts from which they derive. To facilitate the use of a siRNA intervention the MDCK cells were cultured in Matrigel rather than collagen as this has previously been shown to expedite cyst formation.

MDCK cells grown in Matrigel rapidly formed cysts that can be identified by phase contrast microscopy as containing an apical lumen as early as 4 days. The lumen becomes more pronounced with time and growth arrest occurred by day 10 (Figure 3.5A). To characterise the apical domain, cysts were stained for actin (phalloidin stain) or labelled with antibodies for ZO-1, GM130 and aPKC, all previously demonstrated to define the apical region (Day6, Figure 3.5B; Day12, Figure3.6A). To enable the antibody staining, MDCK cysts required detachment from the Matrigel using ice cold EDTA-PBS. The detached cysts were then placed on a poly-L-Lysine slide and gently centrifuged (115g) to encourage attachment. The apical pattern of the ZO-1, GM130 and aPKC correspond to the actin staining. Actin and DNA (Hoechst) staining were robust for the Matrigel (Figure 3.5B, Far Right panel). Following centrifugation of the cysts the mechanical force results in slightly flattened cysts at D6 and collapse of the larger D12 structures. This gives the mistaken impression at D6 of incomplete luminal clearance and at D12 of a double ring of cells (Figure 3.6B). Taken together, the data shows that actin staining is representative of the apical lumen, and can be used to robustly stain cysts embedded in Matrigel ensuring retained structural integrity. The combination of actin and DNA staining was therefore used in all subsequent MDCK 3D growth studies.

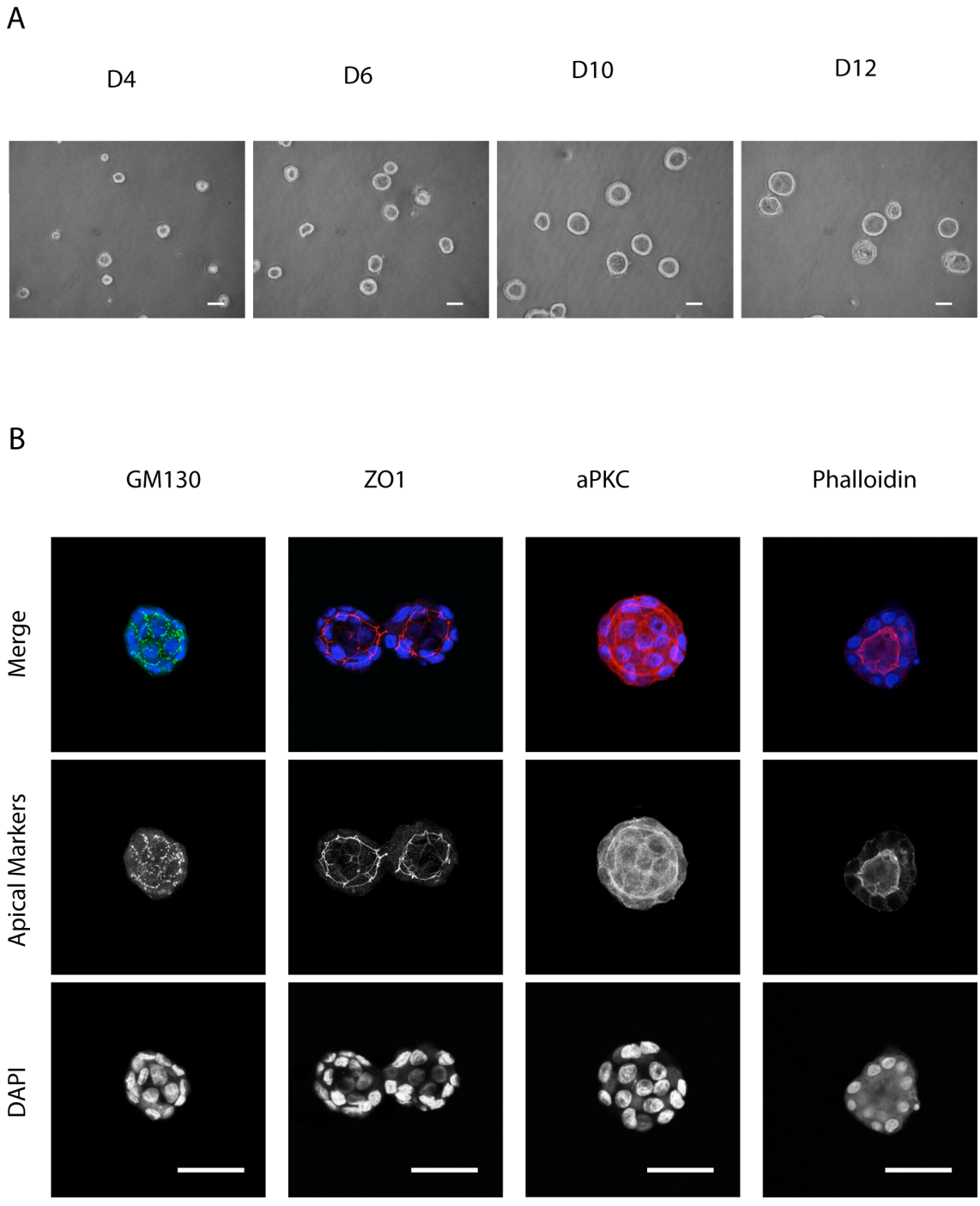

Figure 3.5 Three-dimensional cultures of MDCK cells on Matrigel at day 6
A, MDCK cells embedded in Matrigel form cysts. Phase images were taken at multiple time points as indicated. B, Day 6 MDCK cysts were washed in ice-cold PBS and attached to poly-L-lysine coated slides by centrifugation. The cysts were stained or immunostained for apical markers as indicated. The images are representative of at least 3 separate experiments.

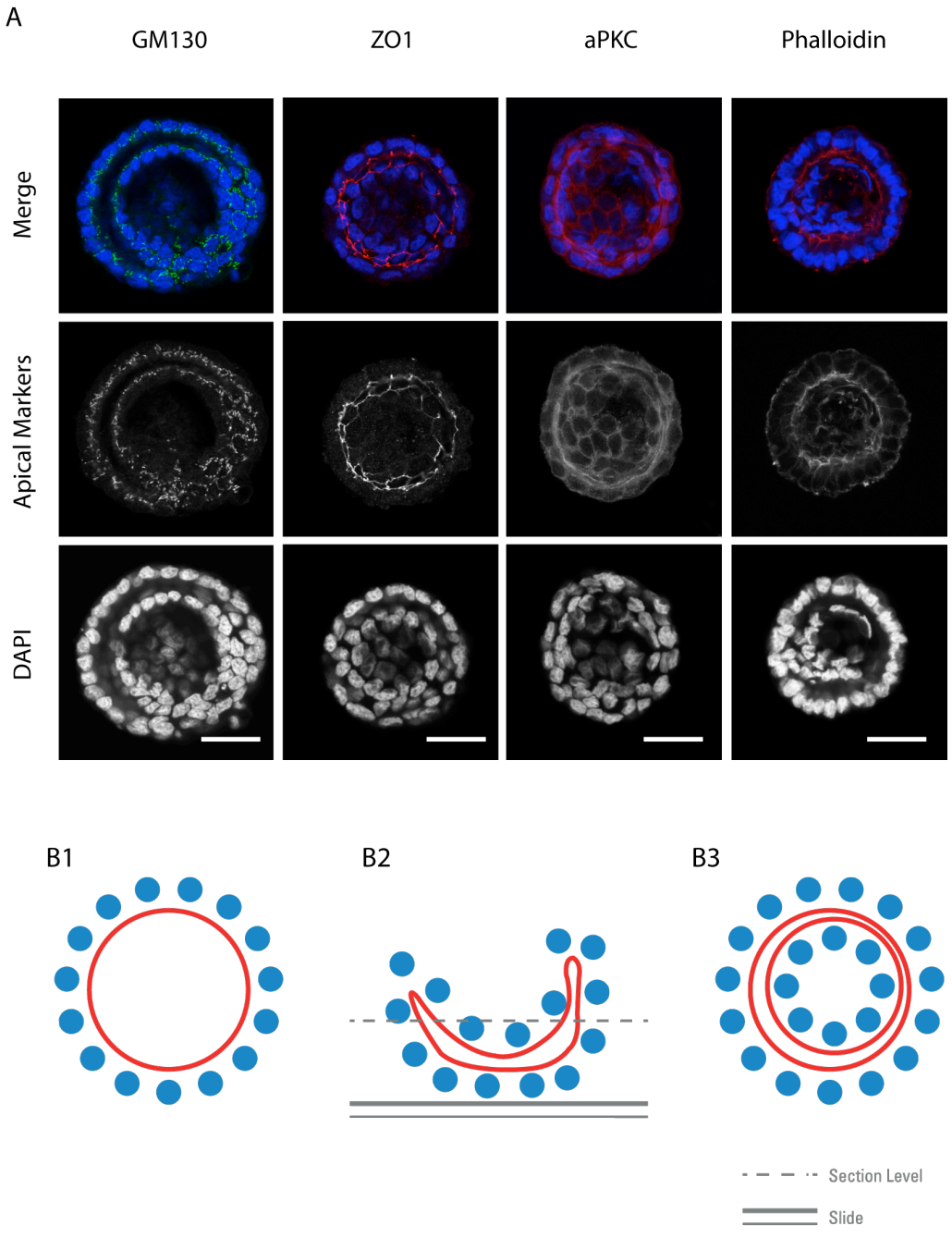

Figure 3.6 Three-dimensional cultures of MDCK cells on Matrigel at day 12.
A, Day 12 MDCK cysts were washed in ice-cold PBS and attached to poly-L-lysine coated slides by centrifugation. The cysts were stained or immunostained for apical markers as indicated. The images are representative of at least 3 separate experiments. B, Schematic depiction of a large MDCK cyst in z-plane revealing the basis of the artifactual double ring cysts. B1, appearance of a MDCK cyst embedded in Matrigel in both X-Y and Z axis. B2, Z-stack appearance of MDCK cyst washed and spun onto the slide. B3, The X-Y appearance of the cyst described in B2.

3.2.5 The altered catalytic activity of PKCι mutants is confirmed by phosphorylation of LLGL2

In order to investigate the role of PKCι in the MDCK model, mutants were generated of wild-type PKCι, constituently active PKCι (A120E) and a kinase dead PKCι (D368N). To test the effectiveness of these mutations an assay was developed exploiting the fact that LLGL2 is phosphorylated by PKCι and antibodies exist for the phosphorylation site. As levels of LLGL2 are low or LLGL2 reagents are of poor sensitivity, exogenous co-expression was required for PKCι-WT induced phosphorylation of LLGL2 to be detected in HEK293 cells. Accordingly, the A120E mutant led to an increased phosphorylation signal and the D368N mutant almost abolished the signal. Transient expression of PKCι constructs showed equal protein expression (Figure 3.7). Moreover, both constitutively active and kinase dead mutants had comparable priming phosphorylation levels to the wild-type, suggesting that mutations did not disrupt the structural competence of the protein.

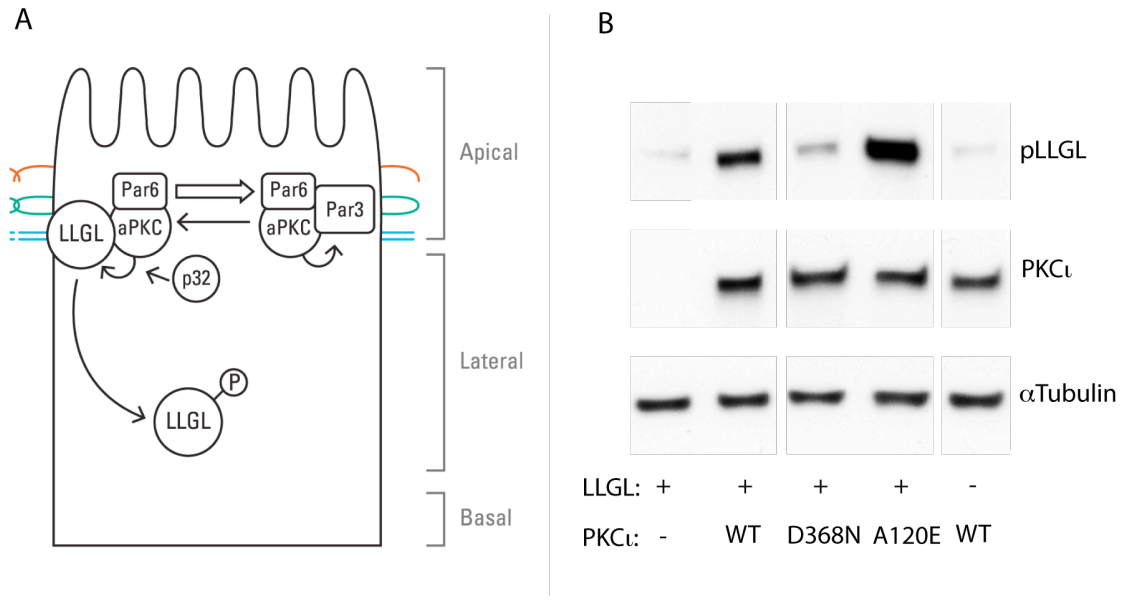

Figure 3.7 Phosphorylated LLGL2 is a marker of PKCι activity.
A, In polarized epithelial cells polarity complexes compete for aPKC interaction and this interaction contributes to complex localisation. aPKC dependent phosphorylation of LLGL, which may be assisted by p32, results in LLGL inactivation and exclusion from the apical cortex of the cell. B, GFP-LLGL and GFP-PKCι/PKCι mutants were co-expressed in HEK293 cells and the affect on phosphorylation of LLGL was measured at 36h. The blot is representative of at least 3 separate experiments. Blot fragmentation is due to editorial removal of bands not relevant to this section.

3.2.6 Altered PKCι expression effects MDCK polarity

The effects of exogenous PKCι, PKCι kinase activity mutants and siRNA knockdown on apical lumen formation in MDCK cysts were investigated. Stably transfected PKCι and PKCι mutant cell lines that were twice FACS sorted for GFP demonstrated equal PKCι protein expression (Figure 3.8A). GFP vector control MDCK cells grown for 6 days in Matrigel form cysts with an actin defined apical lumen in 45% of cysts (Figure 3.8B). For PKCι-WT cysts there was a trend for a higher proportion of cysts with a normal lumen. There was inter-experiment variability and no statistically significant difference was demonstrated. The exogenously expressing PKCι-WT MDCK cysts appeared generally larger. Surprisingly, the A120E and D368N PKCι mutants resulted in a similar phenotype with the loss of normal apical lumen and larger multi-cystic structures. The differences in apical lumen formation were quantified by counting at least 100 cysts per condition per experiment through the eye-piece of the confocal microscope that allowed scanning through the Z axis for each cyst (see figure 3.8B). In keeping with the results for the dominant negative PKCι construct, use of the canine PKCι directed siRNA also disrupted normal acini formation (Figure 3.8D). The level of knockdown was confirmed by western blot analysis using a mouse PKCλ antibody the epitope of which is entirely homologous to both human and dog (Figure 3.8E). Densitometry of the Western blots demonstrated 65% knockdown. Unlike the cysts resulting from over-expression of the dominant negative PKCι, the size of the cysts were observed to be unchanged.

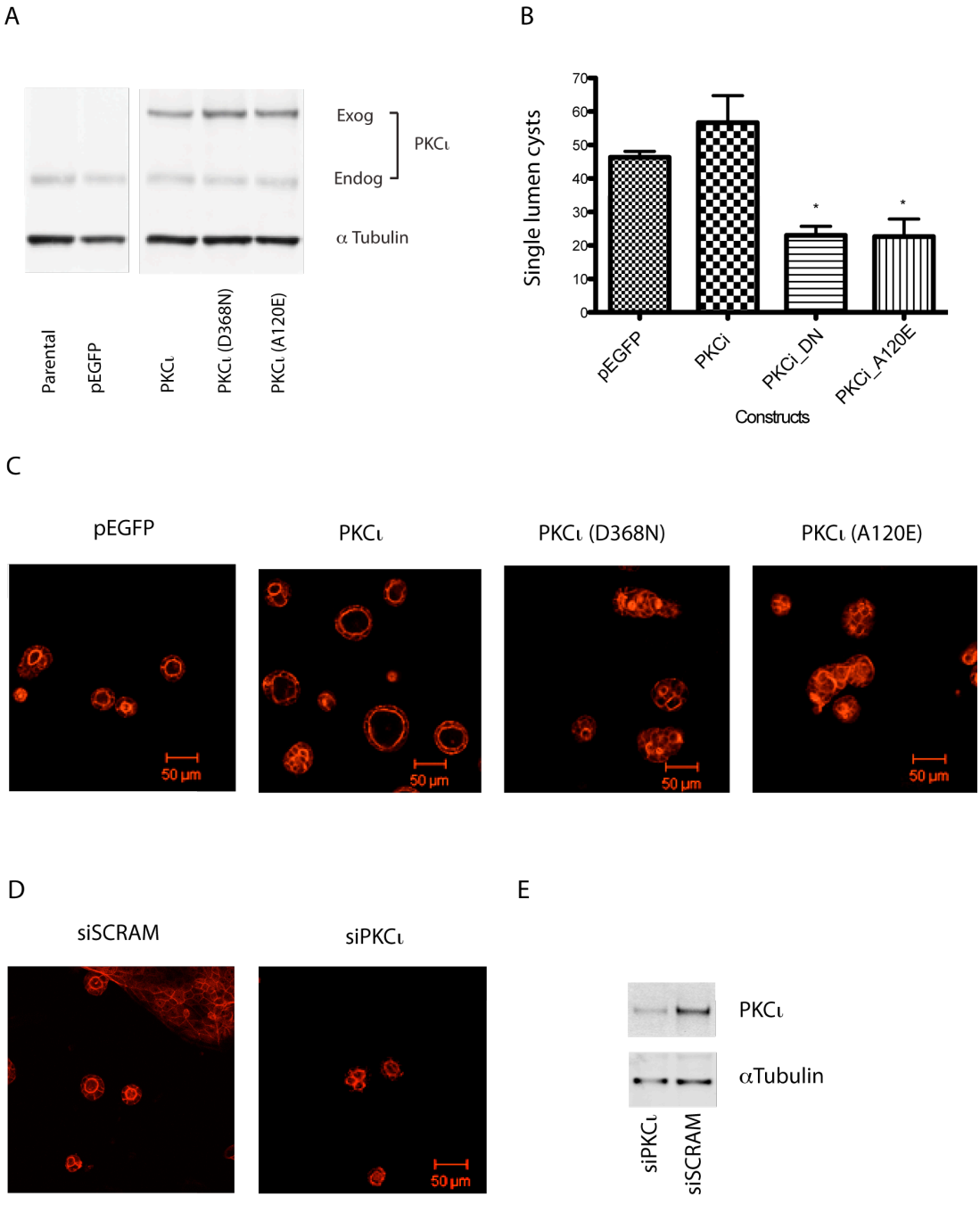

Figure 3.8 Manipulation of PKCι impacts on apical lumen formation in MDCKs.
A, Western blot showing the level of exogenous protein in MDCK cells transfected with PKCι/PKCι mutants. B, Quantification of the number of normal apical lumens. At least 100 spheroids were counted per condition and the results of 3 separate experiments are presented. Error bars represent the SEM. One way ANOVA was used to determine statistical significance of difference *, $p<0.05$. C & D, Representative single confocal images of actin staining (red) are presented. Scale bars represent 50µm. E, Western blot showing the level of knockdown of endogenous PKCι by siRNA. The blot is representative of more than 3 separate experiments.

3.3 Discussion

Using 2 separate systems to perturb PKCι function, chemical inhibition and siRNA knockdown, it was demonstrated that PKCι is dispensable for 2D growth but may play a role in 3D growth. There was a strong structure-activity relationship (SAR) between the known biochemical IC50s of a range of relatively specific PKCι inhibitors and the colony formation in a 3D growth assay, indicating that the PKCι is required for non-adherent growth. The exceptions to the SAR were the competitive inhibitors BIM1 and Gö6983. It was anticipated that at a concentration of 1μM, the pan-PKC inhibitor Gö6983 would inhibit PKCι dependent colony formation but that BIM1, which lacks PKCι inhibition, would not. In fact no difference between the two agents was seen. It is possible that the doses were too low for this analysis as for competitive inhibitors there is typically a 10 to 100 fold drop off in potency in cells compared to the biochemical assay.

This inhibitor-induced effect, however, was not reproduced by the siRNA knockdown. The knockdown efficiency of the HeLa cells used in the colony assay were assessed 72h post transfection in adherent cells in log phase growth. The transfection efficiency of about 70% may be an underestimation as the PKCι antibody also detects PKCζ albeit with a 10-fold lower potency (Appendix 1). Combined knockdown of PKCι and ζ may help address this issue or alternatively mRNA could be assessed although this does not necessarily reflect protein expression levels, probably due to post transcriptional changes (Anderson and Seilhamer, 1997). It is also possible that knockdown efficiency is affected by the 3D matrix and therefore not truly represented in this experiment. The most likely explanation for the lack of colony inhibition, however, is that a short-term intervention was being used in a long-term assay (12 days). siRNA typically has a maximal protein silencing between 2-3 days and duration of action of no longer than 5-7 days. Only if the role of PKCι is critical in the initiation phase of transformed growth would an siRNA induced effect be seen, for example if knock-down led to apoptosis in 3D culture this would have been evident.

This observed difference between adherent and non-adherent growth is consistent with results from the Fields Laboratory who demonstrated that PKCι was necessary for lung adenocarcinoma cell colony formation in soft agar but was dispensable for their growth on plastic (Regala et al., 2005b)(see section 1.3.11). These data are further supported by the finding that transcription is dramatically altered in 3D cell culture compared to 2D. For example, the Eskelinen Laboratory recently demonstrated a robust induction of an additional 118 genes in v-Src transformed MDCK cells in 3D culture compared to 2D (Toyli et al., 2010).

The first attempted technique to investigate the role of mammalian PKCι in 3D growth was the MCF10a 3D morphogenesis assay. This is an elegant assay that has previously been used to study polarity (Debnath et al., 2003, Aranda et al., 2006). Furthermore, MCF10a are immortalized non-transformed human mammary cells that recapitulate the mammary duct architecture when grown in Matrigel. A human study of predominantly invasive ductal carcinomas of the breast had demonstrated a correlation between high PKCι expression and decreased disease free survival (Kojima et al., 2008). During this thesis it was not possible to optimize the model in order to provide a robust polarized morphology. While there are a multitude of possible variables that could account for this failure of technique, the 4 most critical were explored; Matrigel batch, cells, serum and EGF but this proved to be to no avail. It is most likely that the assay was compromised due to Matrigel variability. Matrigel is secreted by Engelbreth-Holm-Swarm (EHS) mouse sarcoma cells, and although a low growth factor version was used, the precise growth factor and protein composition is not controlled for. In hindsight, a critical aspect of this assay is to procure samples of reagents from a Laboratory actively performing the technique. This would help limit the fruitless testing of different variables. A very useful collaboration was established with the Bentires-Alj Laboratory at the Fredrich Miescher Institute(FMI) in Basel and during a visit to this lab the nuances of the technique were demonstrated and a number of reagents were gifted. Unfortunately their working Matrigel stocks, a very precious commodity, were low and could not be spared. It is also well recognised that normal polarization of MCF10a is lost upon cell confluency or late passage. The combination of potential pitfalls makes this assay challenging to set up, an experience shared by a number of different groups

subsequently encountered (personal communications). As the MCF10a polarity assay take at least 12 days, durable shRNA knockdown strategies are necessary. Given the requirements of early passage number and avoidance of confluence for the MCF10a cells, there is a significant risk of clonal drift during longer term culture required for transfection and selection of shRNA. These concerns could be partially negated by the use of inducible shRNAs and without this, MCF10a polarity studies should be viewed with caution.

To develop a long-term knockdown of PKCι it was decided to embrace the up to date shRNA technology and use the Expression Arrest microRNA adapted shRNA (shRNA mir) library. shRNAmir system is based on the endogenous micro-RNA biogenesis pathways. The constructs are designed to mimic natural microRNA primary transcripts, enabling specific processing by the endogenous RNAi pathway and thus more effective knockdown (Stegmeier et al., 2005). The doxycycline induction of turbo-RFP was successful but with no resulting knockdown of the target genes (aPKC). Presumably, despite the launch of whole genome libraries for both human and mouse, the algorithms for developing shRNA-mir sequences are not yet advanced enough. Analogous to siRNA, the development of shRNA-mir may require several years of investigator driven validation. Consistent with this statement and the results fed back to the proprietor, the 7 shRNAs tested during this work have since been withdrawn from sale.

Fortunately, despite being unable to use the MCF10a acini assay, it was possible to directly apply the methodology and reagents to an MDCK cyst assay. Parental MDCK reliably formed cysts with an outer layer of cells and a single lumen that stained with typical apical markers. About 50% of parental MDCK cysts in Matrigel formed with a single lumen. This is consistent with Zheng et al who have also cultured MDCK cells in Matrigel, but substantially lower than reported for MDCK cysts grown in collagen gels (Zheng et al., 2010, Yamanaka et al., 2006). Such differences are not surprising as it has long been recognised that the ECM is critical for cyst morphogenesis. For example, MDCK cells exposed to Hepatocyte growth factor further differentiate into tubes grown in collagen type I, but fail to do so cultured in Matrigel (Santos and Nigam, 1993). Staining of MDCK cysts with antibodies required detachment from the Matrigel and thorough washing. However, Zheng et al were able to stain the apical lumen of

Matrigel embedded MDCK cysts to good effect and there are no reported differences in the growth assay or staining protocol to explain this difference (Zheng et al., 2010).

For functional assessment of PKCι in the MDCK assay catalytic mutants were generated. A point mutation of the conserved pseudosubstrate region within the regulatory domain of PKCι was made (A120E) and has previously been shown to be constitutively active (Pears et al., 1990). For the kinase dead mutant an ATP trans-phosphorylation mutant (D368N) was made rather than the more common mutation of the ATP coordinating lysine (K274M). This action was taken because ATP-coordinating lysine mutants of other PKC family members have been demonstrated to have lower protein expression than wild type PKCs and would not be desirable for functional comparisons. The reason for this has recently been shown to be as a result of decreased protein stability due to lack of nucleotide pocket occupation (Cameron et al., 2009)(see section 1.3.1). The PKCι-D368N kinase dead mutant, that was predicted to bind to ATP, had comparable expression to the PKCι-WT mutant. To validate the (in)activity of the mutant's phosphorylation, a PKCι substrate was sought. Phosphorylation of endogenous LLGL by exogenous aPKC was previously demonstrated by immunodetection of immunocomplexes in HEK293T cells (Plant et al., 2003). In the experiments presented here, phosphorylation of exogenous LLGL2 acted as a good marker of expected activity of the exogenous PKCι proteins and validated the use of the D368N as a kinase dead mutant. Unless more sensitive and specific antibodies to pLLGL1/2 are generated, it is unlikely that endogenous LLGL phosphorylation could be used as a marker of PKCι activity (biomarker).

Over-expression mutants of PKCι have a profound impact on apical lumen formation in MDCK cells. While over-expression of wild type PKCι demonstrated a trend to an increased proportion of cysts with a normal apical lumen, over-expression of the constitutive active PKCι or kinase dead PKCι mutant led to a significant reduction in the proportion of normal apical lumen cysts. The reduction in apical lumen formation was also seen with siRNA-aPKC gene silencing. These data suggest that that PKCι may demonstrate multiple-threshold signalling for polarity. Such multiple-threshold signalling usually requires coordination of several signalling pathways that are linked

by negative and/or positive feedback mechanisms (see section 1.2.7). Intriguingly, there is the possibility that the regulation of polarity is distinct to the growth regulation, as while use of siRNA PKCι disrupted apical lumen formation and had no effect on cyst size, the dominant negative PKCι construct disrupted apical lumen formation but led to increased growth of the multi-cystic structures. One explanation for such a difference may be that growth signalling is dependent of a PKCι scaffold function, whereas the apical lumen formation requires the catalytic activity. Uncontrolled secondary effects of the forced over-expression of the PKCι constructs should also be considered, for example the localization of the over-expressed protein could be erroneous and sequester proteins required for normal polarity signalling away from the endogenous PKCι.

The activity of PKCι has been difficult to assess in vivo. Unlike other AGC kinases, the PKC family of kinases are constitutively phosphorylated at the activation loop and this is therefore likely to be an unreliable marker of activity. At the current time, over-expression of activity mutants remains an important tool in the characterization of PKCι behaviour. The identification of robust biomarkers of PKCι activity is the subject of chapter 6.

In summary, a model of MDCK cell 3D morphogenesis in Matrigel has been established and shown to be PKCι dependent. Due to the relatively short duration of the assay, it is amenable to both stable and transient transfection interventions. Manipulation of PKCι in the MDCK cyst model has suggested possible threshold signalling of polarity.

Chapter 4. PKCι is a downstream effector of oncogenic Ras that controls MDCK polarity

4.1 Introduction

PKCι is has been reported to be over-expressed in human malignancy (Regala et al., 2005b, Eder et al., 2005). In the previous chapter it was suggested that there is a PKCι threshold requirement for normal MDCK cystogenesis, a system commonly used to evaluate polarity. A number of studies have demonstrated an association of aPKC and bona fide human oncogenes such as PI3 Kinase, Ras, Raf, ErbB2 and Src (see section 1.3.3.3). Little is know about potential role of PKCι in collaboration with these oncogenes in the regulation of epithelial cell polarity. Results from a genetic screen in *D.melanogaster* suggested that aberrant expression of polarity genes alone led to tumour formation whereas the cooperation between aberrant polarity gene expression and oncogenic Ras led to invasive and metastatic tumours (Pagliarini and Xu, 2003). The aim of this chapter was to establish whether literature-based candidate oncogenes led to PKCι dependent abnormal polarity in the MDCK model.

4.2 Results

4.2.1 Oncogene expression in MDCK cells disrupts morphology

MDCK cells cultured on plastic grew as epithelial clusters and at confluence adopted a cobblestone appearance (Figure 4.1A). MDCK variants that expressed V12-H-Ras, p110a-CAAX and v-Src activated oncogenes became more fibroblastic in appearance and lost their direct cell-cell contacts. This phenotype was most pronounced in V12-H-Ras MDCK. The MDCK cells that expressed Raf-CAAX and ErbB2 activated oncogenes grew in 2-D as epithelial sheets, but unlike the parental line, small epithelial clusters or islands were not seen even at low confluence.

To identify if the oncogenes impact on normal MDCK cyst formation in 3D, cells from the oncogenic MDCK cell panel were cultured in Matrigel. All the oncogenic MDCK

cells tested resulted in larger cysts or aggregates. In particular V12-Ras-MDCK, ErbB2-MDCK and p110a-MDCKs grew as large spherical aggregates that lacked an apical (central) lumen and an apical actin ring. The v-Src cells developed with a large central lumen surrounded by a ring of smaller lumens. The Raf-CAAX cells formed as large but otherwise normal cysts (Figure 4.1A). As many of these structures derived from the oncogenic MDCK cell panel were not cysts, the collective term of oncogenic MDCK spheroids is used for the remainder of this thesis.

4.2.2 Oncogenic MDCKs do not have altered expression of PKCι

As the oncogenic MDCK spheroids had clear differences in their ability to develop an apical ring and lumen the possible role of PKCι in this process was explored. Firstly the defining protein expression (for example v-Src or ErbB2) of the respective oncogenic MDCK cells was determined. With the exception of p110α a strong signal was seen for their defining protein for each member of the oncogenic MDCK cell panel (see figure 4.1B). Appropriately, phosphorylation of Src at tyrosine 527, that is inactivating and absent in the v-Src mutant, was not elevated in the v-Src-MDCK cells. Using a p110α antibody a 110kD band was detected in each of the oncogenic MDCK cell lines from the panel, but this was not elevated in the p110α-MDCKs. There was, however, a unique unknown band in the p110α-MDCK at 65kD. Total PKCι levels were similar between the parental MDCK cells and the oncogenic MDCK cell panel. Phosphorylation of the activation loop of PKCι at Threonine 403 is a possible marker of PKCι activity but this was also uniform for the MDCK cell panel and parental MDCK. To identify whether PKCι expression or phosphorylation at T403 was altered in the context of 3D cultures, protein was harvested from the Matrigel cultures but the immunoblots using the resulting total cell extracts were un-interpretable as they had significant background and poor detection of PKCι.

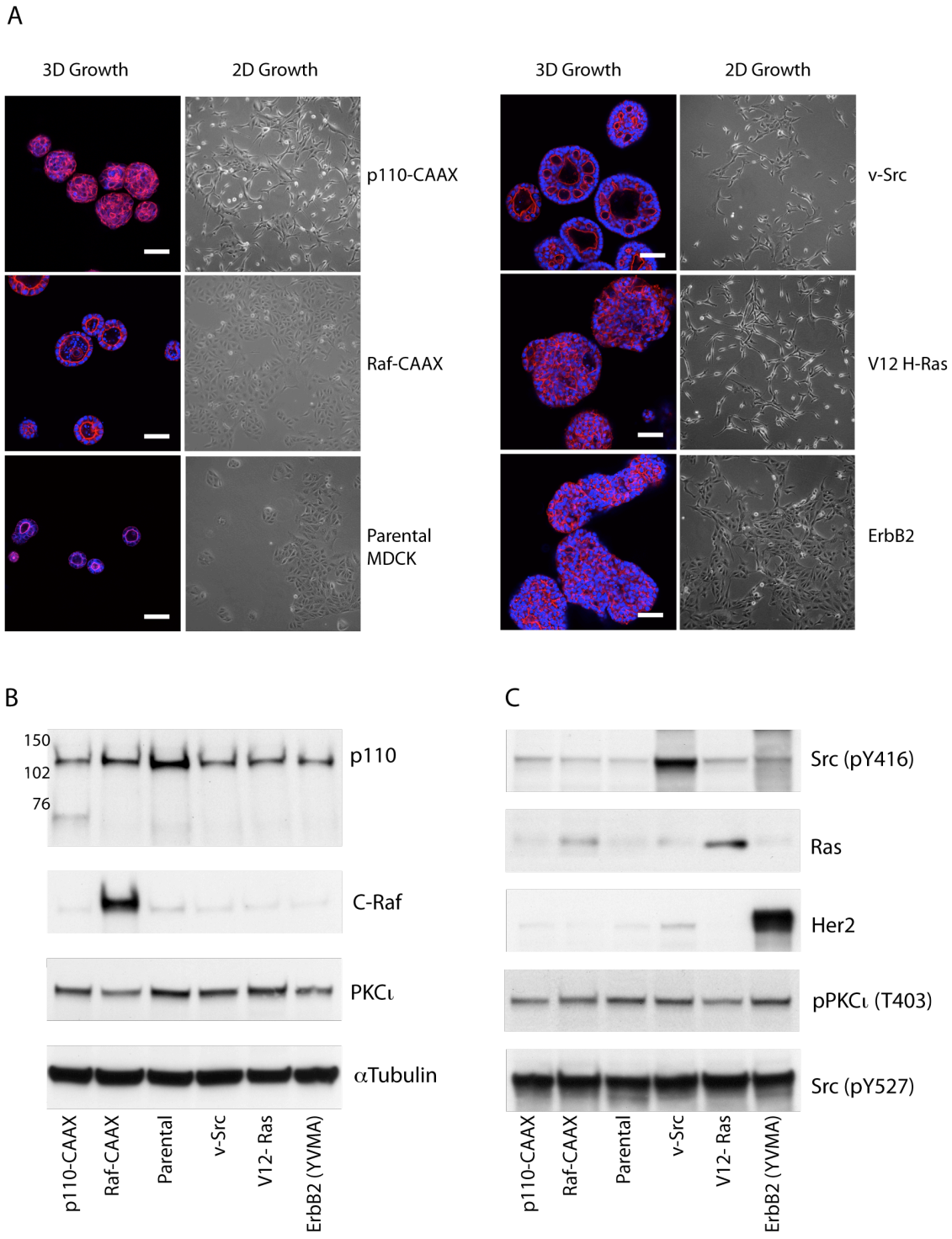

Figure 4.1 Characterisation of Oncogenic MDCK cells
A, MDCK cell variants cultured in Matrigel (3-D) for 6 days alongside phase images of their growth in 2-D. Phalloidin (Red) stained Actin and Hoechst (Blue) identified nuclei. Scale bars represent 50μM. B, Lysates of MDCK cell variants in log phase growth were immunoblotted for defining proteins.

4.2.3 Knockdown of PKCι in H-Ras and ErbB2 spheroids restores an apical lumen

To test further whether PKCι is involved in signalling downstream of key oncogenic proteins a siRNA approach was adopted to transiently knock down PKCι in the oncogenic MDCK series and then culture in Matrigel for 6 days. Initial experiments showed that the best transfection efficiency without significant cell death was obtained at 72hours using Lullaby transfection reagent. The knockdown efficiency of two separate siRNA oligomers ranged from 30% to 80% depending on cell type (see figure 4.2B).

Oncogenic spheroids treated with siRNA-PKCι compared to scrambled control siRNA were generally smaller and had a distinct appearance with regards to their apical actin ring. In a pilot study the apical rings of ErbB2 spheroids with and without siRNA-PKCι were analysed and differential criteria were defined – predominantly single apical lumen (PSAL) (see section 1.2.19.3).

In both H-Ras and ErbB2-MDCK, knockdown of PKCι resulted in smaller spheroids with significantly more PSALs (see figure 4.2A). The v-Src spheroids were smaller in size and lost many of the small lumens in the outer ring. They continued to have a PSAL and therefore no differences between siRNA-PKCι and scrambled siRNA were scored. Although this trend was consistent between experiments the magnitude of the effect was variable between experiments, which is reflected in the wide standard error of the mean.

There was no difference in PSALs between Raf spheroids with and without PKCι knockdown. The percentage of spheroids with PSAL was uniformly high at about 80%. It is worth noting that the average knockdown of PKCι in Raf-MDCK cells was the lowest among the oncogenic MDCK panel although at this level an effect on proliferation was still seen. In the p110 spheroids, there was no difference in PSAL between the siRNA-PKCι and scrambled control but unlike the Raf-MDCK spheroids apical lumens were rarely present.

Upon PKCι knockdown of the parental MDCK cells the spheroids remained a similar size but had a PSAL in less than 50% spheroids. This is compared to over 70% in the group treated with the scrambled control siRNA.

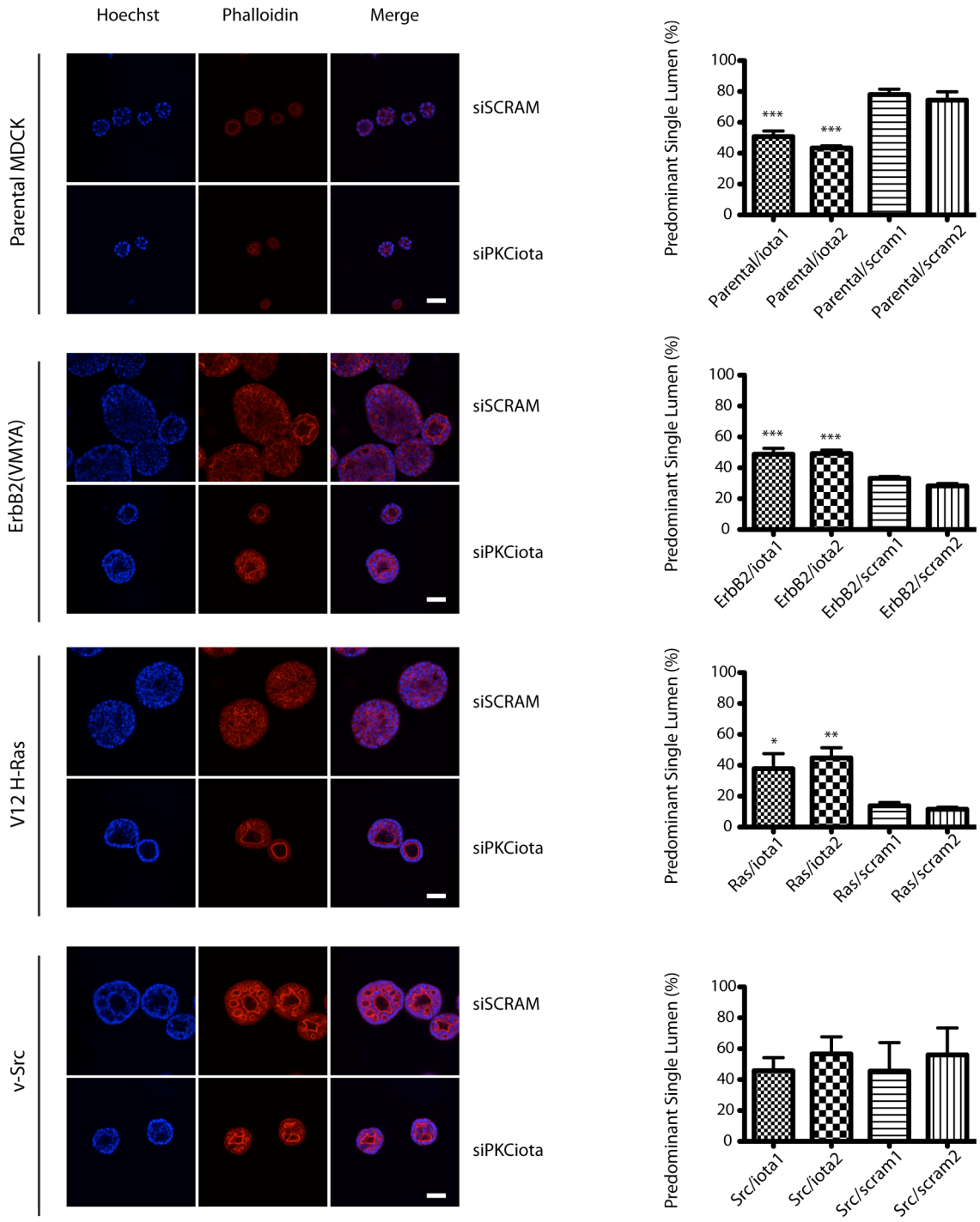

Figure 4.2 (PANEL 1) The effect of PKCι knockdown in oncogenic MDCK.
LEFT COLUMN, MDCK variant cells treated with siRNA-PKCι for 24h prior to culture in Matrigel for 6 days. Single confocal images with phalloidin (Red) stained actin and Hoechst (Blue) identified nuclei. Scale bars represent 50μm. RIGHT COLUMN, Quantification of number of Predominantly Single Apical Lumens (PSALs). The x-axis is labelled with the cell type and siRNA used. At least 100 spheroids were counted per condition and the results of at least 3 separate experiments are presented. Error bars represent the SEM. One way ANOVA was used to determine statistical significance of difference between PKCι knockdown and the scrambled controls ; *, $p<0.05$; **, $p<0.01$; ***, $p<0.001$.

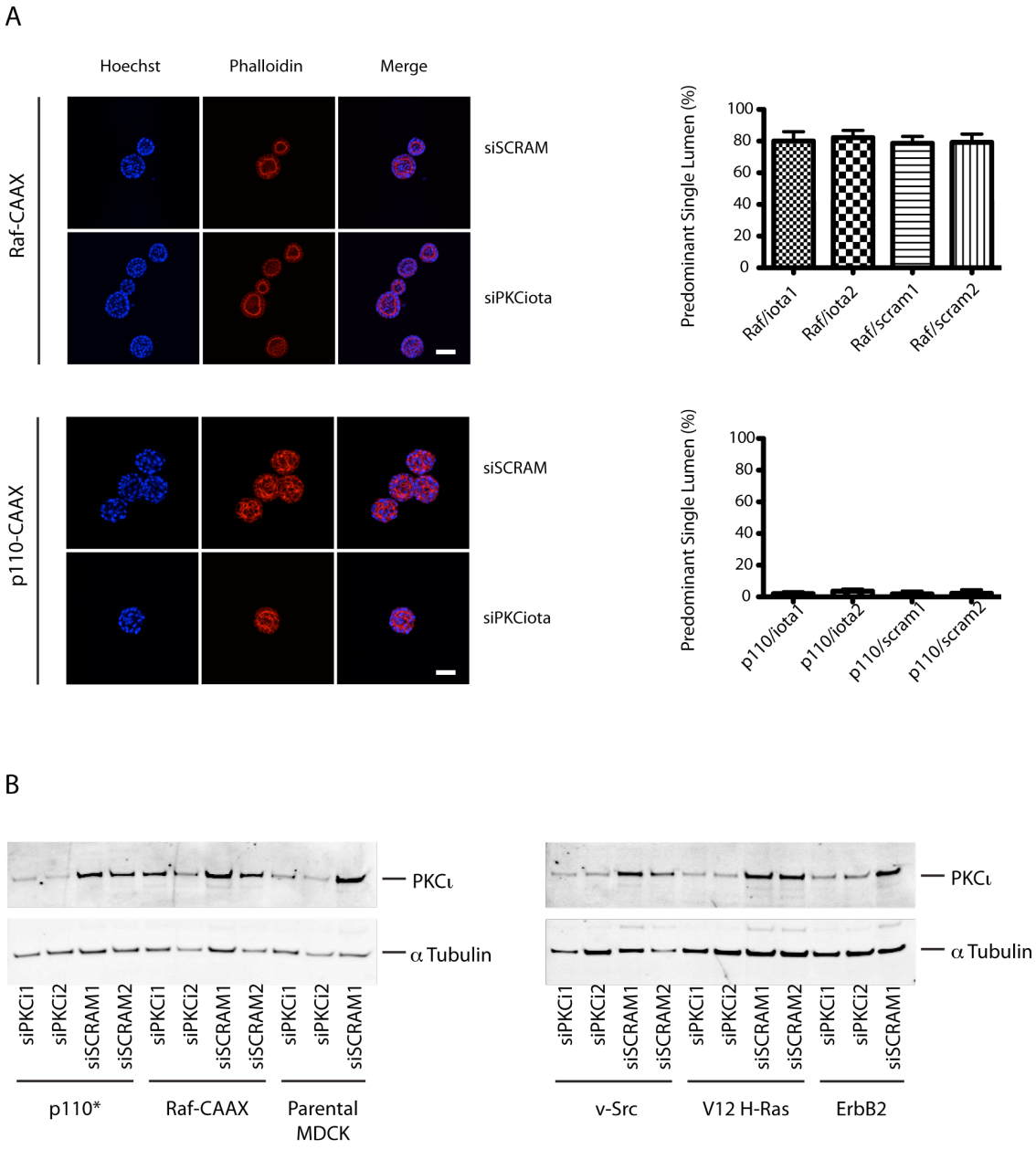

Figure 4.2 (PANEL 2) The effect of PKCι knockdown in oncogenic MDCK.
A (LEFT COLUMN), MDCK variant cells treated with siRNA-PKCι for 24h prior to culture in Matrigel for 6 days. Single confocal images with phalloidin (Red) stained actin and Hoechst (Blue) identified nuclei. Scale bars represent 50μm. A (RIGHT COLUMN), Quantification of the number of Predominantly Single Apical Lumens (PSALs). The x-axis is labelled with the cell type and siRNA used. At least 100 spheroids were counted per condition and the results of at least 3 separate experiments are presented. Error bars represent the SEM. One way ANOVA was used to determine the statistical significance of any differences between PKCι knockdown and the scrambled controls ; *, $p<0.05$; **, $p<0.01$; ***, $p<0.001$. B, MDCK variant cells treated with siRNA-PKCι for 24h were seeded in 6-well plates and total cell extracts were prepared after 48h (72h post transfection). The Western blot is representative of 3 separate experiments.

4.2.4 Expression of PKCι can partially rescue the PKCι-siRNA induced lumen formation

To determine the specificity of the siRNA utilised in the knockdown studies an attempt was made to rescue the siRNA induced phenotype with siRNA resistant cDNA of PKCι (see figure 4.3). The interspecies sequence differences were exploited as the human PKCι sequence was distinct from the canine siRNA-PKCι sequences used and should therefore be resistant. In view of the emerging data to support a functional interaction between oncogenic Ras and PKCι and the implications that this may have for human malignancy the H-Ras-MDCK cell line was selected to test the rescue experiment. H-Ras-MDCK cells were transfected sequentially, first with siPKCι and then after 24 hours with the human cDNA for PKCι. The co-transfection with siPKCι.1 and cDNA-PKCι resulted in considerable cytotoxicity and as such it was not possible to achieve co-transfection with this oligonucleotide.

Following co-transfection of H-Ras-MDCK cells with siPKCι.2 and empty vector, there was a three-fold increase in the number of spheroids with a predominantly single apical lumen (PSAL) compared to the scrambled control (Figure 4.3C). When the Ras-MDCK cells were treated with siPKCι.2 and cDNA-PKCι the increase in spheroids with PSAL was less than 2 fold. Addition of PKCι to scrambled control had little effect on the number of PSALs. Thus a good partial rescue of the siRNA- PKCι induced phenotype with cDNA-PKCι was attained.

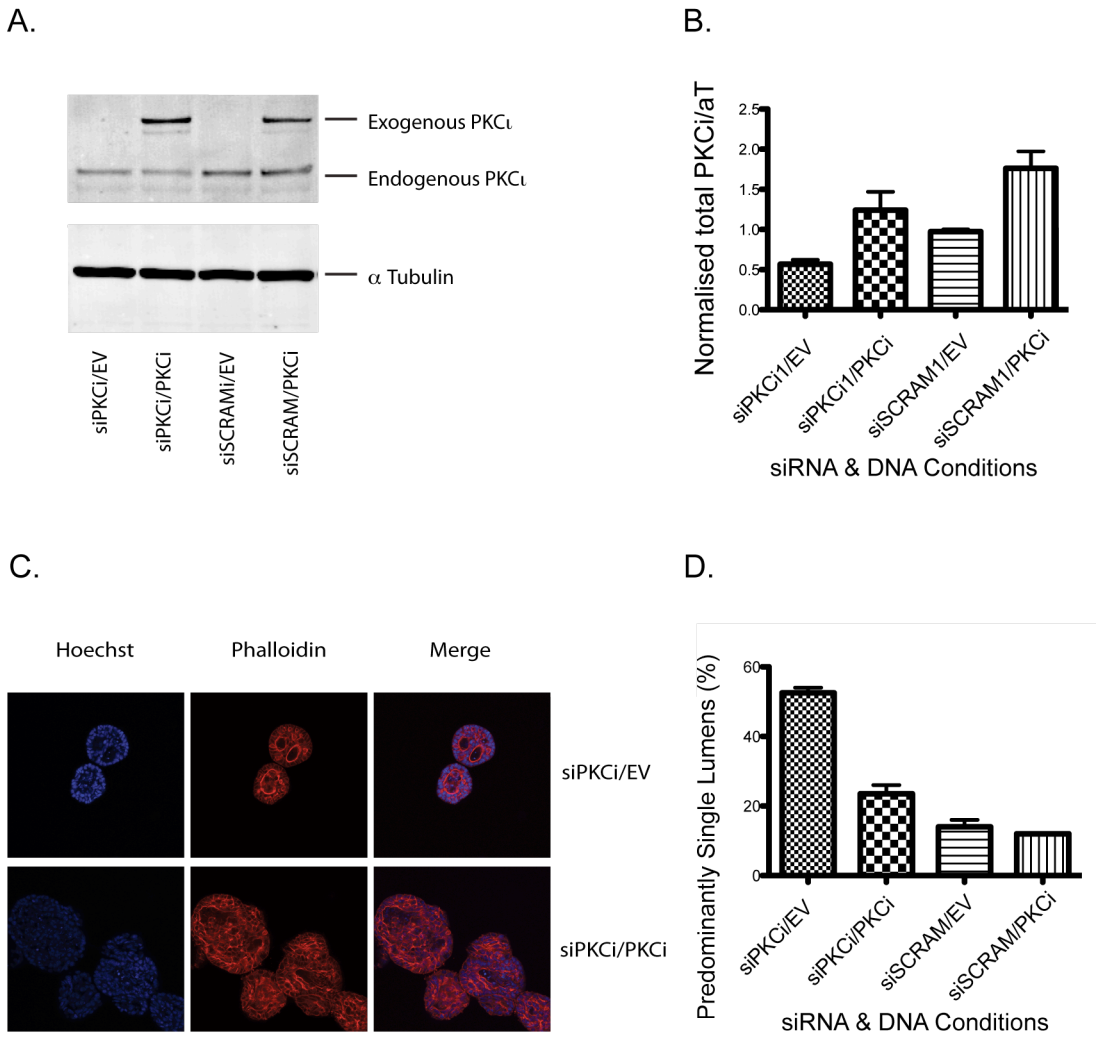

Figure 4.3 PKCι rescue system

A, H-Ras-MDCK cells were sequentially transfected with siRNA-PKCι followed by siRNA resistant PKCι-cDNA. Cells were seeded in 6 well plates and total cell extracts made after 24h. The levels of endogenous PKCι knockdown and GFP-PKCι over-expression were determined by Western blot using the LiCOR system. B, densitometry was performed on the resulting blots. C, the sequentially transfected cells were seeded in Matrigel and after 6 days were fixed and stained for actin (Red) and DNA (blue). Representative single confocal images are presented. D, Quantification of the number of predominantly single lumens is shown. At least 100 spheroids were counted per condition and the results of 3 separate experiments are presented. EV, Empty vector.

4.2.5 PKCι inhibitors can restore apical lumens in MDCK cells

To attempt to further characterise PKCι as an essential component of polarity signalling downstream of Ras in MDCK spheroids, PKCι chemical inhibitors were employed. H-Ras-MDCK spheroids were grown in Matrigel in the presence of either Gö6983, a pan-PKC inhibitor, or CRT66854, a structurally distinct atypical PKC inhibitor. Inhibitors were added on the day of seeding a single cell suspension in Matrigel and replenished on alternate days for 6 days. The inhibitor doses used for compounds were determined based on their individual, previously defined cellular EC50s. Both inhibitors phenocopied the siRNA-PKCι intervention resulting in the induction of apical lumen formation in the spheroids and a reduction in the spheroid size (see Figures 4.4A&B). The maximal effect of Gö6983 on PSALS was at 2μM resulting in a 6 fold increase. At a dose of 3.6 μmol there was extensive cell death making scoring of apical lumens unfeasible. The maximal proportion of PSALs was seen with CRT66854 at the lower dose of 1.2 μM. Above this dosing level the apical lumen formation was impaired and extensive cytotoxicity occurred at 3 μM (see figure 4.4C&D).

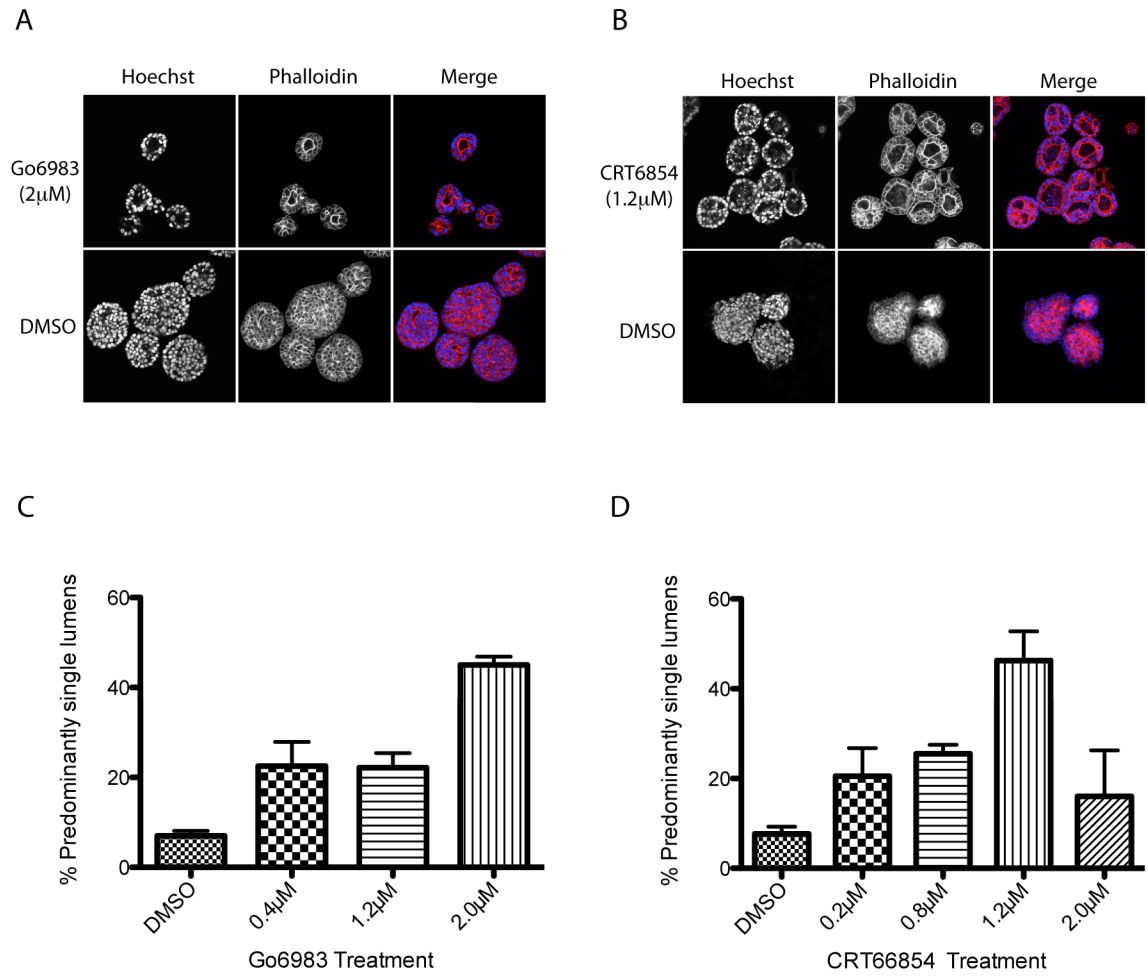

Figure 4.4 PKCι inhibitors induce lumen formation in H-Ras-MDCK spheroids.
H-Ras-MDCK were cultured in Matrigel for 6 days and treated with inhibitors at a range of concentrations. Representative single confocal images of H-Ras-MDCK treated with; A, 2.0μM Go6983 and B, 1.2μM CRT66854 is presented. Spheroids were fixed and stained for actin (Red) and DNA (blue). C&D, Quantification of number of Predominantly Single Apical Lumens (PSALs) at different inhibitor concentrations. At least 100 spheroids were counted per condition and the results of at least 3 separate experiments are shown.

4.2.6 Short-term lung colonisation of H-Ras MDCK cells may be PKCι dependent

As loss of normal polarity is associated with high-grade, poorly differentiated tumours and epithelial to mesenchymal transition we hypothesised that restoration of polarity in H-Ras cells, by knockdown of PKCι, may lead to fewer lung metastases. H-Ras or v-Src MDCK cells were injected subcutaneously into the flank of NOD-SCID mice. The H-Ras group developed rapidly growing tumours at the site of inoculation and required culling at day 22 as they had reached the permitted maximal tumour burden ($1.44cm^3$). The time from detection of a palpable tumour to maximal tumour burden was only 6 days. No lung metastases were detected following Hematoxylin and Eosin (H&E) staining at multiple levels. V-Src MDCK tumours grew considerably slower with a median time to maximal tumour burden of 6 weeks. Again no lung metastases were detected in these mice.

In view of the rapid growth of the H-Ras MDCK cells we postulated that there was insufficient time for the cells to invade and intravasate into blood vessels. To overcome this, a short-term lung colonisation assay was performed. H-Ras-, vSrc- and parental MDCK cells were transfected with GFP-pBABE or Cherry-pBABE empty vectors and selected with puromycin to generate stable fluorescent cells lines. Initial investigations were carried out to detect whether lung colonisation occurred 48 hours after tail vein injection using the fluorescent cell lines. At this time point a high burden of fluorescent cells was seen in the H-Ras MDCK group but no lung colonisation was apparent for the mice injected with v-Src or parental MDCK cells.

The effect of PKCι-siRNA knockdown in H-Ras MDCK cells on lung colonisation was tested relative to scrambled control-siRNA. If for example, the GFP-H-Ras MDCK cells were treated with PKCι-siRNA then the Cherry-H-Ras MDCK cells were treated with siRNA-scrambled control. The experiment was also conducted with the coloured labels switched, i.e. PKCι-siRNA in the Cherry cells and scrambled-siRNA in GFP. 48h after transfection a 1:1 mix of the two conditions was injected into the mice tail veins. After a further 48h the ratio of siPKCι.2 to siScrambled was decreased suggesting a reduction in lung metastasis when PKCι is depleted. This finding,

however, was not corroborated with a second oligonuclotide (PKCι.1) and in fact the inverse result was observed.

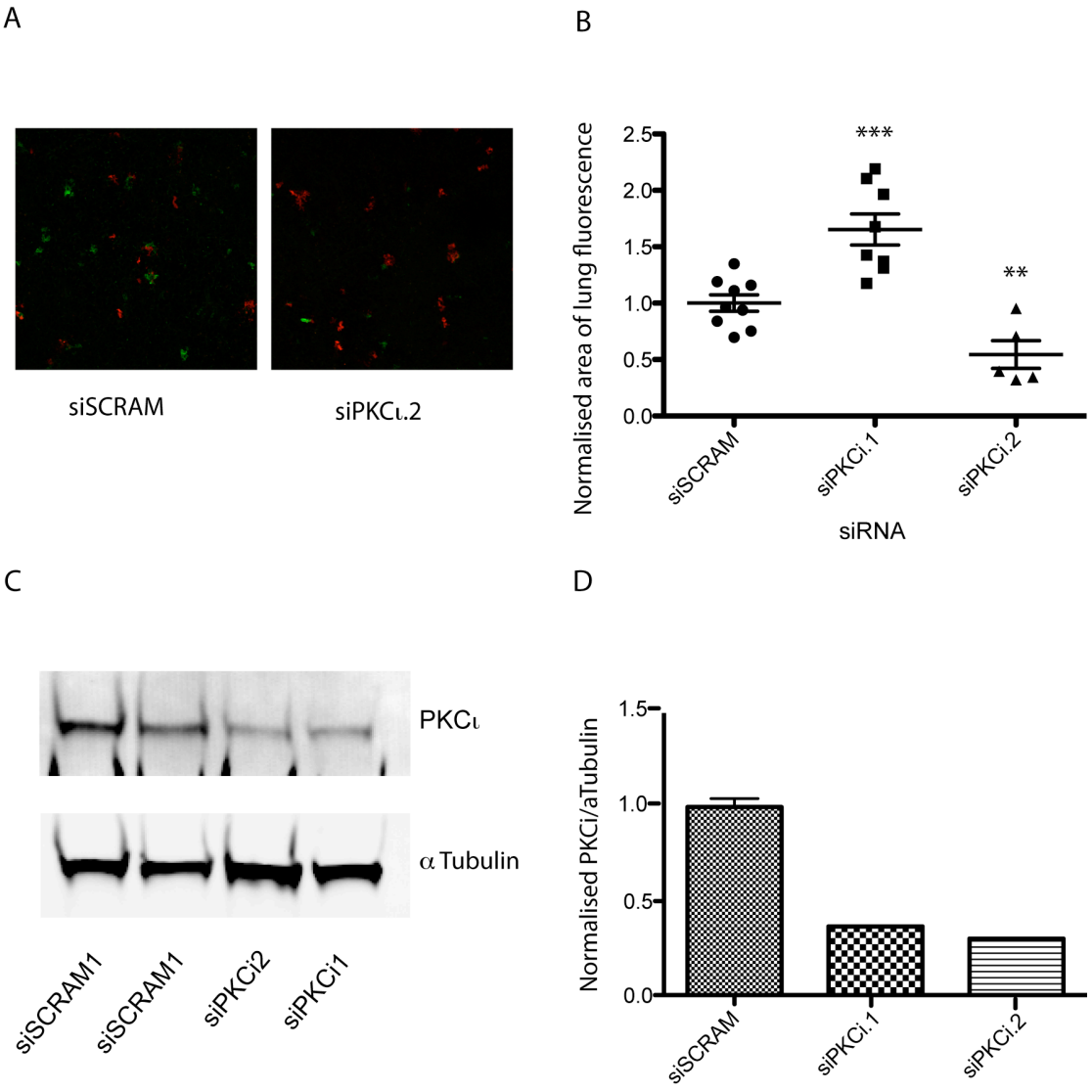

Figure 4.5 Short term lung colonisation may be affected by PKCι knockdown.
A, Fluorescently labelled H-Ras-MDCK cells transfected with siPKCι or siScrambled control were injected into mice tail veins. Representative confocal images (x0.7 magnification) of the lungs 48h post injection are presented. Control siScrambled cells (Red & Green, LEFT) and control (Red) and siPKCι (Green) cells (RIGHT). B, For quantification of lung colonisation the sum area of at least 10 separate images per mouse was calculated for both green and red cells. At least 5 mice are presented for each condition in at least 2 separate experiments. One way ANOVA was used to determine the statistical significance of differences between PKCι knockdown and the scrambled control ; **, $p<0.01$; ***, $p<0.001$. C, the level of knockdown was confirmed by Western blot and D, normalised densitometry was calculated.

4.3 Discussion

MDCK cells that over-express activated H-Ras, C-Raf, p110α, v-Src and Her2 proteins grow with an altered morphological appearance in 2-D and have clearly distinguishable morphologies in 3-D. Using an assessment of predominantly single apical lumens (PSAL) as an indicator of polarity it was demonstrated that the aberrant polarity of H-Ras MDCK and ErbB2-MDCK spheroids could be partially reversed by knock down of PKCι using two separate siRNAs.

Uniform knockdown of PKCι was not achieved between the different cell lines with the more fibroblastic cells (H-Ras, p110α and v-Src) having a better transfection efficiency. The level of knockdown did not exceed 80% for any of the MDCK cell lines despite observing phenotypic effects. From screening of the PKCι antibodies against recombinant PKCι and PKCζ it was demonstrated that the most specific PKCι antibody still cross-reacted with PKCζ at about one tenth of the potency (see appendix 1). It is possible that the knockdown efficiencies are higher than reported and that some of the residual protein identified is in fact PKCζ. The reverse cross-reactivity existed for the preferred PKCζ antibody making it difficult to test out this theory for protein expression. The siRNAi.2 silenced PKCι with greater efficiency than PKCι.1 but this difference in knock down did not correlate with the extent of polarity reversion. This lack of correlation could be explained by a threshold effect (as discussed in chapter 3). For example, in this case if both knockdowns reach the threshold a comparable phenotype rather than one that is proportional to the knockdown level is seen. C-Raf expressing spheroids maintained normal polarity. The c-Raf cells had a poor transfection/knock-down efficiency with both PKCι oligonucleotides. Therefore it may be concluded that activated c-Raf does not drive apical lumen disruption in MDCK cells but the role of PKCι in polarity signalling downstream of c-Raf remains uncertain. This finding may well be cell type specific as it has recently been published that an inducible, activated kinase domain of c-Raf is able to disrupt apical-basal polarity in non-transformed human mammary spheroids (s1 cells) (Beliveau et al., 2010). Using a completely different model system, Raf was also required for establishing dorsoventral polarity during Drosophila development (Brand and Perrimon, 1994).

In this thesis the aberrant polarity induced by activated P110α was not dependent on PKCι. Confirmation of the 110 kD protein expressed in these cells was not obtained. This was not unexpected as the p110α subunit of PI3K requires binding to the p85 subunit to form a stable heterodimeric complex (Yu et al., 1998). The mesenchymal appearance, compared to the epithelial control, provides a level of confidence that this is indeed the p110α over expressing cell line but mRNA expression should be sought to confirm this. Others have demonstrated that the addition of Ly294002, the pan PI3K inhibitor, is able to reverse the disrupted polarity of T4-2 spheroids, derived from a human mammary tumour (Liu et al., 2004). This effect may be cell type specific, due to inhibition of other PI3K isoforms or could be due to greater functional inhibition by the inhibitor as compared to siRNA.

Although multiple oligonucleotides had demonstrated the same phenotype, we set about minimising the risk of off target siRNA effects by performing a rescue experiment. Sequential transfections proved too toxic for experiments involving siPKCι.1. The cDNA transfection reagent used, Lipofectamine 2000, is toxic at low seeding densities and following the slight antiproliferative effect of PKCι.1 the combination of PKCι knockdown and overexpression resulted in cell death. SiPKCi.2 transfection, followed by overexpression human PKCι cDNA gave a good partial rescue of the siRNA phenotype providing a further level of confidence as to the PKCι specific function downstream of Ras in polarity signalling.

Further evidence of an atypical PKC dependent process was provided by inhibitor experiments. Both Gö6983 and CRT66854 were able to revert the aberrant polarity of H-Ras MDCK cells. The dose required for maximal phenotypic effect was higher for Gö6983 than CRT66854. This is not consistent with the reported biochemical IC 50s for these drugs that is 60nM for Gö6983 (Gschwendt et al., 1996) and 161nM for CRT66854 (Barton et al., 2009a). This discrepancy may be a consequence of inhibitor cell permeability, the dosing strategy, drug metabolism or differences in the in vitro kinase assay protocol compared to the published studies. In this experiment media/inhibitor was empirically replenished on alternate days but little is know about the most appropriate dosing strategy or whether these drugs accumulate in Matrigel. In

addition, it is possible that other members of the PKC family, which are also inhibited by Gö6983, impact on polarity signalling.

H-Ras disrupts polarity in MDCK and this may be mediated by PKCι. The three most notable isoforms of Ras (H-Ras, K-Ras and N-Ras) share similar catalytic domains and are thought to differ by virtue of their membrane association and thus activating partners. The G12V-Ras mutant used in this study is insensitive to inactivation by GAP, remains bound to GTP and is therefore constitutively active. In this G12V-Ras form the isoform differences are blurred and it is commonly referred to as oncogenic Ras.

The short-term lung colonisation assay is a useful model to test acute interventions, such as siRNA and single doses of inhibitor, in vivo. The readout from the assay (relative lung fluorescence) is a composite endpoint of multiple processes that occur during metastases but after intravasation; anoikis, endothelial adhesion, invasion and proliferation within the lung. To minimise the impact of proliferation on the readout the lungs were examined 48 hours after tail vein injection. To control for any differences in the number of GFP and mCherry labelled H-Ras-MDCK cells injected into the mouse, cells were plated on a Mattex dish, allowed to adhere overnight, fixed and examined by a confocal microscopy. The results obtained from the lung were then adjusted for this input control. This does make an assumption that the interventions are not having a significant effect on proliferation in the short term Mattex dish culture. To circumvent this problem cells could be seeded onto Poly Lysine and immediately fixed or alternatively the cell populations could be assessed by Fluorescence-activated cell sorting (FACS). The results of this colonisation experiment showed opposing effects for the two PKCι oligonucleotides. To uncover if this is due to off target effects further PKCι oligonucleotides, an in vivo rescue of a siRNA phenotype experiment or an independent mode of intervention (inhibitors) should all be considered. The preliminary results obtained after treatment with CRT66854, an atypical PKCι inhibitor, are consistent with siPKCi.2 (validated by rescue in vitro) in that it decreases early lung colonisation. This experiment was performed by 12 hours inhibitor treatment prior to tail vein injection at which time it would be anticipated that the competitive inhibitor disengages from the PKCι complex. In carrying out this experiment therefore, an

assumption was made that this period of inhibitor pre-treatment was sufficient to alter the transcription of the PKCι signalosome. This could be tested by RNA based micro-arrays over a time course. Alternatively the phosphorylation of an abundant PKCι substrate could be monitored, if such a molecule could be identified. The *in vivo* rescue would be technically difficult and would require a large cohort of mice. Currently the use of further PKCι oligonucleotides in the short-term lung colonisation assay are planned.

PKCι has been associated with polarity signalling in model organisms, human neuroblasts and in migration studies see Chapter 1. Separately, PKCι protein expression has been shown to be prognostic in a number of human malignancies and in a mouse cancer model to function downstream of K-Ras. This study provides, for the first time, the evidence that PKCι dependant polarity signalling is downstream of oncogenic Ras in mammalian epithelium. PKCι is currently one of the most hotly pursued targets in early stage drug development . Target validation has relied on non-adherent growth assays. Whilst these are extremely important in drug development, in the absence of a robust PKCι biomarker, they are susceptible to the common antiproliferative off-target effects of siRNAs and shRNAs. An MDCK polarity assay provides defined morphological information that is likely to be more target-specific than 3D growth alone. The results obtained in this study may also prove valuable for stratification of patients likely to benefit from anti- PKCι therapy, particularly selecting patients with oncogenic Ras and ErbB2. Preliminary *in vivo* results suggest that the strategies to reverse aberrant polarity in vitro may correlate with a decrease in early experimental lung metastasis. The mainstay of treatment of localised primary tumours is surgical resection but it is well recognized that despite expert surgical technique, surgery itself can lead to the dissemination of microscopic disease (Sheen et al., 2004). The *in vivo* results therefore, if confirmed, would point to a possible role for peri-operative anti-PKCι treatment that would be predicted to reduce tumour recurrence.

Chapter 5. Identification of an aPKC-specific recruitment site for LLGL, essential for MDCK polarity

5.1 Introduction

The recent crystal structure determination of PKCι bound to the CRT66854 inhibitor by the Structural Biology Laboratory (SBL) at the LRI defined (1) a detailed interaction map of contacts between chemical ligand and PKCι (2) identified a putative protein interaction motif within the PKCι C-lobe as discussed below. Collaboration with the SBL has provided unique insights into the structure of PKCι and therefore a platform for functional assessment. An intriguing aspect of the 66854-bound PKCι kinase domain structure was the nature of the crystal contacts within the crystal lattice. Each of the three copies of PKCι within the crystal asymmetric unit made equivalent contacts from an Arg-Ile-Pro-Arg motif (RIPR; amino acids 471 to 474) from the C-lobe of one molecule to the B-helix within the N-lobe of an adjacent symmetry-related molecule (see figure 5.1A). This interaction involved a network of hydrogen bonds involving one of the arginine side-chains, phospho-T403, the B-helix and the second arginine making contacts close to where a gamma-phosphate of ATP would lie (see figure 5.1B). Surprisingly, the motif lies between the H and I helices at exactly the same position on the EGFR that makes a trans-activating contact in a trans-activating EGFR dimer. The symmetry contact in PKCι also stabilises the B-helix, which is partially unfolded and not helical in all other PKCι structures (Takimura et al., 2010, Messerschmidt et al., 2005). In contrast, the B-helix is well formed in all previously determined AGC kinases. It was therefore hypothesised that this RIPR motif could be an important protein-protein interaction determinant and may be involved in stabilising a higher-order PKCι kinase structure that plays a crucial functional role.

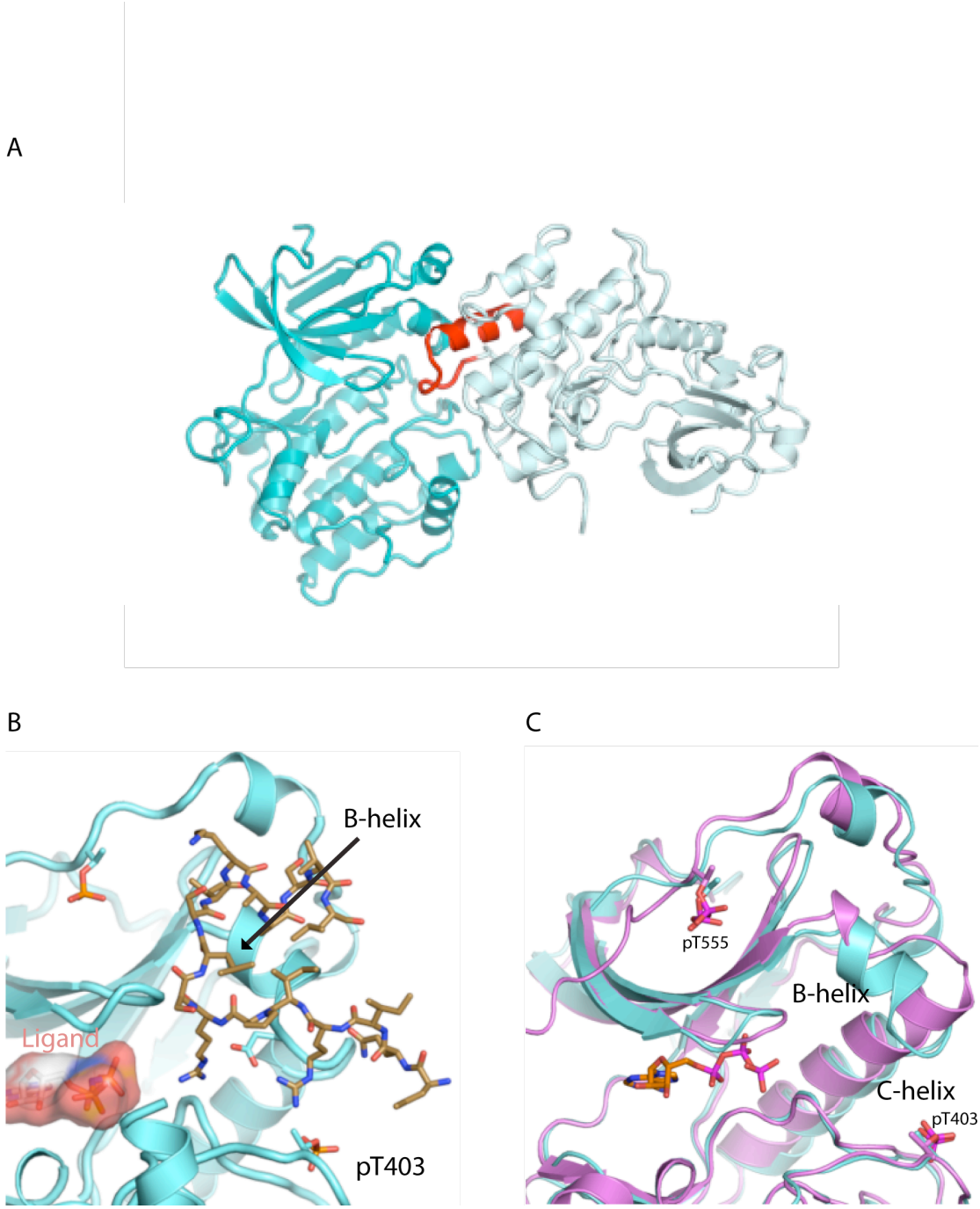

Figure 5.1 PKCι kinase domain crystal lattice

A, The first PKCι kinase domain (grey) is using the RIPR motif (red) to bind the second PKCι kinase domain (cyan). B, the RIPR containing loop (brown) of a PKCι kinase (mainly out of picture) makes contacts with the pT403, the B-helix and close to where the γ-phosphate of ATP would lie. C, In CRT66854 bound PKCι structure (cyan) a formed B-helix is seen in contrast to all other aPKC structures determined, for example PKCζ kinase domain (pink).

5.2 Results

5.2.1 The RIPR region is required for PKCι dependent phosphorylation of LLGL but not in vitro phosphorylation of PKCε pseudosubstrate

To test whether the activity of PKCι in cells was dependent on the RIPR motif, a double arginine mutant (R471A/R474A, creating the sequence AIPA) was made. For the remainder of this thesis this mutant will be referred to as the AIPA mutant. Using phosphorylation of LLGL2 (pLLGL) as a read out of PKCι activity (as validated in chapter 3), GFP-LLGL was co-transfected in HEK293 cells with the full-length PKCι mutant series- GFP-PKCι-WT, GFP-PKCι-AIPA, GFP-PKCι -D368N (kinase dead) or empty vector. Under these conditions pLLGL detected by Western was reduced by 94% with PKCι-D368N and 82% with PKCι-AIPA compared to PKCι-WT (Figure 5.2A). This experiment was repeated using the kinase domain (aa.239-587) versions of the PKCι mutant series and the results mirrored those of the full-length constructs.

To demonstrate that the low activity of the AIPA mutant was a protein autonomous function, HEK293 cells were transfected with the same PKCι mutant series, immuno-complexes were precipitated via the GFP tag and assayed in a classical kinase assay using PKCε pseudosubstrate (PKCεPS) as the substrate. In this assay the PKCι-AIPA had slightly lower activity than PKCι-WT but it was not comparable to the decrease in pLLGL in cells. Both the vector control and the kinase dead had no activity above baseline levels in the kinase assay (Figure 5.2B).

In order to explain this discrepancy between the cell-based phosphorylation and the immunocomplex kinase assay results, a number of different hypotheses were proposed: 1) The RIPR region could participate as a donor in an activating intermolecular interaction. This transactivation would be predicted to require a high localised protein concentration, mimicking the concentrations found in a cellular membrane (2D) but is too weak an interaction to be detected *in vitro*, 2) the AIPA region may provide a docking site for proteins that inhibit activity – these proteins being present in the cell but not the kinase reaction mix, or 3) The RIPR region could

be required for substrate binding but is not required by the short PKCεPS peptide substrate used in the *in vitro* kinase assay.

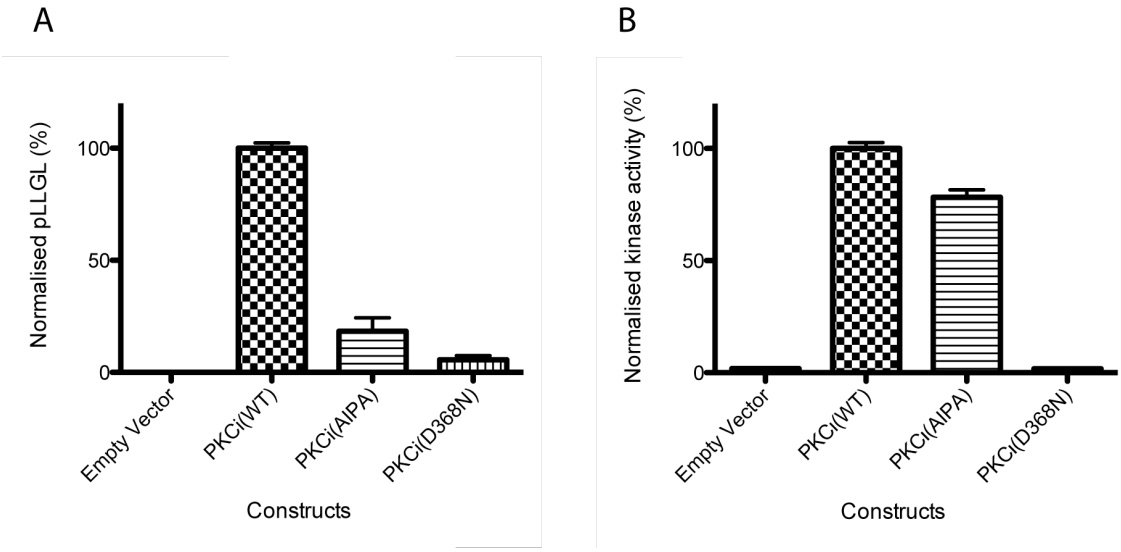

Figure 5.2 In vivo and in vitro substrate phosphorylation by PKCι-AIPA
A, Empty Vector, PKCι-WT, PKC-AIPA (RIPR>AIPA mutant) or PKC-D368N were co-transfected with LLGL2 in HEK293 cells and the phosphorylation of LLGL2 was measured after 36h. Constructs from the PKCι mutant series were co-transfected at a 1:1 ratio along with LLGL2. Total DNA transfected was kept constant for all conditions. Lysates were immunoblotted for pLLGL and PKCι and the densitometry of the pLLGL/PKCι signal is shown. B, PKCι-WT, PKC-AIPA, PKC-D368N and empty vector were transfected in HEK293 cells, immunoprecipitated via their GFP tags and immunocomplex kinase assays were performed. Activity was adjusted for PKCι protein concentration. Both graphs show the mean±SEM of 3 separate experiments normalised to PKCι-WT.

5.2.2 PKCι-DN is unable to rescue PKCι-AIPA activity in HEK293 cells

If the activity of PKCι-AIPA mutant was diminished in cells because it lacked the putative RIPR transactivation region (which by inference might not be operating in an immune complex kinase assay) then the activity might be rescued by a mutant with an intact RIPR region but lacking kinase activity (PKCι-D368N). The two mutant constructs, PKCι-AIPA and PKCι-D368N were mixed at a 1:1 ratio with a constant DNA concentration in the LLGL co-transfection experiment. No appreciable increase in pLLGL was demonstrated compared to PKCι-AIPA alone (figure 5.3).

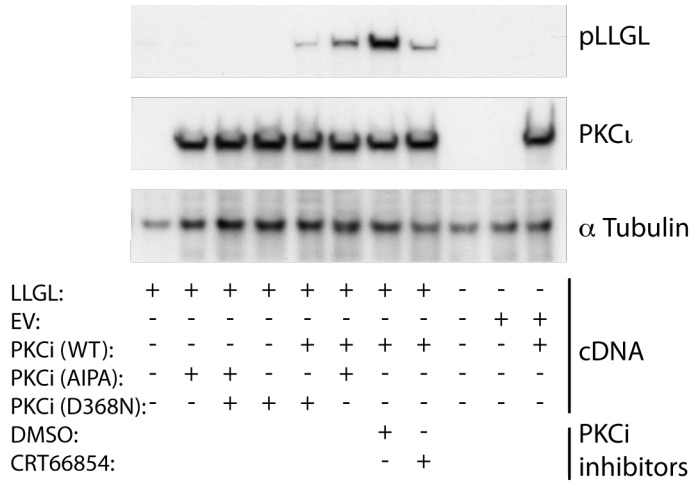

Figure 5.3 Attempted rescue of PKCι-AIPA activity with a kinase dead mutant
HEK293 cells were co-transfected with LLGL and a 1:1 mix of PKCι or PKCι mutants maintaining a constant DNA concentration per condition. After 36h total cell lysates were analysed for pLLGL. As a positive control the PKCι-WT/LLGL co-transfected cells were treated with a specific PKCι inhibitor. The blot is representative of 3 separate experiments.

This lack of rescue could have been a consequence of disproportionate expression of the two proteins or due to an inadequate localised concentration of PKCι. To address the issue of disproportionate expression the experiment was performed mixing GFP-tagged constructs with non-tagged constructs so each could be identified by separation of mass on an SDS-PAGE gel. When expressed individually the PKCι mutant series expressed equally well in both pEGFP-C1 and pcDNA3.1 vectors and had the same effect on LLGL phosphorylation. Initial results indicated that when the 2 vectors were mixed the expression of proteins from pcDNA3 were markedly lower than from pEGFP and this discrepancy could not be overcome by increasing the ratio of construct DNA in favour of pcDNA3.1.

As an alternative strategy to enable the protein ratio to be quantified, full length or kinase domain alone was expressed in the same pEGFP vector. To ensure high-localised concentrations, that were predicted to be required for transactivation, the proteins were myristolated at the N-terminus of the GFP tag. These myristolated proteins were localised to membranes (Figure 5.4A) and had a more robust pLLGL

signal compared to the non-myristolated counterparts (Figure 5.4B). When co-expressed the myristolated kinase domains of the PKCι mutant series expressed slightly better than the myristolated full-length PKCι mutant series and therefore influenced the pLLGL to a greater extent. Despite these optimisations the PKCι-D368N was unable to rescue PKCι-AIPA activity in cells (Figures 5.4C&D).

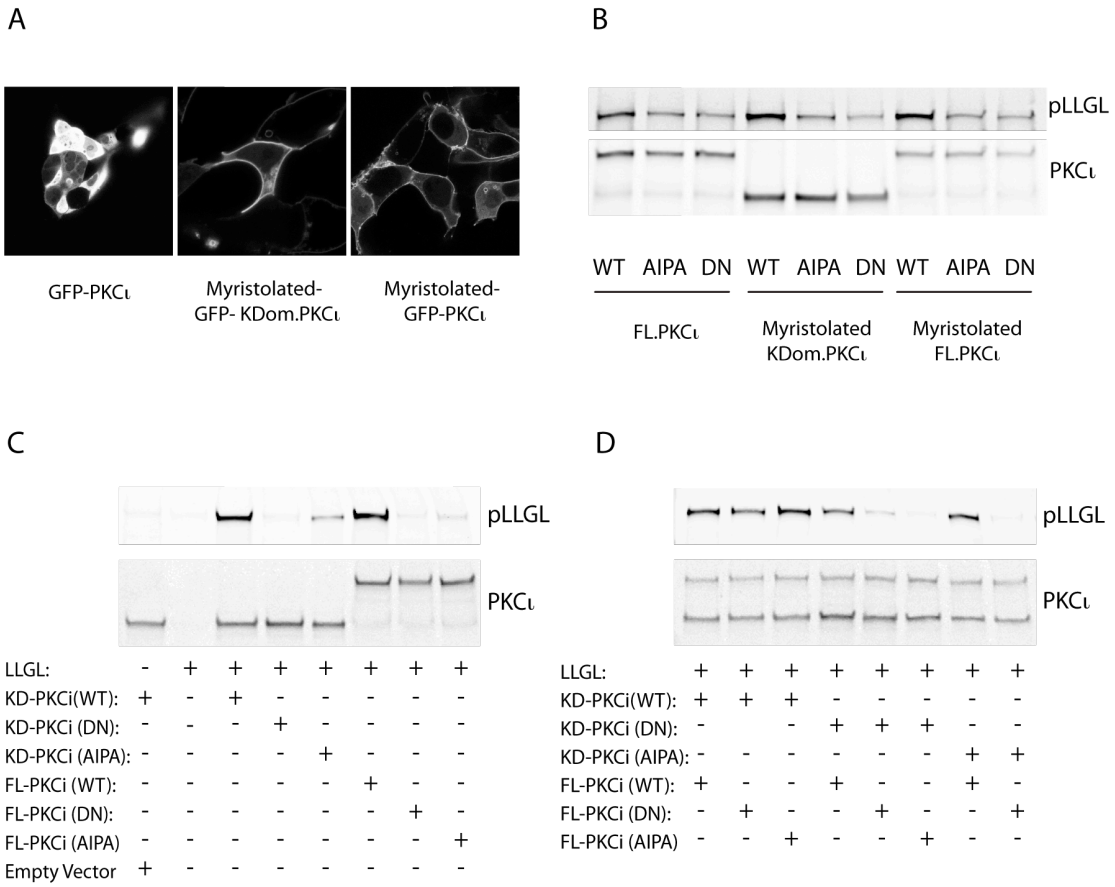

Figure 5.4 Attempted activity rescue following membrane localisation
A, HEK293 were transiently transfected with GFP-PKCι, myristolated GFP-PKCι and myristolated GFP-PKCι kinase domain and fixed after 36h. Representative single confocal images of the GFP (white) are shown. B, HEK293 cells were co-transfected with LLGL2 and different PKCι mutants that were membrane targeted or not. After 36h total cell lysates were analysed for pLLGL. C, Myristolated full length or kinase domain PKCι constructs were co-transfected with LLGL in HEK293 cells. The effect on pLLGL was assessed by immunoblot at 36h. D, Myristolated full length or kinase domain PKCι constructs were co-transfected with LLGL and a 1:1 mix of PKCι mutants maintaining a constant DNA concentration per condition. After 36h total cell lysates were analysed for pLLGL. All blots are representative of 3 separate experiments.

5.2.3 PKCι has concentration dependent specific activity but this does not require the RIPR region

To more directly assess whether high PKCι concentrations were required for optimal activity, recombinant kinase domain was assayed over a broad range of concentrations. To facilitate the high kinase concentrations a modified kinase assay was developed (see section 2.2.13.2). Increased wild type PKCι did indeed result in an increased specific activity reaching a maximum activity at a kinase concentration of 1000 μg/ml (Figure 5.5). If the modified kinase assay was performed without substrate or with BSA as a control for the total protein concentration in the reaction, no increase in specific activity was detected. To investigate whether the RIPR region was necessary for this effect on specific activity, recombinant PKCι-AIPA was used in the reaction. This protein did not result in any impairment in concentration dependent specific activity, and if anything, the relative specific activity was slightly higher. A protein autonomous concentration dependent activation of PKCι was therefore identified in vitro but this was independent of the RIPR region.

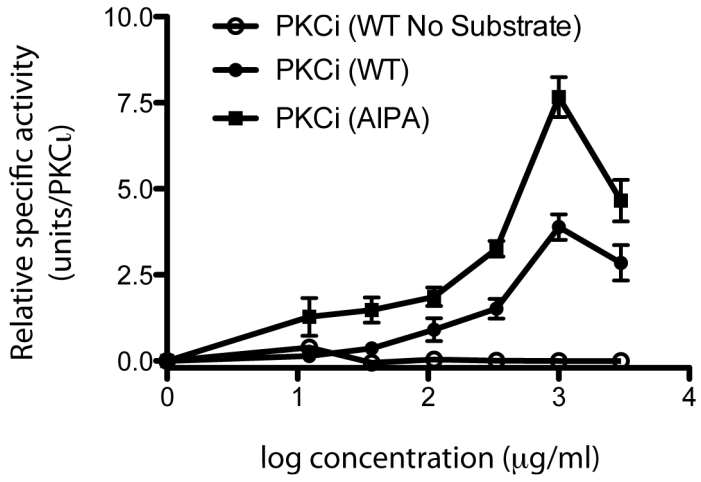

Figure 5.5 Concentration dependent specific activity
Recombinant PKCι and PKCι-AIPA kinase domains (0-2500μg/ml) were used in a modified kinase assay. Data represent mean and the range for at least 2 separate experiments normalised to the median of all experimental data.

A protein overlay strategy was adopted to elicit potential sites of homotypic PKCι protein interactions that could explain the concentration dependent behaviour. To improve the likelihood of detecting interactions, a dimeric form of the kinase was used – recombinant fusion protein of GST and PKCι. Initial experiments have identified 3 possible regions of homotypic PKCι interaction (Appendix 3).

5.2.4 The PKCι RIPR motif is a protein-interaction site.

As the hypothesis that the PKCι RIPR motif was required for allosteric activation was rejected, the possibility that it was involved in protein-protein binding was pursued. Co-immunoprecipitation experiments of exogenously expressed GFP-PKCι-WT, GFP-PKCι-AIPA or GFP alone were performed in HCT116 cells. Protein staining of the resulting SDS page gel did not reveal any clear differentiating bands between the three conditions but demonstrated equal protein loading (Figure 5.6A). Consequently a whole lane mass spectrometry approach was adopted. In total 1194 different proteins were identified. Subtraction of the GFP control interacting proteins reduced the list to 321(Appendix 2). A further 67 proteins that were enriched in unique peptides by at least three times in the experimental groups compared to the GFP-control were also included. To increase the confidence of the reported hits, this list of 388 proteins was filtered based on abundance and reproducibility. To meet the abundance criteria at least three unique peptides must have been identified for each protein and 70 proteins fulfilled this. These 70 proteins were stratified based on the relative abundance of unique peptides after pull down with PKCι-WT or PKCι-AIPA. In this list there were 38 proteins that were at least 3 times more abundant in the PKCι-WT pull down compared to the PKCι-AIPA and the remaining 32 were considered to be similar between the two conditions. There were no proteins in this selection of hits that were 3 times more abundant in the PKCι-AIPA pull down compared to the PKCι-WT.

In parallel, a separate PKCι-based whole lane mass spectrometry experiment was performed in the lab by Dr Philippe Riou. The two independent experiments used the

same cell type, IP protocol and shared two experimental conditions - PKCι-WT and GFP vector control. This separate screen was used to test reproducibility. The recognised PKCι binding proteins, Par3 and Par6 were present in both screens. Of the 38 proteins shown to preferentially bind PKCι-WT over PKCι-AIPA, 5 were present in both screens (Figure 5.6B & Table 5.1). Intriguingly, one of these hits was LLGL2.

A

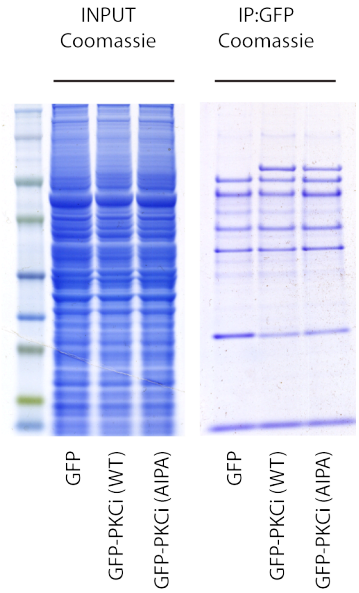

B

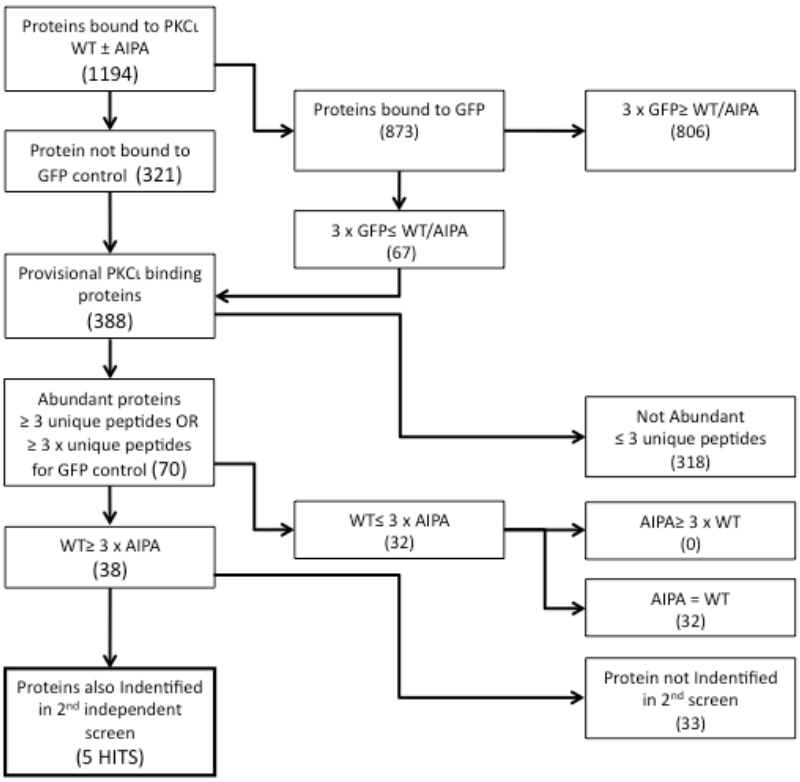

Figure 5.6 Mass spectrometry 'hit' stratification
A, PKCι-WT and PKCι-AIPA immunocomplexes on a Coomassie gel. B, Schematic of the mass spectrometry screening cascade. Number of proteins is in brackets.

Table 5.1 Stringent Hits from the Immunocomplex-mass spectrometry screen.

Entry Name & Accession No.	Protein ID	Abundance of unique peptides		
		GFP	PKCι-WT	PKCι-AIPA
L2GL2_HUMAN Q6P1M3	Lethal(2) giant larvae protein homolog 2	1	16	5
FARP1_HUMAN Q9Y4F1	FERM, RhoGEF and pleckstrin domain-containing protein 2	0	5	0
MAGI1_HUMAN Q96QZ7	Membrane-associated guanylate kinase, WW and PDZ domain-containing protein	0	5	1
MTA2_HUMAN Q94776	Metastasis-associated protein MTA2	0	4	0
PDIA3_HUMAN P30101	Protein disulfide-isomerase A3	2	8	2

To validate that LLGL2 preferentially binds to PKCι-WT over PKCι-AIPA, reciprocal pull down experiments were performed. Subsequent immunoblotting for LLGL2 demonstrated a loss of signal in the PKCι-AIPA pull down (Figure 5.7A) and GFP-LLGL was able to pull down PKCι-WT but not PKCι-AIPA (Figure 5.7B). Par3 and Par6B, known to form a trimeric complex with PKCι, were present in both PKCι-WT and PKCι-AIPA pull downs. The antibody specificity for LLGL2 was demonstrated by loss of the band in GFP- PKCι-WT immunocomplexes pre-treated with siRNA-LLGL2 (Figure 5.7C). When this blot was re-probed for Par6 the level was enhanced in PKCι-WT treated with LLGL siRNA compared to the scramble control in 2 separate experiments. Additionally, the PKCι-WT and PKCι-AIPA pull down experiment was performed and duplicate SDS PAGE gels were run. One gel was used for a Western Blot with a phospho-serine-PKC (pPKC) substrate antibody. A prominent 130kD band was identified in the PKCι-WT lane only (Figure 5.7D). The immunoblot was used to guide the dissection of the equivalent band in the duplicate gel and this was sent for mass spectrometry. This band was also identified as LLGL2.

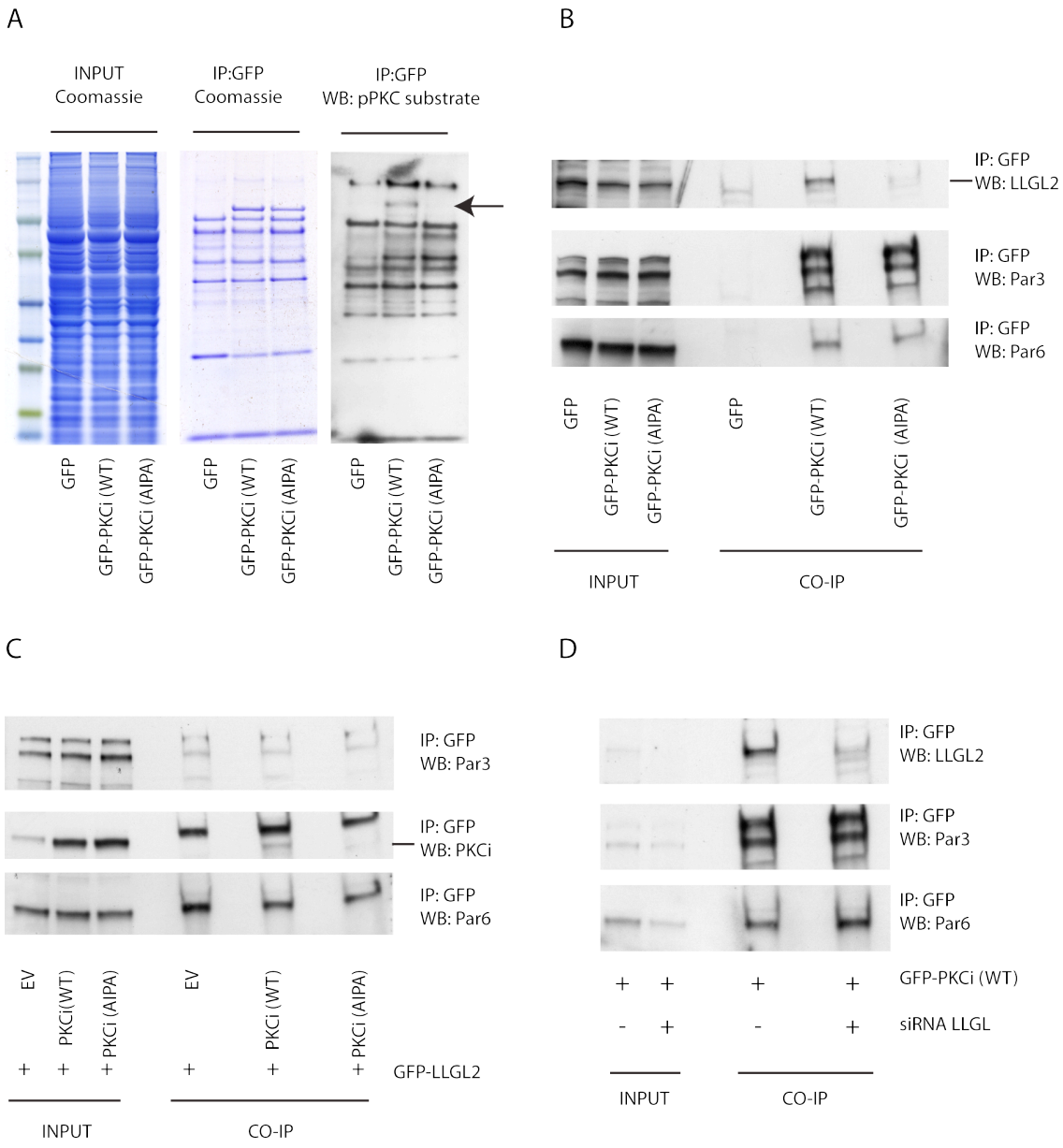

Figure 5.7 Co-immunoprecipitation experiments of the PKCι-AIPA mutant.
A, HCT116 cells were transiently transfected with GFP, GFP-PKCι or GFP-PKCι-AIPA. Immunocomplexes were separated by gel electrophoresis and immunoblotted for LLGL2 and then re-probed for Par6 and Par3. B, cells were co-transfected with GFP-LLGL and empty vector (EV), PKCι or PKCι-AIPA. Immunocomplexes were immunoblotted for PKCι. C, HCT116 cells were reverse-transfected with siRNA-LLGL2 or scrambled siRNA and after 24h transfected with PKCι. After a further 48h immunocomplexes were generated and immunoblotted for LLGL2 and then re-probed for Par6 and Par3. D, Immunoblot from (A) was stained with colloidal coomassie (left and center panel) and immunoblotted with pPKC substrate antibody (right panel) that demonstrated a differential band (arrow).

As the AIPA mutant is deficient in LLGL binding this could provide an explanation for the difference in the in phosphorylation of LLGL in the cell and phosphorylation of PKCε pseudosubstrate peptide (PKCεPS) in vitro (described in section 5.2). To test this directly, an in vitro kinase assay was performed using recombinant kinase domain PKCι-WT, kinase domain PKCι-AIPA and either recombinant full-length LLGL2 or the PKCεPS. There was no difference between the activity detected between PKCι-WT and PKCι-AIPA when PKCεPS was used as substrate but a decrease of 60% for PKCι-AIPA when LLGL was used as substrate for the reaction (Figure 5.8).

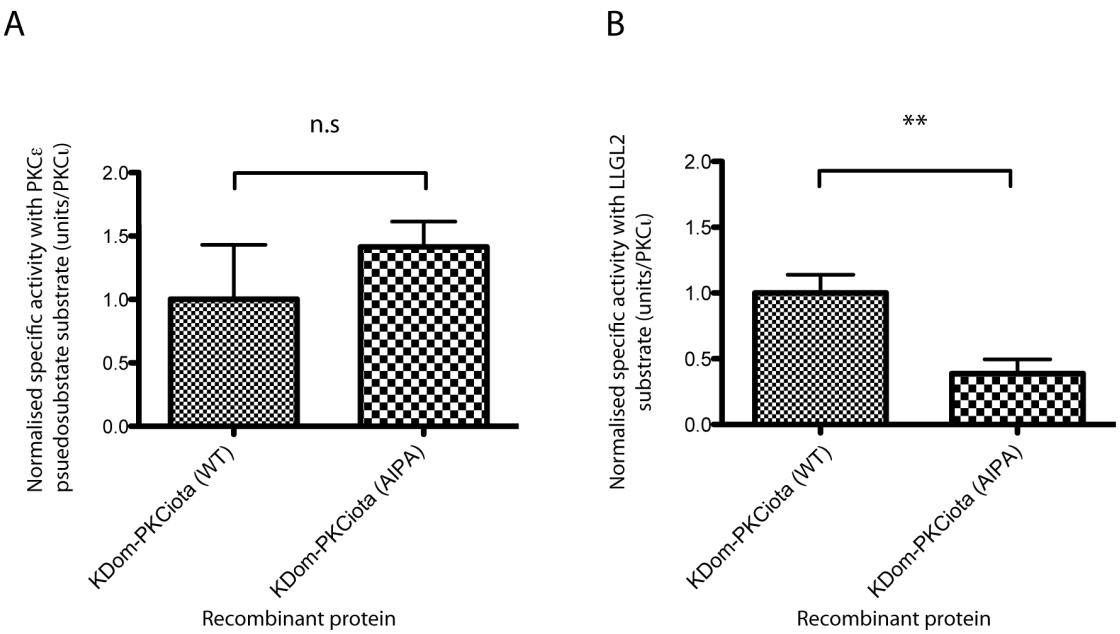

Figure 5.8 Substrate phosphorylation by PKCι - revisited
The effects of mutating the RIPR motif on PKCι induced substrate phosphorylation. A, classical kinase assays were performed using recombinant PKCι, PKCι-AIPA and full length recombinant LLGL as substrate. B, historical control of the classical kinase assay for PKCι and PKCι-AIPA with PKCεPS as substrate. The data is from two separate experiments and represent the mean and the range. Students-t test was used to determine statistical significance of any difference **, $p<0.01$; n.s, no statistical difference.

5.2.5 The RIPR region is a predicted PKN substrate motif.

A substrate screen of PKN1 and 3, protein kinases closely related to PKCι, performed in the lab by Dr Alejandra Collazos defined their substrate motifs. An arginine at the -3 position and a hydrophobic residue at the +1 position flank Serine 477 of PKCι and predict that it would be a good PKN substrate. The arginine (R) at -3 is the second R of the RIPR motif. Putative phosphorylation deficient (S477A) and phosphomimetic (S477E) mutants were used to interrogate whether phosphorylation at this site controls protein interactions at the RIPR region. Using the cell based pLLGL assay, no differences were observed between myristolated PKCι-WT and the S477A or S477E mutants. The pLLGL in the vector and PKCι-AIPA controls, were markedly reduced (Figure 5.9).

A

MSHTVAGGGSGDHSHQVRVKAYYRGDIMITHFEPSISFEGLCNEVRDMCS
FDNEQLFTMKWIDEEGDPCTVSSQLELEEAFRLYELNKDSELLIHVFPCVPE
RPGMPCPGEDKSIYRRGARRWRKLYCANGHTFQAKRFNRRAHCAICTDRI
WGLGRQGYKCINCKLLVHKKCHKLVTIECGRHSLPQEPVMPMDQSSMHS
DHAQTVIPYNPSSHESLDQVGEEKEAMNTRESGKASSSLGLQDFDLLRVIG
RGSYAKVLLVRLKKTDRIYAMKVVKKELVNDDEDIDWVQTEKHVFEQASN
HPFLVGLHSCFQTESRLFFVIEYVNGGDLMFHMQRQRKLPEEHARFYSAEIS
LALNYLHERGIIYRDLKLDNVLLDSEGHIKLTDYGMCKEGLRPGDTTSTFCG
TPNYIAPEILRGEDYGFSVDWWALGVLMFEMMAGRSPFDIVGSSDNPDQN
TEDYLFQVILEKQIRIPRSLSVKAASVLKSFLNKDPKERLGCHPQTGFADIQ
GHPFFRNVDWDMMEQKQVVPPFKPNISGEFGLDNFDSQFTNEPVQLTPDD
DDIVRKIDQSEFEGFEYINPLLMSAEECV

B

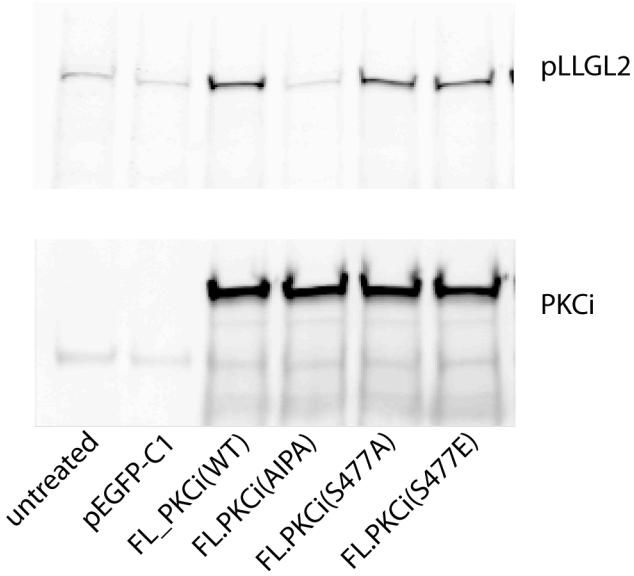

Figure 5.9 Effect on LLGL phosphorylation by PKCι mutated at its putative PKN substrate motif.

A, The human PKCι amino acid sequence and highlighted PKN substrate motifs (yellow). B, Predicted phosphomimetic mutant (S477E) and phosphorylation deficient mutant (S477A) of PKCι were co-expressed with LLGL in HEK293 cells and their effect on pLLGL elicited by Western blot.

5.2.6 The RIPR region is required for normal lumen formation in MDCK cysts

Parental MDCK cells grown in Matrigel form a hollow sphere with an apical lumen that may be characterised by F-actin staining (see section 3.2.4). In MDCK cells stably transfected with PKCι-AIPA they developed a multi-cystic appearance (figure 5.10A) and there was a 58% reduction in the number of spheroids with normal apical lumens compared to the PKCι -WT (figure 5.10B) despite similar protein expression levels (figure 5.10C).

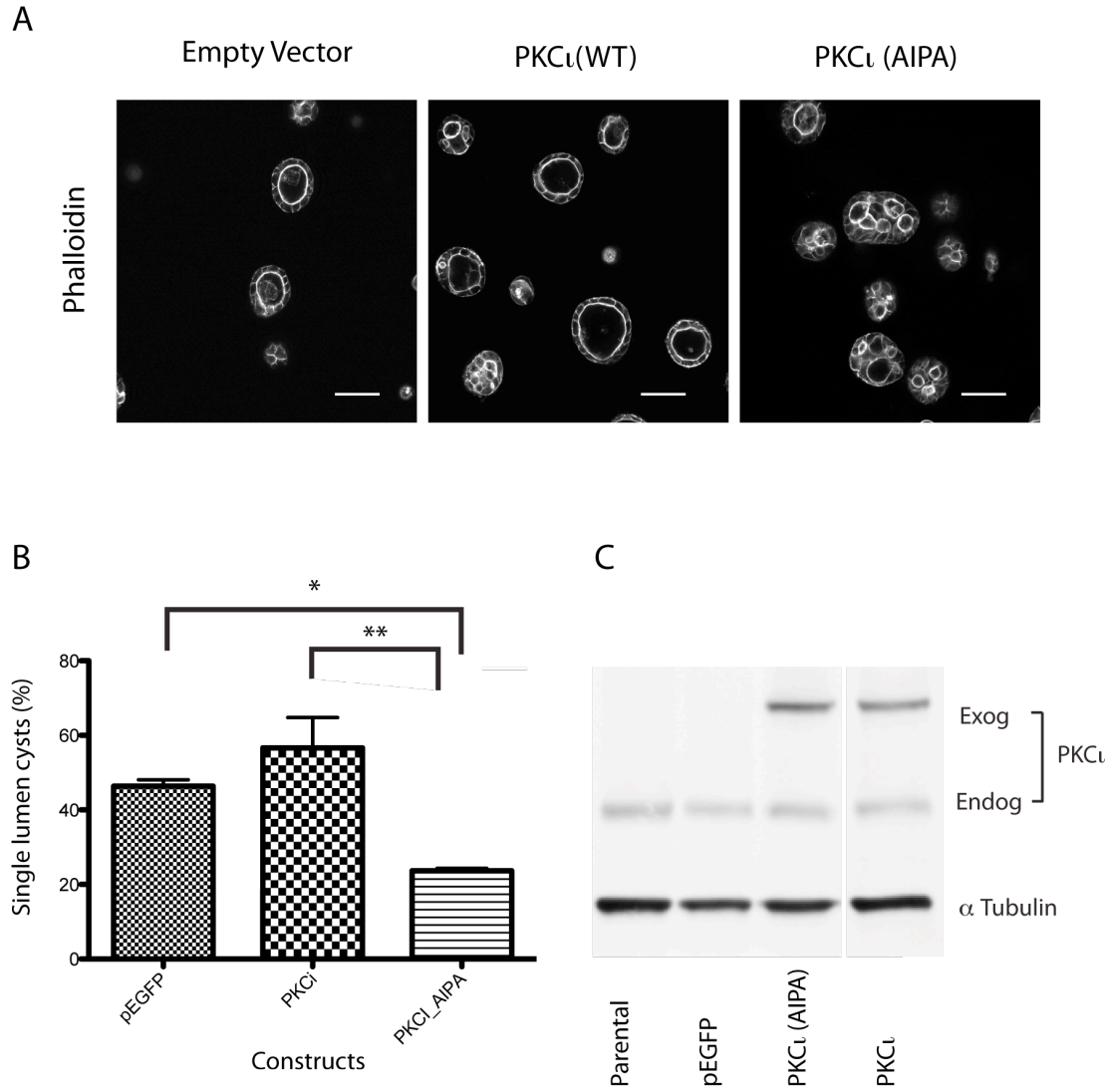

Figure 5.10 The physiological relevance of the RIPR motif.
A, MDCK cells were stably transfected with empty vector, PKCι or PKCι-AIPA and cultured in Matrigel for 6 days. Representative single confocal images of actin staining (white) are presented. Scale bars represent 50μm. B, Western blot showing the exogenous PKCι expression in the mutant cells lines. C, Quantification of number of normal apical lumens. At least 100 spheroids were counted per condition for each experiment and the mean ± SEM of 3 separate experiments are presented. One way ANOVA was used to determine statistical significance of difference; *, $p<0.05$; **, $p<0.01$.

5.3 Discussion

Collaboration with the SBL and with Cancer Research Technology, who provided selective PKCι ligands, presented a unique opportunity to explore the structure-function relationships of PKCι. Predictions from the crystal structure directed initial investigation towards testing whether the RIPR motif was involved in allosteric transactivation of PKCι. Enthusiasm for this line of investigation was fuelled by the finding that in a cell based pLLGL assay, previously shown to correlate with PKCι activity, mutation at the RIPR motif dramatically impaired substrate phosphorylation.

There are significant parallels with this observation and the allosteric activation of the EGFR family of receptors proposed by the Kuryian Laboratory (also see section 1.2.6). From the crystal structure of inactive EGFR kinase domain they were able to identify an intermolecular interaction site and defined donor and acceptor regions. A mutant form of the EGFR kinase domain that was donor deficient (V924R mutant) was mixed with the HER3 kinase, a pseudokinase that lacks catalytic activity, on lipid vesicles and in vitro kinase assays were performed. Both the EGFR-V924R and HER3 lacked appreciable activity when assayed alone but when mixed the kinase inactive HER3, with an intact donor region, was able to rescue the activity of EGFR-V924R (Jura et al., 2009).

For studies on PKCι a putative donor mutant (PKCι-AIPA) and acceptor mutant (the kinase dead PKCι-D368N) were fashioned. Co-expression of PKCι mutants and LLGL were performed to test whether there was an in vivo rescue of PKCι-by PKCι-D368N. Considerable effort was spent optimizing the assay to enable quantification of the co-expressed exogenous proteins and to concentrate the PKCι at the membrane in a fashion analogous to the in vitro lipid vesicles used by Kuryian's group for EGFR. Despite this no rescue of PKCι-AIPA was achieved with PKCι-D368N. We concluded that activation of PKCι does not occur by transactivation in a RIPR dependent fashion. However while testing this first hypothesis several notable observations came to light.

Firstly, the co-expression studies of different PKCι mutants were technically challenging. In order to measure the relative expression of the mutants, different vectors (pcDNA3.1

or pEGFP-C1) were used as a means to differentially introduce GFP tags. While both vectors efficiently expressed protein individually, in co-expression experiments the protein expression from pcDNA3 was markedly suppressed. Following the introduction of a potent transcriptional activator into eukaryotic cells this paradoxical suppression of a co-introduced gene target is a recognised phenomenon and is termed "Squelching". It is thought that Squelching may be a result of competition for general transcription factors (GTFs) and seems to affect transient vector expression more than chromatin-integrated promoters. It is speculated that this discrepancy between integrated and non-integrated promoters may be as a result of separate pools of GTFs for these compartments or possibly the presence of high affinity binding sites for GTFs within the chromatin (Natesan et al., 1997). When pcDNA3 and pEGFP are co-transfected competition takes place between their respective episomal target genes with those derived from pEGFP winning. Both constructs contain a human cytomegalovirus immediate early promoter and contain enhancer regions. It is possible that differences seen are due to variable affinities of GTF binding sites in the two constructs. Such difficulties could be overcome by use of a multicistronic vector where proteins are encoded by a single messenger RNA. When aiming for similar expression of two proteins, use of a 2A peptide might be appropriate. Using this strategy the mRNA transcript contains 2 gene transcripts separated by a 2A-coding region. The 2A-coding region leads to the co-translational production of an abnormal peptide bond between a glycine and proline resulting in cleavage of the nascent peptide at this site and therefore the two gene products in equal ratio (Trichas et al., 2008).

Secondly, as predicted, myristolation of PKCι resulted in membrane targeting as determined by confocal microscopy. This led to increased phosphorylation of LLGL2 compared to non-myristolated proteins. This provides evidence that its activity is enhanced at the membrane, at least for the LLGL2 substrate.

Thirdly, while testing whether any requirement for the RIPR motif was concentration dependent, using a modified kinase assay that permitted high protein concentrations, a quite unexpected observation was made. This was that increased concentration of PKCι kinase domain lead to an increase in measured specific activity and that this was

independent of the RIPR motif. This trend in specific activity was seen in at least five separate experiments derived from two different protein preparations. The data presented in figure 5.3E are two separate experiments from a single protein preparation. From this experiment the specific activity is actually higher for the AIPA compared to the WT at all concentrations but the rate of change is the same. Although the protein preparations were prepared using the same protocol, they were not generated synchronously and previous experiments conducted at single protein concentrations (5 μg/ml) actually showed a lower specific activity for PKCι-AIPA compared to PKCι. It is likely, therefore, that the varying relative specific activities represent differences in protein preparations and further experiments with new protein preparations would be required to confirm this.

The rate of phosphorylation per unit of kinase (specific activity) of PKCι kinase domain went up significantly with increasing kinase concentration. For an increase to this extent it is likely to require increasing efficiency of catalysis. This could be mediated by a protein-protein allosteric activation or increased autophosphorylation.

When autophosphorylation was looked at, in the modified kinase assay without the optimal peptide substrate, the specific activity remained low and constant over a broad range of concentrations. This zero-order kinetic would be expected for cis-autophosphorylation, as previously demonstrated for purified recombinant PKC βII that will autophosphorylate on the C-terminal hydrophobic motif (Behn-Krappa and Newton, 1999). However the modified kinase assay, by virtue of the low reaction volume, would not be expected to be sensitive enough to reliably detect the low levels of phosphorylation associated with stoichiometric reactions of cis- or trans-autophosphorylation. It cannot be ruled out therefore that there is autophosphorylation (particularly in trans) that changes the activity state of the protein. The protein preparations used in this experiment had been co-incubated with PDK1, shown to induce phosphorylation of aPKC at the activation loop (Le Good et al., 1998), and purified by ion exchange to enrich for the phosphorylated form. There are further sites that may be autophosphoylated such at the turn motif (Thr555) and other sites that could be phosphorylated by contaminating tyrosine kinases such as Tyr256, a site thought to be involved in nuclear import (White et al., 2002). One approach to address whether

autophosphorylation is involved in concentration dependent activation would be to carry out the modified kinase assay on a high and low concentration preparations and perform quantitative phosphoproteomics.

As an additional control a low concentration PKCι-kinase domain kinase assay was carried out with incremental concentrations of bovine serum albumin. Adsorption of kinase to the Eppendorf tube can prevent its involvement in catalysis, but above a threshold the surface becomes saturated with protein and this may be perceived as a concentration dependent gain in activity. In this experiment there was no detected increase in activity ruling out significant adsorption and non-specific protein effects. The experiment, however, does not control for differences in substrate binding to phosphocellulose paper (p81) under acidic conditions. The p81 paper is an ion exchange matrix with a net negative charge at low pHs. A phosphorylated peptide will bind if it has a net positive charge. For PKCePS this is achieved by multiple arginines (RPRKRQGAVRRR) that are positively charged at most pHs (pI=10.8). Unlike the classical kinase assay, the modified assay is terminated by mixing with glacial acetic acid before binding to the p81 paper. There is a theoretical situation where this acid treatment prevents peptide adsorption to p81 and this effect is reduced by higher PKCι concentrations. To carry out this control neutral termination solutions could be used, for example EDTA in HEPES.

The preferred explanation for the protein concentration dependent activity is that there is an intra-molecular or homotypic protein interaction that results in an activating conformational change. If proven, this could have significant implications for understanding PKCι function and on the development of potential specific allosteric inhibitors. Initial experiments using a PKCι protein overlay on a PKCι peptide array suggested that there was a number of homotypic PKCι interaction sites. Ongoing work in the Protein Phosphorylation Laboratory will aim to repeat this experiment to confirm the regions of interaction and test whether there is protein-concentration dependence.

The second structure-derived hypothesis tested was that the RIPR motif could be involved in protein-protein interactions. Indeed, through an immunocomplex and whole

lane mass spectrometry screen, proteins that bound to PKCι-WT in preference to the PKCι-AIPA mutant and the GFP PKCι-WT were identified, one of which was LLGL2. In the mass spectrometry there were a large number of proteins that bound to the GFP control in addition to the experimental conditions and were therefore excluded. These excluded proteins may have contained true PKCι-WT/ PKCι-AIPA interacting proteins that happened to also stick to the GFP. An attempt to minimise such false negatives was made by using the GFP-TrapM system, a 13kD protein based on a single domain antibody from Lama Alpaca that has a high affinity, instead of conventional GFP monoclonal antibodies. However a large number of non-GFP binding proteins (388) were identified in the screen. To select hits the protein lists were filtered based on the abundance of unique peptide sequences for each protein and reproducibility. Identification of a unique peptide is more likely if the parent protein occurs at a high concentration in the sample but is not a quantitative measure of abundance. There are a number of caveats to the use of this index. Firstly, abundant peptides ions can be missed if they co elute on the reverse phase front end with other more abundant peptide ions as only the more abundant one is selected for analysis. Secondly, a unique peptide sequence may be detected multiple times if prevalent but this is only recorded as a single unique peptide. Thirdly, the ability for proteins to be detected depends upon the position of tryptic cleavage sites (carboxyl side of lysine and arginine) within the protein and fragment charges and thus the ability of the peptide ions to pass through the spectrometer (‘to fly’). Reproducibility for the predominantly PKCι-WT interacting proteins was assessed by cross-reference to another PKCι based whole lane mass spec screen performed concomitantly in the Lab. The methodology was similar with the exception of high salt IP washes and an additional 2 short IP washes. Surprisingly, there was only a 12% overlap between the proteins identified in the two studies after the GFP-control interacting proteins were subtracted. The Human Proteome Organization (HUPO) conducted an audit of accurate identification of a protein test set and showed markedly varying results despite the same or similar instrumentation (Bell et al., 2009).

LLGL was selected from the hit list to validate the mass spectrometry screen for several reasons. Firstly, it is a well-established interaction partner with PKCι albeit one whose

site of interaction has not been described. Secondly, the reagents for this target had been validated. Analytical immunoprecipitations and immunoblots clearly demonstrated that the PKCι-AIPA mutant is a non-LLGL binding mutant. By an astonishing coincidence, therefore, the very substrate chosen to interrogate the cell-based activity of the PKCι-AIPA mutant was a protein for which the mutant was unable to bind. It is worth noting here that based on the crystal structure, that reveals that the RIPR region is remote from the active site, it would not have been predicted to directly affect substrate binding.

In the knowledge that the RIPR motif was required for LLGL2 binding the initial kinase assay was re-examined, this time also using recombinant LLGL as a substrate for the reaction. Phosphorylation of LLGL2, but not PKCePS, was significantly reduced compared to PKCι-WT. As the protein is capable of phosphorylating the short PKCePS in the absence of RIPR this would suggest that the RIPR site functions as a docking site rather than an allosteric regulator of catalysis. Such a docking site is reminiscent of the Arg-X-Leu motif (RXL) used by cyclin partners of cyclin-dependent kinases (CDKs) to engage substrates. In this case the RXL motif is within the substrate, however the RIPR motif is within the aPKC kinase and we speculate below where the RIPR motif may bind on the LLGL substrate. For CDKs the local sequence motif that is phosphorylated is Ser-Pro-X-Lys. The RXL motif therefore acts as a recruitment site in addition to the phospho-motif of these proline-directed kinases (Jeffrey et al., 1995). Parallels with MAPK substrates and regulators are also known (Tanoue and Nishida, 2003). It is likely therefore that the RIPR motif plays an analogous role in helping to recruit highly selective aPKC substrates.

LLGL is known to be phosphorylated in a low complexity region (LCR) or hinge region that lies within the WD40 β-propellers. In light of the discovery that LLGL binds to PKCι via the RIPR motif an initial attempt has been made to model potential sites of interaction on LLGL. The crystal structure of LLGL has not been solved but the yeast homologue provides a scaffold upon which the human LLGL sequence can be overlaid. From this structural overlay, surface acidic patches that were phylogenetically conserved were identified and considered possible sites of interaction. From this preliminary model it appears plausible that PKCι could bind to LLGL at the interface between the two β-

propellers as four conserved acidic pathches are found at this location. The multiple WD40 regions and the hinge regions of LLGL would provide the length and flexibility to wrap around the PKCι kinase domain and position the LLGL hinge for optimal phosphorylation by PKCι (Figure 5.11).

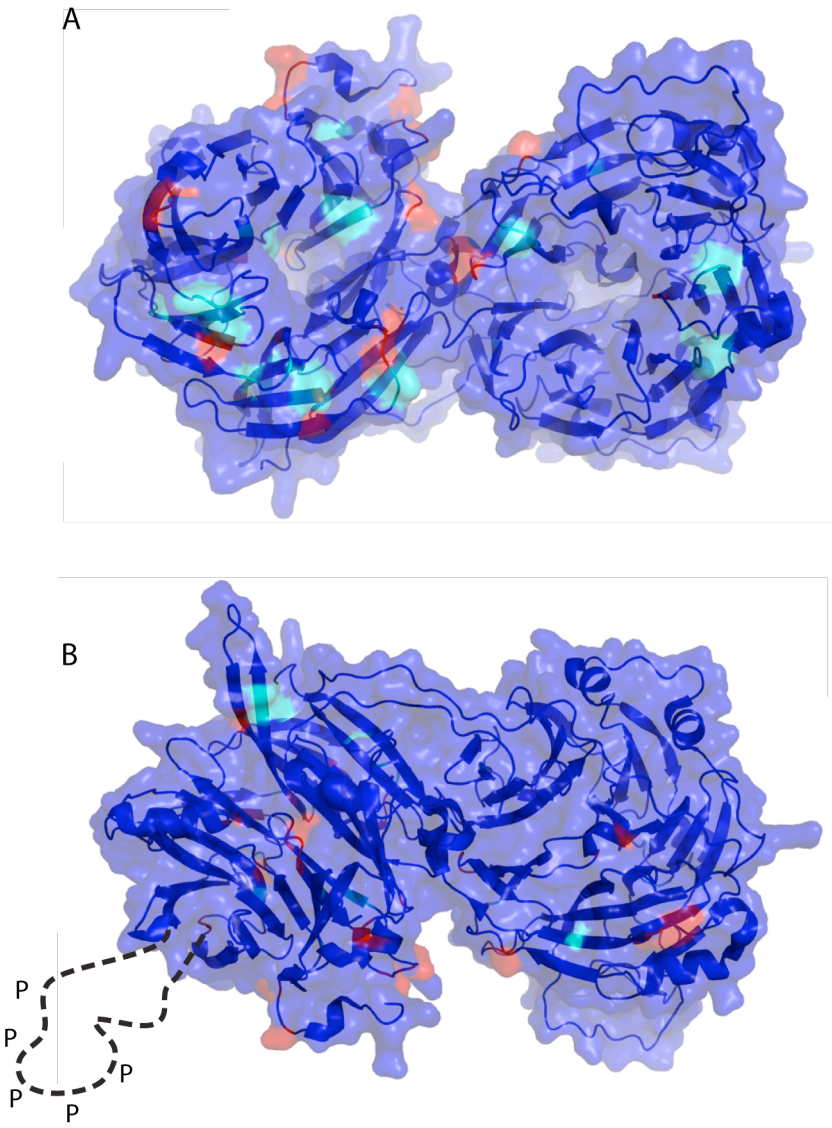

Figure 5.11 Model of LLGL interaction sites with PKCι
A, LLGL2 model with a semi-transparent surface of a view looking into the two WD40 propellers. Conserved acidics (D/E) in red and basics (R/H/K) in cyan. Acidics that co-evolved with a corresponding basic reside in the near vicinity have not been included in the model. B, side on view of LLGL2 model showing the low complexity region (LCR) with multiple phosphorylation sites.

The immunoblots provided further validation for the mass spectrometry screen. Par3, a known binding partner of PKCι was complexed to both PKCι-WT and PKCι-AIPA as supported by the mass spectrometry and number of unique peptides. Par6, that is reported to bind to PKCι via their respective PB1 domains, was also complexed to both PKCι-WT and PKCι-AIPA but was enriched in the PKCι-WT condition. This was also the case in the mass spectrometry results where the ratio of number of unique peptides was 2:1 in favour of PKCι-WT. However, using my hit selection criteria this was considered equal abundance. Endogenous Par6B was able to bind to exogenous LLGL2 in the absence of detectable levels of PKCι. This may be a direct or indirect association - murine Par6 isoforms have previously been shown to bind to murine Lgl (Mlgl). Immunoprecipitation experiments in Cos cells and recombinant murine proteins has suggested that the interaction is mediated via the first PDZ domain of Par6C and the N-terminus of Mlgl (Plant et al., 2003). A further interesting but provisional observation (only 2 separate experiments performed) is that there is greater Par6 interaction with PKCι-WT following LLGL2 knockdown with siRNA. This would imply a degree of competition for binding to the PKCι-complexes.

Having identified a novel protein-binding site in PKCι, excitement was roused by the potential convergence of 2 separate projects in the lab. Dr Alejandra Collazos had identified a PKN consensus substrate motif that overlapped the RIPR motif in PKCι making PKN an ideal candidate as a RIPR binding regulating kinase; independently Dr Collazos had also identified the related PKCζ as a PKN substrate in a screen of over 4000 protein substrates. Phosphorylation of this proposed PKCι phosphorylation site (S477) has previously been noted in mass spectrometry analysis of recombinant PKCι from insect cells (Neil McDonald, unpublished results). While this may not represent the phosphorylation events in mammalian cells, it supported the basis for the subsequent mutagenesis experiments. Attempted phosphomimetic and phosphorylation deficient mutants of S477 were generated but did not effect LLGL phosphorylation, a combined readout of LLGL binding to RIPR and catalytic activity. This suggests that the S477

does not in fact regulate binding to the RIPR binding motif. The ability of S477A and S477E to act as phosphorylation deficient and phosphomimetic mutants has not been formally tested. The S477A hydrophobic substitution will not be able to become phosphorylated but the negatively charged glutamate is often not sufficient to mimic for phosphorylation dependent binding. From this experiment alone therefore, it cannot be ruled out that for example phosphorylation at S477 leads to the binding of an adaptor that is required for binding to PKCι.

In conclusion, the LLGL2 binding site of PKCι has been identified and functional analysis using mutants of this binding site show a disruption in normal polarity in an *ex-vivo* MDCK cyst polarity assay.

Chapter 6. Development of a drug insensitive PKCι mutant and its utilisation for biomarker identification

6.1 Introduction

The interpretation of many studies ascribing PKCι function should be viewed with caution as the tools and reagents to study PKCι specifically have been of poor quality (Garcia-Paramio et al., 1998). Commercial atypical PKC antibodies tested against recombinant atypical PKC isoforms were not specific for PKCι or PKCζ (See Appendix 1). RNAi strategies have been fraught with off-target effects and need corroboration using mechanistically distinct rescue paradigms. Other commonly employed tools include the use of chemical inhibitors. Protein kinase inhibitors fall into 2 main classes, namely competitive and non-competitive. Competitive inhibitors may be type I (DFG-in), where the inhibitor competes with ATP for access to the nucleotide-binding pocket and the conserved Asp-Phe-Gly motif is locked in, or type II (DFG-out) where the Asp-Phe-Gly motif is "flipped out" and the inhibitor binds to an inactive kinase conformation (Knight and Shokat, 2005). The human genome encodes more than 518 kinases with many shared structural and functional features, in particular, the highly homologous ATP binding pocket. Therefore chemical inhibitors specific to a kinase are unusual and multiple off-target effects are reported. Sorafenib (BAY-43-9006), for example, was originally designed as a Raf kinase inhibitor (Lyons et al., 2001) but its subsequent success in clinical trials was probably due to the inhibition of VEGFR and PDGFR, two tyrosine kinases.

One way to circumvent the kinase promiscuity of inhibitors is the use of analogue sensitive kinases modified at their "gatekeeper" residue, an approach pioneered by the Shokat Laboratory (Bishop and Shokat, 1999). The gatekeeper residue is located at the back of the nucleotide-binding pocket and controls access to an enlarged hydrophobic cavity, also known as the selectivity pocket. In nature, secondary resistance to ATP competitive inhibitors is often as a result of a mutation of this gatekeeper residue. For example, the small threonine gatekeeper in EGFR is mutated to a bulky residue,

preventing access to the selectivity pocket, in some tyrosine kinase inhibitor resistant forms of lung cancer (T790M). The same pattern is true for Abl in Chronic Myelogenous Leukaemia (T315I) (Azam et al., 2008, Tamborini et al., 2006, Tamborini et al., 2004). Conversely, the Shokat approach is to exploit the frequently bulky gatekeeper residues in kinases, mutating it to a small residue that enables back-pocket access to a specified chemical ligand. For example, the mutant v-Src kinase (I388G) was exquisitely sensitive to inhibition by 1-NaPP1, a synthesized ligand that has little effect on wild type cells (Bishop and Shokat, 1999).

A second technique of chemical-genetic intervention is to develop a drug-insensitive mutant form of the kinase of interest once a potent compound has been identified. The mutant kinase is altered at the site of interaction between the kinase and an inhibitor while leaving its ATP binding site intact. This approach was first described, for kinases, by the Cohen Laboratory. Overexpression of a drug insensitive Stress Activated Protein Kinase 2a (SAPK2a) prevented reduced phosphorylation by the SB203580 inhibitor of some, but not all of, the previously cited downstream substrates. As such they were able to validate SAPK2a as a target of SB203580 and bona fide SAPK2a substrates (Eyers et al., 1999).

The aim of the work described in this chapter was to apply chemical-genetic techniques to help validate PKCι as a druggable target and develop a platform to facilitate new biomarker discovery.

6.2 Results

6.2.1 PKCι and ligand interaction sites observed in a crystal structure

During the course of this thesis, the crystal structure of human PKCι kinase domain (di-phospho-form phosphorylated at T403 and T555) was determined bound to the CRT66854 ligand. The structure provided a basis for understanding critical drug interaction sites and therefore inhibitor specificity. The CRT66854 ligand has several important features: (1) it has a thieno[2,3-d]pyrimidine scaffold that mimics the adenine

portion of ATP; (2) it has a benzyl moiety that displaces F543 from the nucleotide pocket disordering the loop containing F543; (3) a primary amine adjacent to the benzyl group directly contacts aspartic acid D330 and the main chain carbonyl of D373 close to the ATP pocket and near the PKC substrate binding site (a pyridine substituted hydrogen bonds directly to the PKCι hinge main chain amide of V326 connecting the N- and C-lobes of the kinase). The planar shape of the CRT66854 ligand ensures that no direct contacts are made to the conserved PKCι gatekeeper residue I323 leaving considerable space for chemical elaboration of the small molecule ligand. Each of the above features is likely to contribute towards the selectivity of the CRT66854 ligand for the atypical PKCs.

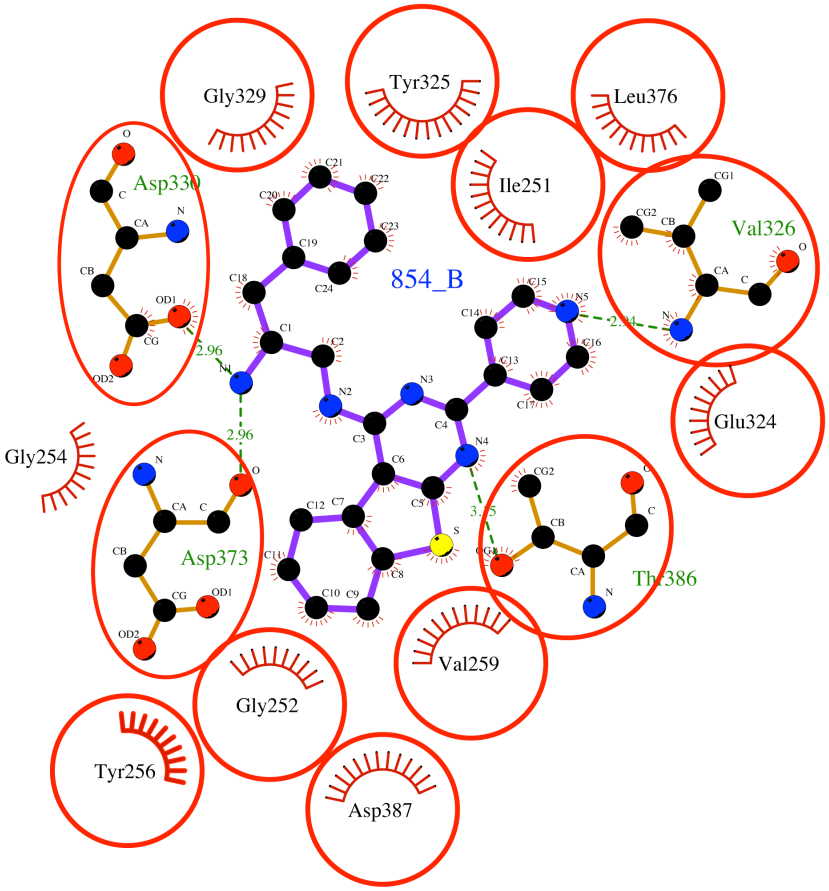

Figure 6.1 Schematic of CRT66854 ligand interactions
PKCι drawn using LIGPLOT software, see http://www.ebi.ac.uk/thornton-srv/software/LIGPLOT/]. CRT66854 is abbreviated to 854.

6.2.2 PKCι mutagenesis of ligand interaction sites results in drug insensitivity

In order to validate the interactions observed within the crystal structure described above, a number of PKCι mutations were generated. The first approach was to use the Shokat system (Figure 6.2A) and create an additional hydrophobic pocket by substituting the relatively bulky gatekeeper isoleucine for a small, hydrophobic alanine (I323A). PP1, an ATP analogue found to inhibit Src kinase, and two derivatives (PP2 and 1-NaPP1) were assessed to see if they could selectively inhibit PKCι-I323A activity in a pLLGL cell based assay. HEK293 cells transfected with PKCι-I323A were treated with the ATP analogues over a range of concentrations (0.001-1μM) for 30mins or with 17.5μM CRT66854, a PKCι selective inhibitor, for 1 hour. Phosphorylation of LLGL was assessed by Western blot but was unaffected by the ATP analogues even up to the highest concentration. As expected the PKCι inhibitor diminished the pLLGL signal for both PKCι-WT and the PKCι-I323A mutant (Figure 6.2B).

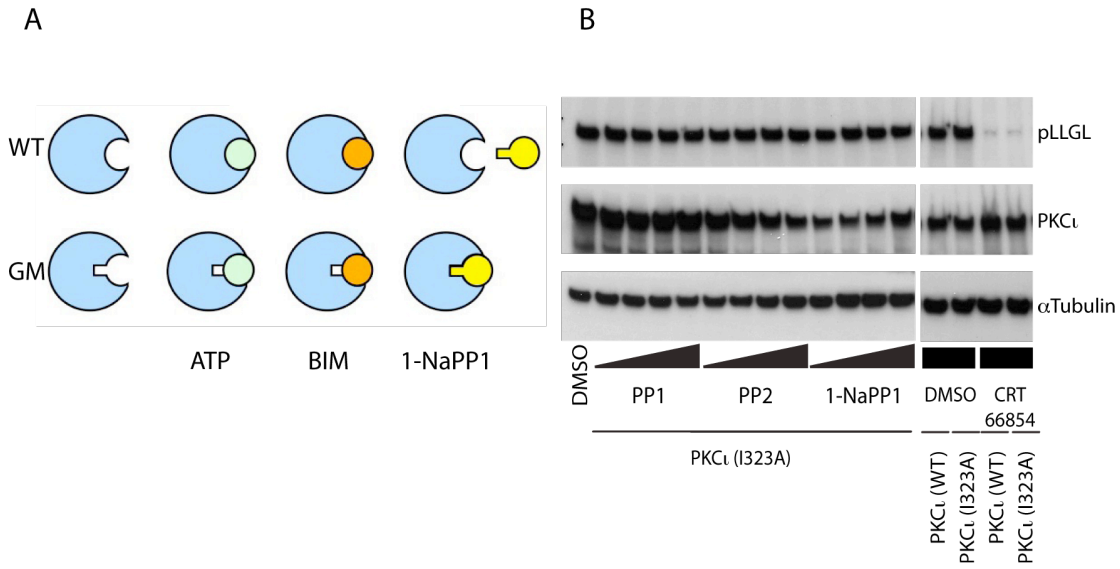

Figure 6.2 Attempted genetic sensitisation of PKCι to ATP analogues
A, schematic representing the 'Shokat' mutant principal. The nucleotide binding pocket of wild type (WT) kinase binds to ATP, and is inhibited by the ATP analogue, Bis-indolylmaleimide (BIM) but not the modified inhibitor 1-NaPP1. The gatekeeper mutant (GM, see text) can still bind ATP and BIM but is exquisitely sensitive to 1-NaPP1. B, HEK293 cells were co-transfected with PKCι gatekeeper mutant (I323A) and LLGL. The cells were treated with different ATP analogues over a range of concentrations (0.001, 0.01, 0.1 and 1μM). pLLGL was used to assess PKCι activity and treatment with CRT66854, a specific PKCι inhibitor was used as the positive control. The Western blot is representative of 3 separate experiments.

As the gatekeeper mutant of PKCι did not allow selective inhibition of the kinase (Shokat system), a second chemical genetic approach was adopted. Point mutants of the two predicted key interaction sites between the active site and the CRT66854 ligand were made. HEK293 cells transfected with PKCι-WT, PKCι-D330A or PKCι-D373A were treated with CRT66854 or DMSO for 1h. At this time point there was no evidence of cytotoxicity from phase microscopy. PKCι-WT cells treated with 3.5μM or 17.5μM of CRT66854 had a decrease in pLLGL of 48% and 80% respectively (Figure 6.3A). Both the point mutants had much less inhibitor induced reductions in pLLGL and at the high inhibitor dose, the level of phosphorylation suppression was 2 fold greater for PKCι-WT.

In an attempt to enhance the drug insensitivity a double substitution mutant was fashioned by sequential mutagenesis. 3.5μM CRT68854 caused minimal suppression of pLLGL in the HEK293 cells over-expressing PKCι-D330A/D373A and at 17.5μM the suppression of pLLGL was 3.4 fold greater for the PKCι-WT (Figure 6.3B). The PKCι western blots reveal a slight band shift between different constructs (Figure 6.3A & B). The constructs that ran fractionally higher contained both GFP and Myc tags whereas those that ran lower did not contain the Myc tag.

To test that the intrinsic catalytic activity was not compromised by the mutations the GFP-tagged constructs were expressed in HEK293 cells and GFP pull-downs of total cell lysates were performed. The immune complex kinase assay demonstrated comparable specific activities for PKCι-WT and the single and double substitution mutants (Figure 6.3C). Importantly there was also no difference in activity between GFP-Myc-PKCι wild type and GFP-PKCι.

In order to demonstrate that the diminished pLLGL signal in the cell based assay was a consequence of a PKCι (or PKCι complex) inhibitory effect, rather than a potential inhibitor 'off target' effect, a dose response curve was generated for one of the mutants. PKCι-D330A, was pulled down and immunocomplexes were added to the reaction mix containing PKCε pseudosubstrate, magnesium and ATP. At low CRT66854 inhibitor concentration (0.1μM) PKCι-WT kinase and PKCι-D330A induced phosphorylation of LLGL was similarly suppressed but at higher inhibitor concentrations (0.1 and 1μM) the PKCι-WT kinase activity, as measured by pLLGL, was inhibited more than PKCι-D330A kinase (Figure 6.3D). The 50% reduction of the relative kinase activity was attained at 0.5μM for PKCι-WT and 1.8μM for PKCι-D330A.

Predicted point mutations of the PKCι kinase domain resulted therefore, in decreased sensitivity to CRT66854 in both in vivo and in vitro phosphorylation studies. In view of the greater level of insensitivity of the double point mutant (PKCι-D330A/D373A), over the single point mutants, this was taken forward for further studies and will be referred to hereafter as the drug insensitive mutant (PKCι-DIM).

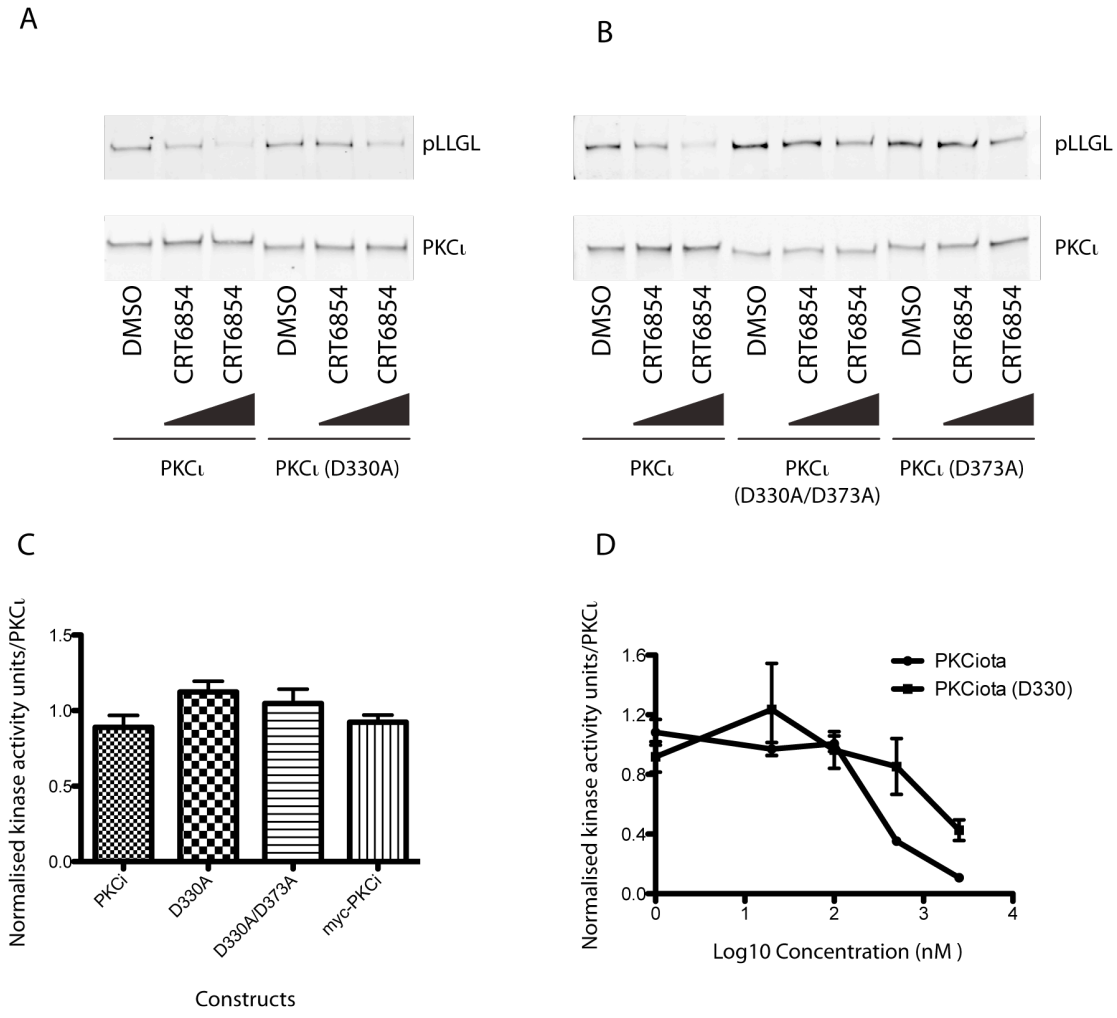

Figure 6.3 Development of a drug insensitive mutant of PKCι
A & B, HEK293 cells were transiently co-transfected with LLGL and PKCι containing point mutations of the ligand-kinase interaction sites. Each PKCι mutant expressing cell line was treated with 3.5μM or 17.5μM of CRT66854. Drug insensitivity is demonstrated by failure to suppress the pLLGL signal. The western blot is representative of 3 separate experiments. C, An immunocomplex kinase assay normalised to the median of all values. Error bars indicate the SEM from 3 separate experiments. D, PKCι or PKCι-D330A immunocomplexes were tested for activity in a kinase assay in the presence of a range of CRT66854 concentrations. Error bars indicate the range from 2 separate experiments.

6.2.3 Drug insensitive mutant is resistant to drug induced cellular phenotype

To further characterize the PKCι-DIM it was incorporated into the MDCK cyst assay, previously defined as a PKCι dependent model (see chapter 3). Inhibition of MDCK

cells, using PKCι siRNA, had resulted in a reduced proportion of MDCK cysts with a normal lumen as defined by apical actin staining. Stable polyclonal cell lines were made expressing GFP-Empty Vector (EV), GFP-PKCι-WT or GFP-PKCι-DIM. The cells were selected by FACS using the same GFP intensity gating for each cell line prior to seeding in Matrigel. The MDCK cultures were treated with inhibitor, at a range of doses between 0 and 3μM, on the day of seeding and then on alternate days for 6 days. Inhibitor treatment diminished the percentage of cysts with a normal lumen for EV and PKCι-WT but had little effect on PKCι-DIM cysts (Figure 6.4A & B). At 3μM CRT66854 there was extensive cytotoxicity precluding any quantification of normal lumens. The basal level of normal lumens was 53% for EV and PKCι-DIM but over 74% for PKCι cysts. In light of the discrepancy between basal expression, particularly between the PKCι and PKCι-DIM, the total cell lysates from the experiment were immunoblotted and a marked difference in PKCι protein expression was seen (Figure 6.4C). The normalised PKCι expression was 2.2 times higher in the PKCι-MDCK cells compared to the PKCι-DIM-MDCK cells. In light of these results, the data is also presented normalised to the basal level of normal lumens for each condition (figure 6.4D). This shows that the rate of drug induced polarity defects is lowest for the PKCι-DIM suggesting that it is indeed relatively drug insensitive.

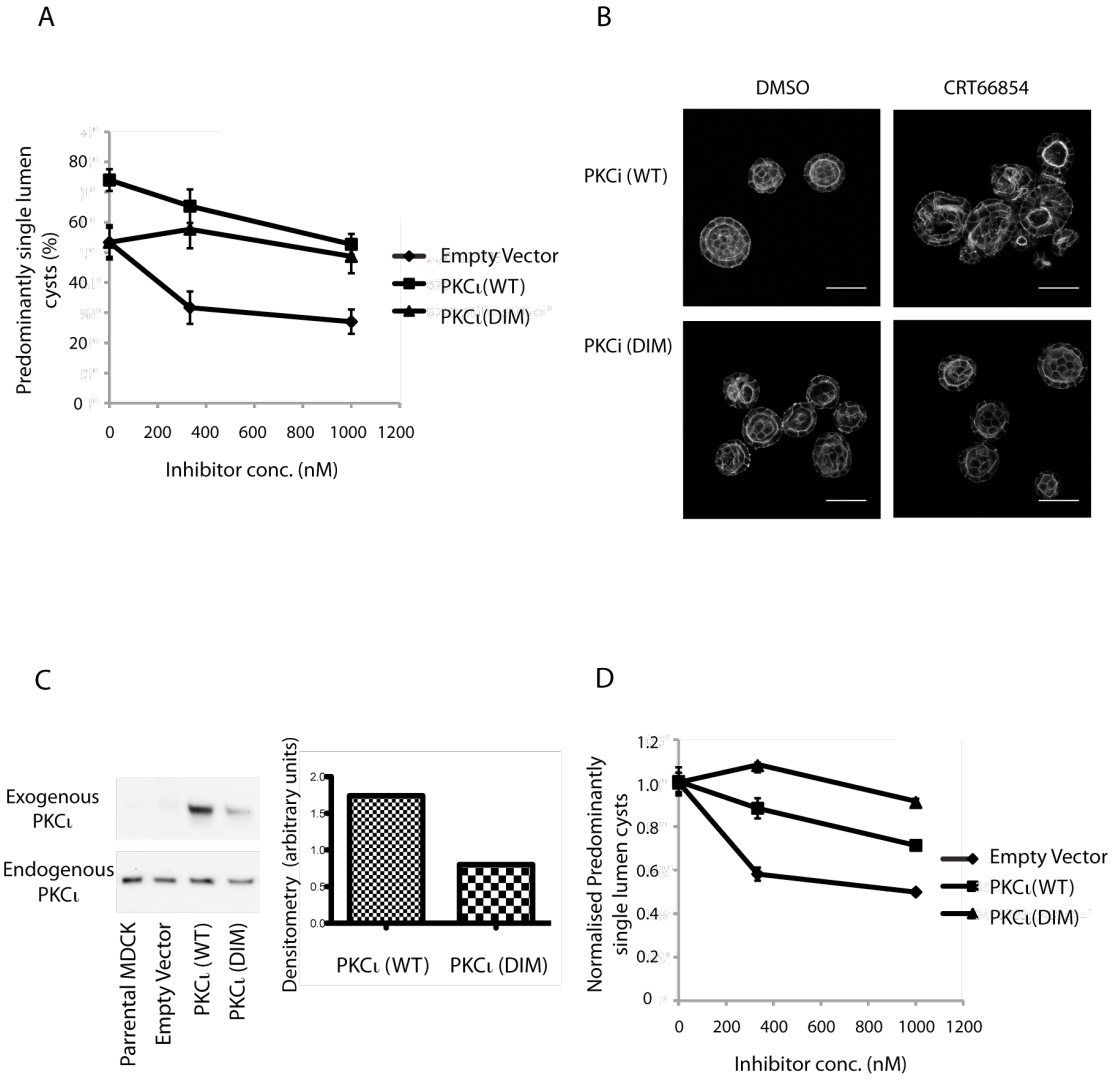

Figure 6.4 The drug insensitive mutant resists drug induced phenotypic change
MDCK cells stably transfected with PKCι-WT, PKCι-DIM or empty vector were cultured in Matrigel for 6 days. The cultures were treated with a range of inhibitor concentrations (0-1μM) which were replenished, along with growth media, on alternate days. Quantification of the number of predominantly single apical lumens (PSALs) was made. At least 100 spheroids were counted per condition in each experiment and the results of at least 3 separate experiments are presented. A, the absolute percentage of single apical lumens. B, Single confocal images of actin staining (white). Scale bars represent 50μM. C, Western blot representing the exogenous PKCι expression in the stable cell lines. The Western blot is representative of duplicate immunoblots. D, the change in single apical lumen formation relative to exogenous PKCι expression and error bars represent the SEM.

6.2.4 PKCι Drug Insensitive Mutant can be applied to biomarker discovery

With a platform for specific PKCι intervention in place, the chemical-genetic strategy was applied to the identification of PKCι substrates. This work was carried out in collaboration with Dr Philippe Riou in the Protein Phosphorylation Laboratory.

HCT 116 cells were transiently transfected with PKCι or PKCι-DIM. 36 hours post transfection the cells were treated with 10 μM CRT66854 for 1 hour followed by immunoprecipitation of the total cell lysates. The colloidal Coomassie stain of the resulting SDS PAGE gel (see figure 6.5A) demonstrated equal protein loading between the four conditions and no obvious differential bands.

The gel was immunoblotted with a phospho-serine-PKC (pPKC) substrate antibody (figure 6.5B). Both the PKCι and PKCι-DIM transfected cells treated with vehicle control showed multiple immunoreactive bands. Treatment of the PKCι transfected cells with CRT66854 led to almost complete loss of pPKC substrate signal whereas the PKCι-DIM transfected cells only had a partial reduction in pPKC signal. To determine whether this PKCι specific effect of CRT66854 was a disruption in complex formation, substrate phosphorylation or both, an in vitro kinase assay was performed on the immunocomplexes extracted from the drug treated, PKCι transfected HCT116 cells. This demonstrated full reversibility of the phosphorylation signal indicating loss of phosphorylation and not loss of associated substrate (see figure 6.5C).

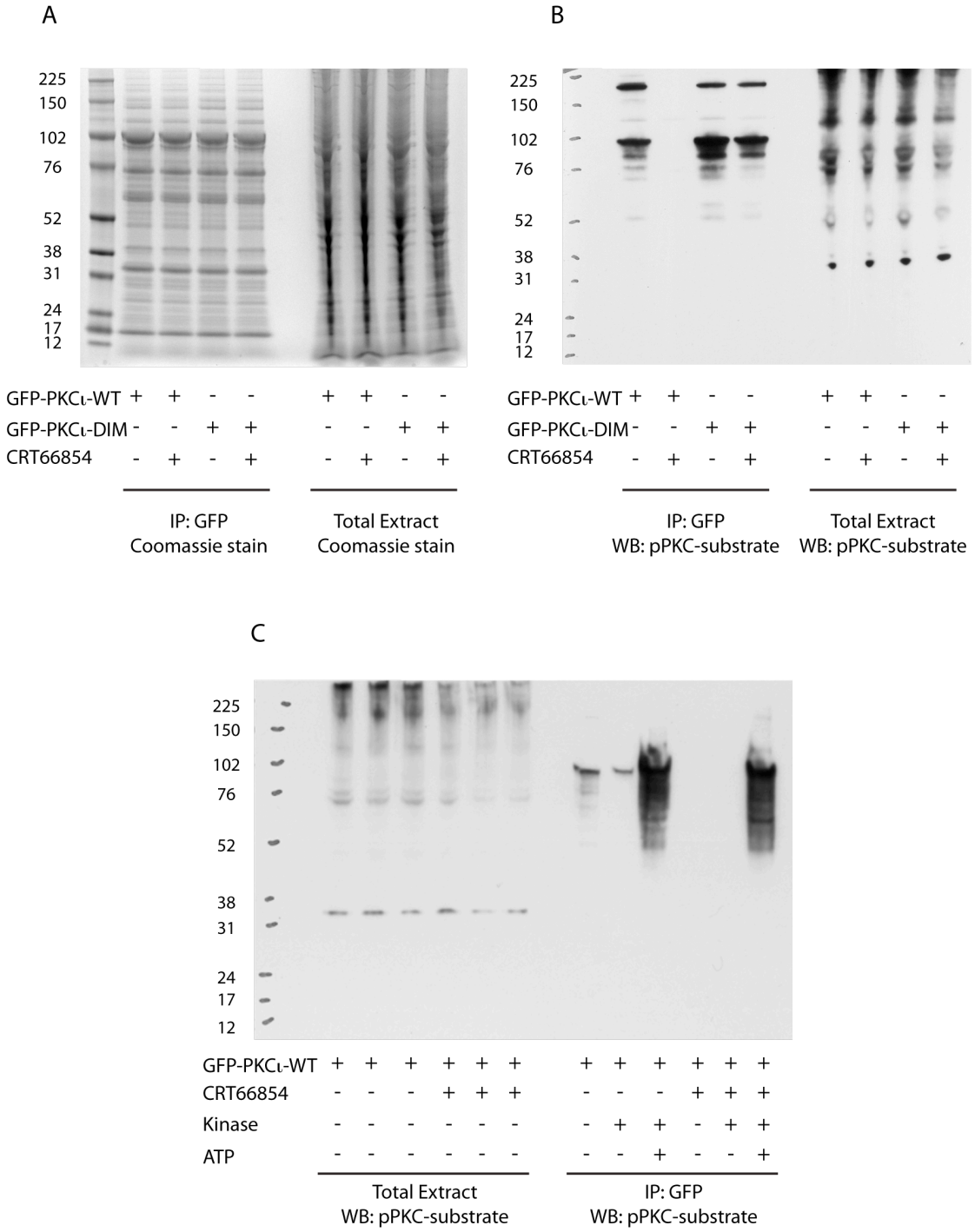

Figure 6.5 Chemical-genetic approach for substrate identification
HCT116 cells were transiently transfected with GFP tagged PKCι-WT or PKC-DIM, treated with CRT66854 for 1 hour, lysed and immunoprecipitated. A, colloidal Coomassie showing protein loading. B, Western blot for pPKC. C, Cell transfected with PKCι-WT cells treated with CRT66854 and then an immunocomplex kinase assay performed. The kinase assay mix was run on an SDS page gel and immunoblotted for pPKC. The western blots shown are representative of at least 3 separate experiments.

6.3 Discussion

In this chapter it was shown that a combined approach of structural biology, cell biology and medicinal chemistry has enabled new strategies to test the specific function of PKCι and potentially identify new clinically relevant biomarkers.

The first strategy attempted however was unsuccessful as the mutated kinase made did not demonstrate any specific sensitivity to the ligands tested. In this experiment the bulky isoleucine gatekeeper residue was substituted for a small hydrophobic alanine. This is in contrast to Bishop et al who mutated the isoleucine of the Src ATP pocket for a glycine. The alanine substitution was chosen over the glycine as this had previously been demonstrated to be highly effective at sensitising other PKC family members (PKCε and PKCα) to 1-NaPP1 inhibition (Saurin et al., 2008, Cameron et al., 2009). The range of doses and treatment duration of PP1 and its analogues were selected based on the previously published results of the 1-NaPP1 and GFP-PKCε-M486A Shokat pair (Cameron et al., 2009). It is possible that higher doses might be required or that a different bulky derivative of another core structure might have worked. While there were no internal positive controls for the PP1 analogue batches, a synchronous experiment in the Parker Laboratory demonstrated the expected 1-NaPP1 induced PKCε-M486A inhibition in HeLa cells, as manifest by cytokinesis failure (personal communication with Dr Nicola Brownlow). For further attempts to establish this model a larger panel of potential ligands should be considered, and in addition, alternative gatekeeper residues utilised. This course of action was not pursued as the Drug Insensitivity mutant strategy, conducted in parallel, showed more promise. Having said this, the Shokat system is particularly elegant for functional studies, as the ligand can be engineered to have virtually no cellular off target effects and therefore a clear background for subsequent studies.

LLGL is a known substrate of PKCι and its phosphorylation was shown in chapter 3, in an exogenous co-expression assay, to be correlated with PKCι activity. In this chapter suppression of pLLGL was achieved in a dose-dependent manner for drug treated PKCι wild type. Doses were chosen as one times and five times the established cellular EC 50 (Barton et al., 2009b). Two main kinase-inhibitor interaction sites were identified

and upon mutation each resulted in drug insensitivity. Unlike Eyers et al, when no additional effect was seen between a single mutation and quadruple mutations of the ATP site (Eyers et al., 1999), a clear additive insensitivity was seen for a double point mutant compared to the single mutants of PKCι. This suggests that both aspartic acids make important charged interactions with the small molecule ligand.

In view of the 3.5 fold difference in phosphorylation inhibition between the wild type and drug insensitive PKCι, a measured difference in a cell phenotypic assay could be anticipated. Consistent with the previously demonstrated siRNA-PKCι results, inhibition with CRT66854 disrupted normal apical lumen formation in control MDCK cysts grown in Matrigel. Kim et al have previously demonstrated abnormal lumen formation, increased apoptosis and proliferation, in parental MDCK cells grown for 6 days in a collagen, in response to a myristolated aPKC pseudosubstrate inhibitor (Kim et al., 2007). They did not include an apical marker in this assessment and so it is not clear whether there is a multi-lumen phenotype, delayed lumen formation or permanent apical-basal disruption.

The sensitivity to CRT66854 induced polarity defects was highest for EV-MDCK, followed by PKCι-MDCK and was lowest for PKCι-DIM-MDCK. This suggests that the exogenous PKCι affords the cell protection against aberrant lumen formation, because cellular substrates are in excess and the increased enzyme concentration leads to more catalytic product despite the presence of a competitive inhibitor. In the drug insensitive mutant, the competition for catalysis by the inhibitor is negated and the rate of catalytic product is likely to be further increased. It is noteworthy that this incremental rate of catalysis for the PKCι-DIM-MDCK cells over the PKCι-MDCK is despite considerably lower expression of the drug resistant protein and the observed effect may be much greater if equal expression could be achieved.

In order to try and attain equal protein expression between PKCι-DIM-MDCK PKCι-MDCK (both expressed in the pEGFP-C1 vector) the populations were FACS sorted using equivalent GFP intensity gating. The polyclonal cell population was expanded over 1 week and then immediately used in the 3D Matrigel assay. The subsequent Western Blot for PKCι, however showed much lower PKCι expression in the PKCι-

DIM-MDCK cells. This could be due to a rapid drift of the polyclonal cell population indicating a potential detrimental effect of the drug insensitive protein or a selective survival advantage of the wild-type protein in MDCK cells. In provisional experiments using the same constructs, no drift was observed in Normal Rat Kidney cells and in experiments by Dr Philippe Riou in the Parker Laboratory there was evidence in HCT116 cells of a rapid drift favouring high expression of PKCι-DIM over PKCι. A further explanation is that within the defined range of GFP-intensity used for sorting the cells they happened to be predominantly at the low end of the range for PKCι-DIM but at the upper end of the range for PKCι.

It is becoming evident that target inhibition as opposed to knock-down is more effective in determining the biological outputs of a target (Weiss et al., 2007). Kinases often have both catalytic and scaffold functions. Inhibition with small molecules will block the catalytic function but will not necessarily affect protein-protein interactions. Knockdown by allelic deletion or RNAi will affect both enzymatic and scaffold functions and remaining proteins from the now redundant complex may impact on other signalling pathways. One example of this anomalous behaviour is the inhibition of p110β, one isoform of the catalytic subunit of PI3 Kinase. In glioma cells siRNA directed against p110β decreased both proliferation and phosphorylation of PKB. A panel of selective inhibitors, however, blocked only PKB phosphorylation. The catalytic PI3 kinase subunits (p110α, β and δ) form a stable heteromer with the regulatory subunit (p85α and β). p110α inhibitors do block proliferation. It has been proposed therefore that siRNA-p110β not only prevents phosphorylation of its downstream targets (PKB), but by virtue of the resulting free p85 sequestering proteins required for p110α complex activation, proliferation signalling is abrogated (Fan et al., 2006). In situations such as these, knockdown would not be helpful for the identification of physiological substrates that may be used as biomarkers for an upstream kinase. As RNAi is commonly used to aid inhibitor target validation it is likely that inhibitor and RNAi incongruence is under-reported in the scientific literature.

The potentially limited specificity of action of inhibitors precludes a simple drug versus no drug analysis. However the use of a modified insensitive target circumvents this issue permitting comparative studies potentially leading to a robust biomarker.

CRT66854 induced loss of phosphorylation of multiple bands of PKCι immunocomplexes compared to the drug insensitive PKCι (PKCι-DIM) immunocomplexes. The magnitude of this difference seen with the HCT116 immunocomplexes was considerably greater than the 3.4 fold difference observed with pLLGL in total HEK293 cell lysates. The differences could relate to cell type specificity, differences in transfection efficiency between the two studies or reduction of background substrate phosphorylation for immunocomplexes compared to total cell lysates. For example, LLGL2 may be phosphorylated by other kinases in the cell and not be part of PKCι complexes. This proportion of LLGL would be unaffected by PKCι inhibitors in a total cell lysate but would not be present in PKCι complexes. The ability to take the PKCι-immunocomplexes of CRT66854 treated cells and then rescue the substrate phosphorylation in an in vitro kinase assay, demonstrates that the small molecule inhibitor is affecting catalytic function, and not complex formation. A concern about protein over-expression studies is that they can result in saturation of the cells translation, sorting and protein modifications, artificially modifying normal signalling cascades. Candidate biomarkers identified using over-expression systems must therefore undergo further validation in control matched disease tissue.

In this study the drug insensitivity strategy worked well and there is the promise of the discovery of clinically relevant PKCι biomarkers. Having established the principle, the mass spectrometry results, for identification of the substrate bands revealed in this study, are eagerly awaited.

Chapter 7. Discussion

7.1 Overview

Protein Kinase C iota (PKCι) is a serine-threonine protein kinase that is a human oncogene, aberrantly expressed in cancer and is a prognostic indicator (Fields and Regala, 2007, Eder et al., 2005). Consequently PKCι is considered a desirable target for drug development. The work performed in this thesis was motivated by the desire to understand mammalian PKCι biology with a view to assisting in rational therapeutic design. On commencing this work, little was known about robust inputs into the PKCι signalling cascade and less still was known about the downstream effectors. PKCι function is essential in normal development as the knock out mouse is embryonic lethal (Soloff et al., 2004). In non-transformed cells PKCι had been demonstrated to play a role in apical-basal polarity (Izumi et al., 1998, Aranda et al., 2006), growth (Grzeschik et al., 2010a) and asymmetric cell division (Atwood and Prehoda, 2009). Additionally, during the period of this thesis, a role in migration and spindle orientation in mitosis were also firmly established (Durgan et al., 2011, Qin et al., 2010).

Initial investigations in this thesis set out to identify a reproducible PKCι dependent phenotype in the context of mammalian oncogenic signalling. In keeping with phenotypes described in non-transformed cells, the data in this thesis shows that PKCι only demonstrated a reliable phenotype following chemical or genetic perturbation in cells grown in 3D cultures. This finding is in keeping with work from the Fields Laboratory that showed that treatment of a lung adenocarcinoma cell line, A549, with dominant negative PKCι mutant had no effect on the adherent cell growth or survival but caused a dramatic decrease in 3D colony formation (Regala et al., 2005a). The differences in phenotypic response between 2D adherent cell growth and growth in 3D matrices is well described (Janda et al., 2002, Weigelt et al., 2010) and is perhaps unsurprising, given the known differential protein expression seen in proteomic studies of transformed cells between the two culture conditions (Toyli et al., 2010).

Based on the well-established ability to form rapid polarised cysts in 3D gels, Madin-Darby canine kidney (MDCK) cells were selected to interrogate PKCι function. Single

apical lumen formation was disrupted by both high activity and dominant negative activity PKCι mutants, as well as siRNA against PKCι. As normal levels of PKCι were required for single apical lumen formation it was hypothesised that PKCι may lie downstream of recognised human oncogenes. Consequently MDCK cells lines transfected with single oncogenes, each one chosen due to their published interaction with PKCι/ζ, were obtained or generated. These cell lines were then screened for their lack of apical lumens in 3D culture and rescue of a predominant apical lumen upon treatment with 2 separate PKCι siRNA. Activated Src- and Raf-MDCK had persistent apical lumens that were largely unaffected by siRNA against PKCι. Activated ErbB2, H-Ras and p110α all had markedly abnormal morphology in 3D culture with large irregular structures often lacking a predominant apical lumen. In structures that did maintain a lumen, the apical marker actin was frequently re-localised to sides facing the basal and lateral surface of the cells. Upon PKCι-siRNA treatment, activated ErbB2- and Ras-MDCK developed a predominant lumen with prominent actin staining whereas activated p110α-MDCK did not. The specificity of PKCι siRNA was demonstrated by overcoming the lumen and polarity induction using a siRNA resistant form of PKCι cDNA. All oncogenic-MDCK spheroids appeared smaller in size following PKCι siRNA treatment but the size of parental MDCK cysts were not diminished. Thus siRNA knockdown of PKCι had a range of effects depending on oncogenic contexts including decreased size alone, decreased size and rescue of apical lumen or unaffected size and disruption of apical lumen.

From the crystal structure of PKCι bound to the CRT66854 ligand, a relatively specific ATP-competitive inhibitor of PKCι, a potential protein-protein interaction region was identified. Mutagenesis of this region of PKCι (RIPR>AIPA) and subsequent mass spectrometry analysis identified a number of proteins that require this motif for binding. One of these hits, Lethal Giant Larvae 2 (LLGL2) was confirmed to require the RIPR motif by reciprocal immunoprecipitation and immunodetection, validating the mass spectrometry approach. Stable transfection of MDCK cells with PKCι-AIPA disrupted normal polarity.

LLGL2, when co-transfected with PKCι, proved to be a useful system to assess the potency of PKCι inhibitors. However, the expression of LLGL2 is variable in transformed cells and the current available antibodies are poor at detecting endogenous levels, limiting its potential application as a clinically relevant biomarker. Low efficiency and off target effects of PKCι siRNA and lack of specific PKCι inhibitors and antibodies has made identification of PKCι-downstream effectors challenging. To circumvent some of these issues a chemical genetic approach was adopted. Based on predictions from the CRT66854 bound PKCι crystal structure a drug resistant mutant form of PKCι was generated. PKCι inhibition with this drug was shown to decrease kinase activity in vitro, reduce LLGL phosphorylation in a cell based assay and lead to abnormal lumen formation in an MDCK cyst assay. The PKCι drug insensitive mutant partially rescued each of these parameters, consistent with its reduced sensitivity.

7.2 PKCι as a downstream Ras effector in polarity signalling

For the first time, the work in this thesis has demonstrated that PKCι may sit downstream of oncogenic Ras in a pathway responsible for regulating MDCK polarity. Over recent years a number of other groups have identified a role of PKCι downstream of oncogenic Ras in both tissue culture and murine models. It has been suggested that PKCι plays a role in transformed growth and survival mediated by Rac1 and NF-κB signalling pathways respectively (see section 1.3.3.3). It was also shown in this thesis that ErbB2 seems to act upstream of PKCι in MDCK polarity signalling. This is in keeping with the findings of the Muthuswamy Laboratory which showed, in a MCF10a 3D culture model, that activated ErbB2 induced a multicystic appearance, failed luminal clearance and relocalisation of apical markers to basal and lateral cell surfaces. Genetic disruption of aPKC-Par6 binding partially rescued this activated ErbB2 induced phenotype. It was also demonstrated, in both MDCK and MCF10a cells, that aPKC-Par6 co-immunoprecipitated with ErbB2 although a direct interaction was not proven (Aranda et al., 2006). It is well recognised that persistent ErbB2 signalling promotes oncogenic transformation that is mediated, at least in part, by activation of Ras (Satoh et

al., 1990, Eckert et al., 2004). It is possible therefore that an ErbB2>Ras>PKCι polarity signalling axis exists.

Activated Ras is now known to relay signals to multiple pathways including Raf, PI3-K, phospholipase Cε and RalGEFs (Buday and Downward, 2008, Ferro et al., 2008) (see section 1.2.8). The results from this screen of iota dependence, downstream of selected oncogenes, indicate that this polarity signalling is not via c-Raf or p110α. Of course there are other isoforms of Raf (A-Raf and B-Raf) and PI3K (p110β, p110δ, p110γ catalytic subunits) that could mediate this response but it is intriguing to speculate about a third but less well recognized Ras signalling effector, Ral. RalA, one of the two Ral isoforms, is a small GTPase that has been implicated as potentiating the interaction between par-3, aPKC, and the exocyst complex thus regulating neuronal polarity (Lalli, 2009). RalA has also been shown to be activated in human samples of Ras mutant colorectal cancer (Martin et al., 2011).

A bioinformatics search for co-expressed gene products in epithelial cancers was performed using the oncomine database (www.oncomine.com). Surprisingly, the gene mRNAs that were co-overexpressed with PKCι mRNA were the same genes identified as being upstream of PKCι in polarity signalling in this thesis, namely Ras and ErbB2 . In addition, RalA and its binding partner RalBP1, were also concomitantly overexpressed with PKCι. V-Src, c-Raf and p110α are not concomitantly overexpressed and this is despite the fact that p110α is found within the same chromosomal band (3q26.3) as PKCi. It should be noted that this result could be affected by a sampling bias as gene analysis studies that included PKCι were less likely to screen for Src, c-Raf and p110α. Mechanistic studies into the potential role of RalA as a signalling intermediary between Ras and PKCι in epithelial polarity should be pursued. The case to do so is further strengthened by the finding that Ral A co-immunoprecipitated with exogenous PKCι in HCT116 cells (personal communication from Philippe Riou).

Median Rank	p-Value	Gene
239.5	2.10E-5	PRKCI
703.0	0.009	RALA
1154.0	0.027	KRAS
1192.0	0.001	HRAS
1385.5	0.019	RALBP1
2331.5	6.46E-4	NRAS
2456.0	0.009	ERBB2
2945.0	0.061	PIK3CA
3324.0	0.126	RALB
3984.0	0.902	SRC
5572.0	0.500	RAF1

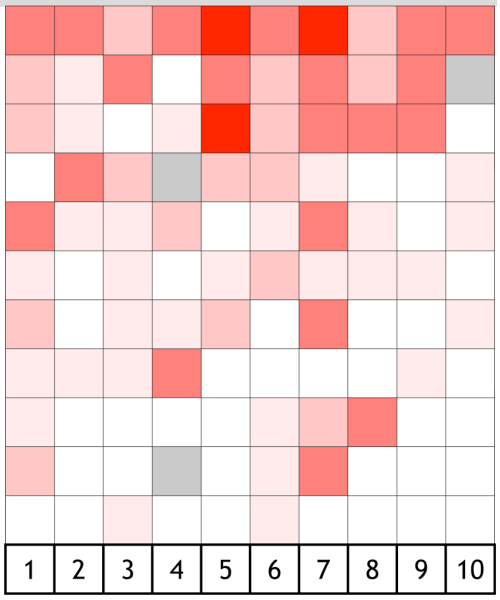

Figure 7.1 Oncomine analysis of selected gene expression in epithelial cancer
The top 10% of epithelial cancer studies from the Oncomine database with at least a two-fold over-expression of PKCι in cancer samples compared to normal controls were selected. Concurrent expression of selected genes was analysed. The heat map indicates the level of expression: over-expression (red), under-expression (blue), un-changed (white) and not measured (grey). Tumour types: 1, Pancreatic; 2, Squamous cell carcinoma (SCC) of the lung; 3, Bladder; 4, SCC lung; 5, Ovarian; 6, Skin; 7, Pancreatic; 8, Pancreatic; 9, Ovarian; 10, Ovarian.

7.3 Polarised cysts

Cell polarity is the restricted and organised localisation of cell components to distinct regions within the cell. Loss of cell polarity is commonly observed in advanced tumours and correlates with their invasion into adjacent tissues and the formation of metastases (Wodarz and Nathke, 2007). Polarity proteins may function within aberrant growth signalling pathways in cancer and intact global polarity may suppress signalling that is exploited by malignancy (Wodarz and Nathke, 2007, Lee and Vasioukhin, 2008). In a number of epithelial malignancies PKCι expression levels correlated to cancer stage and prognosis. This clinical correlation suggests that PKCι is involved in cancer progression and metastasis rather than cancer initiation (Eder et al., 2005, Regala et al., 2005b).

Cells lining ductal structures exhibit apical-basal polarity in which proteins asymmetrically distribute along the apical-basal axis (Huang and Muthuswamy, 2010). In order to study this process techniques have been devised to culture specialised epithelial cells in a 3D extracellular matrix (O'Brien et al., 2001, Debnath et al., 2003). The principle technique used in this thesis was MDCK cytogenesis in Matrigel. From a single cyst of cells several parameters may be determined; proliferation, apoptosis, central luminal clearance and polarised protein distribution (Elia and Lippincott-Schwartz, 2009).

For the purposes of the screen undertaken in this work, looking into the role of PKCι downstream of selected oncogenes, a robust read-out was required. The criteria chosen was the determination of predominantly single apical lumens (PSAL). This was a composite end-point of lumen formation and polarity. The apical polarity component was defined by the presence of more intense actin staining at the lumen than at basal and lateral cell aspects. This assessment was deliberately simple and could be performed down the eye-piece of a confocal microscope which allowed for the inclusion of large, statistically relevant numbers of spheroids. To take this assay further an automated determination of the centre of the spheroid, image capture and actin intensity would be desirable. Aside from time, one of the excepted limitations of this assay was the difficulty in identifying normal apical polarity in the absence of a lumen.

In this thesis manipulation of PKCι activity in parental MDCK cells led to irregular growth and multiple lumens. In some cases, but not all, these multiple lumens continued to be have polarised actin at the apical interface. Recently a number of other groups have identified that perturbation of ‘polarity proteins’ in epithelial cysts can, in some cases, lead to a multi-luminal phenotype that has normal apical protein localisation. Potentially the multi-luminal phenotype is a more sensitive indicator of impending polarity failure. Alternatively, the multi-luminal phenotype may be the result of aberration of a PKCι dependent signalling pathway that is distinct from or a different mechanism of polarity, for example mitotic spindle orientation (Durgan et al., 2011, Qin et al., 2010, Jaffe et al., 2008). At the current time therefore, the multi-lumen phenotype should not be considered a surrogate for polarity.

The MDCK assay was designed to identify differences in apical lumen polarity. During the course of these investigations interesting preliminary observations were also made regarding the size of both parental MDCK cysts and the oncogenic-MDCK spheroids. The measurement of spheroid size is really a combination of two processes; proliferation and apoptosis (no evidence of larger cells). In order to improve the understanding of the role of PKCι in cyst and spheroid growth, future studies would benefit from immunostaining with markers of proliferation and apoptosis such as Ki67 and Caspase-3.

7.4 Threshold effects of PKCι signalling

PKCι manipulation in MDCK cells appears to result in an all or nothing response with regard to normal lumen formation. For example, over-expression of wild type PKCι had no detrimental effect on MDCK polarity but constitutively active PKCι expressed at a comparable level resulted in large, multi-cystic structures with poorly defined apical markers. This observation suggests that above a particular activity level of PKCι a different signalling response is initiated. Such a threshold effect is common in cellular signalling pathways and requires positive feedback mechanisms to achieve the binary response (see section 1.2.7).

PKCι seems to exhibit multiple thresholding in MDCK cytogenesis. Expression of activated PKCι or dominant negative PKCι both caused a decrease in normal cystogenesis, as does inhibition of PKCι with siRNA. This strongly suggests that a normal activity of PKCι is tightly regulated. It would be predicted that the improvement in polarity upon PKCι siRNA treatment of H-Ras-MDCK cells is derived from a reduction in activated PKCι. By analogy to parental MDCK it would also be predicted that knockdown below a particular threshold would revert back to abnormal polarity. With this in mind it is perhaps fortuitous that the siRNA knockdown in H-Ras-MDCK only achieved a moderate knockdown, thus revealing the dramatic rescue

of a polarised lumen. It would be interesting to test for the potential role of thresholding in Ras-MDCK but it may not be possible to achieve a good enough knockdown with siRNA. Instead dominant negative PKCι constructs or titrated PKCι inhibitors could be used to test this hypothesis.

While it has been inferred that the threshold behaviour described in this thesis is due to differing PKCι activity levels, the evidence to support this is lacking. No increase in total PKCι or phosphorylated PKCι levels were detected in oncogenic-MDCK spheroids. These findings may still be compatible with an activated PKCι state as PKC family members adopt an activated open configuration that is more sensitive to protease degradation (Gao et al., 2008). Therefore, chronic activation of PKC could theoretically lead to decreased protein levels at steady state. PKCι priming phosphorylation is only representative of activity levels in restricted cellular contexts as typically PKCs are constitutively primed. PKCι protein turnover could be measured using a pulse-chase approach and may reveal increased turnover as a consequence of upstream oncogenic signalling. In addition the identification of robust PKCι biomarker would be invaluable in this setting.

7.5 Distinct PKCι polarity and growth pathways

In murine mammary cells the presence of endogenous PKCζII, a protein homologous to the PKCζ regulatory domain that acts as a PKCζ inhibitor, disrupted tight junction formation following calcium switch and caused cellular overgrowth (Parkinson et al., 2004). These findings led to the hypothesis that abnormal epithelial growth is a secondary effect of globally deregulated cell polarity. In this thesis, knockdown of PKCι in 3D growth assays of oncogenic-MDCK cells revealed two features; decreased size and induction of a polarised apical lumen. While all MDCK oncogenic spheroids (p110α-, c-Raf-, v-Src-, H-Ras- and ErbB2-MDCK) were diminished in size following PKCι siRNA only H-Ras- and ErbB2-MDCK cells demonstrated induction of a polarised apical lumen. One explanation for this is that two distinct PKCι dependent pathways exist for growth and polarity and that the polarity pathway is only functional

in particular cellular contexts. Similarly, the Hall Laboratory identified two separate functions of aPKC in Caco2 cystogenesis in 3D growth assays; multiple lumen formation and cell survival. By titrating the siRNA concentration and thus the level of PKCι knockdown it was shown that the morphological changes were sensitive to partial PKCι knockdown whereas decreased cell survival only occurred with more robust knockdown (Durgan et al., 2011). These data support the notion that PKCι is involved in distinct pathways.

Three recent studies in *D.melanogaster* have all demonstrated that the polarity proteins Lgl, scrib and crb regulate tissue growth independently of cell polarity. (Ling et al., 2010); (Robinson et al., 2010); (Grzeschik et al., 2010a). In particular, control of growth (proliferation and apoptosis) was mediated by the Salvador/Warts/Hippo (SWH) pathway (see (Parsons et al., 2010) for review). The SWH pathway is a kinase cascade where Hippo (Hpo) binds to its adapter protein Salvador (Sav) to enable phosphorylation of Warts (Wts) that phosphorylates and excludes from the nucleus the transcription factor Yorkie (Yki). Among the transcriptional targets of Yki are cell cycle regulators E2F1 and CycE and the Drosophila inhibitor of apoptosis 1 (DIAP1). Upon knockdown of Lgl or over expression of aPKC or Crb the transcriptional targets of the SWH pathway were elevated suggesting that disruption of the polarity machinery leads to up regulation of this proliferation and anti-apoptotic pathway.

Over-expression of a CrbΔPDZ–transgene, that lacked polarity complex binding, (see section 1.2.5.3) up regulated the SWH pathway and was sufficient for wing tissue overgrowth. Conversely, a CrbΔFERM-transgene, that had intact polarity complex binding but was unable to bind FERM domain proteins did not affect the SWH transcription targets or result in tissue overgrowth (Grzeschik et al., 2010a). Surprisingly, knockdown of Crb led to overgrowth but with preserved polarity (Robinson et al., 2010, Richardson and Pichaud, 2010). A possible explanation for this is that expanded (Ex), a FERM domain binding protein that negatively regulates the transcription activity of Yki, is reduced as a result of Crb over-expression and is increased but mislocalised in response to Crb knockout (Ling et al., 2010). It has been proposed that the Ex protein is unable to inhibit Yki, as it is either absent or in a

location distinct from Yki, thereby resulting in increased SWH target transcription and growth.

In larval eye disks Lgl knockout or aPKC overexpression, in addition to upregulation of the SWH pathway, caused co-mislocalisation of Hpo and RASSF (Grzeschik et al., 2010b). The Tapon Laboratory demonstrated that RASSF competes with Sal for Hpo binding and therefore inhibits Hpo (Polesello et al., 2006). Expression of a membrane targeted dominant negative aPKC construct in an Lgl knockout clone rescued both the tissue overgrowth and the RASSF/Hpo mislocalisation. Taken together, these data suggest that a disrupted balance between aPKC and Lgl leads to mislocalisation of RASSF and Hpo, suppression of Hpo catalytic activity and resulting Yki induced transcription and proliferation. Eliciting the mechanism by which the aPKC-Lgl balance impacts on RASSF-Hpo localization is undoubtedly a hotly pursued area of biological research at the current time.

Based on the current understanding, it seems likely that global polarity aberration can contribute to deregulated growth but is neither necessary nor sufficient. The growth signalling resulting from neoplastic gene products is regulated by feedback mechanisms and cellular localisation and is interwoven with recognised hypertrophic growth pathways. In addition these pathways may be cell type and species specific.

7.6 RIPR protein binding region of PKCι

During the work undertaken in this thesis a novel protein-binding region of PKCι was identified between residues 471 and 474 (RIPR). Using stringent stratification criteria 5 protein hits that require the RIPR motif for immunocomplex formation were identified from a mass spectrometry screen. One of the hits was lethal giant larvae 2.

The finding that this double arginine motif is conserved in a number of protein kinases including PKCζ, PKB and EGFR suggests that it is likely to be a functional motif. This led to question of whether the RIPR binding domain has any physiological relevance. LLGL was identified as a tumour suppressor gene in *D.melanogaster* where its deletion

leads to a neoplastic phenotype (Gateff and Schneiderman, 1969). LLGL plays an important role in epithelial polarity. While genetic experiments have demonstrated LLGL to be a tumour suppressor gene in *D.melanogaster* the understanding of its role in mammalian tissue is less well understood (see section 1.3.5.4). Both knockdown and over expression of LLGL has been shown to disrupt apical lumen formation in 3D-MDCK cysts (Horikoshi et al., 2009, Yamanaka et al., 2006, Yamanaka et al., 2003). In the studies presented in this thesis it was shown that expression of the AIPA mutant, that is unable to bind and unable to phosphorylate LLGL, caused MDCK cysts to be overgrown, poorly circumscribed and with multi-luminal cysts. This would be consistent with the notion that LLGL displays polarity threshold behaviour, as described for PKCι, wherein either knockout or over expression results in a loss of polarity. While often referred to as "the best studied tumour suppressor gene in Drosophila" (Merz et al., 1990) this label does not necessarily relate to expression array data available in human cancer. From two separate analyses of the Oncomine gene expression array and the EBI array, LLGL2 is significantly over-expressed in a number of human malignancies especially in breast, ovarian, pancreatic and bladder cancer. LLGL2 is under-expressed predominantly in non-epithelial malignancies such as leukaemia, renal cancer, melanoma and sarcoma.

From searching the COSMIC database for somatic mutations in cancer, 3 mutations of PKCι have been identified in human samples. One of those mutations was a substitution of R471C, the first arginine of the RIPR motif, and occurred in a patient with ovarian carcinoma (1 out of 24 samples). Thus the RIPR motif is an LLGL2 binding region, that when mutated disrupts polarity in MDCK cells and may be associated with human epithelial cancer. This intriguing finding should be followed up, firstly by determining whether the R471C mutation is sufficient to affect protein binding to the RIPR region. This could be tested by measuring the phosphorylation of LLGL2 in a cell-based assay. If R471C is confirmed as a functional binding mutant, then there is a strong case to sequence the PKCι gene (or specifically this exon) in human ovarian cancer samples as this could represent a new mechanism-based cancer driver-mutation.

It would be of considerable interest to further interrogate the molecular basis behind the PKCι-RIPR protein-binding site. The recently defined PKN consensus substrate motif (Collazos et al., 2011) overlaps with the RIPR binding motif. Provisional mutagenesis experiments of the proposed phosphorylated serine (S477) has not demonstrated a role of this residue in LLGL binding and phosphorylation. However, it was recently shown that the recombinant PKCι protein generated from insect cells was phosphorylated at stoichiometric levels at S475 and not S477, (R-I-P-R-S-L-S-V-K) (personal communication Neil McDonald). It would be interesting to test whether this second serine site is phosphorylated by an as yet unidentified kinase at S475 and whether this contributes to binding of protein interaction modules at this site. These interaction modules potentially include the WD40 domains within LLGL2 although the RIPR region would be an unusual consensus motif for WD40 binding. Identification of putative upstream kinases could be screened for using a kinase panel and a peptide substrate incorporating the RIPR motif. The role of S475 in LLGL interaction could easily be tested by the generation of phosphorylation deficient and phosphomimetic mutants at this site.

The 5 hits from the mass spectrometry screen included a diverse array of proteins. While searching for any commonality between these proteins that might point to a binding mechanism, it was identified that 4 out of 5 proteins (MTA2, MAGI1, FARP2, PDIA3 with LLGL2 being the exception) contained a strong predicted mode II 14.3.3 binding site. 14.3.3 are a family of adapter proteins that have two modes of binding (mode I and II) and can greatly impact on protein-protein interactions (see section 1.2.5). PKCι itself contains a suboptimal Mode I 14.3.3 binding site that also overlaps the RIPR motif. To determine the likelihood that this enrichment for strong 14.3.3 binding motifs was by chance, a bioinformatics screen was performed on 71809 human protein sequences. Strong type I 14.3.3 binding motifs were identified in 2.6% of sequences and strong type II 14.3.3 binding motifs were present in 17.4% of sequences. It is highly unlikely therefore that this enrichment for Type II 14.3.3 binding in the protein hits was by chance suggesting that their interaction with PKCι is stabilised by 14.3.3.

7.7 Downstream effectors

Guided by the crystal structure of PKCι bound to CRT66854, a relatively potent inhibitor, a drug insensitive PKCι mutant was designed, PKCι-D330A/D373A (PKCι-DIM). PKCι-DIM and CRT66854 have been validated as a resistant protein-inhibitor pairing both in vitro and in vivo and provide a platform for specifically interrogating PKCι biology.

This chemical genetic system, which has the advantage of minimising 'off target effects' commonly seen with RNAi and inhibitors alone, could be exploited in a number of ways. Using cells expressing exogenous PKCι-WT or PKCι-DIM, cells may be subjected to PKCι inhibition (PKCι-WT and CRT66854) or not (PKCι-DIM and CRT66854). Analysis of modified patterns of transcription expression between the two conditions could be performed using micro-array technology. Alternatively, using stable isotope labelling with amino acids in cell culture (SILAC) and mass spectrometry the (phospho) proteome as a function of specific PKCι inhibition may be assessed. Both of these techniques would ideally be carried out in 2 separate cell lines and any hits individually validated. The transcriptional and proteomic data could potentially provide a marker or signature for PKCι activation/inhibition. A biomarker of this type could be used to drive forward clinical PKCι drug development and in particular enable dose determination, patient selection and monitoring of response to potential anti-PKCι therapies.

7.8 Concluding Remarks

During the course of the work in this thesis, a role of PKCι in regulation of polarity downstream of oncogenic Ras has been identified, a new PKCι protein-protein binding domain has been described and a platform for biomarker discovery has been established. Hopefully, a measure of the success of this work can be summed up by the seemingly paradoxical statement that there are more unanswered questions at the end than there were at the beginning.

Appendicies

Appendix 1 Western blot of aPKC antibodies against recombinant aPKC proteins.
Different concentrations of recombinant aPKCζ or aPKCι protein kinase domains were probed with the different antisera overnight at a dilution of 1/1000. Molecular weights markers are shown on the left and the stated antibody and catalogue number is on the right. The blots are representative of 2 separate experiments.

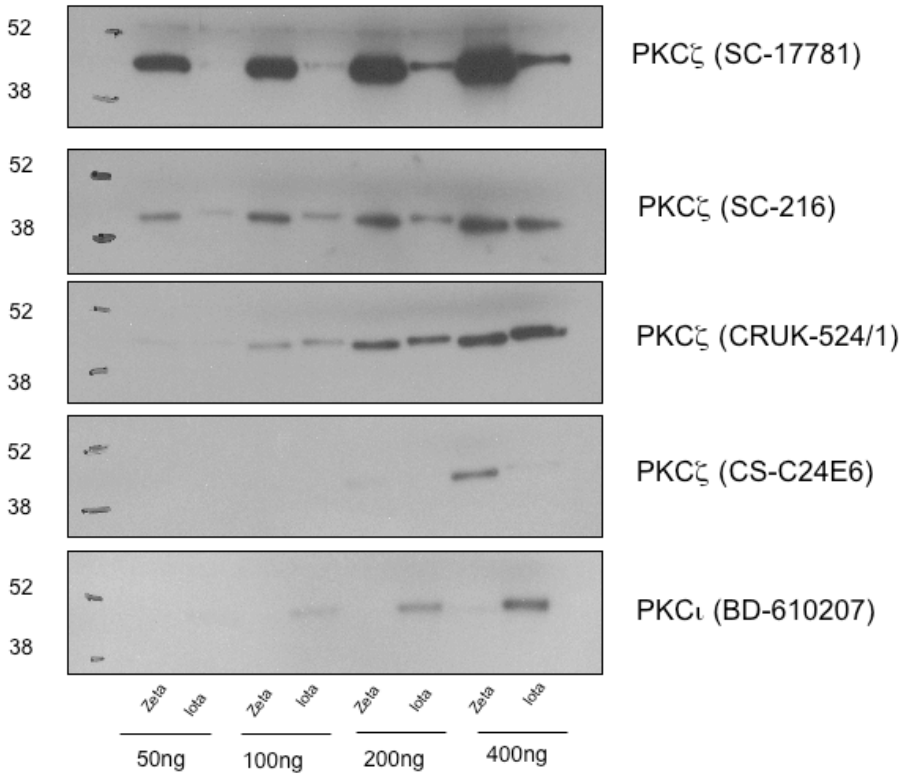

Appendix 2. Abundant Hits from the Immunocomplex-mass spectrometry screen.

Abundant proteins were defined as 3 or more unique peptides or 3 times or more unique peptides than observed in the GFP control. Coloured boxes refer to the relative abunance of unique peptides between PKCι-WT and PKCι-AIPA mutant. Yellow, WT≥ 3x AIPA; Red, AIPA≥ 3x WT; Blue, WT≈AIPA

Entry Name & Accession No.	Protein ID	Protein Mass	Abundance of unique peptides		
			GFP	PKCι-WT	PKCι-AIPA
PLCB3_HUMAN	1-phosphatidylinositol-4,5-bisphosphate phosphodiesterase beta-3 OS=Homo sapiens GN=PLCB3 PE=1 SV=2	139 kDa	0	2	3
1433F_HUMAN (+10)	14-3-3 protein eta OS=Homo sapiens GN=YWHAH PE=1 SV=4	28 kDa	0	2	1
1433T_HUMAN (+13)	14-3-3 protein theta OS=Homo sapiens GN=YWHAQ PE=1 SV=1	28 kDa	1	3	2
KI67_HUMAN	Antigen KI-67 OS=Homo sapiens GN=MKI67 PE=1 SV=2	359 kDa	0	11	1
API5_HUMAN (+7)	Apoptosis inhibitor 5 OS=Homo sapiens GN=API5 PE=1 SV=2	58 kDa	1	6	0
AATM_HUMAN (+3)	Aspartate aminotransferase, mitochondrial OS=Homo sapiens GN=GOT2 PE=1 SV=3	48 kDa	1	5	1
A8K092_HUMAN (+7)	ATP synthase subunit alpha OS=Homo sapiens PE=2 SV=1	54 kDa	1	5	5

E41L5_HUMAN (+5)	Band 4.1-like protein 5 OS=Homo sapiens GN=EPB41L5 PE=1 SV=3	82 kDa	0	5	0
B4DR68_HUMAN (+5)	cDNA FLJ58608, highly similar to Heat shock protein 75 kDa, mitochondrial OS=Homo sapiens PE=2 SV=1	74 kDa	0	4	0
B4DLN1_HUMAN	cDNA FLJ60124, highly similar to Mitochondrial dicarboxylate carrier OS=Homo sapiens PE=2 SV=1	48 kDa	1	4	4
A8K5H7_HUMAN (+5)	cDNA FLJ77542, highly similar to Homo sapiens YME1-like 1 (S. cerevisiae) (YME1L1), transcript variant 3, mRNA OS=Homo sapiens PE=2 SV=1	80 kDa	0	4	1
A8MPX7_HUMAN (+4)	Chromosome X open reading frame 56, isoform CRA_b OS=Homo sapiens GN=CXorf56 PE=2 SV=1	20 kDa	1	6	4
COIL_HUMAN	Coilin OS=Homo sapiens GN=COIL PE=1 SV=1	63 kDa	0	5	2
HEM6_HUMAN	Coproporphyrinogen-III oxidase, mitochondrial OS=Homo sapiens GN=CPOX PE=1 SV=3	50 kDa	1	4	2
H2AY_HUMAN (+5)	Core histone macro-H2A.1 OS=Homo sapiens GN=H2AFY PE=1 SV=4	40 kDa	1	4	1
KCRB_HUMAN (+3)	Creatine kinase B-type OS=Homo sapiens GN=CKB PE=1 SV=1	43 kDa	0	4	2
CYFP1_HUMAN (+4)	Cytoplasmic FMR1-interacting protein 1 OS=Homo sapiens GN=CYFIP1 PE=1 SV=1	145 kDa	0	4	0

CKAP4_HUMAN (+3)	Cytoskeleton-associated protein 4 OS=Homo sapiens GN=CKAP4 PE=1 SV=2	66 kDa	2	7	4
Q86X36_HUMAN (+15)	DEAH (Asp-Glu-Ala-His) box polypeptide 8 OS=Homo sapiens GN=DHX8 PE=2 SV=2	139 kDa	0	4	2
TFB1M_HUMAN (+2)	Dimethyladenosine transferase 1, mitochondrial OS=Homo sapiens GN=TFB1M PE=1 SV=1	40 kDa	1	4	0
MCM2_HUMAN (+3)	DNA replication licensing factor MCM2 OS=Homo sapiens GN=MCM2 PE=1 SV=4	102 kDa	1	5	0
Q4G0F4_HUMAN (+1)	DNA-directed RNA polymerase OS=Homo sapiens GN=POLRMT PE=2 SV=1	139 kDa	1	6	1
B7Z823_HUMAN (+1)	DNA-directed RNA polymerase OS=Homo sapiens PE=2 SV=1	132 kDa	1	4	0
RPAC1_HUMAN (+3)	DNA-directed RNA polymerases I and III subunit RPAC1 OS=Homo sapiens GN=POLR1C PE=1 SV=1	39 kDa	0	4	2
Q9NX84_HUMAN	Erythrocyte membrane protein band 4.1 like 4B, isoform CRA_b OS=Homo sapiens GN=EPB41L4B PE=2 SV=1	51 kDa	1	7	2
EIF2A_HUMAN (+2)	Eukaryotic translation initiation factor 2A OS=Homo sapiens GN=EIF2A PE=1 SV=3	65 kDa	0	4	1
SSRP1_HUMAN (+8)	FACT complex subunit SSRP1 OS=Homo sapiens GN=SSRP1 PE=1 SV=1	81 kDa	0	4	2
FARP2_HUMAN	FERM, RhoGEF and pleckstrin domain-	120 kDa	0	5	0

	containing protein 2 OS=Homo sapiens GN=FARP2 PE=1 SV=3				
B2ZZ83_HUMAN (+4)	Filamin B OS=Homo sapiens GN=FLNB PE=2 SV=1	282 kDa	0	4	1
B4DE36_HUMAN (+3)	Glucose-6-phosphate isomerase OS=Homo sapiens PE=2 SV=1	60 kDa	1	4	3
KT33B_HUMAN	Keratin, type I cuticular Ha3-II OS=Homo sapiens GN=KRT33B PE=1 SV=3	46 kDa	0	6	0
O60382_HUMAN (+1)	KIAA0324 (Fragment) OS=Homo sapiens GN=KIAA0324 PE=2 SV=1	191 kDa	0	6	0
L2GL1_HUMAN	Lethal(2) giant larvae protein homolog 1 OS=Homo sapiens GN=LLGL1 PE=1 SV=3	115 kDa	0	5	3
L2GL2_HUMAN	Lethal(2) giant larvae protein homolog 2 OS=Homo sapiens GN=LLGL2 PE=1 SV=2	113 kDa	1	16	5
SYLC_HUMAN (+3)	Leucyl-tRNA synthetase, cytoplasmic OS=Homo sapiens GN=LARS PE=1 SV=2	134 kDa	1	5	0
MAGI1_HUMAN (+8)	Membrane-associated guanylate kinase, WW and PDZ domain-containing protein 1 OS=Homo sapiens GN=MAGI1 PE=1 SV=3	165 kDa	0	5	1
MTA2_HUMAN (+6)	Metastasis-associated protein MTA2 OS=Homo sapiens GN=MTA2 PE=1 SV=1	75 kDa	0	4	0
E5KSU5_HUMAN (+8)	Mitochondrial transcription factor A OS=Homo sapiens PE=4 SV=1	29 kDa	0	3	4

E5KSY5_HUMAN (+1)	Mitochondrial twinkle protein OS=Homo sapiens PE=4 SV=1	77 kDa	0	5	0
PLPL6_HUMAN (+3)	Neuropathy target esterase OS=Homo sapiens GN=PNPLA6 PE=1 SV=2	150 kDa	0	5	3
NOG1_HUMAN (+5)	Nucleolar GTP-binding protein 1 OS=Homo sapiens GN=GTPBP4 PE=1 SV=3	74 kDa	1	7	0
PARD3_HUMAN (+2)	Partitioning defective 3 homolog OS=Homo sapiens GN=PARD3 PE=1 SV=2	151 kDa	0	19	17
PAR6B_HUMAN (+3)	Partitioning defective 6 homolog beta OS=Homo sapiens GN=PARD6B PE=1 SV=1	41 kDa	0	6	3
PCID2_HUMAN (+2)	PCI domain-containing protein 2 OS=Homo sapiens GN=PCID2 PE=1 SV=2	46 kDa	1	4	4
A8K401_HUMAN (+7)	Prohibitin, isoform CRA_a OS=Homo sapiens GN=PHB PE=2 SV=1	30 kDa	1	4	5
A8K3Z3_HUMAN (+21)	Proteasome (Prosome, macropain) 26S subunit, ATPase, 5, isoform CRA_b OS=Homo sapiens GN=PSMC5 PE=2 SV=1	45 kDa	0	4	1
DEK_HUMAN	Protein DEK OS=Homo sapiens GN=DEK PE=1 SV=1	43 kDa	1	5	0
PDIA3_HUMAN (+5)	Protein disulfide-isomerase A3 OS=Homo sapiens GN=PDIA3 PE=1 SV=4	57 kDa	2	8	2
FA32A_HUMAN (+6)	Protein FAM32A OS=Homo sapiens GN=FAM32A PE=1 SV=2	13 kDa	0	8	2

KPCI_HUMAN	Protein kinase C iota type OS=Homo sapiens GN=PRKCI PE=1 SV=2	68 kDa	0	46	33
POP1_HUMAN (+1)	Ribonucleases P/MRP protein subunit POP1 OS=Homo sapiens GN=POP1 PE=1 SV=2	115 kDa	0	4	1
Q53EP4_HUMAN (+5)	Ribophorin I variant (Fragment) OS=Homo sapiens PE=2 SV=1	69 kDa	0	4	2
RBM27_HUMAN	RNA-binding protein 27 OS=Homo sapiens GN=RBM27 PE=1 SV=2	119 kDa	1	7	2
Q9Y6G0_HUMAN (+1)	RNA-binding protein OS=Homo sapiens PE=2 SV=1	32 kDa	1	4	3
RUVB1_HUMAN (+8)	RuvB-like 1 OS=Homo sapiens GN=RUVBL1 PE=1 SV=1	50 kDa	1	7	2
SQSTM_HUMAN	Sequestosome-1 OS=Homo sapiens GN=SQSTM1 PE=1 SV=1	48 kDa	0	10	11
SPS2L_HUMAN (+2)	SPATS2-like protein OS=Homo sapiens GN=SPATS2L PE=1 SV=2	62 kDa	1	6	1
SMC1A_HUMAN (+10)	Structural maintenance of chromosomes protein 1A OS=Homo sapiens GN=SMC1A PE=1 SV=2	143 kDa	0	4	1
SQRD_HUMAN (+3)	Sulfide:quinone oxidoreductase, mitochondrial OS=Homo sapiens GN=SQRDL PE=1 SV=1	50 kDa	0	5	2
THSD4_HUMAN	Thrombospondin type-1 domain-containing protein 4 OS=Homo sapiens GN=THSD4 PE=2 SV=2	112 kDa	0	5	0

TAF2_HUMAN (+4)	Transcription initiation factor TFIID subunit 2 OS=Homo sapiens GN=TAF2 PE=1 SV=3	137 kDa	0	4	1
TBL2_HUMAN (+4)	Transducin beta-like protein 2 OS=Homo sapiens GN=TBL2 PE=1 SV=1	50 kDa	1	4	3
Q53G69_HUMAN (+2)	Translocase of inner mitochondrial membrane 44 homolog (Fragment) OS=Homo sapiens PE=2 SV=1	51 kDa	0	4	0
TPP2_HUMAN (+4)	Tripeptidyl-peptidase 2 OS=Homo sapiens GN=TPP2 PE=1 SV=4	138 kDa	0	2	5
TRM1L_HUMAN (+2)	TRMT1-like protein OS=Homo sapiens GN=TRMT1L PE=1 SV=2	82 kDa	0	4	3
NSUN2_HUMAN (+2)	tRNA (cytosine-5-)-methyltransferase NSUN2 OS=Homo sapiens GN=NSUN2 PE=1 SV=2	86 kDa	1	5	1
CJ018_HUMAN	Uncharacterized protein C10orf18 OS=Homo sapiens GN=C10orf18 PE=1 SV=1	269 kDa	0	4	2
E7ENH9_HUMAN (+6)	Uncharacterized protein OS=Homo sapiens GN=ACLY PE=4 SV=1	125 kDa	1	5	0
A6NDY9_HUMAN (+5)	Uncharacterized protein OS=Homo sapiens GN=FLNA PE=4 SV=3	246 kDa	2	7	0
WDR61_HUMAN	WD repeat-containing protein 61 OS=Homo sapiens GN=WDR61 PE=1 SV=1	34 kDa	1	5	2

Appendix 3 PKCι protein overlay

PKCι peptide array membrane was incubated with A, GST-C3 fusion protein or B, No protein or C, GST-PKCι (kinase domain) for 20minutes. The protein was cross-linked to the membrane, washed and then incubated with anti-GST antibody and species specific secondary-HRP antibody. There were three areas of enhanced binding of GST-PKCι as compared to the control (red boxes numbered 1-3). The yellow box highlights a region of unexpected binding of the GST antibody in the control despite no GST tagged protein being present. D, when the 3 regions of putative homotypic interaction were overlayed on the PKCι-inhibitor bound crystal structure of two interacting PKCι kinase domains (kinase 1 = green and kinase 2 =brown), 2 of the regions formed a contiguous region (red) on the surface of the peptide at the interface between the two kinases. Sites of bound inhibitor (cyan). This experiment has only been performed under these conditions on a single occasion.

A

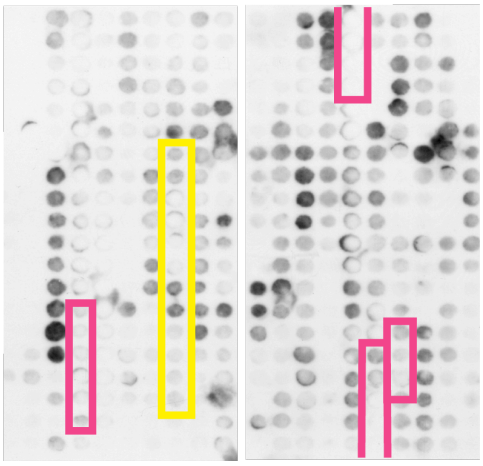

Control: GST Fusion Protein

B

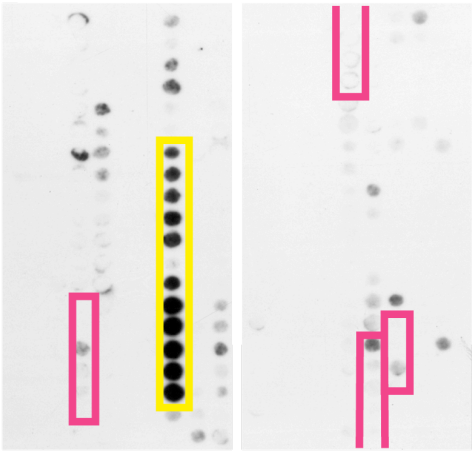

Control: untreated

C

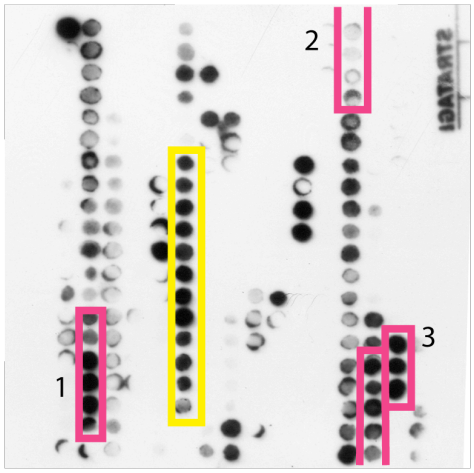

GST-PKCι

D

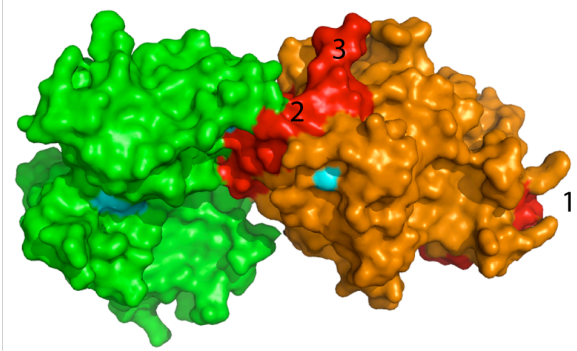

References

ACEVEDO-DUNCAN, M., PATEL, R., WHELAN, S. & BICAKU, E. (2002) Human glioma PKC-iota and PKC-betaII phosphorylate cyclin-dependent kinase activating kinase during the cell cycle. *Cell Prolif,* 35**,** 23-36.

AKIMOTO, K., MIZUNO, K., OSADA, S., HIRAI, S., TANUMA, S., SUZUKI, K. & OHNO, S. (1994) A new member of the third class in the protein kinase C family, PKC lambda, expressed dominantly in an undifferentiated mouse embryonal carcinoma cell line and also in many tissues and cells. *J Biol Chem,* 269**,** 12677-83.

AKIMOTO, K., NAKAYA, M., YAMANAKA, T., TANAKA, J., MATSUDA, S., WENG, Q. P., AVRUCH, J. & OHNO, S. (1998) Atypical protein kinase Clambda binds and regulates p70 S6 kinase. *Biochem J,* 335 (Pt 2)**,** 417-24.

AKIMOTO, K., TAKAHASHI, R., MORIYA, S., NISHIOKA, N., TAKAYANAGI, J., KIMURA, K., FUKUI, Y., OSADA, S., MIZUNO, K., HIRAI, S., KAZLAUSKAS, A. & OHNO, S. (1996) EGF or PDGF receptors activate atypical PKClambda through phosphatidylinositol 3-kinase. *EMBO J,* 15**,** 788-98.

ANDERSON, L. & SEILHAMER, J. (1997) A comparison of selected mRNA and protein abundances in human liver. *Electrophoresis,* 18**,** 533-7.

ANDREYEV, H. J., NORMAN, A. R., CUNNINGHAM, D., OATES, J., DIX, B. R., IACOPETTA, B. J., YOUNG, J., WALSH, T., WARD, R., HAWKINS, N., BERANEK, M., JANDIK, P., BENAMOUZIG, R., JULLIAN, E., LAURENT-PUIG, P., OLSCHWANG, S., MULLER, O., HOFFMANN, I., RABES, H. M., ZIETZ, C., TROUNGOS, C., VALAVANIS, C., YUEN, S. T., HO, J. W., CROKE, C. T., O'DONOGHUE, D. P., GIARETTI, W., RAPALLO, A., RUSSO, A., BAZAN, V., TANAKA, M., OMURA, K., AZUMA, T., OHKUSA, T., FUJIMORI, T., ONO, Y., PAULY, M., FABER, C., GLAESENER, R., DE GOEIJ, A. F., ARENDS, J. W., ANDERSEN, S. N., LOVIG, T., BREIVIK, J., GAUDERNACK, G., CLAUSEN, O. P., DE ANGELIS, P. D., MELING, G. I., ROGNUM, T. O., SMITH, R., GOH, H. S., FONT, A., ROSELL, R., SUN, X. F., ZHANG, H., BENHATTAR, J., LOSI, L., LEE, J. Q., WANG, S. T., CLARKE, P. A., BELL, S., QUIRKE, P., BUBB, V. J., PIRIS, J., CRUICKSHANK, N. R., MORTON, D., FOX, J. C., AL-MULLA, F., LEES, N., HALL, C. N., SNARY, D., WILKINSON, K., DILLON, D., COSTA, J., PRICOLO, V. E., FINKELSTEIN, S. D., THEBO, J. S., SENAGORE, A. J., HALTER, S. A., WADLER, S., MALIK, S., KRTOLICA, K. & UROSEVIC, N. (2001) Kirsten ras mutations in patients with colorectal cancer: the 'RASCAL II' study. *Br J Cancer,* 85**,** 692-6.

ARANDA, V., HAIRE, T., NOLAN, M. E., CALARCO, J. P., ROSENBERG, A. Z., FAWCETT, J. P., PAWSON, T. & MUTHUSWAMY, S. K. (2006) Par6-aPKC uncouples ErbB2 induced disruption of polarized epithelial organization from proliferation control. *Nat Cell Biol,* 8**,** 1235-45.

ATWOOD, S. X. & PREHODA, K. E. (2009) aPKC phosphorylates Miranda to polarize fate determinants during neuroblast asymmetric cell division. *Curr Biol,* 19**,** 723-9.

AZAM, M., SEELIGER, M. A., GRAY, N. S., KURIYAN, J. & DALEY, G. Q. (2008) Activation of tyrosine kinases by mutation of the gatekeeper threonine. *Nat Struct Mol Biol,* 15**,** 1109-18.

BALDWIN, R. M., PAROLIN, D. A. & LORIMER, I. A. (2008) Regulation of glioblastoma cell invasion by PKC iota and RhoB. *Oncogene,* 27**,** 3587-95.

BALENDRAN, A., BIONDI, R. M., CHEUNG, P. C., CASAMAYOR, A., DEAK, M. & ALESSI, D. R. (2000) A 3-phosphoinositide-dependent protein kinase-1 (PDK1) docking site is required for the phosphorylation of protein kinase Czeta (PKCzeta) and PKC-related kinase 2 by PDK1. *J Biol Chem,* 275**,** 20806-13.

BANDYOPADHYAY, G., SAJAN, M. P., KANOH, Y., STANDAERT, M. L., QUON, M. J., REED, B. C., DIKIC, I. & FARESE, R. V. (2001) Glucose activates protein kinase C-zeta /lambda through proline-rich tyrosine kinase-2, extracellular signal-regulated kinase, and phospholipase D: a novel mechanism for activating glucose transporter translocation. *J Biol Chem,* 276**,** 35537-45.

BARFORD, D. & JOHNSON, L. N. (1989) The allosteric transition of glycogen phosphorylase. *Nature,* 340**,** 609-16.

BARROS, C. S., PHELPS, C. B. & BRAND, A. H. (2003) Drosophila nonmuscle myosin II promotes the asymmetric segregation of cell fate determinants by cortical exclusion rather than active transport. *Dev Cell,* 5**,** 829-40.

BARTON, C., SOUDY, C., WYNNE, E., OLOWOYE, I., PATEL, B., KAYE, S., LEJEUNE, A., EAST, P., LINCH, M., PARKER, P. J., DILLON, C. & ROFFEY, J. (2009a) Identification and characterisation of small molecule inhibitors of atypical protein kinase C (aPKC) as anti-cancer targets. *EACR,* 130.

BARTON, C., SOUDY, C., WYNNE, E., OLOWOYE, I., PATEL, B., KAYE, S., LEJEUNE, A., EAST, P., LINCH, M., PARKER, P. J., DILLON, C. & ROFFEY, J. (2009b) Identification and characterisation of small molecule inhibitors of atypical protein kinase C (aPKC) as anti-cancer targets. *EACR Abstract,* 130.

BEHN-KRAPPA, A. & NEWTON, A. C. (1999) The hydrophobic phosphorylation motif of conventional protein kinase C is regulated by autophosphorylation. *Curr Biol,* 9**,** 728-37.

BELIVEAU, A., MOTT, J. D., LO, A., CHEN, E. I., KOLLER, A. A., YASWEN, P., MUSCHLER, J. & BISSELL, M. J. (2010) Raf-induced MMP9 disrupts tissue architecture of human breast cells in three-dimensional culture and is necessary for tumor growth in vivo. *Genes Dev,* 24**,** 2800-11.

BELL, A. W., DEUTSCH, E. W., AU, C. E., KEARNEY, R. E., BEAVIS, R., SECHI, S., NILSSON, T. & BERGERON, J. J. (2009) A HUPO test sample study reveals common problems in mass spectrometry-based proteomics. *Nat Methods,* 6**,** 423-30.

BENTON, R. & ST JOHNSTON, D. (2003) Drosophila PAR-1 and 14-3-3 inhibit Bazooka/PAR-3 to establish complementary cortical domains in polarized cells. *Cell,* 115**,** 691-704.

BERRIDGE, M. J. (2006) Cell Signalling Biology. Portand Press.

BERRIDGE, M. J. (2009) Inositol trisphosphate and calcium signalling mechanisms. *Biochim Biophys Acta,* 1793**,** 933-40.

BETSCHINGER, J., EISENHABER, F. & KNOBLICH, J. A. (2005) Phosphorylation-induced autoinhibition regulates the cytoskeletal protein Lethal (2) giant larvae. *Curr Biol,* 15**,** 276-82.

BETSCHINGER, J., MECHTLER, K. & KNOBLICH, J. A. (2003) The Par complex directs asymmetric cell division by phosphorylating the cytoskeletal protein Lgl. *Nature,* 422**,** 326-30.

BEZPROZVANNY, I., WATRAS, J. & EHRLICH, B. E. (1991) Bell-shaped calcium-response curves of Ins(1,4,5)P3- and calcium-gated channels from endoplasmic reticulum of cerebellum. *Nature,* 351**,** 751-4.

BIALUCHA, C. U., FERBER, E. C., PICHAUD, F., PEAK-CHEW, S. Y. & FUJITA, Y. (2007) p32 is a novel mammalian Lgl binding protein that enhances the activity of protein kinase Czeta and regulates cell polarity. *J Cell Biol,* 178**,** 575-81.

BILDER, D. (2004) Epithelial polarity and proliferation control: links from the Drosophila neoplastic tumor suppressors. *Genes Dev,* 18**,** 1909-25.

BILDER, D., BIRNBAUM, D., BORG, J. P., BRYANT, P., HUIGBRETSE, J., JANSEN, E., KENNEDY, M. B., LABOUESSE, M., LEGOUIS, R., MECHLER, B., PERRIMON, N., PETIT, M. & SINHA, P. (2000a) Collective nomenclature for LAP proteins. *Nat Cell Biol,* 2**,** E114.

BILDER, D., LI, M. & PERRIMON, N. (2000b) Cooperative regulation of cell polarity and growth by Drosophila tumor suppressors. *Science,* 289**,** 113-6.

BISHOP, A. C. & SHOKAT, K. M. (1999) Acquisition of inhibitor-sensitive protein kinases through protein design. *Pharmacol Ther,* 82**,** 337-46.

BJORKOY, G., PERANDER, M., OVERVATN, A. & JOHANSEN, T. (1997) Reversion of Ras- and phosphatidylcholine-hydrolyzing phospholipase C-mediated transformation of NIH 3T3 cells by a dominant interfering mutant of protein kinase C lambda is accompanied by the loss of constitutive nuclear mitogen-activated protein kinase/extracellular signal-regulated kinase activity. *J Biol Chem,* 272**,** 11557-65.

BOECKELER, K., ROSSE, C., HOWELL, M. & PARKER, P. J. (2010) Manipulating signal delivery - plasma-membrane ERK activation in aPKC-dependent migration. *J Cell Sci,* 123**,** 2725-32.

BOELLMANN, F. & THOMAS, R. S. (2010) The identification of protein kinase C iota as a regulator of the Mammalian heat shock response using functional genomic screens. *PLoS One,* 5**,** e11850.

BOURBON, N. A., YUN, J. & KESTER, M. (2000) Ceramide directly activates protein kinase C zeta to regulate a stress-activated protein kinase signaling complex. *J Biol Chem,* 275**,** 35617-23.

BRAND, A. H. & PERRIMON, N. (1994) Raf acts downstream of the EGF receptor to determine dorsoventral polarity during Drosophila oogenesis. *Genes Dev,* 8**,** 629-39.

BRANDMAN, O. & MEYER, T. (2008) Feedback loops shape cellular signals in space and time. *Science,* 322**,** 390-5.

BRIDGES, D. & MOORHEAD, G. B. (2005) 14-3-3 proteins: a number of functions for a numbered protein. *Sci STKE,* 2005**,** re10.

BUDAY, L. & DOWNWARD, J. (2008) Many faces of Ras activation. *Biochim Biophys Acta,* 1786**,** 178-87.

BURKHART, D. L. & SAGE, J. (2008) Cellular mechanisms of tumour suppression by the retinoblastoma gene. *Nat Rev Cancer,* 8**,** 671-82.

CAMERON, A. J., ESCRIBANO, C., SAURIN, A. T., KOSTELECKY, B. & PARKER, P. J. (2009) PKC maturation is promoted by nucleotide pocket occupation independently of intrinsic kinase activity. *Nat Struct Mol Biol,* 16**,** 624-30.

CAMERON, A. J., LINCH, M. D., SAURIN, A. T., ESCRIBANO, C. & PARKER, P. J. (2011) Dissecting the role of Sin1 in AGC kinase regulation by TORC2. *Biochem J*.

CANTLEY, L. C. (2002) The phosphoinositide 3-kinase pathway. *Science,* 296**,** 1655-7.

CARRASCO, S. & MERIDA, I. (2007) Diacylglycerol, when simplicity becomes complex. *Trends Biochem Sci,* 32**,** 27-36.

CHEN, X. & MACARA, I. G. (2005) Par-3 controls tight junction assembly through the Rac exchange factor Tiam1. *Nat Cell Biol,* 7**,** 262-9.

CHISHTI, A. H., KIM, A. C., MARFATIA, S. M., LUTCHMAN, M., HANSPAL, M., JINDAL, H., LIU, S. C., LOW, P. S., ROULEAU, G. A., MOHANDAS, N., CHASIS, J. A., CONBOY, J. G., GASCARD, P., TAKAKUWA, Y., HUANG, S. C., BENZ, E. J., JR., BRETSCHER, A., FEHON, R. G., GUSELLA, J. F., RAMESH, V., SOLOMON, F., MARCHESI, V. T., TSUKITA, S., HOOVER, K. B. & ET AL. (1998) The FERM domain: a unique module involved in the linkage of cytoplasmic proteins to the membrane. *Trends Biochem Sci,* 23**,** 281-2.

CHUANG, L. Y., GUH, J. Y., LIU, S. F., HUNG, M. Y., LIAO, T. N., CHIANG, T. A., HUANG, J. S., HUANG, Y. L., LIN, C. F. & YANG, Y. L. (2003) Regulation of type II transforming-growth-factor-beta receptors by protein kinase C iota. *Biochem J,* 375**,** 385-93.

COLLAZOS, A., MICHAEL, N., WHELAN, R. D., KELLY, G., MELLOR, H., PANG, L. C., TOTTY, N. & PARKER, P. J. (2011) Site recognition and substrate screens for PKN family proteins. *Biochem J,* 438**,** 535-43.

COLOSIMO, P. F., LIU, X., KAPLAN, N. A. & TOLWINSKI, N. S. (2010) GSK3beta affects apical-basal polarity and cell-cell adhesion by regulating aPKC levels. *Dev Dyn,* 239**,** 115-25.

CROCE, C. M. (2008) Oncogenes and cancer. *N Engl J Med,* 358**,** 502-11.

DEBNATH, J. & BRUGGE, J. S. (2005) Modelling glandular epithelial cancers in three-dimensional cultures. *Nat Rev Cancer,* 5**,** 675-88.

DEBNATH, J., MUTHUSWAMY, S. K. & BRUGGE, J. S. (2003) Morphogenesis and oncogenesis of MCF-10A mammary epithelial acini grown in three-dimensional basement membrane cultures. *Methods,* 30**,** 256-68.

DESAI, S., PILLAI, P., WIN-PIAZZA, H. & ACEVEDO-DUNCAN, M. (2011) PKC-iota promotes glioblastoma cell survival by phosphorylating and inhibiting BAD through a phosphotidylinositol 3-kinase pathway. *Biochim Biophys Acta*.

DIAZ-MECO, M. T., LOZANO, J., MUNICIO, M. M., BERRA, E., FRUTOS, S., SANZ, L. & MOSCAT, J. (1994) Evidence for the in vitro and in vivo interaction of Ras with protein kinase C zeta. *J Biol Chem,* 269**,** 31706-10.

DIAZ-MECO, M. T. & MOSCAT, J. (2001) MEK5, a new target of the atypical protein kinase C isoforms in mitogenic signaling. *Mol Cell Biol,* 21**,** 1218-27.

DIAZ-MECO, M. T., MUNICIO, M. M., SANCHEZ, P., LOZANO, J. & MOSCAT, J. (1996) Lambda-interacting protein, a novel protein that specifically interacts with the zinc finger domain of the atypical protein kinase C isotype lambda/iota and stimulates its kinase activity in vitro and in vivo. *Mol Cell Biol,* 16**,** 105-14.

DOLLAR, G. L., WEBER, U., MLODZIK, M. & SOKOL, S. Y. (2005) Regulation of Lethal giant larvae by Dishevelled. *Nature,* 437**,** 1376-80.

DOMINGUEZ, I., SANZ, L., ARENZANA-SEISDEDOS, F., DIAZ-MECO, M. T., VIRELIZIER, J. L. & MOSCAT, J. (1993) Inhibition of protein kinase C zeta subspecies blocks the activation of an NF-kappa B-like activity in Xenopus laevis oocytes. *Mol Cell Biol,* 13**,** 1290-5.

DOORNBOS, R. P., THEELEN, M., VAN DER HOEVEN, P. C., VAN BLITTERSWIJK, W. J., VERKLEIJ, A. J. & VAN BERGEN EN HENEGOUWEN, P. M. (1999) Protein kinase Czeta is a negative regulator of protein kinase B activity. *J Biol Chem,* 274**,** 8589-96.

DOWNWARD, J. (2001) The ins and outs of signalling. *Nature,* 411**,** 759-62.

DOWNWARD, J. (2006) Signal transduction. Prelude to an anniversary for the RAS oncogene. *Science,* 314**,** 433-4.

DU, Q. & MACARA, I. G. (2004) Mammalian Pins is a conformational switch that links NuMA to heterotrimeric G proteins. *Cell,* 119**,** 503-16.

DURAN, A., DIAZ-MECO, M. T. & MOSCAT, J. (2003) Essential role of RelA Ser311 phosphorylation by zetaPKC in NF-kappaB transcriptional activation. *EMBO J,* 22**,** 3910-8.

DURAN, A., LINARES, J. F., GALVEZ, A. S., WIKENHEISER, K., FLORES, J. M., DIAZ-MECO, M. T. & MOSCAT, J. (2008) The signaling adaptor p62 is an important NF-kappaB mediator in tumorigenesis. *Cancer Cell,* 13**,** 343-54.

DURAN, A., SERRANO, M., LEITGES, M., FLORES, J. M., PICARD, S., BROWN, J. P., MOSCAT, J. & DIAZ-MECO, M. T. (2004) The atypical PKC-interacting protein p62 is an important mediator of RANK-activated osteoclastogenesis. *Dev Cell,* 6**,** 303-9.

DURGAN, J., KAJI, N., JIN, D. & HALL, A. (2011) Par6B and atypical PKC (aPKC) regulate mitotic spindle orientation during epithelial morphogenesis. *J Biol Chem*.

EBNET, K., SUZUKI, A., HORIKOSHI, Y., HIROSE, T., MEYER ZU BRICKWEDDE, M. K., OHNO, S. & VESTWEBER, D. (2001) The cell polarity protein ASIP/PAR-3 directly associates with junctional adhesion molecule (JAM). *Embo J,* 20**,** 3738-48.

ECKERT, L. B., REPASKY, G. A., ULKU, A. S., MCFALL, A., ZHOU, H., SARTOR, C. I. & DER, C. J. (2004) Involvement of Ras activation in human breast cancer cell signaling, invasion, and anoikis. *Cancer Res,* 64**,** 4585-92.

EDER, A. M., SUI, X., ROSEN, D. G., NOLDEN, L. K., CHENG, K. W., LAHAD, J. P., KANGO-SINGH, M., LU, K. H., WARNEKE, C. L., ATKINSON, E. N., BEDROSIAN, I., KEYOMARSI, K., KUO, W. L., GRAY, J. W., YIN, J. C., LIU, J., HALDER, G. & MILLS, G. B. (2005)

Atypical PKCiota contributes to poor prognosis through loss of apical-basal polarity and cyclin E overexpression in ovarian cancer. *Proc Natl Acad Sci U S A,* 102**,** 12519-24.

ELIA, N. & LIPPINCOTT-SCHWARTZ, J. (2009) Culturing MDCK cells in three dimensions for analyzing intracellular dynamics. *Curr Protoc Cell Biol,* Chapter 4**,** Unit 4 22.

ERDOGAN, E., KLEE, E. W., THOMPSON, E. A. & FIELDS, A. P. (2009) Meta-analysis of oncogenic protein kinase Ciota signaling in lung adenocarcinoma. *Clin Cancer Res,* 15**,** 1527-33.

ERDOGAN, E., LAMARK, T., STALLINGS-MANN, M., LEE, J., PELLECCHIA, M., THOMPSON, E. A., JOHANSEN, T. & FIELDS, A. P. (2006) Aurothiomalate inhibits transformed growth by targeting the PB1 domain of protein kinase Ciota. *J Biol Chem,* 281**,** 28450-9.

ETIENNE-MANNEVILLE, S. & HALL, A. (2003) Cdc42 regulates GSK-3beta and adenomatous polyposis coli to control cell polarity. *Nature,* 421**,** 753-6.

ETIENNE-MANNEVILLE, S., MANNEVILLE, J. B., NICHOLLS, S., FERENCZI, M. A. & HALL, A. (2005) Cdc42 and Par6-PKCzeta regulate the spatially localized association of Dlg1 and APC to control cell polarization. *J Cell Biol,* 170**,** 895-901.

EYERS, P. A., VAN DEN, I. P., QUINLAN, R. A., GOEDERT, M. & COHEN, P. (1999) Use of a drug-resistant mutant of stress-activated protein kinase 2a/p38 to validate the in vivo specificity of SB 203580. *FEBS Lett,* 451**,** 191-6.

FACCHINETTI, V., OUYANG, W., WEI, H., SOTO, N., LAZORCHAK, A., GOULD, C., LOWRY, C., NEWTON, A. C., MAO, Y., MIAO, R. Q., SESSA, W. C., QIN, J., ZHANG, P., SU, B. & JACINTO, E. (2008) The mammalian target of rapamycin complex 2 controls folding and stability of Akt and protein kinase C. *EMBO J,* 27**,** 1932-43.

FAN, Q. W., KNIGHT, Z. A., GOLDENBERG, D. D., YU, W., MOSTOV, K. E., STOKOE, D., SHOKAT, K. M. & WEISS, W. A. (2006) A dual PI3 kinase/mTOR inhibitor reveals emergent efficacy in glioma. *Cancer Cell,* 9**,** 341-9.

FARFEL, Z., BOURNE, H. R. & IIRI, T. (1999) The expanding spectrum of G protein diseases. *N Engl J Med,* 340**,** 1012-20.

FEDOROV, Y. V., JONES, N. C. & OLWIN, B. B. (2002) Atypical protein kinase Cs are the Ras effectors that mediate repression of myogenic satellite cell differentiation. *Mol Cell Biol,* 22**,** 1140-9.

FENG, W., WU, H., CHAN, L. N. & ZHANG, M. (2007) The Par-3 NTD adopts a PB1-like structure required for Par-3 oligomerization and membrane localization. *EMBO J,* 26**,** 2786-96.

FERRO, E., MAGRINI, D., GUAZZI, P., FISCHER, T. H., PISTOLESI, S., POGNI, R., WHITE, G. C. & TRABALZINI, L. (2008) G-protein binding features and regulation of the RalGDS family member, RGL2. *Biochem J,* 415**,** 145-54.

FIELDS, A. P. & REGALA, R. P. (2007) Protein kinase C iota: human oncogene, prognostic marker and therapeutic target. *Pharmacol Res,* 55**,** 487-97.

FINCH, E. A., TURNER, T. J. & GOLDIN, S. M. (1991) Calcium as a coagonist of inositol 1,4,5-trisphosphate-induced calcium release. *Science,* 252**,** 443-6.

FLYNN, P., MELLOR, H., PALMER, R., PANAYOTOU, G. & PARKER, P. J. (1998) Multiple interactions of PRK1 with RhoA. Functional assignment of the Hr1 repeat motif. *J Biol Chem,* 273**,** 2698-705.

FREDERICK, L. A., MATTHEWS, J. A., JAMIESON, L., JUSTILIEN, V., THOMPSON, E. A., RADISKY, D. C. & FIELDS, A. P. (2008) Matrix metalloproteinase-10 is a critical effector of protein kinase Ciota-Par6alpha-mediated lung cancer. *Oncogene*.

FUKUHARA, A., IRIE, K., NAKANISHI, H., TAKEKUNI, K., KAWAKATSU, T., IKEDA, W., YAMADA, A., KATATA, T., HONDA, T., SATO, T., SHIMIZU, K., OZAKI, H., HORIUCHI, H., KITA, T. & TAKAI, Y. (2002) Involvement of nectin in the localization of junctional adhesion molecule at tight junctions. *Oncogene,* 21**,** 7642-55.

GALVEZ, A. S., DURAN, A., LINARES, J. F., PATHROSE, P., CASTILLA, E. A., ABU-BAKER, S., LEITGES, M., DIAZ-MECO, M. T. & MOSCAT, J. (2009) PKC{zeta} represses the IL-6 promoter and impairs tumorigenesis in vivo. *Mol Cell Biol*.

GAO, L., JOBERTY, G. & MACARA, I. G. (2002) Assembly of epithelial tight junctions is negatively regulated by Par6. *Curr Biol,* 12**,** 221-5.

GAO, T., BROGNARD, J. & NEWTON, A. C. (2008) The phosphatase PHLPP controls the cellular levels of protein kinase C. *J Biol Chem,* 283**,** 6300-11.

GARCIA-CAO, I., DURAN, A., COLLADO, M., CARRASCOSA, M. J., MARTIN-CABALLERO, J., FLORES, J. M., DIAZ-MECO, M. T., MOSCAT, J. & SERRANO, M. (2005) Tumour-suppression activity of the proapoptotic regulator Par4. *EMBO Rep,* 6**,** 577-83.

GARCIA-PARAMIO, P., CABRERIZO, Y., BORNANCIN, F. & PARKER, P. J. (1998) The broad specificity of dominant inhibitory protein kinase C mutants infers a common step in phosphorylation. *Biochem J,* 333 (Pt 3)**,** 631-6.

GARRETT, T. P., MCKERN, N. M., LOU, M., ELLEMAN, T. C., ADAMS, T. E., LOVRECZ, G. O., ZHU, H. J., WALKER, F., FRENKEL, M. J., HOYNE, P. A., JORISSEN, R. N., NICE, E. C., BURGESS, A. W. & WARD, C. W. (2002) Crystal structure of a truncated epidermal growth factor receptor extracellular domain bound to transforming growth factor alpha. *Cell,* 110**,** 763-73.

GATEFF, E. (1978) Malignant neoplasms of genetic origin in Drosophila melanogaster. *Science,* 200**,** 1448-59.

GATEFF, E. & SCHNEIDERMAN, H. A. (1969) Neoplasms in mutant and cultured wild-tupe tissues of Drosophila. *Natl Cancer Inst Monogr,* 31**,** 365-97.

GREEN, J. B., SMITH, J. C. & GERHART, J. C. (1994) Slow emergence of a multithreshold response to activin requires cell-contact-dependent sharpening but not prepattern. *Development,* 120**,** 2271-8.

GRIFONI, D., GAROIA, F., BELLOSTA, P., PARISI, F., DE BIASE, D., COLLINA, G., STRAND, D., CAVICCHI, S. & PESSION, A. (2007) aPKCzeta cortical loading is associated with Lgl cytoplasmic release and tumor growth in Drosophila and human epithelia. *Oncogene,* 26**,** 5960-5.

GRIFONI, D., GAROIA, F., SCHIMANSKI, C. C., SCHMITZ, G., LAURENTI, E., GALLE, P. R., PESSION, A., CAVICCHI, S. & STRAND, D. (2004) The human protein Hugl-1 substitutes for Drosophila lethal giant larvae tumour suppressor function in vivo. *Oncogene,* 23**,** 8688-94.

GRZESCHIK, N. A., PARSONS, L. M., ALLOTT, M. L., HARVEY, K. F. & RICHARDSON, H. E. (2010a) Lgl, aPKC, and Crumbs regulate the Salvador/Warts/Hippo pathway through two distinct mechanisms. *Curr Biol,* 20**,** 573-81.

GRZESCHIK, N. A., PARSONS, L. M. & RICHARDSON, H. E. (2010b) Lgl, the SWH pathway and tumorigenesis: It's a matter of context & competition! *Cell Cycle,* 9.

GSCHWENDT, M., DIETERICH, S., RENNECKE, J., KITTSTEIN, W., MUELLER, H. J. & JOHANNES, F. J. (1996) Inhibition of protein kinase C mu by various inhibitors. Differentiation from protein kinase c isoenzymes. *FEBS Lett,* 392**,** 77-80.

GULINO, A., DI MARCOTULLIO, L. & SCREPANTI, I. (2010) The multiple functions of Numb. *Exp Cell Res,* 316**,** 900-6.

GUO, H., MA, Y., ZHANG, B., SUN, B., NIU, R., YING, G. & ZHANG, N. (2009) Pivotal Advance: PKC{zeta} is required for migration of macrophages. *J Leukoc Biol*.

GUO, W., WU, S., LIU, J. & FANG, B. (2008) Identification of a small molecule with synthetic lethality for K-ras and protein kinase C iota. *Cancer Res,* 68**,** 7403-8.

GUSTAFSON, W. C., RAY, S., JAMIESON, L., THOMPSON, E. A., BRASIER, A. R. & FIELDS, A. P. (2004) Bcr-Abl regulates protein kinase Ciota (PKCiota) transcription via an Elk1 site in the PKCiota promoter. *J Biol Chem,* 279**,** 9400-8.

HADORN, E. (1938) Die Degerneration der Imaginalscheiben bei letalen Drosophila-Larven der Mutation Lethal-giant. *Rev Suisse Zool***,** 425-429.

HAN, Y., WEI, F., XU, X., CAI, Y., CHEN, B., WANG, J., XIA, S., HU, H., HUANG, X., WU, M. & WANG, M. (2002) [Establishment and comparative genomic hybridization analysis of human esophageal carcinomas cell line EC9706]. *Zhonghua Yi Xue Yi Chuan Xue Za Zhi,* 19**,** 455-7.

HANSRA, G., BORNANCIN, F., WHELAN, R., HEMMINGS, B. A. & PARKER, P. J. (1996) 12-O-Tetradecanoylphorbol-13-acetate-induced dephosphorylation of protein kinase Calpha correlates with the presence of a membrane-associated protein phosphatase 2A heterotrimer. *J Biol Chem,* 271**,** 32785-8.

HAO, Y., DU, Q., CHEN, X., ZHENG, Z., BALSBAUGH, J. L., MAITRA, S., SHABANOWITZ, J., HUNT, D. F. & MACARA, I. G. (2010) Par3 controls epithelial spindle orientation by aPKC-mediated phosphorylation of apical Pins. *Curr Biol,* 20**,** 1809-18.

HARRIS, S. L. & LEVINE, A. J. (2005) The p53 pathway: positive and negative feedback loops. *Oncogene,* 24**,** 2899-908.

HASTIE, C. J., MCLAUCHLAN, H. J. & COHEN, P. (2006) Assay of protein kinases using radiolabeled ATP: a protocol. *Nat Protoc,* 1**,** 968-71.

HATTENDORF, D. A., ANDREEVA, A., GANGAR, A., BRENNWALD, P. J. & WEIS, W. I. (2007) Structure of the yeast polarity protein Sro7 reveals a SNARE regulatory mechanism. *Nature,* 446**,** 567-71.

HAVERTY, P. M., HON, L. S., KAMINKER, J. S., CHANT, J. & ZHANG, Z. (2009) High-resolution analysis of copy number alterations and associated expression changes in ovarian tumors. *BMC Med Genomics,* 2**,** 21.

HIRANO, Y., YOSHINAGA, S., TAKEYA, R., SUZUKI, N. N., HORIUCHI, M., KOHJIMA, M., SUMIMOTO, H. & INAGAKI, F. (2005) Structure of a cell polarity regulator, a complex between atypical PKC and Par6 PB1 domains. *J Biol Chem,* 280**,** 9653-61.

HIROSE, T., IZUMI, Y., NAGASHIMA, Y., TAMAI-NAGAI, Y., KURIHARA, H., SAKAI, T., SUZUKI, Y., YAMANAKA, T., SUZUKI, A., MIZUNO, K. & OHNO, S. (2002) Involvement of ASIP/PAR-3 in the promotion of epithelial tight junction formation. *J Cell Sci,* 115**,** 2485-95.

HOMMEL, U., ZURINI, M. & LUYTEN, M. (1994) Solution structure of a cysteine rich domain of rat protein kinase C. *Nat Struct Biol,* 1**,** 383-7.

HORIKOSHI, Y., SUZUKI, A., YAMANAKA, T., SASAKI, K., MIZUNO, K., SAWADA, H., YONEMURA, S. & OHNO, S. (2009) Interaction between PAR-3 and the aPKC-PAR-6 complex is indispensable for apical domain development of epithelial cells. *J Cell Sci*.

HUANG, H. C., HUANG, C. Y., LIN-SHIAU, S. Y. & LIN, J. K. (2008) Ursolic acid inhibits IL-1beta or TNF-alpha-induced C6 glioma invasion through suppressing the association ZIP/p62 with PKC-zeta and downregulating the MMP-9 expression. *Mol Carcinog*.

HUANG, L. & MUTHUSWAMY, S. K. (2010) Polarity protein alterations in carcinoma: a focus on emerging roles for polarity regulators. *Curr Opin Genet Dev,* 20**,** 41-50.

HUNG, T. J. & KEMPHUES, K. J. (1999) PAR-6 is a conserved PDZ domain-containing protein that colocalizes with PAR-3 in Caenorhabditis elegans embryos. *Development,* 126**,** 127-35.

HUNTER, T. (2000) Signaling--2000 and beyond. *Cell,* 100**,** 113-27.

HURD, T. W., FAN, S., LIU, C. J., KWEON, H. K., HAKANSSON, K. & MARGOLIS, B. (2003) Phosphorylation-dependent binding of 14-3-3 to the polarity protein Par3 regulates cell polarity in mammalian epithelia. *Curr Biol,* 13**,** 2082-90.

HURLEY, J. H., NEWTON, A. C., PARKER, P. J., BLUMBERG, P. M. & NISHIZUKA, Y. (1997) Taxonomy and function of C1 protein kinase C homology domains. *Protein Sci,* 6**,** 477-80.

HUROV, J. B., WATKINS, J. L. & PIWNICA-WORMS, H. (2004) Atypical PKC phosphorylates PAR-1 kinases to regulate localization and activity. *Curr Biol,* 14**,** 736-41.

HUTTERER, A., BETSCHINGER, J., PETRONCZKI, M. & KNOBLICH, J. A. (2004) Sequential roles of Cdc42, Par-6, aPKC, and Lgl in the establishment of epithelial polarity during Drosophila embryogenesis. *Dev Cell,* 6**,** 845-54.

HYODO-MIURA, J., YAMAMOTO, T. S., HYODO, A. C., IEMURA, S., KUSAKABE, M., NISHIDA, E., NATSUME, T. & UENO, N. (2006) XGAP, an ArfGAP, is required for polarized localization of PAR proteins and cell polarity in Xenopus gastrulation. *Dev Cell,* 11**,** 69-79.

IGAKI, T., PAGLIARINI, R. A. & XU, T. (2006) Loss of cell polarity drives tumor growth and invasion through JNK activation in Drosophila. *Curr Biol,* 16**,** 1139-46.

IKENOUE, T., INOKI, K., YANG, Q., ZHOU, X. & GUAN, K. L. (2008) Essential function of TORC2 in PKC and Akt turn motif phosphorylation, maturation and signalling. *EMBO J,* 27**,** 1919-31.

INOUE, T., YOSHIDA, T., SHIMIZU, Y., KOBAYASHI, T., YAMASAKI, T., TODA, Y., SEGAWA, T., KAMOTO, T., NAKAMURA, E. & OGAWA, O. (2006) Requirement of androgen-dependent

activation of protein kinase Czeta for androgen-dependent cell proliferation in LNCaP Cells and its roles in transition to androgen-independent cells. *Mol Endocrinol,* 20**,** 3053-69.

ISHIGURO, H., AKIMOTO, K., NAGASHIMA, Y., KOJIMA, Y., SASAKI, T., ISHIGURO-IMAGAWA, Y., NAKAIGAWA, N., OHNO, S., KUBOTA, Y. & UEMURA, H. (2009) aPKClambda/iota promotes growth of prostate cancer cells in an autocrine manner through transcriptional activation of interleukin-6. *Proc Natl Acad Sci U S A,* 106**,** 16369-74.

ISHIUCHI, T. & TAKEICHI, M. (2011) Willin and Par3 cooperatively regulate epithelial apical constriction through aPKC-mediated ROCK phosphorylation. *Nat Cell Biol,* 13**,** 860-6.

IZUMI, Y., HIROSE, T., TAMAI, Y., HIRAI, S., NAGASHIMA, Y., FUJIMOTO, T., TABUSE, Y., KEMPHUES, K. J. & OHNO, S. (1998) An atypical PKC directly associates and colocalizes at the epithelial tight junction with ASIP, a mammalian homologue of Caenorhabditis elegans polarity protein PAR-3. *J Cell Biol,* 143**,** 95-106.

JAFFE, A. B., KAJI, N., DURGAN, J. & HALL, A. (2008) Cdc42 controls spindle orientation to position the apical surface during epithelial morphogenesis. *J Cell Biol,* 183**,** 625-33.

JANDA, E., LITOS, G., GRUNERT, S., DOWNWARD, J. & BEUG, H. (2002) Oncogenic Ras/Her-2 mediate hyperproliferation of polarized epithelial cells in 3D cultures and rapid tumor growth via the PI3K pathway. *Oncogene,* 21**,** 5148-59.

JEFFREY, P. D., RUSSO, A. A., POLYAK, K., GIBBS, E., HURWITZ, J., MASSAGUE, J. & PAVLETICH, N. P. (1995) Mechanism of CDK activation revealed by the structure of a cyclinA-CDK2 complex. *Nature,* 376**,** 313-20.

JIN, Y. T., YING, X. X., HU, Y. H., ZOU, Q., WANG, H. Y. & XU, Y. H. (2008) aPKC inhibitors might be the sensitizer of chemotherapy and adoptive immunotherapy in the treatment of hASIPa-overexpressed breast cancer. *Oncol Res,* 17**,** 59-68.

JOBERTY, G., PETERSEN, C., GAO, L. & MACARA, I. G. (2000) The cell-polarity protein Par6 links Par3 and atypical protein kinase C to Cdc42. *Nat Cell Biol,* 2**,** 531-9.

JOHNSON, L. N. & O'REILLY, M. (1996) Control by phosphorylation. *Curr Opin Struct Biol,* 6**,** 762-9.

JOSHI, J., FERNANDEZ-MARCOS, P. J., GALVEZ, A., AMANCHY, R., LINARES, J. F., DURAN, A., PATHROSE, P., LEITGES, M., CANAMERO, M., COLLADO, M., SALAS, C., SERRANO, M., MOSCAT, J. & DIAZ-MECO, M. T. (2008) Par-4 inhibits Akt and suppresses Ras-induced lung tumorigenesis. *Embo J*.

JURA, N., ENDRES, N. F., ENGEL, K., DEINDL, S., DAS, R., LAMERS, M. H., WEMMER, D. E., ZHANG, X. & KURIYAN, J. (2009) Mechanism for activation of the EGF receptor catalytic domain by the juxtamembrane segment. *Cell,* 137**,** 1293-307.

JUSTILIEN, V. & FIELDS, A. P. (2009) Ect2 links the PKCiota-Par6alpha complex to Rac1 activation and cellular transformation. *Oncogene*.

JUSTILIEN, V., JAMEISON, L., DER, C. J., ROSSMAN, K. L. & FIELDS, A. P. (2010) The oncogenic activity of ECT2 is regulated through protein kinase C{iota} mediated phosphorylation. *J Biol Chem*.

KALLAY, L. M., MCNICKLE, A., BRENNWALD, P. J., HUBBARD, A. L. & BRAITERMAN, L. T. (2006) Scribble associates with two polarity proteins, Lgl2 and Vangl2, via distinct molecular domains. *J Cell Biochem,* 99**,** 647-64.

KARAPETIS, C. S., KHAMBATA-FORD, S., JONKER, D. J., O'CALLAGHAN, C. J., TU, D., TEBBUTT, N. C., SIMES, R. J., CHALCHAL, H., SHAPIRO, J. D., ROBITAILLE, S., PRICE, T. J., SHEPHERD, L., AU, H. J., LANGER, C., MOORE, M. J. & ZALCBERG, J. R. (2008) K-ras mutations and benefit from cetuximab in advanced colorectal cancer. *N Engl J Med,* 359**,** 1757-65.

KARIN, M. (1999) The beginning of the end: IkappaB kinase (IKK) and NF-kappaB activation. *J Biol Chem,* 274**,** 27339-42.

KELLER, A., NESVIZHSKII, A. I., KOLKER, E. & AEBERSOLD, R. (2002) Empirical statistical model to estimate the accuracy of peptide identifications made by MS/MS and database search. *Anal Chem,* 74**,** 5383-92.

KHWAJA, A., RODRIGUEZ-VICIANA, P., WENNSTROM, S., WARNE, P. H. & DOWNWARD, J. (1997) Matrix adhesion and Ras transformation both activate a phosphoinositide 3-OH kinase and protein kinase B/Akt cellular survival pathway. *EMBO J,* 16**,** 2783-93.

KIM, M., DATTA, A., BRAKEMAN, P., YU, W. & MOSTOV, K. E. (2007) Polarity proteins PAR6 and aPKC regulate cell death through GSK-3beta in 3D epithelial morphogenesis. *J Cell Sci,* 120**,** 2309-17.

KISSELEVA, T., SONG, L., VORONTCHIKHINA, M., FEIRT, N., KITAJEWSKI, J. & SCHINDLER, C. (2006) NF-kappaB regulation of endothelial cell function during LPS-induced toxemia and cancer. *J Clin Invest,* 116**,** 2955-63.

KLEZOVITCH, O., FERNANDEZ, T. E., TAPSCOTT, S. J. & VASIOUKHIN, V. (2004) Loss of cell polarity causes severe brain dysplasia in Lgl1 knockout mice. *Genes Dev,* 18**,** 559-71.

KMIECIK, T. E. & SHALLOWAY, D. (1987) Activation and suppression of pp60c-src transforming ability by mutation of its primary sites of tyrosine phosphorylation. *Cell,* 49**,** 65-73.

KNIGHT, Z. A. & SHOKAT, K. M. (2005) Features of selective kinase inhibitors. *Chem Biol,* 12**,** 621-37.

KOBAYASHI, T., INOUE, T., SHIMIZU, Y., TERADA, N., MAENO, A., KAJITA, Y., YAMASAKI, T., KAMBA, T., TODA, Y., MIKAMI, Y., YAMADA, T., KAMOTO, T., OGAWA, O. & NAKAMURA, E. (2010) Activation of Rac1 is closely related to androgen-independent cell proliferation of prostate cancer cells both in vitro and in vivo. *Mol Endocrinol,* 24**,** 722-34.

KOJIMA, Y., AKIMOTO, K., NAGASHIMA, Y., ISHIGURO, H., SHIRAI, S., CHISHIMA, T., ICHIKAWA, Y., ISHIKAWA, T., SASAKI, T., KUBOTA, Y., INAYAMA, Y., AOKI, I., OHNO, S. & SHIMADA, H. (2008) The overexpression and altered localization of the atypical protein kinase C lambda/iota in breast cancer correlates with the pathologic type of these tumors. *Hum Pathol,* 39**,** 824-31.

KOSTELECKY, B., SAURIN, A. T., PURKISS, A., PARKER, P. J. & MCDONALD, N. Q. (2009) Recognition of an intra-chain tandem 14-3-3 binding site within PKCepsilon. *EMBO Rep,* 10**,** 983-9.

KRISHNAMURTHY, K., WANG, G., SILVA, J., CONDIE, B. G. & BIEBERICH, E. (2007) Ceramide regulates atypical PKCzeta/lambda-mediated cell polarity in primitive ectoderm cells. A novel function of sphingolipids in morphogenesis. *J Biol Chem,* 282**,** 3379-90.

KUPHAL, S., WALLNER, S., SCHIMANSKI, C. C., BATAILLE, F., HOFER, P., STRAND, S., STRAND, D. & BOSSERHOFF, A. K. (2006) Expression of Hugl-1 is strongly reduced in malignant melanoma. *Oncogene,* 25**,** 103-10.

KURIYAN, J. & COWBURN, D. (1997) Modular peptide recognition domains in eukaryotic signaling. *Annu Rev Biophys Biomol Struct,* 26**,** 259-88.

LALLENA, M. J., DIAZ-MECO, M. T., BREN, G., PAYA, C. V. & MOSCAT, J. (1999) Activation of IkappaB kinase beta by protein kinase C isoforms. *Mol Cell Biol,* 19**,** 2180-8.

LALLI, G. (2009) RalA and the exocyst complex influence neuronal polarity through PAR-3 and aPKC. *J Cell Sci,* 122**,** 1499-506.

LARKIN, A. & IMPERIALI, B. (2011) The expanding horizons of asparagine-linked glycosylation. *Biochemistry,* 50**,** 4411-26.

LE GOOD, J. A., ZIEGLER, W. H., PAREKH, D. B., ALESSI, D. R., COHEN, P. & PARKER, P. J. (1998) Protein kinase C isotypes controlled by phosphoinositide 3-kinase through the protein kinase PDK1. *Science,* 281**,** 2042-5.

LEE, G. Y., KENNY, P. A., LEE, E. H. & BISSELL, M. J. (2007) Three-dimensional culture models of normal and malignant breast epithelial cells. *Nat Methods,* 4**,** 359-65.

LEE, M. & VASIOUKHIN, V. (2008) Cell polarity and cancer--cell and tissue polarity as a non-canonical tumor suppressor. *J Cell Sci,* 121**,** 1141-50.

LEHMAN, K., ROSSI, G., ADAMO, J. E. & BRENNWALD, P. (1999) Yeast homologues of tomosyn and lethal giant larvae function in exocytosis and are associated with the plasma membrane SNARE, Sec9. *J Cell Biol,* 146**,** 125-40.

LESEUX, L., LAURENT, G., LAURENT, C., RIGO, M., BLANC, A., OLIVE, D. & BEZOMBES, C. (2008) PKC zeta mTOR pathway: a new target for rituximab therapy in follicular lymphoma. *Blood,* 111**,** 285-91.

LI, H., XING, X., DING, G., LI, Q., WANG, C., XIE, L., ZENG, R. & LI, Y. (2009) SysPTM: a systematic resource for proteomic research on post-translational modifications. *Mol Cell Proteomics,* 8**,** 1839-49.

LI, Q., WANG, J. M., LIU, C., XIAO, B. L., LU, J. X. & ZOU, S. Q. (2008) Correlation of aPKC-iota and E-cadherin expression with invasion and prognosis of cholangiocarcinoma. *Hepatobiliary Pancreat Dis Int,* 7**,** 70-5.

LIMATOLA, C., SCHAAP, D., MOOLENAAR, W. H. & VAN BLITTERSWIJK, W. J. (1994) Phosphatidic acid activation of protein kinase C-zeta overexpressed in COS cells: comparison with other protein kinase C isotypes and other acidic lipids. *Biochem J,* 304 (Pt 3)**,** 1001-8.

LIN, D., EDWARDS, A. S., FAWCETT, J. P., MBAMALU, G., SCOTT, J. D. & PAWSON, T. (2000) A mammalian PAR-3-PAR-6 complex implicated in Cdc42/Rac1 and aPKC signalling and cell polarity. *Nat Cell Biol,* 2**,** 540-7.

LING, C., ZHENG, Y., YIN, F., YU, J., HUANG, J., HONG, Y., WU, S. & PAN, D. (2010) The apical transmembrane protein Crumbs functions as a tumor suppressor that regulates Hippo signaling by binding to Expanded. *Proc Natl Acad Sci U S A,* 107**,** 10532-7.

LISOVSKY, M., DRESSER, K., BAKER, S., FISHER, A., WODA, B., BANNER, B. & LAUWERS, G. Y. (2009) Cell polarity protein Lgl2 is lost or aberrantly localized in gastric dysplasia and adenocarcinoma: an immunohistochemical study. *Mod Pathol,* 22**,** 977-84.

LISOVSKY, M., DRESSER, K., WODA, B. & MINO-KENUDSON, M. (2010) Immunohistochemistry for cell polarity protein lethal giant larvae 2 differentiates pancreatic intraepithelial neoplasia-3 and ductal adenocarcinoma of the pancreas from lower-grade pancreatic intraepithelial neoplasias. *Hum Pathol,* 41**,** 902-9.

LIU, H., RADISKY, D. C., WANG, F. & BISSELL, M. J. (2004) Polarity and proliferation are controlled by distinct signaling pathways downstream of PI3-kinase in breast epithelial tumor cells. *J Cell Biol,* 164**,** 603-12.

LIU, S. G., WANG, B. S., JIANG, Y. Y., ZHANG, T. T., SHI, Z. Z., YANG, Y., YANG, Y. L., WANG, X. C., LIN, D. C., ZHANG, Y., YANG, H., CAI, Y., ZHAN, Q. M. & WANG, M. R. (2011) Atypical Protein Kinase C{iota} (PKC{iota}) Promotes Metastasis of Esophageal Squamous Cell Carcinoma by Enhancing Resistance to Anoikis via PKC{iota}-SKP2-AKT Pathway. *Mol Cancer Res*.

LIU, X. F., XIE, X. & MIKI, T. (2006) Inhibition of protein kinase C zeta blocks the attachment of stable microtubules to kinetochores leading to abnormal chromosome alignment. *Cell Signal,* 18**,** 2314-23.

LIU, Y., WANG, B., WANG, J., WAN, W., SUN, R., ZHAO, Y. & ZHANG, N. (2008) Down-regulation of PKCzeta expression inhibits chemotaxis signal transduction in human lung cancer cells. *Lung Cancer*.

LU, X., FENG, X., MAN, X., YANG, G., TANG, L., DU, D., ZHANG, F., YUAN, H., HUANG, Q., ZHANG, Z., LIU, Y., STRAND, D. & CHEN, Z. (2009) Aberrant splicing of Hugl-1 is associated with hepatocellular carcinoma progression. *Clin Cancer Res,* 15**,** 3287-96.

LYNCH, M. J., HILL, E. V. & HOUSLAY, M. D. (2006) Intracellular targeting of phosphodiesterase-4 underpins compartmentalized cAMP signaling. *Curr Top Dev Biol,* 75**,** 225-59.

LYONS, J. F., WILHELM, S., HIBNER, B. & BOLLAG, G. (2001) Discovery of a novel Raf kinase inhibitor. *Endocr Relat Cancer,* 8**,** 219-25.

MAGNUSON, B. A., CARR, I. & BIRD, R. P. (1993) Ability of aberrant crypt foci characteristics to predict colonic tumor incidence in rats fed cholic acid. *Cancer Res,* 53**,** 4499-504.

MANFRUELLI, P., ARQUIER, N., HANRATTY, W. P. & SEMERIVA, M. (1996) The tumor suppressor gene, lethal(2)giant larvae (1(2)g1), is required for cell shape change of epithelial cells during Drosophila development. *Development,* 122**,** 2283-94.

MANN, M. & JENSEN, O. N. (2003) Proteomic analysis of post-translational modifications. *Nat Biotechnol,* 21**,** 255-61.

MANN, M., ONG, S. E., GRONBORG, M., STEEN, H., JENSEN, O. N. & PANDEY, A. (2002) Analysis of protein phosphorylation using mass spectrometry: deciphering the phosphoproteome. *Trends Biotechnol,* 20**,** 261-8.

MANNING, G., WHYTE, D. B., MARTINEZ, R., HUNTER, T. & SUDARSANAM, S. (2002) The protein kinase complement of the human genome. *Science,* 298**,** 1912-34.

MAO, M., FANG, X., LU, Y., LAPUSHIN, R., BAST, R. C., JR. & MILLS, G. B. (2000) Inhibition of growth-factor-induced phosphorylation and activation of protein kinase B/Akt by atypical protein kinase C in breast cancer cells. *Biochem J,* 352 Pt 2**,** 475-82.

MARTIN, P., DIAZ-MECO, M. T. & MOSCAT, J. (2006) The signaling adapter p62 is an important mediator of T helper 2 cell function and allergic airway inflammation. *EMBO J,* 25**,** 3524-33.

MARTIN, T. D., SAMUEL, J. C., ROUTH, E. D., DER, C. J. & YEH, J. J. (2011) Activation and involvement of Ral GTPases in colorectal cancer. *Cancer Res,* 71**,** 206-15.

MASTRANGELO, D., HADJISTILIANOU, T., DE FRANCESCO, S. & LORE, C. (2009) Retinoblastoma and the genetic theory of cancer: an old paradigm trying to survive to the evidence. *J Cancer Epidemiol,* 2009**,** 301973.

MAURER, M., SU, T., SAAL, L. H., KOUJAK, S., HOPKINS, B. D., BARKLEY, C. R., WU, J., NANDULA, S., DUTTA, B., XIE, Y., CHIN, Y. R., KIM, D. I., FERRIS, J. S., GRUVBERGER-SAAL, S. K., LAAKSO, M., WANG, X., MEMEO, L., ROJTMAN, A., MATOS, T., YU, J. S., CORDON-CARDO, C., ISOLA, J., TERRY, M. B., TOKER, A., MILLS, G. B., ZHAO, J. J., MURTY, V. V., HIBSHOOSH, H. & PARSONS, R. (2009) 3-Phosphoinositide-dependent kinase 1 potentiates upstream lesions on the phosphatidylinositol 3-kinase pathway in breast carcinoma. *Cancer Res,* 69**,** 6299-306.

MCGEHEE, D. S. (1999) Molecular diversity of neuronal nicotinic acetylcholine receptors. *Ann N Y Acad Sci,* 868**,** 565-77.

MECHLER, B. M., MCGINNIS, W. & GEHRING, W. J. (1985) Molecular cloning of lethal(2)giant larvae, a recessive oncogene of Drosophila melanogaster. *EMBO J,* 4**,** 1551-7.

MEDJKANE, S., PEREZ-SANCHEZ, C., GAGGIOLI, C., SAHAI, E. & TREISMAN, R. (2009) Myocardin-related transcription factors and SRF are required for cytoskeletal dynamics and experimental metastasis. *Nat Cell Biol,* 11**,** 257-68.

MERZ, R., SCHMIDT, M., TOROK, I., PROTIN, U., SCHULER, G., WALTHER, H. P., KRIEG, F., GROSS, M., STRAND, D. & MECHLER, B. M. (1990) Molecular action of the l(2)gl tumor suppressor gene of Drosophila melanogaster. *Environ Health Perspect,* 88**,** 163-7.

MESSERSCHMIDT, A., MACIEIRA, S., VELARDE, M., BADEKER, M., BENDA, C., JESTEL, A., BRANDSTETTER, H., NEUEFEIND, T. & BLAESSE, M. (2005) Crystal structure of the catalytic domain of human atypical protein kinase C-iota reveals interaction mode of phosphorylation site in turn motif. *J Mol Biol,* 352**,** 918-31.

MESSORI, L. & MARCON, G. (2004) Gold complexes as antitumor agents. *Met Ions Biol Syst,* 42**,** 385-424.

MICHEL, D., ARSANTO, J. P., MASSEY-HARROCHE, D., BECLIN, C., WIJNHOLDS, J. & LE BIVIC, A. (2005) PATJ connects and stabilizes apical and lateral components of tight junctions in human intestinal cells. *J Cell Sci,* 118**,** 4049-57.

MIZUNO, K., SUZUKI, A., HIROSE, T., KITAMURA, K., KUTSUZAWA, K., FUTAKI, M., AMANO, Y. & OHNO, S. (2003) Self-association of PAR-3-mediated by the conserved N-terminal domain contributes to the development of epithelial tight junctions. *J Biol Chem,* 278**,** 31240-50.

MORA, A., KOMANDER, D., VAN AALTEN, D. M. & ALESSI, D. R. (2004) PDK1, the master regulator of AGC kinase signal transduction. *Semin Cell Dev Biol,* 15**,** 161-70.

MORAIS-DE-SA, E., MIROUSE, V. & ST JOHNSTON, D. (2010) aPKC phosphorylation of Bazooka defines the apical/lateral border in Drosophila epithelial cells. *Cell,* 141**,** 509-23.

MORENO-BUENO, G., FERNANDEZ-MARCOS, P. J., COLLADO, M., TENDERO, M. J., RODRIGUEZ-PINILLA, S. M., GARCIA-CAO, I., HARDISSON, D., DIAZ-MECO, M. T., MOSCAT, J., SERRANO, M. & PALACIOS, J. (2007) Inactivation of the candidate tumor suppressor par-4 in endometrial cancer. *Cancer Res,* 67**,** 1927-34.

MURRAY, N. R. & FIELDS, A. P. (1997) Atypical protein kinase C iota protects human leukemia cells against drug-induced apoptosis. *J Biol Chem,* 272**,** 27521-4.

MURRAY, N. R., JAMIESON, L., YU, W., ZHANG, J., GOKMEN-POLAR, Y., SIER, D., ANASTASIADIS, P., GATALICA, Z., THOMPSON, E. A. & FIELDS, A. P. (2004) Protein kinase Ciota is required for Ras transformation and colon carcinogenesis in vivo. *J Cell Biol,* 164**,** 797-802.

MUSCH, A., COHEN, D., YEAMAN, C., NELSON, W. J., RODRIGUEZ-BOULAN, E. & BRENNWALD, P. J. (2002) Mammalian homolog of Drosophila tumor suppressor lethal (2) giant larvae interacts with basolateral exocytic machinery in Madin-Darby canine kidney cells. *Mol Biol Cell,* 13**,** 158-68.

NAGAI-TAMAI, Y., MIZUNO, K., HIROSE, T., SUZUKI, A. & OHNO, S. (2002) Regulated protein-protein interaction between aPKC and PAR-3 plays an essential role in the polarization of epithelial cells. *Genes Cells,* 7**,** 1161-71.

NATESAN, S., RIVERA, V. M., MOLINARI, E. & GILMAN, M. (1997) Transcriptional squelching re-examined. *Nature,* 390**,** 349-50.

NELSON, W. J. (2008) Regulation of cell-cell adhesion by the cadherin-catenin complex. *Biochem Soc Trans,* 36**,** 149-55.

NG, T., PARSONS, M., HUGHES, W. E., MONYPENNY, J., ZICHA, D., GAUTREAU, A., ARPIN, M., GSCHMEISSNER, S., VERVEER, P. J., BASTIAENS, P. I. & PARKER, P. J. (2001) Ezrin is a downstream effector of trafficking PKC-integrin complexes involved in the control of cell motility. *EMBO J,* 20**,** 2723-41.

NISHIMURA, T. & KAIBUCHI, K. (2007) Numb controls integrin endocytosis for directional cell migration with aPKC and PAR-3. *Dev Cell,* 13**,** 15-28.

O'BRIEN, L. E., JOU, T. S., POLLACK, A. L., ZHANG, Q., HANSEN, S. H., YURCHENCO, P. & MOSTOV, K. E. (2001) Rac1 orientates epithelial apical polarity through effects on basolateral laminin assembly. *Nat Cell Biol,* 3**,** 831-8.

ONO, Y., FUJII, T., OGITA, K., KIKKAWA, U., IGARASHI, K. & NISHIZUKA, Y. (1989) Protein kinase C zeta subspecies from rat brain: its structure, expression, and properties. *Proc Natl Acad Sci U S A,* 86**,** 3099-103.

OSMANI, N., PEGLION, F., CHAVRIER, P. & ETIENNE-MANNEVILLE, S. (2010) Cdc42 localization and cell polarity depend on membrane traffic. *J Cell Biol,* 191**,** 1261-9.

OSMANI, N., VITALE, N., BORG, J. P. & ETIENNE-MANNEVILLE, S. (2006) Scrib controls Cdc42 localization and activity to promote cell polarization during astrocyte migration. *Curr Biol,* 16**,** 2395-405.

PAGLIARINI, R. A. & XU, T. (2003) A genetic screen in Drosophila for metastatic behavior. *Science,* 302**,** 1227-31.

PALMER, R. H., DEKKER, L. V., WOSCHOLSKI, R., LE GOOD, J. A., GIGG, R. & PARKER, P. J. (1995) Activation of PRK1 by phosphatidylinositol 4,5-bisphosphate and phosphatidylinositol 3,4,5-trisphosphate. A comparison with protein kinase C isotypes. *J Biol Chem,* 270**,** 22412-6.

PARKER, P. J., BOSCA, L., DEKKER, L., GOODE, N. T., HAJIBAGHERI, N. & HANSRA, G. (1995) Protein kinase C (PKC)-induced PKC degradation: a model for down-regulation. *Biochem Soc Trans,* 23**,** 153-5.

PARKER, P. J. & MURRAY-RUST, J. (2004) PKC at a glance. *J Cell Sci,* 117**,** 131-2.

PARKINSON, S. J., LE GOOD, J. A., WHELAN, R. D., WHITEHEAD, P. & PARKER, P. J. (2004) Identification of PKCzetaII: an endogenous inhibitor of cell polarity. *EMBO J,* 23**,** 77-88.

PARSONS, L. M., GRZESCHIK, N. A., ALLOTT, M. L. & RICHARDSON, H. E. (2010) Lgl/aPKC and Crb regulate the Salvador/Warts/Hippo pathway. *Fly (Austin),* 4**,** 288-93.

PATEL, R., WIN, H., DESAI, S., PATEL, K., MATTHEWS, J. A. & ACEVEDO-DUNCAN, M. (2008) Involvement of PKC-iota in glioma proliferation. *Cell Prolif,* 41**,** 122-35.

PAWSON, T., GISH, G. D. & NASH, P. (2001) SH2 domains, interaction modules and cellular wiring. *Trends Cell Biol,* 11**,** 504-11.

PAWSON, T. & NASH, P. (2003) Assembly of cell regulatory systems through protein interaction domains. *Science,* 300**,** 445-52.

PAWSON, T., RAINA, M. & NASH, P. (2002) Interaction domains: from simple binding events to complex cellular behavior. *FEBS Lett,* 513**,** 2-10.

PEARCE, L. R., KOMANDER, D. & ALESSI, D. R. (2010) The nuts and bolts of AGC protein kinases. *Nat Rev Mol Cell Biol,* 11**,** 9-22.

PEARS, C. J., KOUR, G., HOUSE, C., KEMP, B. E. & PARKER, P. J. (1990) Mutagenesis of the pseudosubstrate site of protein kinase C leads to activation. *Eur J Biochem,* 194**,** 89-94.

PERKINS, D. N., PAPPIN, D. J., CREASY, D. M. & COTTRELL, J. S. (1999) Probability-based protein identification by searching sequence databases using mass spectrometry data. *Electrophoresis,* 20**,** 3551-67.

PETRONCZKI, M. & KNOBLICH, J. A. (2001) DmPAR-6 directs epithelial polarity and asymmetric cell division of neuroblasts in Drosophila. *Nat Cell Biol,* 3**,** 43-9.

PILLAI, P., DESAI, S., PATEL, R., SAJAN, M., FARESE, R., OSTROV, D. & ACEVEDO-DUNCAN, M. (2011) A novel PKC-iota inhibitor abrogates cell proliferation and induces apoptosis in neuroblastoma. *Int J Biochem Cell Biol*.

PLANT, P. J., FAWCETT, J. P., LIN, D. C., HOLDORF, A. D., BINNS, K., KULKARNI, S. & PAWSON, T. (2003) A polarity complex of mPar-6 and atypical PKC binds, phosphorylates and regulates mammalian Lgl. *Nat Cell Biol,* 5**,** 301-8.

POLESELLO, C., HUELSMANN, S., BROWN, N. H. & TAPON, N. (2006) The Drosophila RASSF homolog antagonizes the hippo pathway. *Curr Biol,* 16**,** 2459-65.

PU, Y., PEACH, M. L., GARFIELD, S. H., WINCOVITCH, S., MARQUEZ, V. E. & BLUMBERG, P. M. (2006) Effects on ligand interaction and membrane translocation of the positively charged arginine residues situated along the C1 domain binding cleft in the atypical protein kinase C isoforms. *J Biol Chem,* 281**,** 33773-88.

PULS, A., SCHMIDT, S., GRAWE, F. & STABEL, S. (1997) Interaction of protein kinase C zeta with ZIP, a novel protein kinase C-binding protein. *Proc Natl Acad Sci U S A,* 94**,** 6191-6.

QIN, J., VINOGRADOVA, O. & PLOW, E. F. (2004) Integrin bidirectional signaling: a molecular view. *PLoS Biol,* 2**,** e169.

QIN, Y., MEISEN, W. H., HAO, Y. & MACARA, I. G. (2010) Tuba, a Cdc42 GEF, is required for polarized spindle orientation during epithelial cyst formation. *J Cell Biol,* 189**,** 661-9.

QIU, R. G., ABO, A. & STEVEN MARTIN, G. (2000) A human homolog of the C. elegans polarity determinant Par-6 links Rac and Cdc42 to PKCzeta signaling and cell transformation. *Curr Biol,* 10**,** 697-707.

QIU, R. G., CHEN, J., KIRN, D., MCCORMICK, F. & SYMONS, M. (1995) An essential role for Rac in Ras transformation. *Nature,* 374**,** 457-9.

REGALA, R. P., DAVIS, R. K., KUNZ, A., KHOOR, A., LEITGES, M. & FIELDS, A. P. (2009) Atypical Protein Kinase C{iota} Is Required for Bronchioalveolar Stem Cell Expansion and Lung Tumorigenesis. *Cancer Res*.

REGALA, R. P., THOMPSON, E. A. & FIELDS, A. P. (2008) Atypical protein kinase C iota expression and aurothiomalate sensitivity in human lung cancer cells. *Cancer Res,* 68**,** 5888-95.

REGALA, R. P., WEEMS, C., JAMIESON, L., COPLAND, J. A., THOMPSON, E. A. & FIELDS, A. P. (2005a) Atypical protein kinase Ciota plays a critical role in human lung cancer cell growth and tumorigenicity. *J Biol Chem,* 280**,** 31109-15.

REGALA, R. P., WEEMS, C., JAMIESON, L., KHOOR, A., EDELL, E. S., LOHSE, C. M. & FIELDS, A. P. (2005b) Atypical protein kinase C iota is an oncogene in human non-small cell lung cancer. *Cancer Res,* 65**,** 8905-11.

REN, L., HONG, S. H., CASSAVAUGH, J., OSBORNE, T., CHOU, A. J., KIM, S. Y., GORLICK, R., HEWITT, S. M. & KHANNA, C. (2009) The actin-cytoskeleton linker protein ezrin is regulated during osteosarcoma metastasis by PKC. *Oncogene,* 28**,** 792-802.

RICHARDSON, E. C. & PICHAUD, F. (2010) Crumbs is required to achieve proper organ size control during Drosophila head development. *Development,* 137**,** 641-50.

ROBINSON, B. S., HUANG, J., HONG, Y. & MOBERG, K. H. (2010) Crumbs regulates Salvador/Warts/Hippo signaling in Drosophila via the FERM-domain protein Expanded. *Curr Biol,* 20**,** 582-90.

RODRIGUEZ, E. M., DUNHAM, E. E. & MARTIN, G. S. (2009) Atypical protein kinase C activity is required for extracellular matrix degradation and invasion by Src-transformed cells. *J Cell Physiol,* 221**,** 171-82.

RODRIGUEZ-FRATICELLI, A. E., VERGARAJAUREGUI, S., EASTBURN, D. J., DATTA, A., ALONSO, M. A., MOSTOV, K. & MARTIN-BELMONTE, F. (2010) The Cdc42 GEF Intersectin 2 controls mitotic spindle orientation to form the lumen during epithelial morphogenesis. *J Cell Biol,* 189**,** 725-38.

ROSSE, C., FORMSTECHER, E., BOECKELER, K., ZHAO, Y., KREMERSKOTHEN, J., WHITE, M. D., CAMONIS, J. H. & PARKER, P. J. (2009) An aPKC-exocyst complex controls paxillin phosphorylation and migration through localised JNK1 activation. *PLoS Biol,* 7**,** e1000235.

ROSSE, C., HATZOGLOU, A., PARRINI, M. C., WHITE, M. A., CHAVRIER, P. & CAMONIS, J. (2006) RalB mobilizes the exocyst to drive cell migration. *Mol Cell Biol,* 26**,** 727-34.

SAADAT, I., HIGASHI, H., OBUSE, C., UMEDA, M., MURATA-KAMIYA, N., SAITO, Y., LU, H., OHNISHI, N., AZUMA, T., SUZUKI, A., OHNO, S. & HATAKEYAMA, M. (2007) Helicobacter pylori CagA targets PAR1/MARK kinase to disrupt epithelial cell polarity. *Nature,* 447**,** 330-3.

SAKISAKA, T., BABA, T., TANAKA, S., IZUMI, G., YASUMI, M. & TAKAI, Y. (2004) Regulation of SNAREs by tomosyn and ROCK: implication in extension and retraction of neurites. *J Cell Biol,* 166**,** 17-25.

SANCHEZ, P., DE CARCER, G., SANDOVAL, I. V., MOSCAT, J. & DIAZ-MECO, M. T. (1998) Localization of atypical protein kinase C isoforms into lysosome-targeted endosomes through interaction with p62. *Mol Cell Biol,* 18**,** 3069-80.

SANTOS, O. F. & NIGAM, S. K. (1993) HGF-induced tubulogenesis and branching of epithelial cells is modulated by extracellular matrix and TGF-beta. *Dev Biol,* 160**,** 293-302.

SATOH, T., ENDO, M., NAKAFUKU, M., AKIYAMA, T., YAMAMOTO, T. & KAZIRO, Y. (1990) Accumulation of p21ras.GTP in response to stimulation with epidermal growth factor and oncogene products with tyrosine kinase activity. *Proc Natl Acad Sci U S A,* 87**,** 7926-9.

SAURIN, A. T., DURGAN, J., CAMERON, A. J., FAISAL, A., MARBER, M. S. & PARKER, P. J. (2008) The regulated assembly of a PKCepsilon complex controls the completion of cytokinesis. *Nat Cell Biol,* 10**,** 891-901.

SCHIMANSKI, C. C., SCHMITZ, G., KASHYAP, A., BOSSERHOFF, A. K., BATAILLE, F., SCHAFER, S. C., LEHR, H. A., BERGER, M. R., GALLE, P. R., STRAND, S. & STRAND, D. (2005) Reduced expression of Hugl-1, the human homologue of Drosophila tumour suppressor gene lgl, contributes to progression of colorectal cancer. *Oncogene,* 24**,** 3100-9.

SCHLESSINGER, J. (2002) Ligand-induced, receptor-mediated dimerization and activation of EGF receptor. *Cell,* 110**,** 669-72.

SCOTTI, M. L., BAMLET, W. R., SMYRK, T. C., FIELDS, A. P. & MURRAY, N. R. Protein Kinase C{iota} Is Required for Pancreatic Cancer Cell Transformed Growth and Tumorigenesis. *Cancer Res*.

SCOTTI, M. L., BAMLET, W. R., SMYRK, T. C., FIELDS, A. P. & MURRAY, N. R. (2010) Protein kinase Ciota is required for pancreatic cancer cell transformed growth and tumorigenesis. *Cancer Res,* 70**,** 2064-74.

SENGUPTA, A., DURAN, A., ISHIKAWA, E., FLORIAN, M. C., DUNN, S. K., FICKER, A. M., LEITGES, M., GEIGER, H., DIAZ-MECO, M., MOSCAT, J. & CANCELAS, J. A. (2011) Atypical protein kinase C (aPKC{zeta} and aPKC{lambda}) is dispensable for mammalian hematopoietic stem cell activity and blood formation. *Proc Natl Acad Sci U S A,* 108**,** 9957-62.

SHEEN, I. S., JENG, K. S., SHIH, S. C., WANG, P. C., CHANG, W. H., WANG, H. Y., SHYUNG, L. R., LIN, S. C., KAO, C. R., TSAI, Y. C. & WU, T. Y. (2004) Does surgical resection of hepatocellular carcinoma accelerate cancer dissemination? *World J Gastroenterol,* 10**,** 31-6.

SHERR, C. J. & MCCORMICK, F. (2002) The RB and p53 pathways in cancer. *Cancer Cell,* 2**,** 103-12.

SHIBATA, H., MUKAI, H., INAGAKI, Y., HOMMA, Y., KIMURA, K., KAIBUCHI, K., NARUMIYA, S. & ONO, Y. (1996) Characterization of the interaction between RhoA and the amino-terminal region of PKN. *FEBS Lett,* 385**,** 221-4.

SINGH, A. B. & HARRIS, R. C. (2005) Autocrine, paracrine and juxtacrine signaling by EGFR ligands. *Cell Signal,* 17**,** 1183-93.

SNADDON, J., PARKINSON, E. K., CRAFT, J. A., BARTHOLOMEW, C. & FULTON, R. (2001) Detection of functional PTEN lipid phosphatase protein and enzyme activity in squamous cell carcinomas of the head and neck, despite loss of heterozygosity at this locus. *Br J Cancer,* 84**,** 1630-4.

SOLOFF, R. S., KATAYAMA, C., LIN, M. Y., FERAMISCO, J. R. & HEDRICK, S. M. (2004) Targeted deletion of protein kinase C lambda reveals a distribution of functions between the two atypical protein kinase C isoforms. *J Immunol,* 173**,** 3250-60.

SONAWANE, M., MARTIN-MAISCHEIN, H., SCHWARZ, H. & NUSSLEIN-VOLHARD, C. (2009) Lgl2 and E-cadherin act antagonistically to regulate hemidesmosome formation during epidermal development in zebrafish. *Development*.

SOTILLOS, S., DIAZ-MECO, M. T., CAMINERO, E., MOSCAT, J. & CAMPUZANO, S. (2004) DaPKC-dependent phosphorylation of Crumbs is required for epithelial cell polarity in Drosophila. *J Cell Biol,* 166**,** 549-57.

SRIPATHY, S., LEE, M. & VASIOUKHIN, V. (2011) Mammalian Llgl2 Is Necessary for Proper Branching Morphogenesis during Placental Development. *Mol Cell Biol,* 31**,** 2920-33.

ST JOHNSTON, D. & AHRINGER, J. (2010) Cell polarity in eggs and epithelia: parallels and diversity. *Cell,* 141**,** 757-74.

STALLINGS-MANN, M., JAMIESON, L., REGALA, R. P., WEEMS, C., MURRAY, N. R. & FIELDS, A. P. (2006) A novel small-molecule inhibitor of protein kinase Ciota blocks transformed growth of non-small-cell lung cancer cells. *Cancer Res,* 66**,** 1767-74.

STANDAERT, M. L., BANDYOPADHYAY, G., KANOH, Y., SAJAN, M. P. & FARESE, R. V. (2001) Insulin and PIP3 activate PKC-zeta by mechanisms that are both dependent and independent of phosphorylation of activation loop (T410) and autophosphorylation (T560) sites. *Biochemistry,* 40**,** 249-55.

STEFANOVA, I., HEMMER, B., VERGELLI, M., MARTIN, R., BIDDISON, W. E. & GERMAIN, R. N. (2003) TCR ligand discrimination is enforced by competing ERK positive and SHP-1 negative feedback pathways. *Nat Immunol,* 4**,** 248-54.

STRAND, D., JAKOBS, R., MERDES, G., NEUMANN, B., KALMES, A., HEID, H. W., HUSMANN, I. & MECHLER, B. M. (1994) The Drosophila lethal(2)giant larvae tumor suppressor protein forms homo-oligomers and is associated with nonmuscle myosin II heavy chain. *J Cell Biol,* 127**,** 1361-73.

SUGITA, M., TANAKA, N., DAVIDSON, S., SEKIYA, S., VARELLA-GARCIA, M., WEST, J., DRABKIN, H. A. & GEMMILL, R. M. (2000) Molecular definition of a small amplification domain within 3q26 in tumors of cervix, ovary, and lung. *Cancer Genet Cytogenet,* 117**,** 9-18.

SUN, R., GAO, P., CHEN, L., MA, D., WANG, J., OPPENHEIM, J. J. & ZHANG, N. (2005) Protein kinase C zeta is required for epidermal growth factor-induced chemotaxis of human breast cancer cells. *Cancer Res,* 65**,** 1433-41.

SUZUKI, A., YAMANAKA, T., HIROSE, T., MANABE, N., MIZUNO, K., SHIMIZU, M., AKIMOTO, K., IZUMI, Y., OHNISHI, T. & OHNO, S. (2001) Atypical protein kinase C is involved in the evolutionarily conserved par protein complex and plays a critical role in establishing epithelia-specific junctional structures. *J Cell Biol,* 152**,** 1183-96.

TABUSE, Y., IZUMI, Y., PIANO, F., KEMPHUES, K. J., MIWA, J. & OHNO, S. (1998) Atypical protein kinase C cooperates with PAR-3 to establish embryonic polarity in Caenorhabditis elegans. *Development,* 125**,** 3607-14.

TAKAGAWA, R., AKIMOTO, K., ICHIKAWA, Y., AKIYAMA, H., KOJIMA, Y., ISHIGURO, H., INAYAMA, Y., AOKI, I., KUNISAKI, C., ENDO, I., NAGASHIMA, Y. & OHNO, S. (2009) High Expression of Atypical Protein Kinase C lambda/iota in Gastric Cancer as a Prognostic Factor for Recurrence. *Ann Surg Oncol*.

TAKAI, Y., IKEDA, W., OGITA, H. & RIKITAKE, Y. (2008) The immunoglobulin-like cell adhesion molecule nectin and its associated protein afadin. *Annu Rev Cell Dev Biol,* 24**,** 309-42.

TAKAYAMA, T., KATSUKI, S., TAKAHASHI, Y., OHI, M., NOJIRI, S., SAKAMAKI, S., KATO, J., KOGAWA, K., MIYAKE, H. & NIITSU, Y. (1998) Aberrant crypt foci of the colon as precursors of adenoma and cancer. *N Engl J Med,* 339**,** 1277-84.

TAKIMURA, T., KAMATA, K., FUKASAWA, K., OHSAWA, H., KOMATANI, H., YOSHIZUMI, T., TAKAHASHI, I., KOTANI, H. & IWASAWA, Y. (2010) Structures of the PKC-iota kinase domain in its ATP-bound and apo forms reveal defined structures of residues 533-551 in the C-terminal tail and their roles in ATP binding. *Acta Crystallogr D Biol Crystallogr,* 66**,** 577-83.

TAMBORINI, E., BONADIMAN, L., GRECO, A., ALBERTINI, V., NEGRI, T., GRONCHI, A., BERTULLI, R., COLECCHIA, M., CASALI, P. G., PIEROTTI, M. A. & PILOTTI, S. (2004) A new mutation in the KIT ATP pocket causes acquired resistance to imatinib in a gastrointestinal stromal tumor patient. *Gastroenterology,* 127**,** 294-9.

TAMBORINI, E., PRICL, S., NEGRI, T., LAGONIGRO, M. S., MISELLI, F., GRECO, A., GRONCHI, A., CASALI, P. G., FERRONE, M., FERMEGLIA, M., CARBONE, A., PIEROTTI, M. A. & PILOTTI, S. (2006) Functional analyses and molecular modeling of two c-Kit mutations responsible for imatinib secondary resistance in GIST patients. *Oncogene,* 25**,** 6140-6.

TANOUE, T. & NISHIDA, E. (2003) Molecular recognitions in the MAP kinase cascades. *Cell Signal,* 15**,** 455-62.

TAYLOR, S. S. & KORNEV, A. P. (2011) Protein kinases: evolution of dynamic regulatory proteins. *Trends Biochem Sci,* 36**,** 65-77.

TEPASS, U., THERES, C. & KNUST, E. (1990) crumbs encodes an EGF-like protein expressed on apical membranes of Drosophila epithelial cells and required for organization of epithelia. *Cell,* 61**,** 787-99.

THIERY, J. P. (2002) Epithelial-mesenchymal transitions in tumour progression. *Nat Rev Cancer,* 2**,** 442-54.

THOMAS, J. E., SORIANO, P. & BRUGGE, J. S. (1991) Phosphorylation of c-Src on tyrosine 527 by another protein tyrosine kinase. *Science,* 254**,** 568-71.

TISDALE, E. J. & ARTALEJO, C. R. (2006) Src-dependent aprotein kinase C iota/lambda (aPKCiota/lambda) tyrosine phosphorylation is required for aPKCiota/lambda association with Rab2 and glyceraldehyde-3-phosphate dehydrogenase on pre-golgi intermediates. *J Biol Chem,* 281**,** 8436-42.

TOKER, A. & NEWTON, A. C. (2000) Cellular signaling: pivoting around PDK-1. *Cell,* 103**,** 185-8.

TOYLI, M., ROSBERG-KULHA, L., CAPRA, J., VUORISTO, J. & ESKELINEN, S. (2010) Different responses in transformation of MDCK cells in 2D and 3D culture by v-Src as revealed by microarray techniques, RT-PCR and functional assays. *Lab Invest,* 90**,** 915-28.

TRAWEGER, A., WIGGIN, G., TAYLOR, L., TATE, S. A., METALNIKOV, P. & PAWSON, T. (2008) Protein phosphatase 1 regulates the phosphorylation state of the polarity scaffold Par-3. *Proc Natl Acad Sci U S A*.

TRICHAS, G., BEGBIE, J. & SRINIVAS, S. (2008) Use of the viral 2A peptide for bicistronic expression in transgenic mice. *BMC Biol,* 6**,** 40.

TSUKITA, S., FURUSE, M. & ITOH, M. (2001) Multifunctional strands in tight junctions. *Nat Rev Mol Cell Biol,* 2**,** 285-93.

TSUKITA, S., YAMAZAKI, Y., KATSUNO, T., TAMURA, A. & TSUKITA, S. (2008) Tight junction-based epithelial microenvironment and cell proliferation. *Oncogene,* 27**,** 6930-8.

UBERALL, F., HELLBERT, K., KAMPFER, S., MALY, K., VILLUNGER, A., SPITALER, M., MWANJEWE, J., BAIER-BITTERLICH, G., BAIER, G. & GRUNICKE, H. H. (1999) Evidence

that atypical protein kinase C-lambda and atypical protein kinase C-zeta participate in Ras-mediated reorganization of the F-actin cytoskeleton. *J Cell Biol,* 144**,** 413-25.

UEMURA, T., SHEPHERD, S., ACKERMAN, L., JAN, L. Y. & JAN, Y. N. (1989) numb, a gene required in determination of cell fate during sensory organ formation in Drosophila embryos. *Cell,* 58**,** 349-60.

VAN DER HOEVEN, P. C., VAN DER WAL, J. C., RUURS, P., VAN DIJK, M. C. & VAN BLITTERSWIJK, J. (2000) 14-3-3 isotypes facilitate coupling of protein kinase C-zeta to Raf-1: negative regulation by 14-3-3 phosphorylation. *Biochem J,* 345 Pt 2**,** 297-306.

VAN DIJK, M. C., HILKMANN, H. & VAN BLITTERSWIJK, W. J. (1997) Platelet-derived growth factor activation of mitogen-activated protein kinase depends on the sequential activation of phosphatidylcholine-specific phospholipase C, protein kinase C-zeta and Raf-1. *Biochem J,* 325 (Pt 2)**,** 303-7.

VENTER, J. C., ADAMS, M. D., MYERS, E. W., LI, P. W., MURAL, R. J., SUTTON, G. G., SMITH, H. O., YANDELL, M., EVANS, C. A., HOLT, R. A., GOCAYNE, J. D., AMANATIDES, P., BALLEW, R. M., HUSON, D. H., WORTMAN, J. R., ZHANG, Q., KODIRA, C. D., ZHENG, X. H., CHEN, L., SKUPSKI, M., SUBRAMANIAN, G., THOMAS, P. D., ZHANG, J., GABOR MIKLOS, G. L., NELSON, C., BRODER, S., CLARK, A. G., NADEAU, J., MCKUSICK, V. A., ZINDER, N., LEVINE, A. J., ROBERTS, R. J., SIMON, M., SLAYMAN, C., HUNKAPILLER, M., BOLANOS, R., DELCHER, A., DEW, I., FASULO, D., FLANIGAN, M., FLOREA, L., HALPERN, A., HANNENHALLI, S., KRAVITZ, S., LEVY, S., MOBARRY, C., REINERT, K., REMINGTON, K., ABU-THREIDEH, J., BEASLEY, E., BIDDICK, K., BONAZZI, V., BRANDON, R., CARGILL, M., CHANDRAMOULISWARAN, I., CHARLAB, R., CHATURVEDI, K., DENG, Z., DI FRANCESCO, V., DUNN, P., EILBECK, K., EVANGELISTA, C., GABRIELIAN, A. E., GAN, W., GE, W., GONG, F., GU, Z., GUAN, P., HEIMAN, T. J., HIGGINS, M. E., JI, R. R., KE, Z., KETCHUM, K. A., LAI, Z., LEI, Y., LI, Z., LI, J., LIANG, Y., LIN, X., LU, F., MERKULOV, G. V., MILSHINA, N., MOORE, H. M., NAIK, A. K., NARAYAN, V. A., NEELAM, B., NUSSKERN, D., RUSCH, D. B., SALZBERG, S., SHAO, W., SHUE, B., SUN, J., WANG, Z., WANG, A., WANG, X., WANG, J., WEI, M., WIDES, R., XIAO, C., YAN, C., et al. (2001) The sequence of the human genome. *Science,* 291**,** 1304-51.

VOGELSTEIN, B. & KINZLER, K. W. (1993) The multistep nature of cancer. *Trends Genet,* 9**,** 138-41.

WALD, F. A., ORIOLO, A. S., MASHUKOVA, A., FREGIEN, N. L., LANGSHAW, A. H. & SALAS, P. J. (2008) Atypical protein kinase C (iota) activates ezrin in the apical domain of intestinal epithelial cells. *J Cell Sci,* 121**,** 644-54.

WANG, G., KRISHNAMURTHY, K., CHIANG, Y. W., DASGUPTA, S. & BIEBERICH, E. (2008a) Regulation of neural progenitor cell motility by ceramide and potential implications for mouse brain development. *J Neurochem*.

WANG, H. L., LOPATEGUI, J., AMIN, M. B. & PATTERSON, S. D. (2010) KRAS mutation testing in human cancers: The pathologist's role in the era of personalized medicine. *Adv Anat Pathol,* 17**,** 23-32.

WANG, J. M., LI, Q., DU, G. S., LU, J. X. & ZOU, S. Q. (2008b) Significance and Expression of Atypical Protein Kinase C-i in Human Hepatocellular Carcinoma. *J Surg Res*.

WANG, Y. M., SEIBENHENER, M. L., VANDENPLAS, M. L. & WOOTEN, M. W. (1999) Atypical PKC zeta is activated by ceramide, resulting in coactivation of NF-kappaB/JNK kinase and cell survival. *J Neurosci Res,* 55**,** 293-302.

WANG, Z., SANDIFORD, S., WU, C. & LI, S. S. (2009) Numb regulates cell-cell adhesion and polarity in response to tyrosine kinase signalling. *EMBO J,* 28**,** 2360-73.

WATTS, J. L., ETEMAD-MOGHADAM, B., GUO, S., BOYD, L., DRAPER, B. W., MELLO, C. C., PRIESS, J. R. & KEMPHUES, K. J. (1996) par-6, a gene involved in the establishment of asymmetry in early C. elegans embryos, mediates the asymmetric localization of PAR-3. *Development,* 122**,** 3133-40.

WEIGELT, B., LO, A. T., PARK, C. C., GRAY, J. W. & BISSELL, M. J. (2010) HER2 signaling pathway activation and response of breast cancer cells to HER2-targeting agents is dependent strongly on the 3D microenvironment. *Breast Cancer Res Treat,* 122**,** 35-43.

WEINBERG, R. A. (1995) The retinoblastoma protein and cell cycle control. *Cell,* 81**,** 323-30.

WEISS, W. A., TAYLOR, S. S. & SHOKAT, K. M. (2007) Recognizing and exploiting differences between RNAi and small-molecule inhibitors. *Nat Chem Biol,* 3**,** 739-44.

WELCHMAN, D. P., MATHIES, L. D. & AHRINGER, J. (2007) Similar requirements for CDC-42 and the PAR-3/PAR-6/PKC-3 complex in diverse cell types. *Dev Biol,* 305**,** 347-57.

WETTSCHURECK, N. & OFFERMANNS, S. (2005) Mammalian G proteins and their cell type specific functions. *Physiol Rev,* 85**,** 1159-204.

WHITE, W. O., SEIBENHENER, M. L. & WOOTEN, M. W. (2002) Phosphorylation of tyrosine 256 facilitates nuclear import of atypical protein kinase C. *J Cell Biochem,* 85**,** 42-53.

WILSON, M. I., GILL, D. J., PERISIC, O., QUINN, M. T. & WILLIAMS, R. L. (2003) PB1 domain-mediated heterodimerization in NADPH oxidase and signaling complexes of atypical protein kinase C with Par6 and p62. *Mol Cell,* 12**,** 39-50.

WIN, H. Y. & ACEVEDO-DUNCAN, M. (2008) Atypical protein kinase C phosphorylates IKKalphabeta in transformed non-malignant and malignant prostate cell survival. *Cancer Lett*.

WIN, H. Y. & ACEVEDO-DUNCAN, M. (2009) Role of protein kinase C-iota in transformed non-malignant RWPE-1 cells and androgen-independent prostate carcinoma DU-145 cells. *Cell Prolif*.

WODARZ, A. & NATHKE, I. (2007) Cell polarity in development and cancer. *Nat Cell Biol,* 9**,** 1016-24.

WOOTEN, M. W., VANDENPLAS, M. L., SEIBENHENER, M. L., GEETHA, T. & DIAZ-MECO, M. T. (2001) Nerve growth factor stimulates multisite tyrosine phosphorylation and activation of the atypical protein kinase C's via a src kinase pathway. *Mol Cell Biol,* 21**,** 8414-27.

WU, H., FENG, W., CHEN, J., CHAN, L. N., HUANG, S. & ZHANG, M. (2007) PDZ domains of Par-3 as potential phosphoinositide signaling integrators. *Mol Cell,* 28**,** 886-98.

XU, C. & MIN, J. (2011) Structure and function of WD40 domain proteins. *Protein Cell,* 2**,** 202-14.

XU, L. & DENG, X. (2006) Protein kinase Ciota promotes nicotine-induced migration and invasion of cancer cells via phosphorylation of micro- and m-calpains. *J Biol Chem,* 281**,** 4457-66.

YAFFE, M. B. (2002) How do 14-3-3 proteins work?-- Gatekeeper phosphorylation and the molecular anvil hypothesis. *FEBS Lett,* 513**,** 53-7.

YAFFE, M. B. & ELIA, A. E. (2001) Phosphoserine/threonine-binding domains. *Curr Opin Cell Biol,* 13**,** 131-8.

YAMANAKA, T., HORIKOSHI, Y., IZUMI, N., SUZUKI, A., MIZUNO, K. & OHNO, S. (2006) Lgl mediates apical domain disassembly by suppressing the PAR-3-aPKC-PAR-6 complex to orient apical membrane polarity. *J Cell Sci,* 119**,** 2107-18.

YAMANAKA, T., HORIKOSHI, Y., SUGIYAMA, Y., ISHIYAMA, C., SUZUKI, A., HIROSE, T., IWAMATSU, A., SHINOHARA, A. & OHNO, S. (2003) Mammalian Lgl forms a protein complex with PAR-6 and aPKC independently of PAR-3 to regulate epithelial cell polarity. *Curr Biol,* 13**,** 734-43.

YAMANAKA, T., HORIKOSHI, Y., SUZUKI, A., SUGIYAMA, Y., KITAMURA, K., MANIWA, R., NAGAI, Y., YAMASHITA, A., HIROSE, T., ISHIKAWA, H. & OHNO, S. (2001) PAR-6 regulates aPKC activity in a novel way and mediates cell-cell contact-induced formation of the epithelial junctional complex. *Genes Cells,* 6**,** 721-31.

YAMASHITA, A., OHNISHI, T., KASHIMA, I., TAYA, Y. & OHNO, S. (2001) Human SMG-1, a novel phosphatidylinositol 3-kinase-related protein kinase, associates with components of the mRNA surveillance complex and is involved in the regulation of nonsense-mediated mRNA decay. *Genes Dev,* 15**,** 2215-28.

YANG, Y. L., CHU, J. Y., LUO, M. L., WU, Y. P., ZHANG, Y., FENG, Y. B., SHI, Z. Z., XU, X., HAN, Y. L., CAI, Y., DONG, J. T., ZHAN, Q. M., WU, M. & WANG, M. R. (2008) Amplification of PRKCI, located in 3q26, is associated with lymph node metastasis in esophageal squamous cell carcinoma. *Genes Chromosomes Cancer,* 47**,** 127-36.

YASUMI, M., SAKISAKA, T., HOSHINO, T., KIMURA, T., SAKAMOTO, Y., YAMANAKA, T., OHNO, S. & TAKAI, Y. (2005) Direct binding of Lgl2 to LGN during mitosis and its requirement for normal cell division. *J Biol Chem,* 280**,** 6761-5.

YEAMAN, C., GRINDSTAFF, K. K. & NELSON, W. J. (1999) New perspectives on mechanisms involved in generating epithelial cell polarity. *Physiol Rev,* 79**,** 73-98.

YU, J., ZHANG, Y., MCILROY, J., RORDORF-NIKOLIC, T., ORR, G. A. & BACKER, J. M. (1998) Regulation of the p85/p110 phosphatidylinositol 3'-kinase: stabilization and inhibition of the p110alpha catalytic subunit by the p85 regulatory subunit. *Mol Cell Biol,* 18**,** 1379-87.

ZHANG, F., ZHANG, X., LI, M., CHEN, P., ZHANG, B., GUO, H., CAO, W., WEI, X., CAO, X., HAO, X. & ZHANG, N. (2010) mTOR Complex Component Rictor Interacts with PKC{zeta} and Regulates Cancer Cell Metastasis. *Cancer Res*.

ZHANG, J., ANASTASIADIS, P. Z., LIU, Y., THOMPSON, E. A. & FIELDS, A. P. (2004) Protein kinase C (PKC) betaII induces cell invasion through a Ras/Mek-, PKC iota/Rac 1-dependent signaling pathway. *J Biol Chem,* 279**,** 22118-23.

ZHANG, L., HUANG, J., YANG, N., LIANG, S., BARCHETTI, A., GIANNAKAKIS, A., CADUNGOG, M. G., O'BRIEN-JENKINS, A., MASSOBRIO, M., ROBY, K. F., KATSAROS, D., GIMOTTY, P., BUTZOW, R., WEBER, B. L. & COUKOS, G. (2006a) Integrative genomic analysis of protein kinase C (PKC) family identifies PKCiota as a biomarker and potential oncogene in ovarian carcinoma. *Cancer Res,* 66**,** 4627-35.

ZHANG, X., GUREASKO, J., SHEN, K., COLE, P. A. & KURIYAN, J. (2006b) An allosteric mechanism for activation of the kinase domain of epidermal growth factor receptor. *Cell,* 125**,** 1137-49.

ZHANG, X., ZHU, S., LUO, G., ZHENG, L., WEI, J., ZHU, J., MU, Q. & XU, N. (2007) Expression of MMP-10 in lung cancer. *Anticancer Res,* 27**,** 2791-5.

ZHENG, Z., ZHU, H., WAN, Q., LIU, J., XIAO, Z., SIDEROVSKI, D. P. & DU, Q. (2010) LGN regulates mitotic spindle orientation during epithelial morphogenesis. *J Cell Biol,* 189**,** 275-88.

ZHOU, P., ALFARO, J., CHANG, E. H., ZHAO, X., PORCIONATTO, M. & SEGAL, R. A. (2011) Numb links extracellular cues to intracellular polarity machinery to promote chemotaxis. *Dev Cell,* 20**,** 610-22.

ZHU, H., BILGIN, M. & SNYDER, M. (2003) Proteomics. *Annu Rev Biochem,* 72**,** 783-812.